Numerical Simulation of Unsaturated Flow Near a Septic System Drainfield

Volume I. Report and Appendixes A, B, and C

By

Nilesh Waghdare, M.S.,
Ken Rainwater, Ph.D., P.E., DEE, and
Andrew Jackson, Ph.D., P.E.
Texas Tech University Water Resources Center
Box 41022
Lubbock, TX 79409-1022

Submitted to

Texas On-Site Wastewater Treatment Research Council
Texas Commission on Environmental Quality
OSSF Program MC-178
P.O. Box 13087
Austin, TX 78711-3087

December, 2003

ACKNOWLEDGEMENTS

I would like to thank my thesis committee members Dr. Ken Rainwater and Dr. Andrew Jackson for their guidance and support. In particular, I am thankful to Dr. Ken Rainwater for providing me with an invaluable research opportunity and for his patience and understanding during the research process. I am also thankful to Texas On-site Wastewater Treatment Research Council for funding this project.

I would also like to thank Brad Thornhill and Greg Crabtree for their help at the test site during field experiments and for solving computer software problems in the most prompt fashion. Thanks are also due to the entire staff of the Civil Engineering Department who made my stay at Texas Tech University a most memorable one.

I would like to thank my parents and relatives in India for their constant encouragement and support during the last two years of my study. Thanks to my friends who were there to help and encourage me. Last but not the least I would like to thank God for this opportunity.

TABLE OF CONTENTS

ACKNOWLEDGEMENTS....................ii

LIST OF TABLES....................vii

LIST OF FIGURES....................viii

CHAPTER

1. INTRODUCTION....................1

1.1 Problem Statement....................1

1.2 Specific Objectives....................3

2. LITERATURE REVIEW....................5

2.1 Introduction....................5

2.2 Current TCEQ Drainfield Requirements....................5

2.3 Phase 1 Study....................8

2.3.1 Test Site Setup....................9

2.3.2 Operation....................11

2.4 Numerical Modeling....................13

2.4.1 MODFLOW-SURFACT....................14

2.4.1.1 MODFLOW-SURFACT: Introduction and history....................14

2.4.1.2 MODFLOW-SURFACT Version 2.2....................16

2.4.1.3 Formulation of the variably saturated water flow equation....................19

2.4.1.4 Applications of MODFLOW-SURFACT....................21

2.4.2 GMS-FEMWATER....................23

2.4.2.1 GMS-FEMWATER: Introduction and history....................23

2.4.2.2 GMS-FEMWATER Version 3.1 24

2.4.2.2.1 Geometry File..25

2.4.2.2.2 Model File..25

2.4.2.2.3 Initial Condition File..27

2.4.2.2.4 Solution File..28

2.4.2.3 Formulation of FEMWATER 28

2.4.2.4 Soil Characteristic Curves in FEMWATER 31

2.4.2.5 Applications of GMS-FEMWATER 31

3. METHODS..35

3.1 Conceptual Model..35

3.1.1 Geometry.. 36

3.1.2 Soils... 41

3.1.3 Hydrologic Data... 41

3.1.4 Trench Operation 43

3.2 Types of Simulations..44

3.3 Input for MODFLOW-SURFACT..46

3.3.1 Basic Package 47

3.3.1.1 Model Geometry 47

3.3.1.2 Initial Conditions 49

3.3.1.3 Time Discretization... 50

3.3.1.4 Simulation Continuity 51

3.3.2 BCF4 Package.. 51

3.3.3 EVT Package 54

3.3.4 Recharge Package 56

3.3.4.1 Negative Recharge Trial Simulations 56

3.3.4.1.1 First Trial Simulation 58

3.3.4.1.2 Second Trial Simulation 58

3.3.4.1.3 Limitations of negative recharge mechanism 59

3.3.5 RSF4 Package 60

3.3.6 ATO4 Package 61

3.3.7 PCG4 Package 62

3.3.8 NRB1 Package 64

3.3.9 Drain Package 65

3.4 Input Requirements for GMS-FEMWATER 65

3.4.1 Geometry File 66

3.4.2 Model File 68

4. RESULTS 74

4.1 Introduction 74

4.2 MODFLOW-SURFACT Results 74

4.2.1.1 Verification of type-A simulation 75

4.2.1.2 Verification of type-B simulation 76

4.2.2 Soil Characteristic Curves in MODFLOW-SURFACT 78

4.2.3 Processing of Results 81

4.2.4 Comparison of loading pattern with respect to ET domains A and B 81

4.2.5 Results of Simulations Performed..85

4.2.5.1 SL-A Simulation..87

4.2.5.2 SL-B Simulation..88

4.2.5.3 SCL-A Simulation..89

4.2.5.4 SCL-B Simulation..90

4.2.6 Comparison of simulations..92

4.2.6.1 SL-A and SL-B simulations..92

4.2.6.2 SL-B and SCL-B simulations..93

4.2.7 Implications..95

4.3 FEMWATER Results..96

5. CONCLUSIONS AND RECOMMENDATIONS..98

5.1 Conclusion..98

5.2 Recommendations..99

REFERENCES..101

APPENDIX

A. PROCEDURE FOR SETTING UP A MODFLOW-SURFACT SIMULATION MODEL USING GROUNDWATER VISTAS

B. SETTING DAILY VALUES OF LOADING RATE, WASTEWATER ET RATE, AND RAINFALL RATE IN FT/DAY FROM PHASE-1 STUDY

C. CALCULATION OF ERROR FOR 30-DAY EVT TRIAL AND 1000-DAY EVT TRIAL

D. CONTOUR AND VECTOR PLOTS FROM SIMULATIONS RUN

LIST OF TABLES

2.1 Summary of field performance (Rainwater et al., 2001)…………………… 12

3.1 Table showing the layer thicknesses for each group of layers……………... 40

3.2 Van Genuchten parameters for soils (Lin et al., 1997)……………………... 53

3.3 Values used in the computation of primary storage coefficient……………. 54

3.4 Soil Properties used in MODFLOW-SURFACT…………………………... 54

3.5 Input water properties used in GMS-FEMWATER………………………... 69

3.6 Input soil properties used in GMS-FEMWATER………………………….. 69

4.1 Comparison of calculated and model output values of total recharge for SL-A simulation…………………………………………………………….. 76

4.2 Comparison of calculated and model output values of total negative recharge for SL-A simulation………………………………………………. 76

4.3 Comparison of calculated and model output values of total recharge for SL-B simulation…………………………………………………………….. 77

4.4 Comparison of calculated and model output values of total negative recharge for SL-B simulation………………………………………………. 77

4.5 Designation of weather conditions to specific months in the SL-A simulation………………………………………………………………… 83

4.6 Designation of weather conditions to specific months in the SL-B simulation……………………………………………………………….... 84

A.1 Top elevation of layers in the model in feet……………………………... 127

A.2 Bottom elevations of layers in the model in feet…………………………… 129

B.1 Daily values of loading rate, Wastewater ET rate, and Rainfall Rate in ft/day from Phase 1 study…………………………………………………... 148

LIST OF FIGURES

2.1	USDA Soil Textural Classification with TCEQ Soil Classes (TCEQ, 2001)	7
2.2	Simplified Process Flow Diagram (Rainwater et al., 2001)………………..	10
2.3	Field Site Layout (not to scale) (Rainwater et al., 2001)……………………	10
2.4	Cross-Sections for (a) Combined ETA, (b) AB Only, and (c) ET only (Rainwater et al., 2001) ………………………………………………………..	13
3.1	Direction of effluent application and the process of ET and rain in cross-sectional view of the conceptual model……………………………………..	36
3.2	Cross-sectional View of the Conceptual Model……………………………	37
3.3	Plan View of the Conceptual Model………………………………………..	38
3.4	Cross-sectional View of the Modeled ETA Trench…………………………	39
3.5	Cross-sectional view of model showing variation of layer thicknesses…….	40
3.6	Daily ET Rate Recorded During 01/15/2000 to 12/31/2000………………..	42
3.7	Daily Precipitation Rate Recorded from 01/15/2000 to 12/31/2000………..	42
3.8	Daily Net Application Rate Data Over The Modeled ETA Drainfield……..	44
3.9	Plan View of ET Domain Type A of size 60 ft by 60 ft……………………	45
3.10	Plan View of the ET Domain Type B of Size 40 ft by 50 ft………………..	46
3.11	Plan View of Model Grid Showing Trench Application Area……………..	49
4.1	Soil characteristic curves showing relationship between pressure head and moisture content for sandy clay loam soil. …………………………………	79
4.2	Soil characteristic curves showing relationship between pressure head and hydraulic conductivity for sandy clay loam soil. …………………………..	79
4.3	Soil characteristic curves showing relationship between pressure head and moisture content for sandy loam soil. ………………………………………	80

4.4 Soil characteristic curves showing relationship between pressure head and hydraulic conductivity for sandy loam soil. ……………………………….. 80

4.5 Cumulative recharge and ET variation over the SL-A simulation run……... 85

4.6 Cumulative recharge and ET variation over the SL-B simulation run……... 85

4.7 Variation of water saturation contour dimensions over the SL-A simulation run……………………………………………………………………….. 88

4.8 Variation of saturation contour dimensions over the SL-B simulation run… 89

4.9 Variation of water saturation contour dimensions over the SCL-A simulation run…………………………………………………………. 90

4.10 Variation of water saturation contour dimensions over the SCL-B simulation run…………………………………………………………. 91

4.11 Comparison of variation of infiltration depth over the SL-A and SL-B simulation runs………………………………………………………… 93

4.12 Comparison of variation of north-south lateral extent of wetted area in SL-A and SL-B simulation runs……………………………………………... 93

4.13 Comparison of the infiltration depth in SL-B and SCL-B simulation runs… 95

4.14 Comparison of the variation in north-south lateral extent of wetted area over SL-B and SCL-B simulation runs……………………………………... 95

A.1 Groundwater Vistas start-up dialog. ……………………………………….. 105

A.2 GroundWater Vistas model grid initialization dialog. ……………………... 107

A.3 Plan view of the model in GroundWater Vistas. …………………………... 108

A.4 Dialog showing input path to model executable files. ……………………... 109

A.5 Dialog showing the MODFLOW modules selected in the model. ………… 111

A.6 Dialog showing the Basic Package input. ………………………………….. 112

A.7 Dialog showing input to the MODFLOW BCF Package…………………... 114

A.8 Dialog showing input to the Output Control Package. …………………….. 115

A.9 Dialog showing the input to the Recharge Package options. ………………. 116

A.10 Dialog showing the input of stress period data in MODFLOW. …………... 117

A.11 Dialog showing input of the initial pressure head input for the first simulation. ……………………………………………………………….. 118

A.12 Dialog showing input of pressure heads to maintain continuity between simulations. ……………………………………………………………… 120

A.13 Dialog showing the selected MODFLOW-SURFACT packages. …………. 121

A.14 Dialog showing input to the BCF4 package. ………………………………. 122

A.15 Dialog showing the selection of the stress period to edit in the ATO4 package in MODFLOW-SURFACT. ……………………………………… 123

A.16 Dialog showing the input of time stepping parameters in the ATO4 package. ……………………………………………………………………. 124

A.17 Dialog showing the input to the PCG4 package. …………………………... 126

A.18 Input dialog showing the input of the top elevation of layers in the model... 128

A.19 Input dialog showing the input of bottom layer elevation in the model……. 130

A.20 Dialog showing the selection of the color zone. …………………………… 131

A.21 Input dialog showing the input of hydraulic conductivity for material zones in the model. ……………………………………………………………….. 132

A.22 Dialog showing the input of coordinates for the selection of zone area in the model.……………………………………………………………………… 133

A.23 Dialog showing the selection of zone numbers for the zone area selected in the model. ……………………………………………………………….. 133

A.24 Input dialog showing input of soil properties for respective zones in the model. ……………………………………………………………………..... 135

A.25 Dialog showing the input of coordinates for the selection of zone areas in the model. ……………………………………………………………………... 136

A.26 Input dialog showing the input of Van Genuchten parameters and residual saturation in the model for respective zones. ………………………………. 137

A.27 Dialog showing the input of coordinates for the selection of zone area in the model. ………………………………………………………………... 138

A.28 Dialog showing the input of positive and negative recharge values for respective zones in the model. ……………………………………………... 140

A.29 Dialog showing the input of coordinates for the selection of zone area in the model. ………………………………………………………………... 141

A.30 Dialog showing the input of coordinates for the selection of zone area in the model. ………………………………………………………………... 142

A.31 Dialog showing the input of the drain boundary condition in the model…... 143

A.32 Dialog to choose the display of the error/warning file on creation of data files in MODFLOW-SURFACT. …………………………………………….. 144

A.33 Dialog showing the completion of model simulation and prompt for the user to select display of result………………………………………………. 145

A.34 Dialog showing the selected options for processing of simulated results….. 146

D.1 Water saturation contours in plan view for SLA1………………………….. 163

D.2 Water saturation contours in plan view for SLA2………………………….. 164

D.3 Water saturation contours in plan view for SLA3………………………….. 165

D.4 Water saturation contours in plan view for SLA4………………………….. 166

D.5 Water saturation contours in plan view for SLA5………………………….. 167

D.6 Water saturation contours in plan view for SLA6………………………….. 168

D.7 Water saturation contours in plan view for SLA7………………………….. 169

D.8 Water saturation contours in plan view for SLA8………………………….. 170

D.9 Water saturation contours in plan view for SLA9………………………….. 171

D.10 Water saturation contours in plan view for SLA10………………………… 172

D.11 Water saturation contours in plan view for SLA11………………………… 173

D.12 Water saturation contours in plan view for SLA12………………………… 174

D.13 Water saturation contours in cross-section for SLA1………………………. 175

D.14 Water saturation contours in cross-section for SLA2………………………. 176

D.15 Water saturation contours in cross-section for SLA3………………………. 177

D.16 Water saturation contours in cross-section for SLA4………………………. 178

D.17 Water saturation contours in cross-section for SLA5………………………. 179

D.18 Water saturation contours in cross-section for SLA6………………………. 180

D.19 Water saturation contours in cross-section for SLA7………………………. 181

D.20 Water saturation contours in cross-section for SLA8………………………. 182

D.21 Water saturation contours in cross-section for SLA9………………………. 183

D.22 Water saturation contours in cross-section for SLA10……………………... 184

D.23 Water saturation contours in cross-section for SLA11……………………... 185

D.24 Water saturation contours in cross-section for SLA12……………………... 186

D.25 Moisture movement vectors in plan view for SLA1……………………....... 187

D.26 Moisture movement vectors in plan view for SLA4……………………....... 188

D.27 Moisture movement vectors in plan view for SLA8……………………....... 189

D.28 Moisture movement vectors in plan view for SLA12…………………….... 190

D.29 Moisture movement vectors along C-30 for SLA1……………………........ 191

D.30 Moisture movement vectors along C-30 for SLA4……………………........ 192

D.31 Moisture movement vectors along C-30 for SLA8……………………........ 193

D.32 Moisture movement vectors along C-30 for SLA12…………………….…... 194

D.33 Moisture movement vectors along R-30 for SLA1……………………........ 195

D.34 Moisture movement vectors along R-30 for SLA4……………………........ 196

D.35 Moisture movement vectors along R-30 for SLA8……………………........ 197

D.36 Moisture movement vectors along R-30 for SLA12……………………....... 198
D.37 Water saturation contours in plan view for SLB1………………….......... 199
D.38 Water saturation contours in plan view for SLB2………………….......... 200
D.39 Water saturation contours in plan view for SLB3………………….......... 201
D.40 Water saturation contours in plan view for SLB4………………….......... 202
D.41 Water saturation contours in plan view for SLB5………………….......... 203
D.42 Water saturation contours in plan view for SLB6………………….......... 204
D.43 Water saturation contours in plan view for SLB7………………….......... 205
D.44 Water saturation contours in plan view for SLB8………………….......... 206
D.45 Water saturation contours in plan view for SLB9………………….......... 207
D.46 Water saturation contours in plan view for SLB10………………........... 208
D.47 Water saturation contours in plan view for SLB11………………........... 209
D.48 Water saturation contours in plan view for SLB12...……………........... 210
D.49 Water saturation contours in cross-section for SLB1……………….….... 211
D.50 Water saturation contours in cross-section for SLB2……………….….... 212
D.51 Water saturation contours in cross-section for SLB3...…………….….... 213
D.52 Water saturation contours in cross-section for SLB4……………….….... 214
D.53 Water saturation contours in cross-section for SLB5……………….….... 215
D.54 Water saturation contours in cross-section for SLB6……………….….... 216
D.55 Water saturation contours in cross-section for SLB7……………….….... 217
D.56 Water saturation contours in cross-section for SLB8……………….….... 218
D.57 Water saturation contours in cross-section for SLB9……………….….... 219
D.58 Water saturation contours in cross-section for SLB10…………………... 220

D.59 Water saturation contours in cross-section for SLB11……………………... 221

D.60 Water saturation contours in cross-section for SLB12……………………... 222

D.61 Moisture movement vectors in plan view for SLB1……………………...... 223

D.62 Moisture movement vectors in plan view for SLB4……………………...... 224

D.63 Moisture movement vectors in plan view for SLB8……………………...... 225

D.64 Moisture movement vectors in plan view for SLB12…………………….... 226

D.65 Moisture movement vectors along C-30 for SLB1…………………….......... 227

D.66 Moisture movement vectors along C-30 for SLB2…………………….......... 228

D.67 Moisture movement vectors along C-30 for SLB8…………………….......... 229

D.68 Moisture movement vectors along C-30 for SLB12……………………....... 230

D.69 Moisture movement vectors along R-30 for SLB1…………………….......... 231

D.70 Moisture movement vectors along R-30 for SLB4…………………….......... 232

D.71 Moisture movement vectors along R-30 for SLB8…………………….......... 233

D.72 Moisture movement vectors along R-30 for SLB12……………………....... 234

D.73 Water saturation contours in plan view for SCLA1……………………....... 235

D.74 Water saturation contours in plan view for SCLA2……………………....... 236

D.75 Water saturation contours in plan view for SCLA3……………………....... 237

D.76 Water saturation contours in plan view for SCLA4……………………....... 238

D.77 Water saturation contours in plan view for SCLA5……………………....... 239

D.78 Water saturation contours in plan view for SCLA6……………………....... 240

D.79 Water saturation contours in plan view for SCLA7……………………....... 241

D.80 Water saturation contours in plan view for SCLA8……………………....... 242

D.89 Water saturation contours in plan view for SCLA9……………………....... 243

D.81 Water saturation contours in plan view for SCLA10……………………..... 244

D.82 Water saturation contours in plan view for SCLA11……………………..... 245

D.83 Water saturation contours in plan view for SCLA12……………………..... 246

D.84 Water saturation contours in cross-section for SCLA1…………………….. 247

D.85 Water saturation contours in cross-section for SCLA2…………………….. 248

D.86 Water saturation contours in cross-section for SCLA3…………………….. 249

D.87 Water saturation contours in cross-section for SCLA4…………………….. 250

D.88 Water saturation contours in cross-section for SCLA5…………………….. 251

D.89 Water saturation contours in cross-section for SCLA6…………………….. 252

D.91 Water saturation contours in cross-section for SCLA7…………………….. 253

D.92 Water saturation contours in cross-section for SCLA8…………………….. 254

D.93 Water saturation contours in cross-section for SCLA9…………………….. 255

D.94 Water saturation contours in cross-section for SCLA10…………………… 256

D.95 Water saturation contours in cross-section for SCLA11…………………… 257

D.96 Water saturation contours in cross-section for SCLA12…………………… 258

D.97 Moisture movement vectors in plan view for SCLA1……………………..... 259

D.98 Moisture movement vectors in plan view for SCLA4……………………..... 260

D.99 Moisture movement vectors in plan view for SCLA8……………………..... 261

D.100 Moisture movement vectors in plan view for SCLA12…………………….. 262

D.101 Moisture movement vectors along C-30 for SCLA1……………………...... 263

D.102 Moisture movement vectors along C-30 for SCLA4……………………...... 264

D.103 Moisture movement vectors along C-30 for SCLA8……………………...... 265

D.104 Moisture movement vectors along C-30 for SCLA12……………………..... 266

D.105 Moisture movement vectors along R-30 for SCLA1……………………...... 267

D.106 Moisture movement vectors along R-30 for SCLA4……………………...... 268

D.107 Moisture movement vectors along R-30 for SCLA8……………………...... 269

D.108 Moisture movement vectors along R-30 for SCLA12…………………….... 270

D.109 Water saturation contours in plan view for SCLB1……………………....... 271

D.110 Water saturation contours in plan view for SCLB2……………………....... 272

D.111 Water saturation contours in plan view for SCLB3……………………....... 273

D.112 Water saturation contours in plan view for SCLB4……………………....... 274

D.113 Water saturation contours in plan view for SCLB5……………………....... 275

D.114 Water saturation contours in plan view for SCLB6……………………....... 276

D.115 Water saturation contours in plan view for SCLB7……………………....... 277

D.116 Water saturation contours in plan view for SCLB8……………………....... 278

D.117 Water saturation contours in plan view for SCLB9……………………....... 279

D.118 Water saturation contours in plan view for SCLB10……………………...... 280

D.119 Water saturation contours in plan view for SCLB11……………………...... 281

D.120 Water saturation contours in plan view for SCLB12………………….......... 282

D.121 Water saturation contours in cross-section for SCLB1…………………….. 283

D.122 Water saturation contours in cross-section for SCLB2…………………….. 284

D.123 Water saturation contours in cross-section for SCLB3…………………..... 285

D.124 Water saturation contours in cross-section for SCLB4…………………….. 286

D.125 Water saturation contours in cross-section for SCLB5…………………….. 287

D.126 Water saturation contours in cross-section for SCLB6………………….... 288

D.127 Water saturation contours in cross-section for SCLB7…………………….. 289

D.128 Water saturation contours in cross-section for SCLB8…………………….. 290

D.129 Water saturation contours in cross-section for SCLB9…………………….. 291

D.130 Water saturation contours in cross-section for SCLB10…………………… 292

D.131 Water saturation contours in cross-section for SCLB11…………………… 293

D.132 Water saturation contours in cross-section for SCLB12…………………… 294

D.133 Moisture movement vectors in plan view for SCLB1……………………..... 295

D.134 Moisture movement vectors in plan view for SCLB4……………………..... 296

D.135 Moisture movement vectors in plan view for SCLB8……………………..... 297

D.136 Moisture movement vectors in plan view for SCLB12…………………….. 298

D.137 Moisture movement vectors along C-30 for SCLB1…………………….... 299

D.138 Moisture movement vectors along C-30 for SCLB4…………………….... 300

D.139 Moisture movement vectors along C-30 for SCLB8…………………….... 301

D.140 Moisture movement vectors along C-30 for SCLB12…………………….... 302

D.141 Moisture movement vectors along R-30 for SCLB1…………………….... 303

D.142 Moisture movement vectors along R-30 for SCLB4…………………….... 304

D.143 Moisture movement vectors along R-30 for SCLB8…………………….... 305

D.144 Moisture movement vectors along R-30 for SCLB12…………………….... 306

CHAPTER 1

INTRODUCTION

1.1 Problem Statement

Septic tanks and associated drainfields are used throughout the United States as on-site wastewater treatment and disposal systems for individual residences or small communities. The need for on-site wastewater treatment and disposal systems is growing and expected to increase even more rapidly in the future. The decline of federal and state construction grants for public wastewater collection and treatment facilities and the increasing demand for affordable housing in rural as well as suburban areas requires that effective, affordable alternatives be provided (Otis, 1991). The septic tank is used to receive and hold fresh sewage. During the detention period, the sediments in the sewage are allowed to settle to the bottom of the tank where they undergo microbial degradation and form sludge, while the floatable matter, like oils and greases, forms a scum layer on the water surface. The somewhat clarified effluent then flows to the drainfield, where the processes of soil absorption by capillary action, evapotranspiration (ET), and gravity flow allow its disposal. The primary function of the drainfield trenches is to receive the effluent water and discharge it underground or to the atmosphere.

Drainfields are classified based on their method of disposal into three main categories: (1) absorption only (AB-only), (2) evapotranspiration only (ET-only), and (3) evapotranspiration-absorption (ETA). AB-only drainfields depend on percolation and capillary forces for movement of water and are usually applied in areas with permeable soils and relatively deep water tables. ET-only drainfields are lined at the bottoms and sides to prevent soil absorption, thus they depend only on evaporation and plant transpiration for water removal. ET-only drainfields are applied in areas with impermeable soils, like clay with relatively shallow water tables. ETA drainfields consider both absorption as well as ET for water removal. In actuality, when AB-only drainfields are applied in arid regions with high evaporation rates, they lose significant amounts of water to ET and absorption, thus effectively acting as ETA drainfields. The ETA drainfields, unlike the ET-only drainfields, are not restricted with liners on the sides and bottom, and hence have larger effective surface areas for water loss due to ET.

In Texas, under the current Texas Natural Resources Conservation Commission (TNRCC), now known as the Texas Commission on Environmental Quality (TCEQ), guidance, drainfield size is based on either AB-only or ET-only (TCEQ, 2001). In more arid western parts of Texas, where AB-only drainfields are built on permeable soils, it was observed by regulators and installers that drainfields were significantly over-designed as a result of neglecting ET that occurs from the drainfields. Septic tank regulators and installers from the western half of Texas have suggested revision of the current TCEQ (2001) design standards to allow for ETA systems that result in smaller, less costly designs. In an effort to address these concerns, research sponsored by the Texas On-site Wastewater Treatment Research Council (TOWTRC) was performed by the Texas Tech University Water Resources Center (TTUWRC) to demonstrate the combined contributions of ET and absorption in septic tank drainfields (Rainwater et al., 2001). Phase 1 of this project, started in 1999, was a 2-yr study involving construction and operation of the three different types of drainfields to observe and compare loading rates and water quality associated with each drainfield type. Phase 1 also considered weather effects on ET-only and ETA trench loading rates, which resulted in recommendations for a new local loading rate for combined ETA systems.

Based on the relatively short duration of the Phase 1 study, there was a concern that the findings of the study were inadequate to accurately represent the typical 10-yr or longer life of a septic system drainfield. In order to overcome this limitation Phase 2 of the study was initiated to observe ETA trench systems for an additional test period. As part of Phase 2, a three-dimensional groundwater flow model of an ETA drainfield system was developed and a transient simulation was performed using loading rate and weather data from Phase 1 for ETA trenches operated at the experimental station. The groundwater flow model was used to simulate the flow pattern and effective ET area around the drainfield with respect to different soil types found in the West Texas region of the United States. Phase 2 also considered extrapolation of results to other regions in Texas with respect to varying climatic conditions and soil types.

1.2 Specific Objectives

The specific objectives of this study were to (1) select a suitable three-dimensional groundwater flow model capable of performing groundwater flow simulations in the unsaturated media, (2) develop a conceptual groundwater flow model to simulate the conditions pertaining to an ETA drainfield, and (3) apply the numerical groundwater flow model to observed field conditions for the Phase I ETA trenches in order to simulate the effects of seasonal variations on the infiltration and ET patterns around the drainfield.

CHAPTER 2

LITERATURE REVIEW

2.1 Introduction

The literature review for the simulation of ETA drainfields involved a survey of the current TCEQ drainfield requirements, which currently regulate AB-only and ET-only type drainfields. The Phase 1 study carried out by the TTUWRC was also reviewed to select the ETA drainfield from Phase 1 to be modeled in this study. The development and formulation of the two unsaturated flow numerical codes used in this study, MODFLOW-SURFACT, and FEMWATER, were also evaluated. Various applications of the simulation codes for both flow and transport modeling were reviewed in order to learn from the conceptual models developed by other users and to make sure that a similar study was not performed in the past.

2.2 Current TCEQ Drainfield Requirements

Effluent disposal systems in Texas must be installed in accordance with the criteria specified by the TCEQ. The current criteria for acceptable standard disposal methods consider drainfields that disperse the effluent either into adjacent soil (AB-only field) or into the surrounding air through ET (ET-only field). In order to install AB-only fields, all the soil and site criteria should be determined as suitable under the current standards. The subsurface soil texture under the current standards is required to be either TCEQ class Ib, II or III along the sidewall and 2 ft below the bottom of the excavation. In case of class II and III soils, the gravel portion must be less than 30 percent. The TCEQ soil class Ib and II include soil types of sand and sandy loam, respectively, while TCEQ soil class III includes soils of varying percentages of clay and silt, as can be seen from Figure 2.1. Finally, a suitable soil layer of at least 2 ft should be present between the bottom of the excavation and a restrictive horizon or groundwater. The absorptive area calculated by including both the bottom area and the lower 1 ft along the walls of the excavated trench (H), is as shown in Equation 2.1 (TCEQ 2001):

$$A_{AB} = LW + 2(L + W)\, H \tag{2.1}$$

where A_{AB} = absorptive area (ft^2), L = excavation length (ft), and W = excavation width (ft). The last term in Equation 2.1 conservatively accounts for water that leaves through the sides of the trench and then moves downward. The TCEQ design procedure allows for flexibility in the number and dimensions of trenches, type of fluid distribution system, and porous media used in the trench, as long as the absorptive area and the long-term acceptance rate (LTAR) values specified are met. Further design details are provided in the standards (TCEQ 2001).

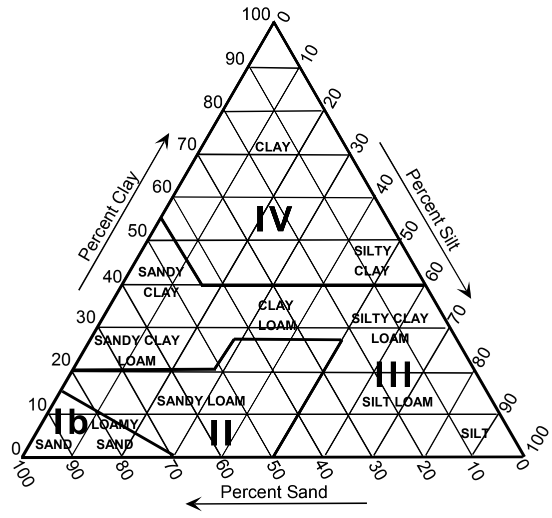

Note: Class **Ia** soils contain >30% gravel, and are not shown here.

Figure 2.1 USDA Soil Textural Classification with TCEQ Soil Classes (TCEQ, 2001)

An ET-only drainfield system may be used when the soil at the site is unsuitable for standard AB-only system with respect to soil texture, restrictive horizons or groundwater (TCEQ, 2001). An ET-only system may also be used in soils of TCEQ soil classes Ia and IV (see Figure 2.1 for details). The ET-only system shall only be used in areas, where the annual average evaporation rate is more than the annual rainfall (TCEQ 2001). An impervious liner must be placed in all TCEQ Class Ia soils, where groundwater tables penetrate the excavation due to seasonal variations, or where a minimum of 2 ft of suitable soil does not exist between the bottom of the excavation and either a restrictive horizon or groundwater. The ET-only trench sizing is critical as undersized beds may pose a health hazard or could restrict the homeowner's water usage if wastewater ponds on the surface of the drainfield. The top surface area in an ET-only system is calculated using Equation 2.2:

$$A_{ET} = \frac{0.067Q}{R_{et}} \qquad (2.2)$$

where A_{ET} = total top surface area of the excavation (ft^2), Q = estimated daily water usage (gpd), R_{et} = net local evaporation rate (in/d). This equation only considers vertical ET loss through the top of the trench.

ET-only systems should be backfilled with TCEQ Class II soil and the final grade of the trench should be revegetated to take maximum advantage of transpiration (TCEQ 2001). Furthermore, ET-only systems should be divided into two or more equal excavations connected by flow control valves, with minimum spacing between trenches of 3 ft. In order to allow for the ET-only system to dry out and decompose biological material that might plug the excavation, one excavation should be removed from service for an extended period of time. During the time when one of the excavations is removed from service, the daily usage rate should be reduced to prevent overloading the existing excavation still in operation. Normally it takes two to three months for biological breakdown to occur; hence an excavation should be taken off-line for two to three months each time.

2.3 Phase 1 Study

The Phase 1 study conducted by TTUWRC during Fall 1999-Spring 2001 was a field experiment that investigated ETA trenches in comparison to ET-only and AB-only trenches. The Phase 1 study was based on the working hypothesis that a combined ETA system provided greater capacity for wastewater disposal than ET-only or AB-only systems. The Phase 1 study was designed to collect field data for each type of drainfield with respect to conditions existing in the Southern High Plains of Texas. The drainfield trenches were laid on TCEQ class II-III soils, which were typical soils found in the Southern High Plains of Texas.

2.3.1 Test Site Setup

The test site was located at Reese Center, approximately 11.2 miles west of Texas Tech University, Lubbock, Texas on a 2 acre plot. The setup involved septic tanks, and eighteen drainfield trenches, installed according to the TCEQ drainfield requirements, and a control building that was used to prepare and distribute artificial wastewater. A weather station kept daily records of wind speed, solar radiation, air temperature, humidity, dew point, barometric pressure, precipitation, and wind direction. The main purpose of the weather station was to collect daily data for the calculation of ET and precipitation rates, which were used for evaluation of drainfield units.

Three replicates of each drainfield type were applied with consistent supply of artificial wastewater (Rainwater et al., 2001), and were referred to as ABW (Absorption only with wastewater), ETW (Evapotranspiration only with wastewater) and ETAW (Evapotranspiration-Absorption with wastewater). A second set of three replicates of the three drainfield types, representing hydraulic experimental controls, were applied with a consistent supply of clean groundwater and were referred to as AB, ET and ETA units. The clean water units were installed and operated to allow quantification of the impact of microbial growth on water movement within the trenches and surrounding soil. Artificial wastewater mixing tanks, septic tanks, header tanks, and clean water tank as shown in the simplified process flow diagram in Figure 2.2 were installed in and around the control building. The location of each type of drainfield was randomly configured as shown in Figure 2.3, so that any bias due to soil heterogeneities would be avoided.

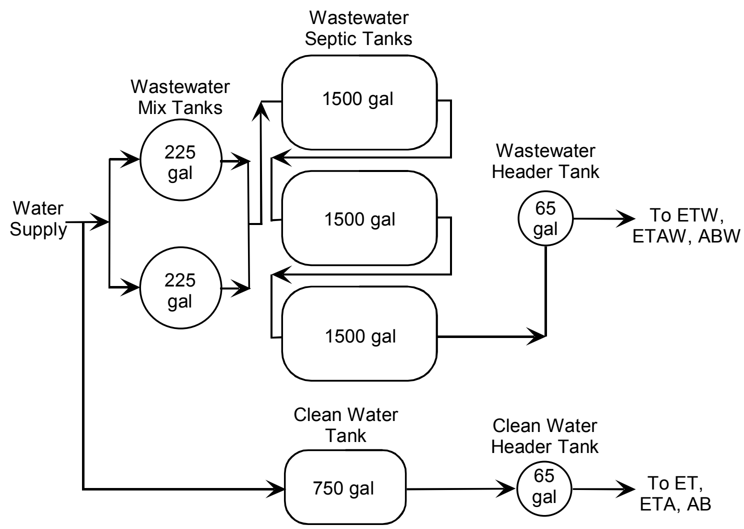

Figure 2.2 Simplified process flow diagram (Rainwater et al., 2001)

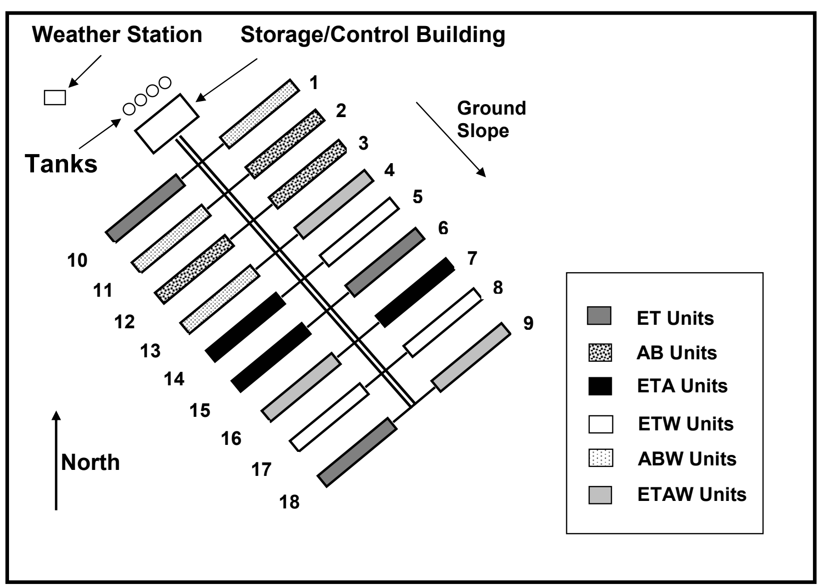

Figure 2.3 Field site layout (not to scale) (Rainwater et al., 2001)

The soil types found at the site were analyzed for percentage of silt, sand, and clay. Based on the percentages of silt, sand, and clay, the soils were classified as either TCEQ soil type III or II. The initial gravimetric moisture content within soil samples ranged from 3.0 to 13 percent, with average and 95 percent confidence interval of 8.8 $\pm$ 0.9 percent. A two-day, double-ring infiltrometer test was carried out to determine the saturated hydraulic conductivity within each non-ET-only trench.

The cross-sectional views of each trench type are shown in Figure 2.4. Typical trenches had a width of 36 in, a depth of 24 in, and a length of 20 ft. All trenches were spaced apart from each other by a distance of 26 ft from centerline to centerline. The field piping allowed for transport of water and wastewater from the septic tanks to the drainfields. Field piping also allowed visual monitoring of fluid level, sample collection, and installation of a level sensing system to monitor water level in each trench throughout the study period. Each trench was carefully filled with gravel using a semi-cylindrical guide form. After the distribution pipe was placed and geofabric was laid over the gravel, the trenches were backfilled with the local soil from the excavation. All disturbed soils were revegetated by reseeding with commonly used turfgrass.

2.3.2 Operation

The operation of the drainfield trench units began in September 1999 and continued till May 2001. All units were not brought on-line at the same time, but in a staggered fashion from late September 1999 to November 1999. The staggered fashion approach was adopted because it was anticipated that initially high hydraulic loading rates might challenge the capacity of the water well supplying the site. Daily flow to each trench was recorded with the help of flow totalizer readings and wastewater septic tank outlet. All readings were recorded at the same time each day to provide consistent data. Artificial wastewater was mixed once to twice daily to meet the loading demand by the wastewater units.

Table 2.1 shows a summary of the field performance of the different types of drainfield at the test site in the Phase 1 study. These results clearly indicate that the combined wastewater ETA drainfields have significantly higher loading capacities as compared to the AB-only and ET-only type drainfields. Complete results were reported by Rainwater et al. (2001).

Table 2.1 Summary of field performance (Rainwater et al., 2001)

Drainfield Type	Average Flow (gpd)	95% Confidence Interval	Average Load (gpd/ft^2)	95% Confidence Interval
ET*	5.9	0.63	0.10	0.01
ETW	6.5	0.40	0.11	0.01
ABW	68.3	25.8	0.64	0.24
ETAW	113.2	18.5	1.07	0.17

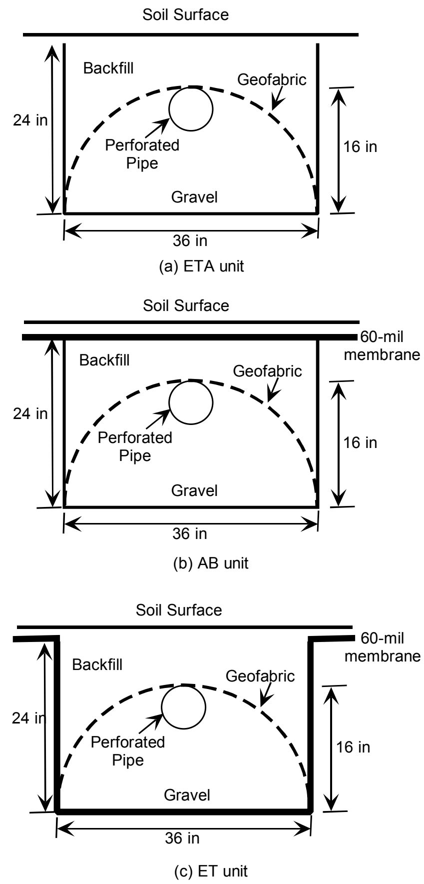

Figure 2.4 Cross-Sections for (a) Combined ETA, (b) AB Only, and (c) ET only (Rainwater et al., 2001)

2.4 Numerical Modeling

The simulation codes MODFLOW-SURFACT and FEMWATER were used for simulating the ETA drainfield in this study. A review of the history, formulation, and applications of each simulation code follows.

2.4.1 MODFLOW-SURFACT

2.4.1.1 MODFLOW-SURFACT: Introduction and history

MODFLOW-SURFACT (Hydrogeologic, Inc., 1996) is a fully integrated flow and transport code, based on the U.S. Geological Survey (USGS) groundwater modeling software, MODFLOW (McDonald and Harbaugh, 1988). MODFLOW-SURFACT provides additional modules to the original MODFLOW code that enhance the physical simulation capabilities of MODFLOW to perform complex, saturated-unsaturated, subsurface flow analysis and contaminant fate transport calculations. MODFLOW-SURFACT version 1.2 was first publicly released in 1996. Version 1.2 incorporated flow packages that enhanced the capability of the original MODFLOW code to handle complex field problems. The additional packages in version 1.2 provided the ability for MODFLOW to do the following tasks.

- Readily accommodate conditions of desaturation/resaturation of aquifer systems.
- Perform axi-symmetric analysis.
- Improve the simulation of multi-layer wells.
- Use additional robust numerical and matrix solution techniques for complex problems.
- Simulate prescribed ponding-recharge and seepage-face boundary conditions.

- Perform transient simulations efficiently using an adaptive time-stepping scheme.

In 1998, Version 2.1 was publicly released. Version 2.1 came with robust numerical schemes and additional physical flow modeling capabilities that are briefly summarized below.

- Rigorous saturated/unsaturated modeling of water flow.
- Rigorous saturated/unsaturated modeling of airflow.
- Newton-Raphson linearization for robustness.

The latest version, MODFLOW-SURFACT version 2.2, provided the following flow modeling enhancements to the previous versions.

- Variable horizontal anisotropy within each model layer.
- Internal computation of saturated leakance between layers when the vertical conductivity of grid blocks is input, thus saving time in the calculation and manual input of the leakance values.
- Generation of non-rectangular grids in the areal plane.
- Plotting breakthrough curves of head or contaminant concentrations at pre-selected nodes in the model domain.
- Mass balance printout to be performed at user-defined intervals, irrespective of the time-step size or the number of time-steps involved in a transient simulation.

All previous versions of MODFLOW-SURFACT, including version 2.2, allow a mix and match of modules between original MODFLOW and MODFLOW-SURFACT.

MODFLOW-SURFACT modules are fully compatible with the modules in original MODFLOW. The modular structure of original MODFLOW is maintained and modules for the enhanced features are still called from the main program. Implementation of new formulations and computational schemes in the additional packages was done on verification using analytical solutions and other numerical models. The input format structure of MODFLOW-SURFACT is straightforward and similar to the format structure for original MODFLOW (Hydrogeologic, Inc., 1996).

2.4.1.2 MODFLOW-SURFACT Version 2.2

Version 2.2 includes several new flow packages that complement or supplement the original MODFLOW version. These packages are referred to as the SURF packages. A brief description of the capabilities of the SURF packages follows.

The BCF4 Package is an alternative to the block-centered flow package in the original MODFLOW version. The BCF4 package allows the simulation of variably saturated flow and axi-symmetric simulation in MODFLOW. Enhancements such as simulation of unsaturated zone moisture movement for air and water using the Richards equation are included in the BCF4 package of version 2.2.

The FWL4 Package enhances the original MODFLOW's capability to model fracture wells as well as extraction/pumping wells. The FWL4 Package simulates a well bore as a high conductivity fracture tube. The high conductivity fracture tube representation connects aquifer cells associated with the well with the 1-D finite diameter cylindrical well-cells, thus overcoming several problems associated with the original well package and truly representing a multilayer well.

The RSF4 Package is a recharge-seepage face boundary condition package that improves the simulation of seepage-face and recharge-ponding conditions. The ponding depth parameter included in this package automatically adjusts the proportion of surface runoff and recharge when the model domain is completely saturated.

The ATO4 Package is an adaptive time stepping package that allows the user to pre-select the times when the output results should be printed. The ATO4 package also allows for automatic adjustment of time-step size corresponding to the complexity of the algebraic equations, solved for convergent solutions.

The PCG4 (Poly Conjugate Gradient Scheme) package is based on partial LU decomposition as a preconditioner. LU decomposition is a standard way of solving the simultaneous matrix equation of the form

$$Ax = b \tag{2.3}$$

where x is a variable matrix and b is the constant matrix. Every square matrix can be expressed as

$$A = PLU \tag{2.4}$$

where P is a permutation matrix, L is a unit lower triangular matrix and U is upper triangular matrix. The LU decomposition method decomposes a matrix A into an upper and lower triangular matrix. The triangular matrices are further solved by successive substitution into corresponding linear equations. This method of decomposition is a modified form of the Gaussian Elimination method (Computational Science Education

Project, 1996). The PCG4 package thus provides a more robust and efficient solver to the slice-successive overrelaxation (SSOR) or the strongly implicit procedure (SIP) solvers of the original MODFLOW version and enhances the capabilities of MODFLOW to handle complex unsaturated zone modeling simulations.

Non-linear algebraic equations are needed to solve the Richards equation for unsaturated flow. Several types of linearization and/or iterative methods are used to solve the non-linear algebraic equations. The Picard and the Newton schemes are standard iterative procedures that are used for solving discrete equations. The modified Picard scheme proposed by Celia et al. (1990) alleviates the mass balance problems associated with unsaturated flow computations. The modified Picard scheme applies a fully implicit time approximation to a mixed form of the unsaturated flow equation, producing a simple computational algorithm by proper expansion of the time derivative, which can be solved easily to arrive at a numerical solution (Williams et al., 1996). The NRB1 (Newton-Raphson Backtracking) Package in MODFLOW-SURFACT includes Newton-Raphson linearization and a backtracking scheme to stabilize the Newton iterations. This scheme is helpful in alleviating convergence difficulties in unsaturated zone flow simulations that cannot be handled efficiently with the Picard or modified Picard iteration schemes used in the earlier versions of MODFLOW or MODFLOW-SURFACT.

The OBS1 (observation node) package is included to assist in post-processing at user-selected nodes for transient simulations. The pressure-time relationship and the concentration-time relationship can be plotted for flow and contaminant transport simulations, respectively, using the OBS1 package.

MODFLOW-SURFACT version 2.2 is capable of performing rigorous modeling of saturated-unsaturated water flow as well as air flow. In the present study, it was used to model an unsaturated water flow simulation and hence more information specific to the formulation of unsaturated water flow is provided in the following section.

2.4.1.3 Formulation of the variably saturated water flow equation

MODFLOW-SURFACT uses the Richards equation to solve the variably saturated flow problem. The three-dimensional movement of water in a variably saturated media can be represented by the following modified form of the Richards Equation (Huyakorn et al,. 1986):

$$\frac{\partial}{\partial x}\left(K_{xx}k_{rw}\frac{\partial h}{\partial x}\right)+\frac{\partial}{\partial y}\left(K_{yy}k_{rw}\frac{\partial h}{\partial y}\right)+\frac{\partial}{\partial z}\left(K_{zz}k_{rw}\frac{\partial h}{\partial z}\right)-W=\phi\frac{\partial S_w}{\partial t}+S_wS_s\frac{\partial h}{\partial t} \tag{2.5}$$

where x, y, and z are Cartesian coordinates [L], K_{xx}, K_{yy} and K_{zz} are the principal components of hydraulic conductivity along the x, y, and z axes, respectively [LT^{-1}], k_{rw} is the relative permeability, which is a function of water saturation, h is the hydraulic head [L], W is a volumetric flux per unit volume and represents sources and/or sinks of water [T^{-1}], ϕ is the drainable porosity taken to be equal to the specific yield S_y, S_w is the degree of saturation of water, which is a function of the pressure head, S_s is the specific storage of the porous material [L^{-1}], and t is time [T].

To solve Equation 2.5, the relationships of relative permeability versus saturation and pressure head versus saturation are required as input. There are two alternatives to specifying the relationship of relative permeability versus saturation, the Brooks and

Corey (1966) equation and the Van Genuchten (1997) equation. The Brooks and Corey equation calculates the relative hydraulic conductivity given the effective saturation in the soil as follows:

$$k_{rw} = S_e^n \tag{2.6}$$

where n is an empirical parameter, and S_e is the effective saturation, defined as

$$S_e = \frac{(S_w - S_{wr})}{(1 - S_{wr})}, \tag{2.7}$$

and S_{wr} is the residual water saturation. The Van Genuchten equation calculates the relative hydraulic conductivity given the effective saturation and the empirical parameter γ for the soil.

$$k_{rw} = S_e^{1/2}[1-(1-S_e{}^{1/\gamma})^{\gamma}]^2, \tag{2.8}$$

where γ is an empirical parameter, where z = vertically upward coordinate [L].

The relationship of pressure head versus water saturation is described by the following function (Van Genuchten, 1977; Mualem, 1976).

$$S_e = \frac{S_w - S_{wr}}{1 - S_{wr}} = \left\{ \frac{1}{\left[1 + (\alpha h_c)^{\beta}\right]^{\gamma}} \right\} for\, \psi < 0 \tag{2.9}$$

$$S_e = 1\, for\, \psi \geq 0 \tag{2.10}$$

where α and β are empirical parameters, h_c is the capillary head defined as $(h_{ap} - \psi)$ [L], h_{ap} is the pressure in air taken as atmospheric (= 0), parameters β and γ are related by

$$\gamma = 1\text{-}1/\beta. \tag{2.11}$$

$$\psi = \text{Pressure head} = h - z \text{ [L]}, \tag{2.12}$$

The effective water saturation is equal to one for pressure head values greater than 1. The Brookes and Corey and Van Genuchten functions for the moisture retention and relative permeability characteristics can be measured in the laboratory for a given soil.

2.4.1.4 Applications of MODFLOW-SURFACT

MODFLOW-SURFACT has been used for the modeling of flow and transport in saturated and unsaturated media in several groundwater flow and transport studies. Doherty (2001) compared pressure head values calculated through the use of pseudo-soil functions by MODFLOW-SURFACT to verify a modified MODFLOW code. The MODFLOW code was modified by making adjustments to the MODFLOW Block-Centered-Flow package. The modifications allowed layers to transmit water with vastly reduced transmissivities, even when the cells in the layer were unsaturated. The reduced transmissivities allowed the desaturation and resaturation of cells with the vertical movement of the water table without making the unsaturated cells inactive in the simulation. It was observed that the pressure head values calculated by the modified MODFLOW code and MODFLOW-SURFACT for a simulation with same input data were nearly identical.

Ronayne et al. (1999) used MODFLOW-SURFACT to perform predictive modeling of mine pit lake recovery and evaluate long-term hydrologic impacts of pit lakes on surrounding groundwater systems. An open-pit porphyry mine located in the southwestern U.S. was modeled for this study. The results of the simulation showed that the pit lakes would reach quasi-steady-state levels within 100 years after the dewatering activities were stopped. The results of the simulation were similar to the lake-stage recovery data collected at the site, which indicated that the variably saturated flow formulation provided accurate representation of lake-pit recovery.

Krambis (2002) investigated the stratigraphy and hydrogeology of the inner margin of the coastal plains of South Carolina using MODFLOW-SURFACT. The simulation was performed to determine the sources and sinks of the study aquifer and to assess the availability of groundwater for supply purposes. The findings of the study revealed that the Aiken County aquifer was isolated with respect to other sources of groundwater and was susceptible to droughts.

Hung (2002) evaluated the merits and potential errors expected as a result of the incorporation of Hung’s 1-D groundwater transport model into the PRESTO-EPA model. Comparison of typical releases calculated during simulations revealed that the errors in Hung’s 1-D model can be kept below 3 percent as compared to the calculated values from MODFLOW-SURFACT. Thus, it was concluded that Hung’s 1-D groundwater transport model was useful since the computation efficiency of the model outweighed the limited impact of its simplifying assumptions.

Peng et al. (2000) tested several MODFLOW-based models, including MODFLOW-SURFACT, MT3D, MODFLOWT, and MOC3D, for their predictive capacity as compared to a specialized contaminant transport model used in 1986. The specialized contaminant transport model used in 1986 had successfully predicted the solute breakthrough curve from a two-well tracer test. The test simulation involved injection of water spiked with bromide for three days; the outflow concentration was then monitored for a month. Results of the study revealed that all the models predicted breakthrough curves as accurately as the specialized contaminant transport code used in 1986; however, it was found that the predictive capacity of the MODFLOW-based models reduced as the number of layers and/or grid blocks was reduced.

2.4.2 GMS-FEMWATER

2.4.2.1 GMS-FEMWATER: Introduction and history

The Athens laboratory of the U.S. Environmental Protection Agency (AERL) and the U.S. Army Corps of Engineers (USACOE) Waterways Experiment Station (WES) were conducting independent evaluations of a wide variety of groundwater models for their in-house applications in the early 1990's. AERL was evaluating models that could be adapted to simulate three-dimensional variably saturated flow with capability to model irregular geometries. WES was also interested in the capability to model irregular geometries, but in addition to flow simulations, they were evaluating models to conduct groundwater remediation studies at contaminated Department of Defense (DoD) sites and for salinity intrusion application in the USACOE navigation projects. As a result of their evaluations, both agencies independently selected the 3DFEMWATER (Yeh 1987b) and 3DLEWASTE (Yeh 1990), respectively, for further development and implementation for their specific purposes. Once it was known that WES and AERL shared similar interests and research responsibilities as far as groundwater models were concerned, a cooperative research agreement was reached and the development of a single groundwater modeling system to support both agencies began. FEMWATER was a result of the cooperative research efforts of these two agencies.

FEMWATER was assembled by integrating the 3DFEMWATER (flow) and 3DLEWASTE (transport) models so that FEMWATER was capable of performing coupled flow and transport simulations. The original 3DFEMWATER and 3DLEWASTE was developed by Dr. G.T. Yeh at the Pennsylvania State University, while the new integrated FEMWATER was developed with the collaborative effort of Dr. Yeh and Dr. H.C. Lin at WES (Lin et al., 1997). FEMWATER included three major improvements, first, the code was integrated into DoD Groundwater Modeling System (GMS), a state-of-the-art graphical user environment that provided efficient pre-and post-processing tools for model setup and visualization. Second, the block-iterative solvers used in older models were replaced with a series of new solvers that allowed an arbitrary node numbering scheme, which enabled easier graphical user interface connections and improved computational efficiency. Third, the capability to perform density-driven transport simulations to conduct high salinity intrusion studies in coastal aquifers was added.

2.4.2.2 GMS-FEMWATER Version 3.1

The main source of information about GMS-FEMWATER version 3.1 was Lin et al. (1997) unless otherwise specified in this study. The input data sets created in GMS-FEMWATER are organized into a set of files. When FEMWATER is launched, the user is prompted for the name of the super file. A super file is a file that contains a list of all the appropriate input and output files required for a simulation, and it is the only file that the user is prompted for while performing a FEMWATER simulation. The super file eliminates the need to enter the name of each individual file separately every time a simulation is performed; also, accessing all the files through a single file simplifies file management. FEMWATER is made up of four basic files, namely the geometry, model, initial condition, and solution files. A brief description of the basic files follows.

2.4.2.2.1 Geometry file

The geometry file is made up of input data required to set up a three-dimensional finite element grid in FEMWATER. The model grid is made up of linear elements such as hexahedra, prisms, and/or tetrahedra. Each element in the three-dimensional grid is assigned a material identification (ID) and usually grouped into zones representing stratigraphic units. The geometry file includes data like the coordinates of the mesh nodes and the element topology.

2.4.2.2.2 Model File

The model file is one of the main files in FEMWATER. The model file contains data regarding the analysis options, material properties, and boundary conditions for a simulation. Each group will be individually described below.

The analysis option includes selection of a solver for computations in the simulation, relaxation parameters to aid convergence of simulation, sorption options, and the simulation type (steady-state or transient). FEMWATER is equipped with efficient and robust numerical solvers to handle rigorous unsaturated flow and transport simulations. The Pointwise iterative matrix solver is the most simple solver in FEMWATER and can employ the successive iteration, Gauss-Seidel, successive under-relaxation, or successive over-relaxation methods to solve the matrix equations. The Preconditioned Conjugate solver employs the conjugate gradient method to solve the matrix equations, and is theoretically faster to converge than the Pointwise iterative solver. The Preconditioned Conjugate Gradient method (incomplete Choleski) solver employs the incomplete Choleski decomposition as a preconditioner into the conjugate gradient method. This last solver is theoretically faster than the previous solvers and should be used if the convergence is either too slow or not achieved at all with the other two solvers. Other options that must be specified while selecting a solver are, the quadrature used for the numerical integration, weighting factor options, and relaxation parameters, which help to overcome convergence difficulties. Quadrature is the weighted sum of a function sampled at a set of points, which means that an integral is solved numerically using quadrature formulas or Gaussian quadrature (Wolfram Research). The weighting factor parameter determines the evaluation of the time derivative terms associated with the velocity in the flow equation. The relaxation parameters are used to estimate pressure head and concentration needed to compose the matrix equation in numerical analysis.

The material properties include the properties of different types of soils, and properties of fluids (water and/or contaminant) used in the model. A single set of fluid properties is specified for the entire model, and a separate set of soil properties have to be specified for each different material used in the model. The soil water retention curves are required to be computed for each type of soil

Specified head, specified flux, flux gradient, and rainfall/seepage boundary conditions are supported by FEMWATER. The boundary conditions assigned can be steady-state or transient. The default boundary conditions for a flow and transport simulation are the no-flux and no-diffusion boundary conditions, respectively.

2.4.2.2.3 Initial Condition File

All simulations require a set of initial conditions from which the simulation progresses. The initial condition file contains data related to the variation of pressure head and contaminant concentration across the model domain. FEMWATER allows for the specification of three types initial conditions, namely cold start, hot start and flow solutions. Cold starts are used while performing simulations with a set of initial values at the beginning of a steady-state or transient simulation. Hot starts use the end condition of a preceding simulation as initial condition for the next simulation to maintain continuity between the two simulations. Flow solutions are a type of initial condition used for transport-only simulations. A transport-only simulation needs a previously computed flow solution (steady-state or transient) to define a three-dimensional flow field so that the contaminant migration can be properly modeled. Flow solutions use either pressure head only, or pressure head and velocity data sets from previous simulations to define the initial moisture content, pressure head, and velocity distribution.

2.4.2.2.4 Solution File

The output generated by a FEMWATER simulation is made up of a diagnostic output file and a number of solution files. The diagnostic output file is a text file summarizing information about the input data, iterations, convergence data, and solution summaries for the simulation performed. The solution files are saved either in binary or ASCII format and contain pressure head, moisture content, velocity, and concentration results for each iteration of the simulation performed. The solution files can be used for post-processing or as initial conditions for subsequent simulations.

2.4.2.3 Formulation of FEMWATER

FEMWATER simulates the flow of water and transport of contaminants in the unsaturated media. The modified Richards equation, subject to initial and boundary condition equations, is the governing flow equation that describes flow through the saturated-unsaturated porous media in FEMWATER. The modified Richards equation is thus used for computations required in a flow only simulation in FEMWATER. The set of matrix equations generated in FEMWATER are solved using the Galerkin finite element method. The modified Richards equation for three-dimensional water movement in saturated-unsaturated media used in FEMWATER is as shown:

$$\frac{\rho}{\rho_o} F \frac{\partial h}{\partial t} = \nabla \left[k' \left(\nabla h + \frac{\rho}{\rho_o} \nabla z \right) \right] + \frac{\rho^*}{\rho_o} q \tag{2.13}$$

with F calculated by

$$F = \alpha' \frac{\theta}{n} + \beta' \theta + \eta \frac{dS}{dh} \tag{2.14}$$

where F = storage coefficient [L^{-1}], k' =hydraulic conductivity tensor [LT^{-1}], z = potential head [L], q = source and/or sink [L^2T^{-1}], ρ = water density at chemical concentration C [ML^{-3}], ρ_o = referenced water density at zero chemical concentration [ML^{-3}], ρ^* = density of either the injection fluid or the withdrawn water [ML^{-3}], θ = moisture content, α' = modified compressibility of the medium[LT^2M^{-1}], β' = modified compressibility of the water [LT^2M^{-1}], η = porosity of the medium, and S = saturation. The hydraulic conductivity K' for unsaturated media is given by

$$K' = \frac{\rho g}{\mu} k = \frac{(\rho/\rho_o)}{(\mu/\mu_o)} \frac{\rho_o g}{\mu_o} k_s k_r = \frac{\rho/\rho_o}{\mu/\mu_o} K_{so} k_r \tag{2.15}$$

where μ = dynamic viscosity of water at chemical concentration C [$ML^{-1}T^{-1}$], μ_o = referenced dynamic viscosity at zero chemical concentration [$ML^{-1}T^{-1}$], k = permeability tensor [L^2], k_s = saturated permeability tensor [L^2], k_r = relative permeability or relative hydraulic conductivity, K_{so} = referenced saturated hydraulic conductivity tensor [LT^{-1}]. The referenced values are generally taken at a chemical concentration of zero. The density and dynamic viscosity of water are functions of chemical concentration and are assumed to take the following form.

$$\frac{\rho}{\rho_o} = a_1 + a_2 C + a_3 C^2 + a_4 C^3 \tag{2.16}$$

and

$$\frac{\mu}{\mu_o} = a_5 + a_6 C + a_7 C^2 + a_8 C^3 \tag{2.17}$$

where a_1, a_2, …., a_8 are the parameters used to define concentration dependence of water density and viscosity and C is the chemical concentration.

The Darcy velocity, V, is calculated as

$$V = -K.\left(\frac{\rho_o}{\rho}\nabla h + \nabla z\right) \tag{2.18}$$

The flow equation (2.13) is subject to the following initial condition equation.

$$h = h_i(x, y, z) \text{ in } R, \tag{2.19}$$

where R is the region of interest and h_i is the prescribed initial condition.

The flow equation (2.13) is also subject to boundary conditions such as Dirichlet, gradient flux, specified flux, and variable conditions during precipitation and non-precipitation conditions. The Dirichlet boundary condition is a specified head boundary condition where the pressure head over a boundary can be assigned and maintained constant throughout the length of simulation. The gradient boundary condition allows the user to assign a flux rate variable with time. The variable boundary condition is applied to the top face of the model and is used to simulate evaporation and seepage. Variable boundary conditions change between Dirichlet and flux boundary conditions depending on the potential evaporation, the conductivity of the media, the availability of water such as rainfall and the level of the groundwater in the model. Further information about the boundary condition equations can be found in Lin et al. (1997).

2.4.2.4 Soil Characteristic Curves in FEMWATER

The unsaturated flow computation in FEMWATER needs a set of parameters specified for a soil type defining the relationship between moisture content-pressure head, relative conductivity-pressure head, and water capacity-pressure head in the unsaturated zone. These relationships are specified in FEWWATER with the help of material property curves.

Moisture content in the unsaturated zone is a function of pressure head and is directly proportional to the numerical value of pressure head. Thus, more negative the pressure head, lower the value of moisture content. The pressure head varies between the limits of residual moisture content and saturated moisture content. The water capacity curve represents the variation of pressure head with respect to the slope of the moisture content curve. The curve is added to alleviate the computational difficulties experienced during rigorous unsaturated zone flow and transport simulations. GMS-FEMWATER automatically generates the material property curve using the Van Genuchten functions (Van Genuchten, 1977), which were described from Equation 2.7 to 2.12 earlier.

2.4.2.5 Applications of GMS-FEMWATER

GMS-FEMWATER has been used in several studies involving groundwater flow and transport in the unsaturated media. Some of the relevant work done was reviewed for the purpose of the study and is presented below. Ng et al. (2001) conducted 3-D numerical analysis to investigate the effect of rainfall patterns on groundwater pressure responses considered to directly influence slope failure mechanisms. The Lai Ping Road in Hong Kong was modeled in this study and subjected to rainfall patterns of 24 h duration with a 10-yr, 100-yr, and 1000-yr return periods. The computed results from the study showed that rainfall patterns have a significant impact on pore-water pressure in soil layers near the ground surface, but its influence gradually diminishes with depth. It was found that the rainfall from an advanced storm pattern of 24-h duration was the most critical because it resulted in the highest pore-water pressure in the slope.

Evans et al. (1995) developed a three-dimensional finite element mesh of central O'ahu, Hawaii using the GMS interface. The model covered a large portion of central O'ahu, with 24 separate aquifer systems. The vadose zone thickness in some areas of the model was between 98 and 590 ft. The model was verified with respect to water elevations, geochemistry data, groundwater age dates, and pump test results supplied by Harding Lawson Associates. The developed model was verified so that it could be used to estimate downstream receptors and evaluate concentration of migrating contaminants from point and non-point sources. The model is also being developed as a standard model for the EPA's wellhead protection purposes and general purpose use by the DoD.

Uwiera et al. (2000) performed three-dimensional flow and transport simulations using GMS-FEMWATER to model the seepage of brine from waste management areas located at Saskatchewan potash mines. A simple, three-layered, hydrostratigraphic section was modeled and several simulations with brine concentration of 2 g/L, 20 g/L, and 200 g/L were performed. The results of the simulations indicated that denser brine plume migrated more rapidly downwards as compared to less dense brine plumes. Also at low dispersivities, it was found that the spreading of the contaminant plume was minimal.

Chen et al. (2002) performed simulation of water-infiltration applied to rice paddy fields using GMS-FEMWATER. The simulations were performed to identify and evaluate the controlling factors in the vertical percolation/lateral seepage process in the field. Also, the recharge to the groundwater from the paddy fields was estimated. Numerical simulations with and without plow sole were run and the results of the simulations indicated that the infiltration rate in the simulation without plow sole was three time larger than the infiltration rate in the simulation with plow sole. Thus, it was concluded that the plow sole was a major factor that controlled infiltration rate. It was further found that the length of the wet to dry boundaries, area of flooded paddy field, and difference between initial and final water content between flooded and dry field soils, determined the ratio of lateral seepage to vertical infiltration.

Lin et al. (1995) conducted two case studies involving flow and transport to demonstrate the GMS-FEMWATER model's flexibility and versatility for application to real-world problems. The first case study simulated alternative scenarios to reduce water levels in the agricultural lands near the city of Homestead, Florida, during the wet season. The second case study was intended to conduct a preliminary exposure assessment for the impact of application of agrichemicals used in the Walnut Creek watershed located in central Iowa on groundwater quality. The results of both the simulations indicated that GMS enhanced the utility of FEMWATER to model complex environments.

Heinzer (1998) modeled the Dura Landfill Avenue in Toledo, Ohio, to investigate the effect of locating a series of extraction wells along the perimeter of the landfill bordering the Ottawa river. Two scenarios were simulated, one with gravity drainage and the other with extraction wells to dewater the landfill. Results of the simulation indicated that it would take 11 years to dewater the landfill with gravity drainage only, while it will take only 2 years to dewater the landfill with extraction wells. Thus, use of perimeter extraction wells for dewatering at the landfill was recommended.

Ouyang et al. (1999) simulated the transport of two environmentally sensitive chemicals, very soluble (aldicarb) and more hydrophobic (acephate) to ascertain the role of density-driven transport of dissolved chemicals through an unsaturated sandy soil. The model was a 33 ft by 33 ft by 2.56 ft zone with constant, uniform concentrations of the residual chemicals. The simulations were performed with and without the effects of density-driven force and the results were then compared. The results indicated that the effect of density-driven flow on migration of low water solubility chemical acephate was negligible while that on high water solubility chemical aldicarb was significant.

CHAPTER 3

METHODS

3.1 Conceptual Model

A conceptual model representing the essential processes involved in the operation of an ETA trench was developed in this study. The main processes necessary to simulate the operation of an ETA trench are application of effluent to the trench surface, precipitation, and ET of the applied water due to weather conditions. The application of water to the trench was simulated by assigning inflow (recharge) in the trench for approximately 12 months. The weather conditions consisted of ET and precipitation. Figure 3.1 shows the direction and application of the different processes involved in an ETA trench. ET was simulated by assigning outflow (as evaporation or negative recharge) while precipitation was simulated by assigning inflow (recharge). In the conceptual model, the trench was represented by a rectangular volume over which inflow conditions were assigned. The cross-section of the modeled trench was made up of two zones representing the soil layers in the actual trench. A cross-sectional view of the conceptual model is shown in Figure 3.2. The units of length and time used in the model were feet and days, respectively. The following paragraphs discuss the conceptual model in further detail.

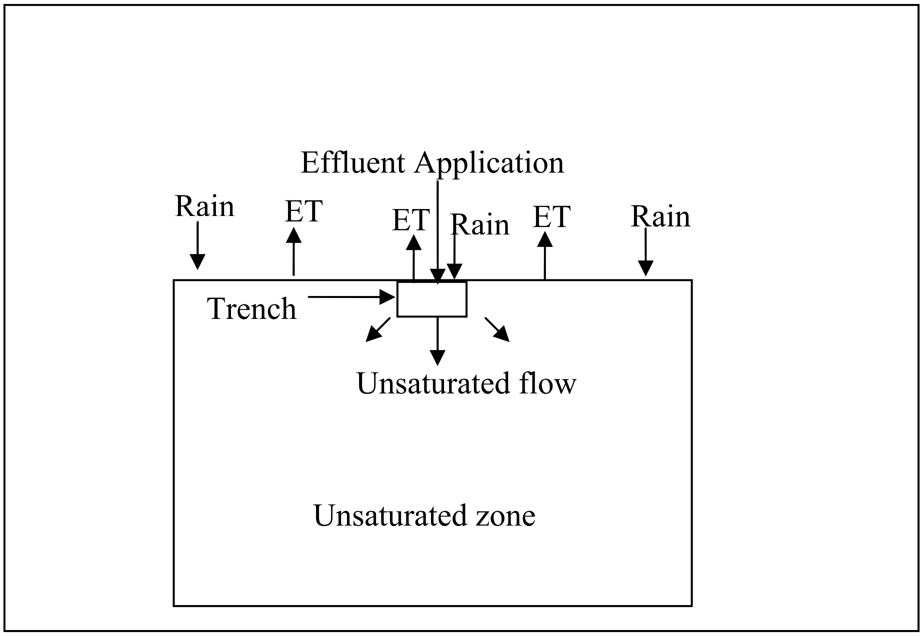

Figure 3.1 Direction of effluent application and the process of ET and Rain in cross-sectional view of the conceptual model

3.1.1 Geometry

The geometry of the model was made up of the length, width and depth of the model domain. The X and Y dimensions of the model domain must be large enough to properly represent the surface and subsurface processes so that boundary conditions would not control the simulation. ET occurs in an area surrounding the trench, and removes part of the applied wastewater effluent that travels laterally through the side-walls of the trench or precipitation that has infiltrated at the surface. The ET area influencing water removal from the trench was approximated by the area wetted by the laterally moving water from the drainfield. The lateral distance traveled by the applied water was influenced by the pressure gradients between the trench and the surrounding soil. Thus, the assumed ET area and the area wetted by the laterally moving applied water are interrelated. Hence, a trial-and-error approach was employed and lateral dimensions of 60 ft by 60 ft were selected, which were found to adequately represent the field conditions. The choice of ET area used in the selection of dimensions of the model was arbitrary and was initially selected as the whole top surface area of the model.

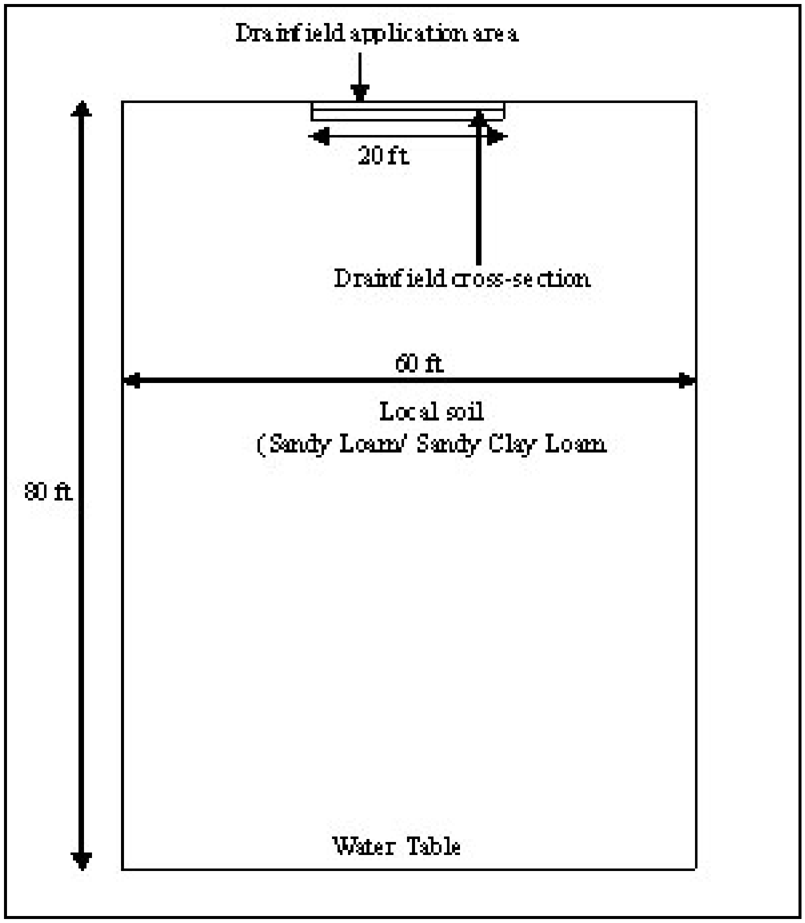

Figure 3.2 Cross-sectional view of the conceptual model

The depth of the water table at the test site was 80 ft (McReynolds, 1995); hence a model domain vertical dimension of 80 ft was selected. The cross-sectional dimensions of the trench according to TCEQ (2001) drainfield requirements were 3 ft wide by 2 ft deep. The length of the trench in the model was 20 ft, as at the test site. The dimensions of the overall model and the conceptual drainfield in cross-sectional view and plan view are shown in Figures 3.2 and 3.3, respectively.

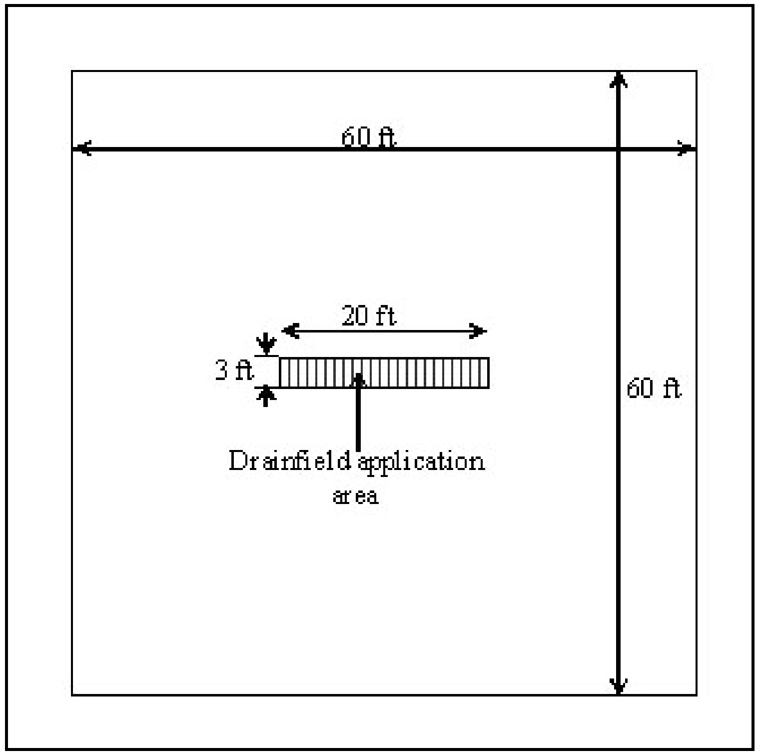

Figure 3.3 Plan view of the conceptual model

The layers of local soil and gravel in the conceptual trench as shown in Figure 3.4 were represented in the modeled trench by assigning soil properties of local soil and sand, respectively. As can be seen from Figure 3.4, the local soil layer was 0.67 ft thick and was the first layer of soil from the surface. The gravel layer was below the top local soil layer and was 1.33 ft thick. As shown in the cross-sectional view of the modeled trench in Figure 3.5, the first two layers of the modeled trench were of 0.335 ft thick and together represented the local soil layer, while each of the layers 3, 4, and 5 were 0.443 ft thick, which together represented the gravel layer in the trench. The rest of the model was assigned soil properties of the local soil.

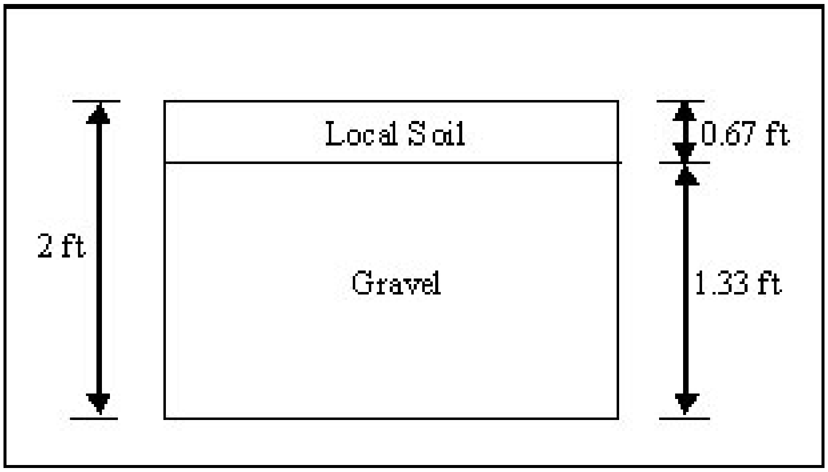

Figure 3.4 Cross-sectional view of the modeled ETA trench

The vertical dimension of the model was divided into 46 layers of varying thicknesses. The thickness of model layers was gradually increased from the top towards the bottom of the model, with the exception of the bottom-most layer, which was set at a thickness of 0.5 ft. The thickness of layers varied gradually from 0.335 ft for the top layer to 3 ft for the bottom layers as shown in Table 3.1 and Figure 3.5. The bottom-most layer was set at a thickness of 0.5 ft as this layer was assigned the drain boundary condition to represent a water table. The drain boundary condition is activated only if the drain cells are completely saturated, thus a smaller cell thickness facilitated immediate activation of the drain boundary condition even when small quantities of water infiltrated to the bottom layer cells and saturated them. However, the drain boundary condition was not activated in any of the simulations performed in this study as sufficient water did not infiltrate to the bottom layer of the model.

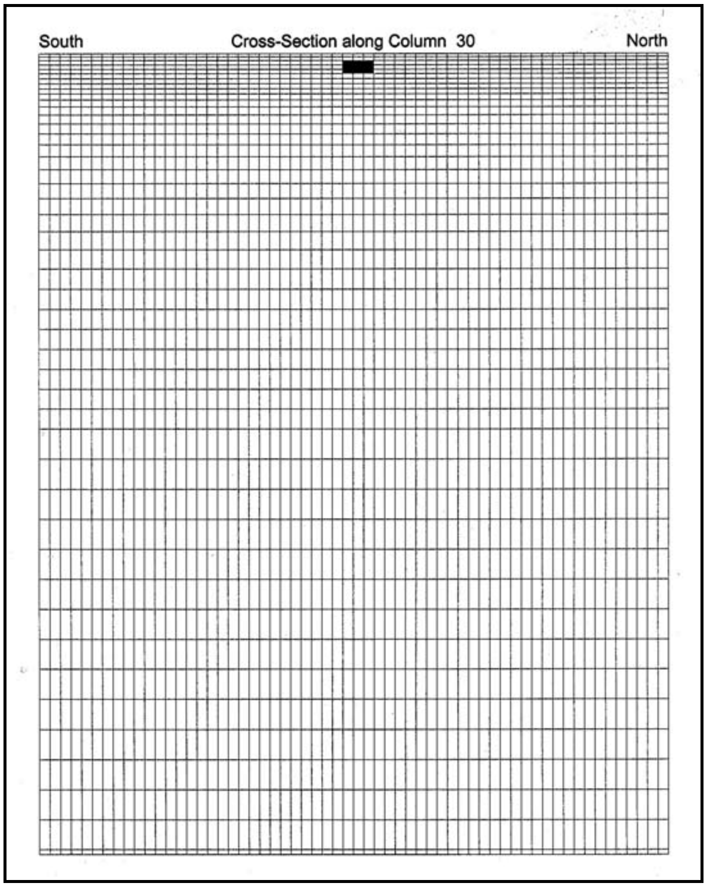

Figure 3.5 Cross-sectional view of model showing variation of layer thicknesses

Table 3.1 Table showing the layer thicknesses for each group of layers

Layer numbers	Layer thickness (ft)
1-2	0.335
3-5	0.433
6-9	0.5
10-24	Thickness was increased by 0.1 ft for each successive layer
24-31	2 ft
32-45	3 ft
46	0.5 ft

3.1.2 Soils

The soils at the test site were found to be mainly TCEQ class II and III soils (Rainwater et al., 2001). The percentages of silt, clay and sand found in the local soils at the test site revealed that the local soil was mainly TCEQ class II soil (sandy loam) and class III soil (sandy clay loam) as can be seen from Figure 2.1 (TCEQ, 2001). These soils are commonly found in the Southern High Plains of Texas (Rainwater et al., 2001). The gravimetric moisture content of the local soil from the test site at the beginning of the field study ranged from 3 to 13 percent. For the purpose of the model, an initial gravimetric moisture content of 12 percent was assumed. A two-day, double-ring infiltrometer test performed in the drainfield trenches, prior to the Phase 1 experiments, indicated an average rate of infiltration of 0.5 ft/d. The backfilled trenches were revegetated by seeding with commonly used turfgrass to enable ET from the drainfields. The soil outside and below the trench was assumed to be homogenous and isotropic throughout the model domain.

3.1.3 Hydrologic Data

The hydrologic data for the study comprised of the daily ET and precipitation data, which was recorded during the period 01/15/2000 to 12/31/2000 at the test site as part of the Phase 1 study. The modeled test site was subject to observed weather effects such as evaporation, precipitation, wind effects, and seasonal variation of temperature and pressure. Potential ET rates were calculated by an on-site weather station, and reported as daily values. Precipitation was also measured by the weather station. Thus, the ET rate and precipitation rate were the two main parameters used to represent weather conditions in the model. Since an ET-only drainfield loses water exclusively by the processes of transpiration and evaporation, the average daily loading rates for the three WW-ET-only drainfields was taken as the ET rate at the ETAW trenches. The observations of daily ET rate and precipitation rate were recorded during the period 01/15/2000 to 12/31/2000 of the Phase 1 study and are shown graphically in Figures 3.6 and 3.7, respectively.

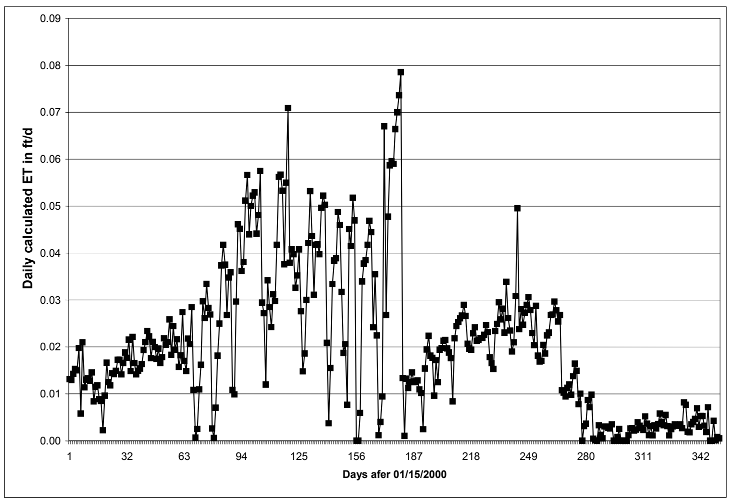

Figure 3.6 Daily ET Rate Recorded During 01/15/2000 to 12/31/2000

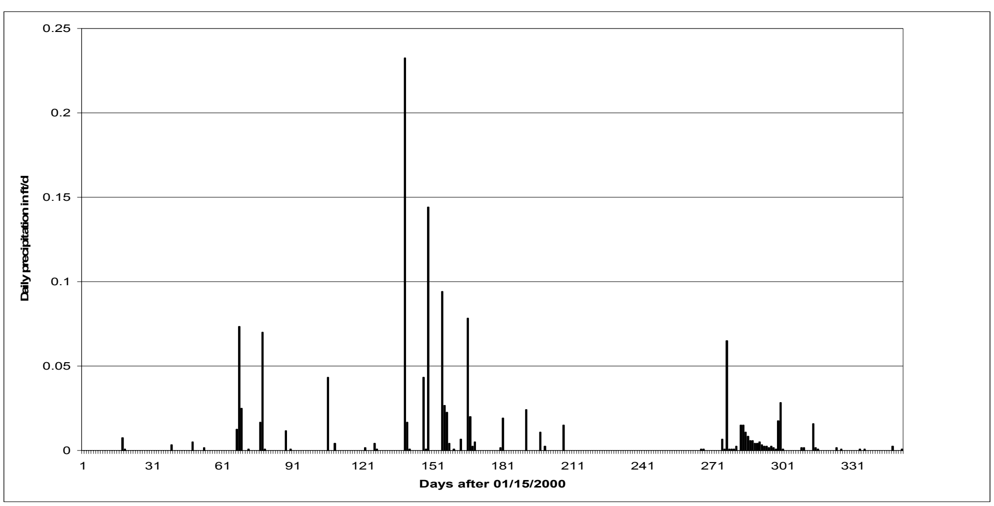

Figure 3.7 Daily Precipitation Rate Recorded from 01/15/2000 to 12/31/2000

The recorded duration of the daily ET rate and precipitation rate governed the duration of the modeling study. ET was applied on the top surface of the model within the ET domain as negative recharge. It was assumed for the purpose of the study that ET would cease completely during precipitation events.

3.1.4 Trench Operation

The actual trenches in the Phase 1 study were maintained at saturated conditions by the application of wastewater effluent throughout the study period. The saturated conditions at the actual trench were simulated by maintaining a recharge boundary condition over the surface of the modeled trench throughout the period of simulation. The wastewater effluent applied over the actual trench was represented by water at standard temperature and pressure (STP) conditions. The trench at the actual site received wastewater effluent whenever water level sensors in the trench indicated a drop in water level below 0.5 in of the top of the gravel envelope. Loading was simulated uniformly over each 24-hr period in the model. The average daily application rate of wastewater effluent to the ETA trench, ET rate, and precipitation rate were converted into units of ft/d for this study. The net application rate over the modeled ETA drainfield was a sum of the effluent application rate, ET rate, and precipitation rate on a given day. The ET rate was considered negative as it removed water from the model, while precipitation rate was considered positive. The average daily application rate data from 01/15/2000 to 12/31/2000 for ETA drainfield 9 from the Phase 1 study was used to calculate the net application rate. The net application rates with respect to date are tabulated in Appendix B and shown graphically in Figure 3.8

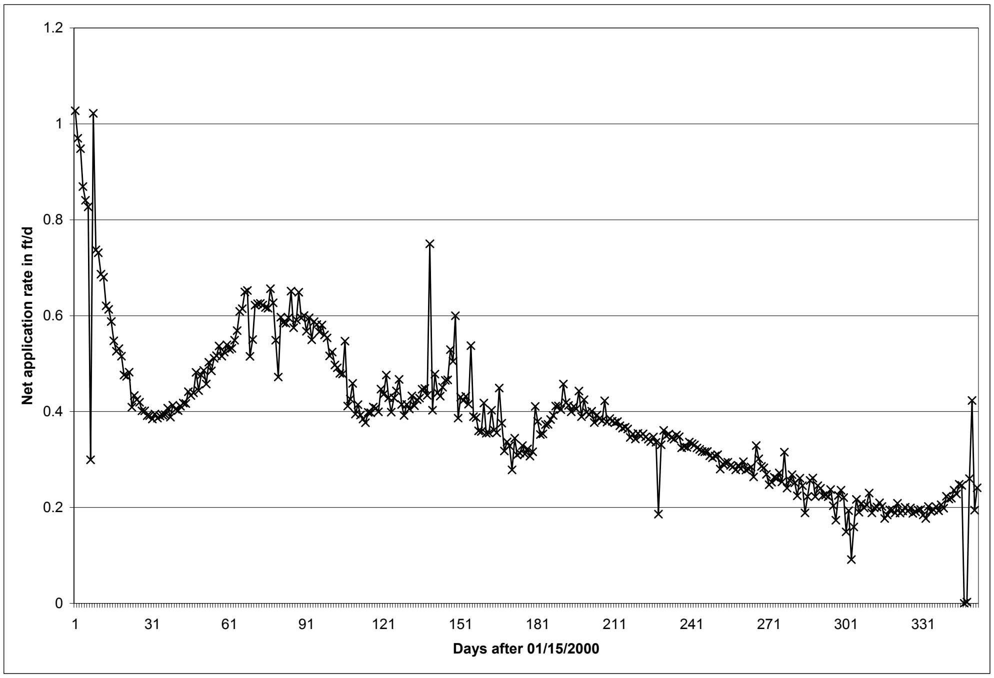

Figure 3.8 Daily net application rate data over the modeled ETA drainfield

3.2 Types of Simulations

In this study, four main simulations were performed. The conceptual model was varied with respect the local soil type and ET domain size. The local soil was of two types: sandy loam (SL) and sandy clay loam (SCL). The ET domain sizes used in the study were (A) 60 ft by 60 ft, and (B) 40 ft by 50 ft as shown in Figure 3.9 and Figure 3.10, respectively. The two ET domain sizes were selected because the actual ET area that influenced the removal of water from the trench due to ET was not known. Thus two domain sizes were selected so that a closer approximation of the actual ET area affecting disposal of water from the ETA trench can be made after analyzing the results. The four simulations were referred to as SL-A, SL-B, SCL-A, and SCL-B.

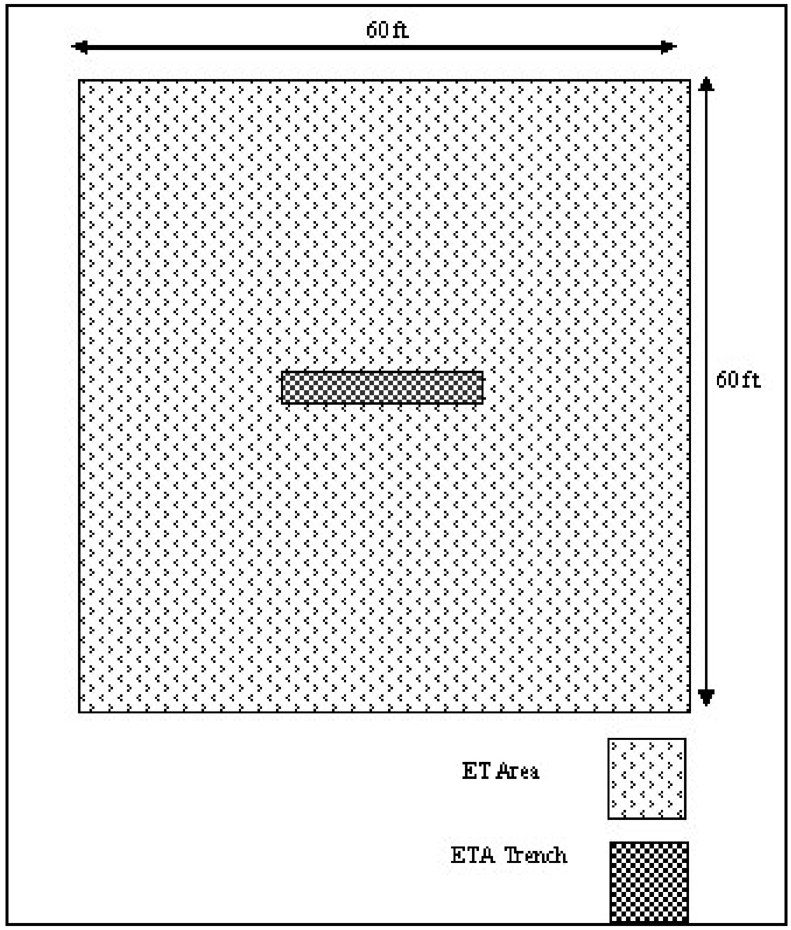

Figure 3.9 Plan view of ET domain Type A of size 60 ft by 60 ft

.

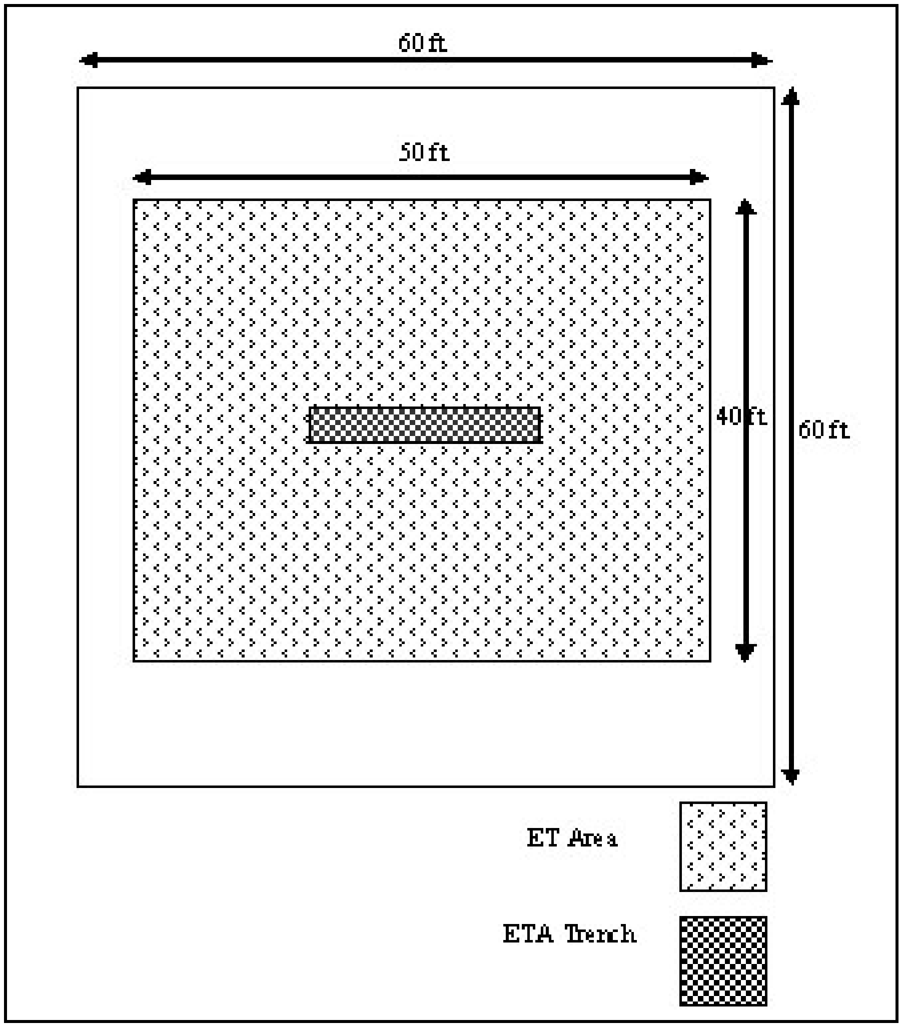

Figure 3.10 Plan view of the ET domain Type B of Size 40 ft by 50 ft

3.3 Input for MODFLOW-SURFACT

The conceptual model was simulated using the finite difference code MODFLOW SURFACT (Hydrogeologic, Inc., 1996), which has similar input requirements as the original MODFLOW (McDonald and Harbaugh, 1988). This section describes the parameters required as input to MODFLOW-SURFACT and MODFLOW files used for the simulation of the conceptual model. The BASIC, BCF4, Recharge, Drain, ATO4, RCH4, PCG4, and NRB1 packages of MODFLOW-SURFACT were used in the development and simulation of an ETA drainfield trench model. The input files were created using the graphical user interface (GUI) pre-processor of Groundwater Vistas version 3.45 (Rumbaugh et al., 2002).

3.3.1 Basic Package

The Basic package is the first package read by the MODFLOW code for any model. The Basic package contains information about model geometry, selected modules, time discretization, and initial pressure head data.

3.3.1.1 Model Geometry

Model geometry includes information about number of rows, columns, and layers in the model. The row and column width for an unsaturated zone model should be as small as possible to improve precision and accuracy of results, but close spatial discretization results in large data files, which result in slower simulation speed. After considering cell widths of 0.5 ft, 1 ft and 2 ft, it was decided that a cell width of 1 ft would be optimal for the model. Thus a 60 row by 60 column grid was selected for the model.

The layer thicknesses of the top layers in the model ranged from 0.335 ft to 1 ft, while the layer thicknesses of the bottom layers ranged from 0.5 ft to 3 ft. This was done since layers near the surface of the model were subjected to significant moisture movement during simulation due to recharge and ET boundary conditions on the top surface of the model. Significant moisture movement results in convergence difficulties and high computation time, which can be reduced by close discretization of cells in the region subjected to significant moisture movement. Thus to aid convergence and precision of the simulation, small values of layer thickness were used for layers near the surface of the model. Layer thicknesses were increased gradually to 3 ft towards the bottom of the model. It is considered a good model development practice to maintain the difference between thicknesses of adjoining layers in a model to less than 1.5 times the thickness of the smaller layer. This practice dictated the choice of number of layers in the model. The vertical dimension of the model was thus divided into 46 layers. The exact top and bottom elevations assigned to the model layers are shown in Table A.1 and A.2 in Appendix A. The variation of layer thicknesses can be seen in the cross-sectional view as shown in Figure 3.5.

The drainfield application area was spread over 60 cells in the top layer of the model. The application area included cells between rows 29 to 31 and columns 20 to 39. The drainfield application area is as shown in Figure 3.11. The different soils in the drainfield were represented by assigning material zones in the layers below the drainfield application area. The top two layers of the model were assigned material zone representing local soil while the cells in layers 3, 4 and 5, under the drainfield application area, were assigned material zone representing sand. The application area and the material zones were assigned with the help of pre-processors in GroundWater Vistas and following the procedure described under the section “Assigning Material Property Zones”, in Appendix A.

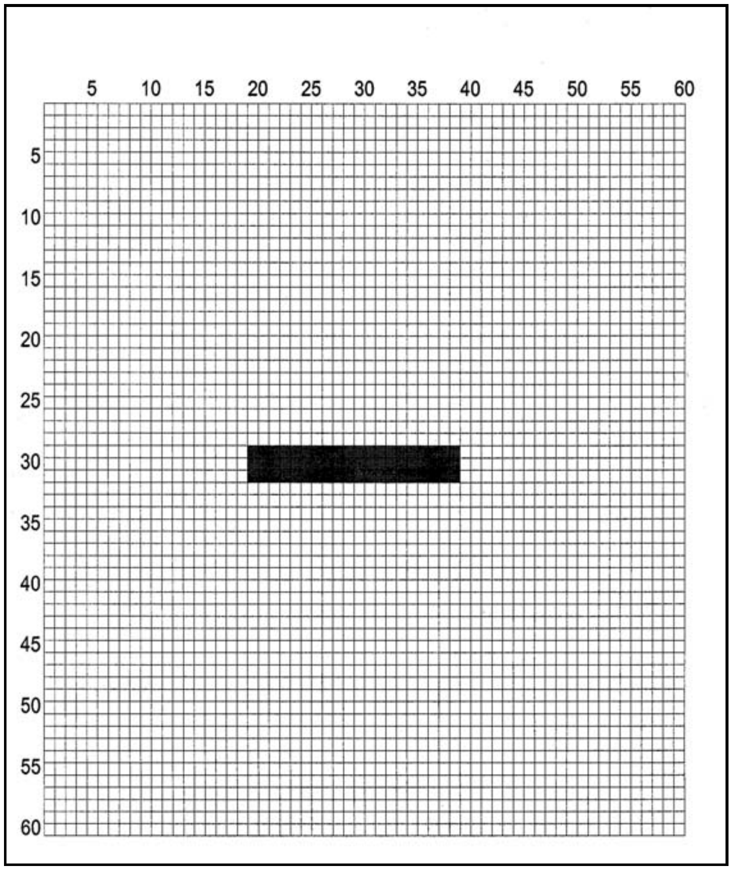

Figure 3.11 Plan view of model grid showing trench application area

3.3.1.2 Initial Conditions

The initial conditions were input in the form of the pressure head distribution. The pressure head at the beginning of the first simulation for each SL and SCL simulation was selected such that water saturation in the model was the same as the water saturation measured at the beginning of the field study at the test site. The gravimetric moisture content measured at the test site was 12 percent, which in terms of water saturation was 48 percent for sandy loam and 52 percent for sand clay loam. The pressure head values representing the initial water saturation in the model were calculated by trial-and-error using the Van Genuchten Equations 2.9 to 2.12. The pressure heads were found to be

-1055 ft and -2800 ft for sandy loam and sandy clay loam, respectively. These values were input as initial pressure head for all the layers in the model. The gravel in the trench was assumed to have similar water saturation as the local soil. Hence, it was assumed for the purpose of this study that the initial water saturation of the gravel would not be critical to model results as saturation values in the gravel layer would be achieved immediately after the trenches were in operation. Thus, pressure head values used for the local soil were used for both layers in the trench.

3.3.1.3 Time Discretization

In this study, the total time to be simulated was 352 days. Each day had a different application rate and ET rate; hence, the simulation time was divided into 352 stress periods. It was found that the simulation became unstable when it was performed with more than 30 stress periods; hence the 352-day period was divided into 12 consecutive simulations, with 30 stress periods and the twelfth simulation with 22 stress periods. The ATO4 package in MODFLOW-SURFACT handles the time discretization on the stress period level. The ATO4 package automatically assigned the number of time-steps for each stress period, thus the number of time-steps in a stress period depended on convergence difficulty for that particular stress period and were not fixed. However, it was found for all simulations that the 30th stress period of each simulation was made up of nine time-steps.

3.3.1.4 Simulation Continuity

Since the 352-day model period was divided into 12 different simulations, it was critical to transfer final pressure head data between consecutive simulations in order to maintain continuity. Continuity was achieved by using pressure head data from stress period 30 and time-step 9 from each preceding simulation as initial pressure head data for the next simulation.

3.3.2 BCF4 Package

The input data format for the BCF4 package is the same as the BCF package in the original MODFLOW. The BCF4 package adds the additional capability of simulating variably saturated flow conditions to the original MODFLOW version. Model properties like horizontal saturated hydraulic conductivity, vertical leakance, top and bottom elevations of cells, and specific yield for transient simulations are the main input parameters in the BCF4 file. These properties depend on the input LAYCON values assigned to each layer. The input LAYCON value is a flag that indicates the type of aquifer being simulated in a given layer. MODFLOW-SURFACT allows the simulation of two types of aquifers: (1) strictly confined, and (2) confined/unconfined. MODFLOW-SURFACT programmers set the input LAYCON values for each type of condition, with 40 for a strictly confined layer and 43 for confined/unconfined conditions. In variably saturated flow simulations, layers are generally assumed to be confined/unconfined aquifers; hence a LAYCON value of 43 was assigned to all the layers in the model.

The saturated hydraulic conductivity for the local soil was taken as the average of the values obtained from double-ring, two-day infiltrometer tests carried out at the test site as part of the Phase 1 study. The average saturated hydraulic conductivity of the local soil at the test site was 0.5 ft/d; hence the local soil simulated in the model was assigned a saturated vertical hydraulic conductivity of 0.5 ft/d. The hydraulic conductivity of 25 ft/d was used to represent gravel based on values obtained from Fetter (2001) for well sorted sand. The function of the gravel layer in the trench was to allow rapid infiltration of water from the trench; since a hydraulic conductivity of 25 ft/d was sufficient to represent a highly permeable layer of soil, the value of 25 ft/d, though typical for well sorted sand, was used to represent the relatively permeable soil layer in this study. Also, it is generally accepted that numerical models converge slowly or produce convergence difficulties when there is a sharp change in material property values between two adjoining layers of the model. Convergence problems occurred during FEMWATER simulations when a large difference in hydraulic conductivity between adjoining layers was input, thus a relatively low value of 25 ft/d, which was adequate for simulating a porous and highly permeable soil layer (gravel), was used in MODFLOW-SURFACT simulations.

The leakance, or VCONT, values required by MODFLOW-SURFACT were computed internally in the BCF4 package by dividing the vertical hydraulic conductivity by the layer thickness. The Van Genuchten relation in Equation 2.8 for simulation of water flow through soil was selected. Next, the upstream weighting option for the calculation of the relative permeability term was selected. The Van Genuchten parameters for sand were used to represent gravel as sand represented a highly porous, permeable soil type and the Van Genuchten parameters for gravel were not found in the literature reviewed. Van Genuchten parameters for the different soils were taken from Table 3.1 adopted from Lin et al. (1997), who adopted it from Carsel and Parrish (1988). The residual saturation in Table 3.2 was calculated using

$$S_{wr} = \frac{\theta_{rs}}{\eta}, \tag{3.1}$$

where θ_{rs} = volumetric residual moisture content. The values of volumetric residual moisture content were taken from Lin et al. (1997). The Van Genuchten parameters alpha and beta, and residual saturation were then assigned to the respective material zones in the model.

Table 3.2 Van Genuchten parameters for soils (Lin et al., 1997)

Parameters	Sandy Loam	Sandy Clay Loam	Gravel	Units
Alpha	$2.46\text{x}10^{-3}$	$1.94\text{x}10^{-3}$	$4.76\text{x}10^{-3}$	Per feet
Beta	1.89	1.48	2.68	No unit
Residual Saturation ratio	0.16	0.26	0.11	No unit

The primary storage coefficient or specific storage was calculated using the following equation from Fetter (2001).

$$S_S = \rho_w g(\alpha + \eta\beta) \tag{3.2}$$

where, ρ_w = density of the water [ML^{-3}], g = acceleration due to gravity [LT^{-2}], α = compressibility of the aquifer [$ML^{-1}T^{-2}$], and β = compressibility of the water [$ML^{-1}T^{-2}$]. The values of parameters used for the computation of primary storage coefficient using Equation 3.2 were adopted from Fetter (2001), and Domenico and Schwartz (1990), and are shown in Table 3.3.

Table 3.3 Values used in the computation of primary storage coefficient

Parameters	Values	Units
Density of water	1.94	Slug /ft^3
Acceleration due to gravity	$2.4x10^{11}$	ft /day^2
Compressibility of soil	$3.09x10^{-17}$	ft.day^2/slug
Compressibility of water	$2.95x10^{-18}$	ft.day^2/slug

The porosity and the volumetric residual moisture content for the soil types used were adopted from Lin et al., (1997), and the specific yield was calculated by using Equation 3.3 given below.

$$S_y = \eta - \theta_{rs} \tag{3.3}$$

where S_y = is the specific yield for the soil, and θ_{rs} = is the volumetric residual moisture content of the soil. The computed values for primary storage coefficient, specific yield and porosity were assigned for the respective materials and are shown in Table 3.4.

Table 3.4 Soil properties used in MODFLOW-SURFACT

Parameter	Sandy Loam	Sandy Clay Loam	Sand
Storage Coefficient	$1.56x10^{-4}$	$1.56x10^{-4}$	$1.56x10^{-4}$
Specific Yield	0.35	0.29	0.39
Porosity	0.41	0.39	0.43

3.3.3 EVT Package

The EVT package in MODFLOW is used to simulate plant transpiration and evaporation from the saturated groundwater regime. The main input parameters in the EVT package were the maximum ET rate and the extinction depth. The user is able to assign an ET surface in the model, typically the model top surface is the default ET surface. The ET surface is at a specified elevation in the model where the ET rate assumes a user-specified maximum value if the water table is at or above the ET surface elevation. The extinction depth is the depth from the ET surface at which the ET rate becomes zero if the water table falls below the extinction depth. The ET rate assumes values from zero to the user specified maximum when the water table is between the extinction depth and the ET surface.

The EVT package was the first choice for simulation of ET in this study. Based on numerous attempted trial simulations, both MODFLOW and MODFLOW-SURFACT were found incapable of properly simulating ET from a variably saturated zone of the model using the EVT package. The EVT package only removes moisture from saturated cells in the model. This condition was confirmed during several simulations involving increasing values of extinction depth for a model with water table at a depth of 80 ft and constant head cells in the lower layer of the trench. All other boundaries for the EVT trial simulation were no-flow boundaries. The constant head cells in the lower layer of the trench represented an infinite supply of water to the model, which gradually saturated the model cells from the bottom up, resulting in a rising water table in the model. It was found that the EVT rate was zero as long as the water table was below the extinction depth specified in the model. As the simulation progressed and the water table rose from its initial depth of 80 ft to the extinction depth specified, the ET rate increased proportionally, eventually assuming the maximum value of ET rate specified in input when the water table had risen near the surface of the model. It was thus concluded that the EVT package could not be used for simulating ET from variably saturated cells above the water table.

3.3.4 Recharge Package

The Recharge package was used to simulate effluent application on the surface of the drainfield, and ET from the area around the drainfield. ET was simulated as negative recharge, while effluent application and precipitation was simulated as recharge. Recharge was applied to the cells in the top layer of the model when an inflow condition such as precipitation or application of water was simulated. Negative recharge was applied to the cells in the top layer of the model when an outflow condition like ET was simulated. Negative recharge meant that the negative values of ET rate were input as recharge, so that water would be removed from the model by reversing the normal mechanism of recharge, thus simulating ET. Since the reverse mechanism of recharge was used to remove water from the model by using a negative value of recharge rate, trial simulations were conducted to test the negative recharge application at the land surface and to assess the limitations of using negative recharge to simulate ET.

3.3.4.1 Negative Recharge Trial Simulations

Trial simulations involving negative recharge were carried out to determine if the simulated negative recharge actually removed water from the unsaturated zone and if the water removal was accurately printed in the diagnostic output. A simulation was run for an extended period of time to find the behavior of the negative recharge mechanism when the top layer of the model reached completely dry conditions or residual saturation.

Two transient-state trial simulations were performed. The difference between the two trial simulations was only in the total duration. The first trial was simulated for 30 days, while the second one was simulated for 1000 days. The conceptual model in the trial simulations represented an ET-only condition in which water was being removed from the soil surface without any addition of water through any other mechanism. Negative recharge was applied to represent ET to the whole top surface of a simple three-layered model of dimension 60 ft by 60 ft by 80 ft, with sandy loam soil, and cell widths of 10 ft. Initial pressure head in all the layers of the model was set at -650 ft.

The water removal due to negative recharge was necessary to be calculated separately in order to verify the negative recharge condition. The initial water saturation in the model layers was calculated from the initial pressure head value input and using Van Genuchten Equations 2.9 to 2.12. The final water saturation was recorded with the help of the post-processing tools in GroundWater Vistas in each model layer. Equation 3.4 shown below was used to calculate the difference between the initial and final values of water saturation in the model cells.

$$\nabla S = S_i - S_f \tag{3.4}$$

where ∇S = the difference in the initial and final water saturation in the model layers, S_i = the initial water saturation in the model layers, and S_f = the final water saturation at the last stress period of the trial simulation. The values of ∇S were computed for each model layer, and multiplied by the volume and porosity of the model layer to determine the calculated loss of water from the model due to negative recharge. A cumulative volume of water loss in cubic feet was calculated by summation of the water loss values for each layer.

3.3.4.1.1 First Trial Simulation

In the first trial, the negative recharge mechanism removed moisture from the top layer only. The removal of moisture from the top layer created a pressure gradient between the top layer and the adjoining layer that caused moisture to move from the adjoining layer to the top layer. This effect continued to the full depth of 80 ft of the model domain. The water removal in this simulation was printed in the diagnostic output results and had a value of 2160 cubic feet. The diagnostic output results were compared with calculated values of water removal using Equation 3.4 on a layer-by-layer basis for the final time-step of the simulation. The calculated water removal was 2125.71 cubic feet, thus an error of 1.59 percent was observed between the values of water removal from the diagnostic output and the calculation. Please refer to Appendix C for detailed calculations related to the trial.

3.3.4.1.2 Second Trial Simulation

The second trial was considered for a period of 1000 days. A 1000 day simulation period was selected so that changes in diagnostic output results could be observed when the top layer of the model reached residual saturation and no further removal of water from the top layer was logically possible. All other conditions for this simulation were similar to the first trial simulation. As was seen in the first trial simulation, the water removal rate in the diagnostic output remained constant throughout the simulation. The actual removal of water from the model stopped when the top layer of the model reached residual saturation or became dry. However, water removal was recorded in the diagnostic output file. Thus, even though the actual removal of water from the model had stopped, the diagnostic output kept recording water removal till the end of the simulation. The water removal shown by the diagnostic output was 72,000 cubic feet, while the calculated water removal was 48,025.2 cubic feet, thus an error of 33.3 percent was observed between the calculated value and the diagnostic output value. The lack of correlation between water removal values calculated from saturation values in the model cells and printed output results produces a large difference between the calculated values and values printed in the diagnostic output. The error increases in direct proportion to the duration of the simulation after the top layer of the model becomes dry or reaches residual saturation. Please refer to Appendix C for detailed calculations related to the trial.

3.3.4.1.3 Limitations of negative recharge mechanism

In spite of the fact that the negative recharge mechanism was verified, some limitations exist while using negative recharge to simulate ET. The first limitation is that the water budget from the diagnostic output would provide accurate values only if the top layer of the model does not become completely dry or reach residual saturation during the simulation. The second limitation is that the negative recharge mechanism eventually draws water from the full depth of the model. Thus, water is removed from very deep layers of the model that likely remain unaffected by ET processes in actuality. It should also be noted that the negative recharge mechanism does not exclusively remove water applied to the drainfield but any moisture that finds its way into a particular cell with specified negative recharge. Thus, the values presented by the negative recharge in the diagnostic output may not precisely represent the potential loss of water due to ET from an ETA trench. However, negative recharge was found to be the only available alternative to simulate ET in the unsaturated zone and hence was used in this study.

3.3.5 RSF4 Package

The RSF4 package was used to activate the ponding-recharge condition for the recharge applied to the trench surface. The ponding condition in the RSF4 package accounts for the surface runoff from the recharge surface. The RSF4 package enables printing of the amount of surface runoff over the recharge surface in the diagnostic output, when accumulation of water over the recharge surface exceeds the specified ponding depth. The RSF4 package required input of a limiting ponding depth value. The ponding depth is the depth of ponded or accumulated water over the recharge surface. If the ponding on the recharge surface is more than the limiting ponding depth specified, the excess water is removed from the recharge surface and printed as surface runoff in the diagnostic output. A ponding depth of 0.5 ft was arbitrarily selected, it was however not expected that there would be any surface runoff from the trench during the simulation as the applied recharge over the trench was rarely at a high enough rate to cause ponding. The RSF4 package was nevertheless included in the study so that potential users and readers of this thesis may be aware of the option should they need to use it in future applications.

3.3.6 ATO4 Package

The ATO4 package is an adaptive time-step selection scheme and an output control package. The output control in the ATO4 package allows the user to print the output of the simulation at predetermined time intervals and also to decide the detail of the requested output. The user can specify which heads, drawdowns, mass budgets, and cell-by-cell flow terms should be printed for a particular stress period. The ATO4 package adjusts the time-step size to perform computations at user-selected times so that the output can be printed at the requested time. The ATO4 package requires the specification of initial time-step, minimum time-step, maximum time-step, length of time-step, time-step increment factor, and time-step reduction factor. The user also has the choice to select the times when the output should be printed or the number of times the output should be printed in every stress period.

The ATO4 package starts the simulation with the initial time-step specified by the user. If the simulation converges in less than 35% of the maximum number of iterations assigned, the next time-step size is then increased by the time-step increment factor. If the simulation convergence rate is between 35% and 65% of the maximum number of iterations assigned, no change in the time-step size is made as the time-step size is considered optimum for convergence. If the simulation convergence rate is more than 65% of the maximum number of iterations, the next time-step size is then reduced by the time-step reduction factor. The simulation is aborted if the time-step size is reduced below the minimum time-step size assigned.

The parameters specified in the ATO4 package vary within stress periods. All stress periods were of the same time duration, i.e., 1 day, in this application. The initial time-step size for stress periods varied from 0.01 to 0.5 days. The maximum time-step size for stress periods varied from 0.5 to 1 day. The range of values for the initial and maximum time-step size were selected by trial-and-error, so that solutions converged for all the stress periods within a given simulation. The minimum time-step size was kept constant at 1×10^{-4} day. The time-step increment factor and the time-step reduction factor were assigned default values of 1.2 and 2.0, respectively. The output was requested at every 0.5 day, 0.75 day, and 1.0 day for each stress period.

3.3.7 PCG4 Package

The PCG4 package provides an additional solver that is more robust and efficient to solve complex non-linear equations in variably saturated flow simulations than MODFLOW's Slice Successive Over-Relaxation (SSOR) and Strongly Implicit Procedure (SIP) solvers. The Preconditioned Conjugate Gradient Method (PCG) has emerged as one of the most promising iterative methods for solving large sparse symmetric matrix equations generated by finite element or finite difference approximations of multi-dimensional field problems (Hydrogeologic Inc., 1996). The PCG4 solver utilizes the symmetric PCG solver that is based on a two-step procedure developed by Meijerink and van der Vorst (1977) and extended and implemented by Kershaw (1978) and Anderson (1983). The PCG solver is used to solve the system of algebraic equations resulting from the iterative Picard scheme of the finite element flow formulation.

The input required in the PCG4 solver is straightforward and simple. The PCG4 solver requires input of the closure tolerance limits and a maximum limit of solver iterations. There are two types of solver iterations, outer and inner. Outer iterations are calls to the solution routine, and inner iterations are calls to the PCG routine. The user also has the choice to hide or suppress the solver output, which is the display of the preliminary step that the PCG solver performs and is not crucial in the output of converged solutions. The maximum number of outer iterations for a linear problem is recommended in the range of 1 to 10. The maximum number of outer iterations for non-linear problems should be between 10 and 100. The maximum number of inner iterations should be in the range of 6 to 600 depending on the complexity of the problem. The maximum numbers of inner and outer iterations assigned in the simulation were 600 and 100 respectively. A converged solution in MODFLOW-SURFACT is assumed to be achieved when the maximum head change values computed for successive iterations is less than a user specified maximum head change criteria. The closure tolerance for the maximum head change was set at 0.001 ft. Another closure criterion, called the relative closure criterion is used for convergence of the inner iterations when the relative head change closure is less than the prescribed value. Convergence is achieved when either the head closure criteria or the relative closure criteria is satisfied. In case the maximum head change criterion is not met, MODFLOW-SURFACT changes the water saturation in the model cells in order to achieve convergence. When the change in saturation content is less than $1x10^{-7}$, convergence is assumed.

3.3.8 NRB1 Package

The NRB1 package works in conjunction with the PCG4 package and can be used when the Picard or modified Picard schemes fail to produce a converged solution or produce excessive iterations. The NRB1 package employs the Newton-Raphson linearization and backtracking scheme to stabilize the Newton iterations and can be used in non-linear situations to alleviate convergence difficulties. The NRB1 package needs to be selected first in order to be used in the simulation with the PCG4 solver. The NRB1 package can be selected either by assigning a value of 1 to INEWT (a flag in the NRB1 input file) or by selecting the option through the PCG4 solver input dialog in Groundwater Vistas. The other input parameters required in the NRB1 package are the backtracking parameters, BFACT and RESRED. It is generally suggested that, in case the Picard iteration schemes fail to converge, BFACT should be left blank and RESRED should be assigned a value greater than or equal to 10^{15}, which would employ the Newton-Raphson scheme without backtracking. If convergence difficulties persist, then a value of 0.1 to 0.2 should be assigned to BFACT and 1 to 2 to RESRED, which would allow severe step cuts in the simulation for a slight increase in the residual value. If the convergence problems still persist, then the user should assign a value of BFACT between 0.1 and 0.2, and RESRED from 10 to 50 so that severe step cuts are performed allowing for a considerable increase in the residual to escape the local minima in the error surface. The ETA drainfield simulation converged with the BFACT values of 0.1 and the RESRED value of 1.0.

3.3.9 Drain Package

The Drain package was used to apply drains to the bottom layer in the model. Drains were applied to the bottom layer in order to determine precisely how much water was reaching the groundwater table during the simulation time. Drains were selected because they could be set to only remove water from the model and did not add any water to the model under any circumstances. Also, the drains remove water only when the head in the drain cells rises above the drain elevation, which was precisely the condition intended to be simulated. The number of drains that would simultaneously function at one time was assigned a value of 3600, which was the total number of cells in the bottom layer. The drains were assigned to layer number 46, and the stage of the drain was assigned a value of 0 ft so that any build-up of water at the bottom of the model would be immediately removed. The hydraulic conductivity of the drains was assigned a value similar to the saturated vertical hydraulic conductivity of the local soil, which was 0.5 ft/d. The drains were applied during all stress periods of each simulation.

3.4 Input Requirements for GMS-FEMWATER

The main source of information regarding the input to GMS-FEMWATER was Lin et al. (1997) unless otherwise specified in this study. The input data in FEMWATER (Lin et al., 1997) is organized into three main files. These files are geometry file, model file, and the initial condition file. The data input for the FEMWATER simulations was done using the GMS pre-processor and the following modules.

- GMS 3.1 pre-processor,
- Mesh Package (2D Mesh and 3D Mesh modules),
- Map Module,
- TIN (Triangular Integrated Network) module,
- Geostatistics package (2D Scatter Point module), and
- FEMWATER numerical code.

3.4.1 Geometry File

The Geometry file consists of input data related to the finite element grid. A conceptual model of the simulation was first built using the Map module in GMS. To start with, the FEMWATER coverage was initialized and the model surface elevation was assigned a value of 80 ft. The units used for the simulation were then selected. Feet were chosen to be the unit of length, days as the unit of time, and slugs as the unit of mass. Next, construction of the finite element grid was started. A 60 ft by 60 ft boundary of the model was first drawn using the “Create Arc” tool. The vertices on the arcs were then redistributed such that spacing between adjacent vertices would be 1.5 ft. Next, using the arcs and vertices, the Map module internally constructed a two-dimensional mesh made up of triangular elements. The two-dimensional mesh was created by selecting the “Map→2-D Mesh” command. The two-dimensional mesh was then used to create four duplicate TINs located at elevations of 80 ft, 60 ft, 20 ft, and 0 ft, respectively.

A three-dimensional mesh was created by filling the space between adjacent TINs with layers. The "Fill Between TINs→ 3-D Mesh" command was used to add layers between each set of adjacent TINs. Areas with significant moisture movement were subjected to more changes in pressure head than other areas of the model. The surface of the model and the area near the water table were identified as the regions where significant moisture movement may produce oscillation of pressure head values during simulation; such oscillations could be reduced by close discretization of layers within the high flux regions. Close vertical discretization of 0.5 ft at the top layer was done as maximum flux, i.e. simulated boundary conditions representing ET, precipitation, and effluent application, occurred mostly in the top layer. The bottom layers were subjected to high flux due to the subsequent change in water table elevation when water due to infiltration reached the water table, thus vertical discretization of 0.5 ft was also applied in the bottom layers. The thickness of layers or vertical discretization between the second and third TINs, where relatively fewer changes in flux were anticipated, was 1 foot.

Next, the materials were assigned. Each node in the Geometry file was assigned a material identification (material ID) based on the different materials (soils) represented in the model. The Geometry file did not store the soil properties of the material used, but the material properties were assigned to specific nodes in the model through the Geometry file. The material ID was stored in the Geometry file, hence the assignment of material properties only are discussed in this section. The model was made up of two types of soils, the local soil and sand (representing gravel) used in the trench. The rectangular volume of the trench located centrally on the top surface of the model was selected and isolated from the rest of the model. The isolation of the rectangular trench volume allowed the selection and modification of material properties of specific layers. Please refer to DoD's GMS version 3.1, Tutorial manual for procedure to assign material properties. The top layer of the isolated trench volume was assigned the properties of the local soil, while the next three layers were assigned the properties of sand.

The Map module allows creation of a conceptual model, which can be converted into data files specific to any type of simulation code supported by GMS 3.1. The procedure discussed above was used in the creation of the conceptual model of an ETA trench in GMS 3.1, which was further converted into a FEMWATER Geometry file by using the "Map→ FEMWATER" command in the "Feature Objects" menu of the Map module.

3.4.2 Model File

The Model file contains a variety of data like the material properties, analysis options, and boundary and initial conditions for a model. The material properties consisted of a single set of fluid properties and two sets of soil properties. Water was used as the model fluid for this flow simulation; hence the fluid properties of water as shown in Table 3.5 were used. The soil properties for the local soil (sandy loam) and sand (representing gravel) were as shown in Table 3.6. The soils were assumed to be homogeneous and isotropic throughout the model domain. Data contained in Table 3.5

and Table 3.6 was adopted from Lin et al. (1997), Domenico and Schwartz (1990), and Fetter (2001).

Table 3.5 Input water properties used in GMS-FEMWATER

Property	Value	Units
Density of water	1.94	Slug/cubic feet
Viscosity of water	2.57	Slug feet/day
Compressibility of water	2.95×10^{-18}	Feet-day^2/slug
Acceleration of gravity	2.4×10^{11}	feet /day^2

Table 3.6 Input soil properties used in GMS-FEMWATER

Property	Sandy Loam	Gravel	Units
Hydraulic Conductivity	0.5	25	feet/day
Compressibility of soil	3.1×10^{-17}	3.0×10^{-16}	feet-day^2/slug

The soil moisture retention curves for the materials used in the model were automatically computed using the “Generate Curves” command in the FEMWATER Material dialog. The soil moisture retention curves were computed using the Van Genuchten Equations 2.8 to 2.11. In order to compute the soil moisture retention curves, 79.5 ft was entered as the maximum height of the model top surface from the water table, thus an unsaturated zone of 79.5 ft instead of 80 ft had to be selected as GMS-FEMWATER compulsorily required a representation of the water table within the model domain. The preset parameter values for sand and sandy loam were used to compute the moisture retention curves. The Van Genuchten parameters for sand were used to represent gravel as sand represented a highly porous, permeable soil type and the Van Genuchten parameters for gravel were not found in the literature reviewed.

After numerous checks of the input values, units used, and trying different boundary conditions, convergence difficulties still persisted. Hence, help was sought from the EMS-i Technical Support (software vendor) and also several internet-based forums for possible solutions to similar problems that other GMS-FEMWATER users might have encountered. Suggestions were made by many GMS-FEMWATER users on several interne-based forums, and EMS-i Technical Support that the sharp curvature of the soil moisture retention curves resulted in non-convergent, oscillating solutions in FEMWATER. It was suggested to manually manipulate the soil moisture retention curves by flattening or smoothing the sharp change in curvature and thus alleviate the convergence difficulties. The manipulation of the soil moisture retention curves was found to produce convergent solutions, but at the expense of heavily compromising the accuracy of the soil property curves.

Next, the analysis options were input. The option for a flow-only type, transient simulation was selected. In problems with large partially unsaturated regions such as the one beneath the drainfield, the larger the unsaturated zone, the more difficult it was to get FEMWATER to converge. For these types of problems, the Nodal/Nodal quadrature option is generally selected as it is more stable than the more accurate Gaussian/Gaussian quadrature. Thus, the Nodal/Nodal quadrature was selected as an unsaturated depth of 79.5 feet was being simulated in the current model. The Crank-Nicholson Central weighting scheme was selected as it is more suitable to theoretical studies. The mass lumping and spline-smoothing of unsaturated curves were also selected as these help in reducing the convergence difficulties during simulation.

Non-linear equations used in unsaturated zone flow simulations require an estimate of pressure head values for their solution. Relaxation parameters in FEMWATER are the variables involved in selection of an estimate of the pressure head needed to compose the matrix equation. There are three types of relaxation parameters in FEMWATER for estimating pressure head values based on previous guesses, and newly obtained values: (1) under-relaxation, (2) exact relaxation, and (3) over-relaxation. The relaxation parameters provide guidance to the progress of simulation based on the type of convergence difficulties encountered. If convergence history shows signs of oscillations then under-relaxation should be used. If convergence history shows a slow monotonic decrease in the computed pressure head values then over-relaxation should be used. Initially the exact relaxation method is preferred, and if it does not produce a convergent solution then the other methods are employed. In the current model, exact relaxation was selected initially, which was later modified to over-relaxation as the convergence history showed a slow monotonic decrease in computed pressure head values while using exact relaxation.

Next, the iteration parameters were selected. The maximum number of iterations for non-linear flow was initially selected to be 40 and later increased to alleviate convergence difficulties. The maximum cycles/time-steps for variable boundary conditions was initially selected to be 1 and was later successively increased up to 100 to reduce convergence difficulties. The maximum iterations to solve the linear equations was assigned a value of 400 to start with and later increased up to 1800, most linear equations converged at this value. The steady-state convergence criterion, though not required for a transient simulation, was assigned a value of 0.001 ft, as it was used later when the transient simulation was converted to a steady-state simulation by slight modification of input parameters. The transient-state convergence criterion was initially assigned a value of 0.001 ft and later successively increased up to 10 to achieve convergence.

Next, the time control options were selected. The maximum time of simulation was set at 12 days as it was considered a sufficient duration to produce clearly observable changes in the pressure head distribution in the model. The constant time-step interval was successively reduced from 1 day to $1x10^{-4}$ day without any stable solution to the simulation. These options were different from those used for MODFLOW-SURFACT as FEMWATER was only being tested during these simulations.

The boundary condition simulated in the model was the specified flux boundary condition. The flux was constant and positive over the trench surface and negative (ET) elsewhere around the trench. The positive flux simulated the infiltration of water through the trench and the negative flux simulated ET from the areas surrounding the trench. The boundary condition was selected using the Map module and was later applied to the FEMWATER code by using the "Map→ FEMWATER" command.

The cold start initial condition option was selected for the simulation. As the topography of the model was flat and the water table was also expected to be flat. The option to apply a level groundwater table was selected. The initial condition was input in terms of the pressure head. A constant total head value of -79.5 ft for the surface of the model was entered. The constant total head value is interpreted by FEMWATER to mean that the water table elevation is equal to the pressure head minus the model surface elevation. Thus the groundwater table elevation was 0.5 ft for the data input above. The options for the initial conditions were stored in the Model file, but the pressure head data was stored in the Initial condition file.

The simulation file was then saved in a separate directory and executed. To perform the steady-state simulations, the transient-state simulation file was saved under a separate file name, and only the option for the type of simulation was modified from transient-state simulation to steady-state simulation. All other data in the simulation remained same and did not affect the performance of the steady-state simulation.

CHAPTER 4

RESULTS AND DISCUSSION

4.1 Introduction

This study used the GMS-FEMWATER and MODFLOW-SURFACT numerical codes to model flow near an ETA drainfield trench. The FEMWATER code developed convergence difficulties during the simulation process and could not successfully model the ETA trench conditions. The problems encountered with GMS-FEMWATER are discussed later in this chapter. MODFLOW-SURFACT was successful in providing numerical solutions for flow near the ETA trench with limitations resulting due to the unrealistic simulation of evapotranspiration process in the model. All simulations performed with MODFLOW-SURFACT converged within the set criteria and the results of the simulation are presented in the following sections.

4.2 MODFLOW-SURFACT Results

The results of the MODFLOW-SURFACT simulations were first verified in order to determine if the input values of net application rate, precipitation rate, and ET rate were accurately processed in the simulations. Since the cumulative recharge and negative recharge varied only with respect to ET-domain size, diagnostic output results were verified for SL-A and SL-B simulations only. The total recharge and ET values were hand-calculated from the net application rate, precipitation, and ET for the two ET domain sizes A and B. The values were accumulated over several consecutive 30 day runs from 01/15/2000 so that the hand-calculated values could be compared with the values printed in the diagnostic output at the end each simulation within the SL-A or SL-B simulation model. The diagnostic output in MODFLOW-SURFACT printed cumulative values of total recharge (precipitation and application) and total negative recharge (ET) at the end of the 9th time-step of the last stress period of sub-simulation. The total recharge in to the model domain was hand-calculated as the sum of net application rate and precipitation rate, while the total negative recharge was equal to ET.

4.2.1.1 Verification of type-A simulation

The hand-calculated recharge and negative recharge values for ET domain type A were compared with values obtained from the diagnostic output files for each 30-d sub-simulation of the SL-A simulation. Table 4.1 compares the recharge values from the diagnostic output and the hand-calculations, while Table 4.2 compares the negative recharge values from the diagnostic output and hand-calculations. It can be seen from Tables 4.1 and 4.2 that the maximum error between the hand-calculated values and the values from the diagnostic output file was less than 4 percent, which was within the acceptable level of error of 5 percent for this study.

Table 4.1 Comparison of calculated and model output values of total recharge for SL-A simulation

Date	Recharge IN (ft^3)	Calculated Recharge-IN (ft^3)	% Error
2/13/2000	1127.20	1125.97	-0.11
3/14/2000	838.87	835.73	-0.38
4/13/2000	1816.90	1810.91	-0.33
5/13/2000	1031.80	1028.49	-0.32
6/12/2000	2393.40	2378.26	-0.64
7/12/2000	1591.00	1574.25	-1.06
8/11/2000	967.12	962.6	-0.47
9/10/2000	617.45	618.7	0.20
10/10/2000	543.76	539.77	-0.74
11/9/2000	1176.40	1180.46	0.34
12/9/2000	432.55	431.56	-0.23
12/31/2000	286.96	286.41	-0.19

Table 4.2 Comparison of calculated and model output values of total negative recharge for SL-A simulation

Date	Negative Recharge (ft^3)	Calculated Negative Recharge (ET) (ft^3)	% Error
2/13/2000	1352.30	1351.79	0.04
3/14/2000	1858.50	1854.28	0.23
4/13/2000	1738.10	1734.64	0.20
5/13/2000	4322.30	4325.15	-0.07
6/12/2000	2800.10	2791.41	0.31
7/12/2000	3072.70	3069.07	0.12
8/11/2000	1320.40	1332.07	-0.88
9/10/2000	2488.60	2492.97	-0.18
10/10/2000	2368.30	2366.75	0.07
11/9/2000	217.71	209.04	3.98
12/9/2000	237.18	241.12	-1.66
12/31/2000	230.10	234.28	-1.82

4.2.1.2 Verification of type-B simulation

The hand-calculated recharge and negative recharge values for ET domain type B were compared with values obtained from the diagnostic output files for each 30-d sub-simulation of the SL-B simulation. Table 4.3 compares the recharge values from the diagnostic output and the hand-calculations, while Table 4.4 compares the negative recharge values from the diagnostic output and hand-calculations. It can be seen from Tables 4.3 and 4.4 that the maximum error between the calculated values and the values from the diagnostic output file was less than 4.2 percent, which was within the acceptable level of error of 5 percent for this study.

Table 4.3 Comparison of calculated and model output values of total recharge for SL-B simulation

Date	Recharge IN (ft^3)	Calculated Recharge-IN (ft^3)	% Error
2/13/2000	1113.8	1113.27	-0.05
3/14/2000	822.87	822.93	0.01
4/13/2000	1478.3	1480.16	0.13
5/13/2000	955.76	955.82	0.01
6/12/2000	1681.4	1681.46	0.00
7/12/2000	1171	1170.99	0.00
8/11/2000	852.45	852.49	0.00
9/10/2000	617.45	618.7	0.20
10/10/2000	541.1	539.36	-0.32
11/9/2000	840.45	845.37	0.58
12/9/2000	392.55	392.57	0.01
12/31/2000	278.97	279.01	0.01

Table 4.4 Comparison of calculated and model output values of total negative recharge for SL-B simulation

Date	Negative Recharge (ft^3)	Calculated Negative Recharge (ET) (ft^3)	% Error
2/13/2000	741.08	740.81	-0.04
3/14/2000	1018.5	1016.19	-0.23
4/13/2000	952.54	950.62	-0.20
5/13/2000	2368.7	2370.28	0.07
6/12/2000	1534.5	1529.75	-0.31
7/12/2000	1683.9	1681.92	-0.12
8/11/2000	723.62	730	0.87
9/10/2000	1363.8	1366.2	0.18
10/10/2000	1297.9	1297.03	-0.07
11/9/2000	119.31	114.56	-4.15
12/9/2000	129.98	132.14	1.63
12/31/2000	126.1	128.39	1.78

4.2.2 Soil Characteristic Curves in MODFLOW-SURFACT

In the MODFLOW-SURFACT simulations, the Van Genuchten parameters, alpha and beta for sandy loam and sandy clay loam soils were input. The residual water saturation and porosity values were also input for each soil type included in the model. The values of the Van Genuchten parameters, residual water saturation and porosity are shown in Table 3.2. The input of these values was sufficient for the model to perform unsaturated zone flow simulations. The soil characteristic curves showing the relationship between pressure head and moisture content, and pressure head and hydraulic conductivity are included below to illustrate the fundamental relationships on which the results of the simulations in this study are based. The Van Genuchten parameters, residual water saturation and porosity values used to plot these curves were used from Table 3.2 and 3.3. Figures 4.1 and 4.2 show the soil characteristic curves for sandy clay loam soil, while Figures 4.3 and 4.4 show the soil characteristic curves for sandy loam soil.

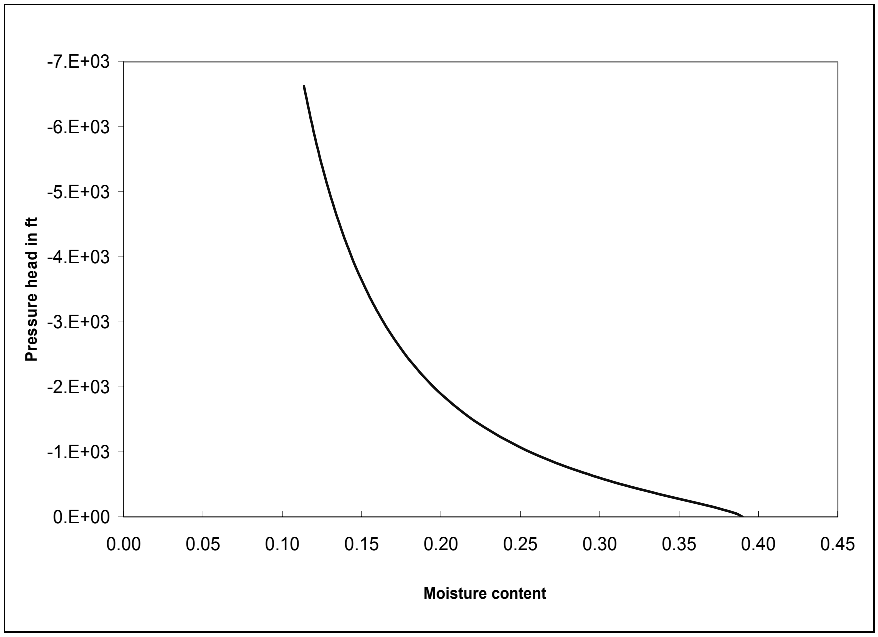

Figure 4.1 Soil characteristic curve showing relationship between pressure head and moisture content for sandy clay loam soil

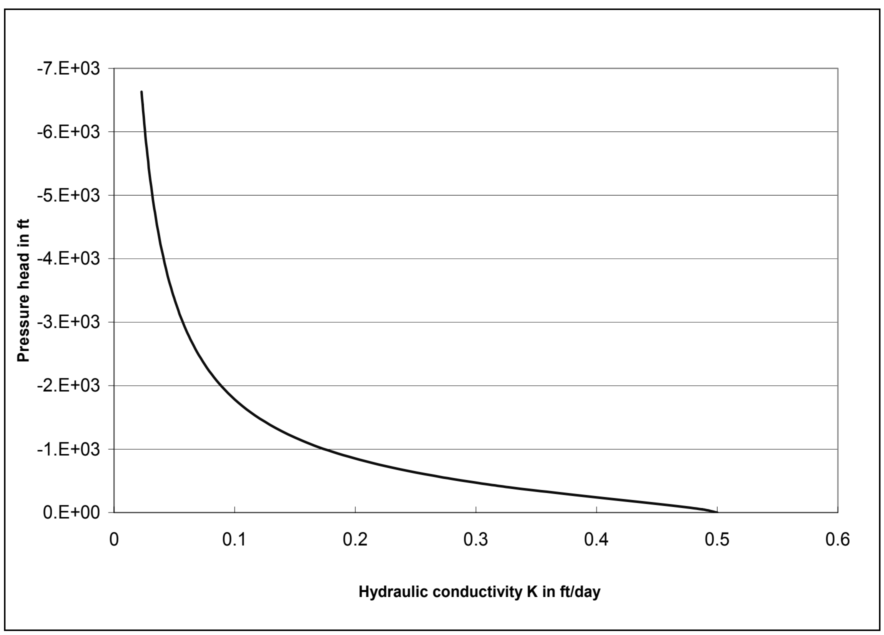

Figure 4.2 Soil characteristic curve showing relationship between pressure head and hydraulic conductivity for sandy clay loam soil.

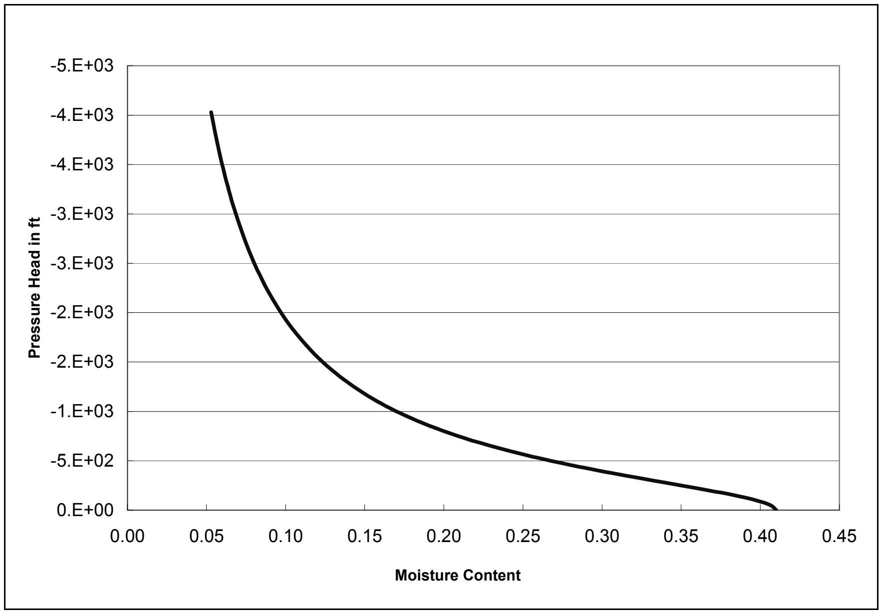

Figure 4.3 Soil characteristic curve showing relationship between pressure head and moisture content in sandy loam soil.

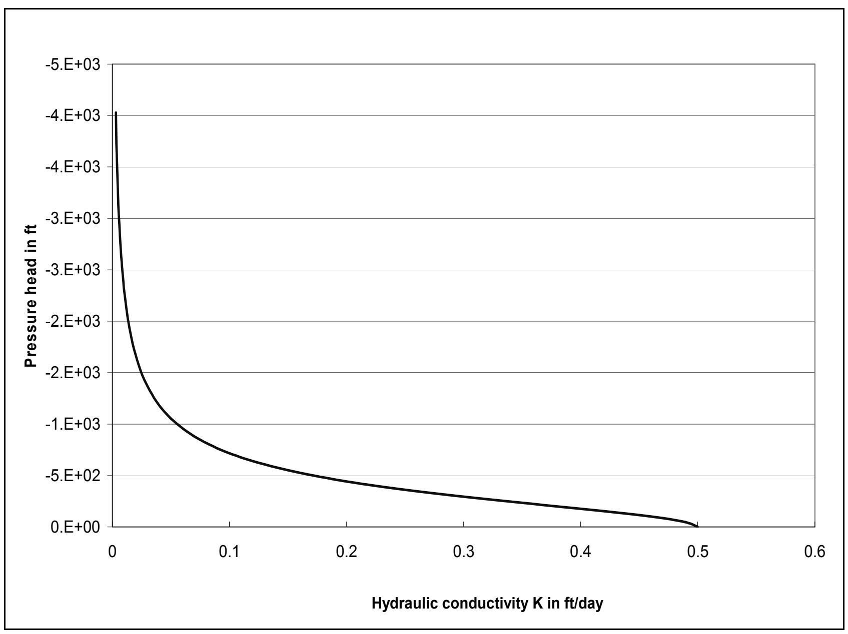

Figure 4.4 Soil characteristic curve showing relationship between pressure head and hydraulic conductivity in sandy loam soil.

4.2.3 Processing of results

The post-processing tools in GroundWater Vistas were used to graphically view the results of the MODFLOW-SURACT simulations. Contour maps of water saturation were plotted at the 9th time-step of the last stress period of each 30-d sub-simulation within the SLA, SLB, SCLA and SCLB runs. The water saturation contours were plotted in plan view for the top layer of the model, and as cross-sectional views along the 30th row and 30th column of the model domain. Please refer to Appendix D for plan and cross-sectional views of the contour maps plotted in this study. Vector plots in cross-sectional and plan views were also plotted after every 120 days during the simulation period to demonstrate the direction of flow in the subsurface and to provide a better understanding of the actual subsurface flow taking place. Distinct water saturation contour levels were selected for SL and SCL type simulations, such that the dimensions of the selected contour level could be measured and compared in the plan and cross-sectional views for all printed contour plots for a particular run. The selected saturation contour was monitored over the entire span of the run, and used to compare the size of the wetted area due to applied water and precipitation and movement of the infiltration depth over the entire span of the simulation. The simulations are discussed individually and compared in the following sections.

4.2.4 Comparison of loading pattern with respect to ET domains A and B

In this study, two ET domain sizes, A (60 ft by 60 ft) and, B (40 ft by 50 ft) were tested. The ET domain represented the area surrounding the ETA trench that influenced removal of water due to ET from the trench. An appropriate size of ET domain is critical in modeling an ETA trench, as disproportionately large or small ET domain sizes may provide misleading results. A very large ET domain size may indicate that water is lost from the whole domain primarily due to ET, while a very small ET domain size may indicate that water is lost mainly due to infiltration from the trench. The SL-A and SCL-A runs had similar loading pattern and the SL-B and SCL-B runs had similar loading patterns. Thus loading patterns depended on the ET domain size and not on the soil type selected for the simulation run. The simulations with ET domain type A indicated that the total water loss due to ET from the model was typically more than the total applied water to the drainfield during the simulation run. Also, background moisture from the soil surrounding the trench was removed, making the soil dry, which resulted in very high pressure gradients for lateral flow of water from the ETA trench. The high pressure gradients do not well represent actual field conditions; hence a smaller sized ET domain was applied to better display any changes in infiltration depth and/or wetted area.

To better compare seasonal variations in infiltration depth and lateral extent of the wetted area around the ETA trench, the ratio of total recharge over ET was calculated for each 30-d sub-simulation. A ratio of 1.3 or higher indicated a very wet period (W), while a ratio of 0.7 or less indicated a very dry period (D). Ratios from 1.1 to 1.3 were indicative of slightly wet periods (S_w) and those from 0.9 to 0.7 indicated slightly dry periods (S_d). Ratios from 0.9 to 1.1 were considered stable (S) as recharge was approximately equal to ET. Hereafter in this study, months are used instead of dates to give the reader an idea about the seasonal variation of weather throughout the year. The last two sub-simulations end in the month of December and hence are differentiated by labeling the last sub-simulation as December-2 and the second last sub-simulation as December-1. As shown in Tables 4.5 and 4.6 the weather conditions for ET domain type A and type B were similar, but not equal, for the months of May (D), June (S), September (D), October (D), November (W), and December-1 (W). Thus, change in ET domain size was found to significantly alter the impact of weather conditions on the ETA trench and thus made a significant change in results.

Table 4.5 Designation of weather conditions to specific months in the SL-A simulation

Month	Recharge (ft^3)	ET (ft^3)	Ratio Recharge/ET	Designation
Feb	1127.20	1352.30	0.8	S_d
Mar	838.87	1858.50	0.5	D
Apr	1816.90	1738.10	1.0	S
May	1031.80	4322.30	0.2	D
Jun	2393.40	2800.10	0.9	S
Jul	1591.00	3072.70	0.5	D
Aug	967.12	1320.40	0.7	S_d
Sep	617.45	2488.60	0.2	D
Oct	543.76	2368.30	0.2	D
Nov	1176.40	217.71	5.4	W
Dec-1	432.55	237.18	1.8	W
Dec-2	286.96	230.10	1.2	S_w

Table 4.6 Designation of weather conditions to specific months in the SL-B simulation

Month	Recharge	ET	Ratio	Designation
	(ft^3)	(ft^3)	Recharge/ET	
Feb	1113.80	741.08	1.5	W
Mar	822.87	1018.50	0.8	S_d
Apr	1478.30	952.54	1.6	W
May	955.76	2368.70	0.4	D
Jun	1681.40	1534.50	1.1	S
Jul	1171.00	1683.90	0.7	S_d
Aug	852.45	723.62	1.2	S_w
Sep	617.45	1363.80	0.5	D
Oct	541.10	1297.90	0.4	D
Nov	840.45	119.31	7.0	W
Dec-1	392.55	129.98	3.0	W
Dec-2	278.97	126.10	2.2	W

The cumulative recharge and ET for the twelve 30-d sub-simulations with ET domain type A and type B are shown in Figures 4.5 and Figure 4.6, respectively. It can be seen from the two figures that the values of ET in Figure 4.6 are significantly less those in Figure 4.5. This difference results from the reduction in ET domain size in simulation model with ET domain type B.

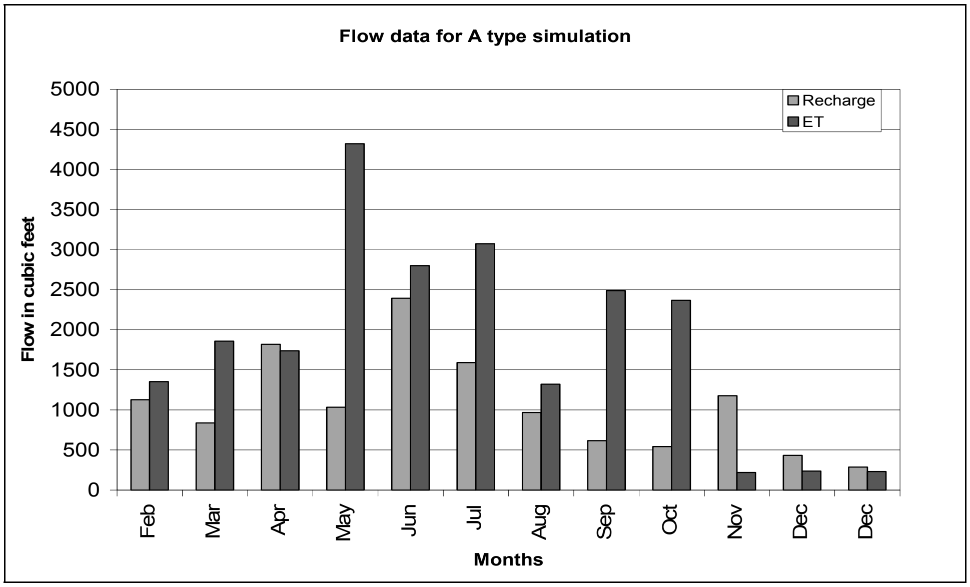

Figure 4.5 Cumulative recharge and ET variation over the SL-A simulation run

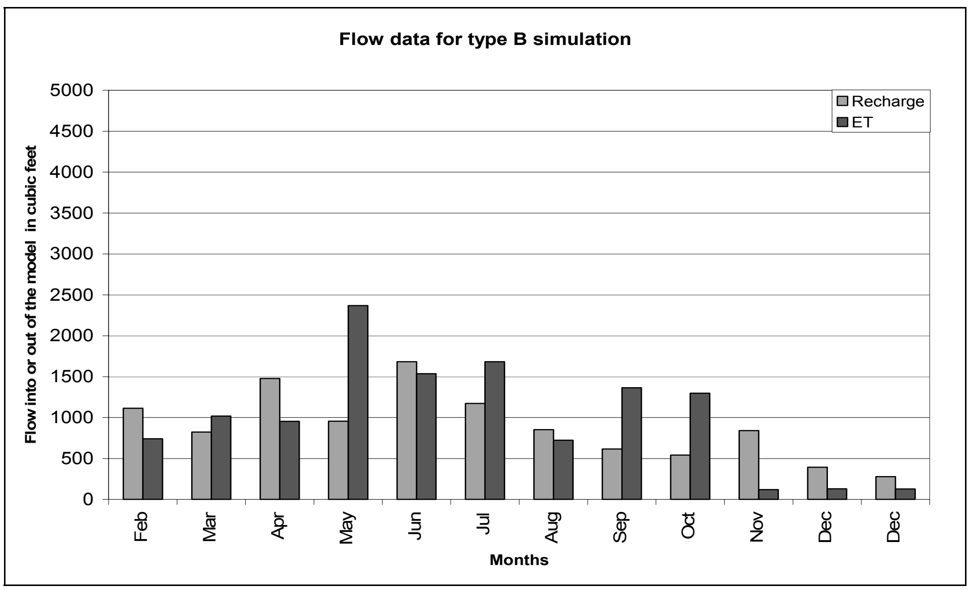

Figure 4.6 Cumulative recharge and ET variation over the SL-B simulation run

4.2.5 Results of Simulations Performed

The results of each simulation performed in this study are presented in the following paragraphs. Selected simulation runs are then compared with each other with respect to infiltration depth, and north-south lateral extents of wetted area. Measurements of infiltration depth, north-south lateral extent, and east-west lateral extent of the wetted area were taken from the water saturation contours printed with the help of the post-processing tools in GroundWater Vistas. Measurements were taken from the contour plots included in Appendix D.

The initial water saturation in the sandy loam soil was 0.48 and water saturation contours at a saturation level of 0.49 were typically considered in the SL-A and SL-B runs to monitor the wetted area and infiltration depth. The initial water saturation in case of SCL-A and SCL-B runs was 0.52 and a saturation level of 0.59 was monitored in these simulation runs. Although the selected saturation level for a simulation run does not accurately represent the actual wetted area or the actual infiltration depth, it does however, give a relatively close approximation of the wetted area and infiltration depth. The monitoring of the approximated wetted area and infiltration depth provide information about the seasonal variation of the size of actual wetted area, and infiltration depth.

The east-west lateral extent of the saturation contour was measured along the length of the trench (20 ft), while the north-south lateral extent of the saturation contour was measured along the width of the trench (3 ft). Thus the sideward distance traveled by water from the trench in the east-west direction is equal to the east-west lateral extent of saturation contour minus length of the trench (20 ft). The sideward distance traveled by water from the trench in the north-south direction is equal to the north-south lateral extent of the saturation contour minus width of the trench (3 ft).

4.2.5.1 SL-A Simulation

The SL-A simulation run was analyzed for variation of the wetted area dimensions and infiltration depth over a 352 day period. At times when the water saturation contour of 0.49 was not displayed in the contour map, lower values of water saturation contours were selected. It is seen in Figure 4.7 that infiltration depth of water was as high as 12 ft in the first month of February; dropped sharply after the very dry month of May, and then remained below 5 ft for the rest of the simulation. The lateral extent of the wetted area was comparatively larger than the infiltration depth, which indicated the predominance of lateral movement of water over downward movement from the trench. The applied water from the trench spread more in the north-south direction as compared to the east-west direction, as the largest side (20 ft) of the trench allowed more water to spread in the north-south direction. Dimensions of the wetted area reduced substantially after the very dry month of May and more or less remained constant till the end of the simulation.

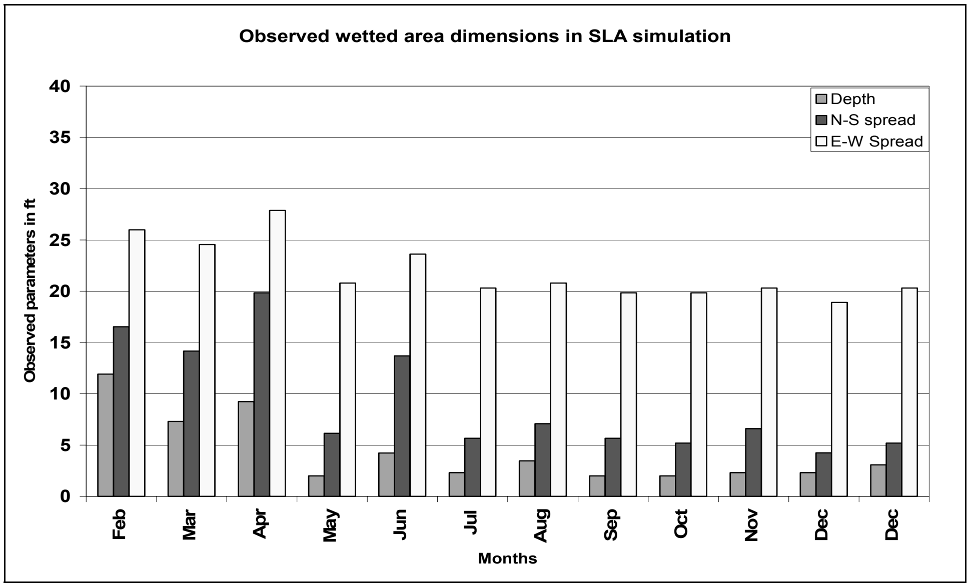

Figure 4.7 Variation of water saturation contour dimensions over the SL-A simulation

4.2.5.2 SL-B Simulation

The SL-B simulation was analyzed in the same way as the SL-A simulation. Water saturation contours at a saturation level of 0.49 were measured from the contour maps plotted for each month of the simulation. Lower saturation level values were considered whenever the saturation level of 0.49 was not displayed in the contour map. It can be seen from Figure 4.8 that maximum infiltration of water to a depth of 24.5 ft was found in the month of April, which was designated as a very wet month (recharge/ET = 1.6). The lateral dimensions of the wetted area were relatively larger than the infiltration depth, which indicates that there was more lateral movement of water from the trench as compared to downward movement. Infiltration depth steadily increased from the months of October to December with relatively less change in lateral extent of wetted area. During the wet periods more water is lost to infiltration than evapotranspiration, and hence the wetted area dimensions remains relatively constant and the excess water is infiltrated. During the month of June, which was a stable period preceded by a very dry period, the lateral extent of the wetted area increased significantly as compared to infiltration as more water moved laterally due to the high pressure gradients created in the soil surrounding the trench in the very dry month of May (recharge/ET=0.4).

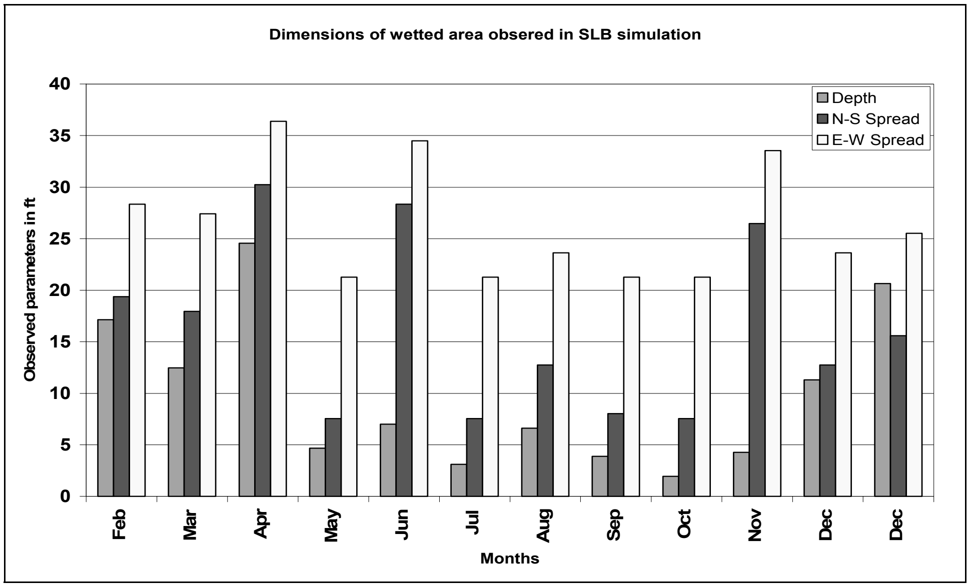

Figure 4.8 Variation of saturation contour dimensions over the SL-B simulation run

4.2.5.3 SCL-A Simulation

The SCL-A simulation was analyzed for the variation of infiltration depth and wetted area lateral extent over the 352-day simulation run. Water saturation contours at a level of 0.58 were plotted, and dimensions of the contour were measured in the plan view and the cross-sectional views. Please refer to Figure 4.9 for variation of wetted area dimensions in the SCL-A simulation. The maximum infiltration of water in the SCL-A simulation was 21 ft during the month of February. The infiltration depth remained fairly constant till the month of April, after which it dropped to 10 ft, as May was a very dry month and a lot of water was removed by ET. The infiltration depth from the month of May remained at approximately 5 ft for the remaining months of the simulation. The lateral extent of the wetted area increased in the months of November to December as these were wet months, which were preceded by very dry months and hence there was more lateral movement of water compared to downward movement.

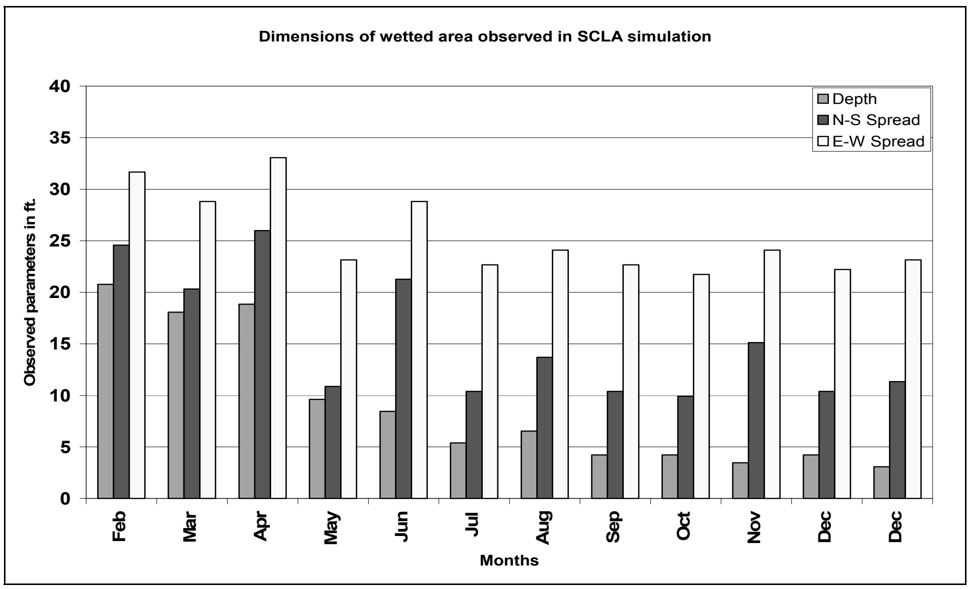

Figure 4.9 Variation of water saturation contour dimensions over the SCL-A simulation

4.2.5.4 SCL-B Simulation

Infiltration depth and lateral dimensions of the wetted area were analyzed by measuring the water saturation contours plotted typically at a level of 0.58 in the plan view and cross-sectional views for the SCL-B simulation run. Please refer to Figure 4.10 for variation of wetted area dimensions in the SCL-B simulation. The infiltration depth in SCL-B simulation was found to be maximum in the month of May, which was a very dry month preceded by a wet period. The reason for the infiltration even during a dry period may be explained by the fact that sandy clay loam soils have a higher percentage of clay and smaller pore diameters, which result in relatively high capillary forces. Thus the water that entered the sandy clay loam soil in the month of April was not completely removed in spite of the ET acting on the surface. However, one can see the delayed response by the fact that the infiltration depth drops sharply in the month of June, even though it was a stable month with similar values of recharge and ET. The lateral extent of the wetted area was larger than infiltration depth, which indicates relatively more lateral movement than downward movement. Sandy clay loam does seem to respond slowly to changing patterns of weather as there was rarely a sharp change in wetted area dimensions or infiltration depth during the simulation.

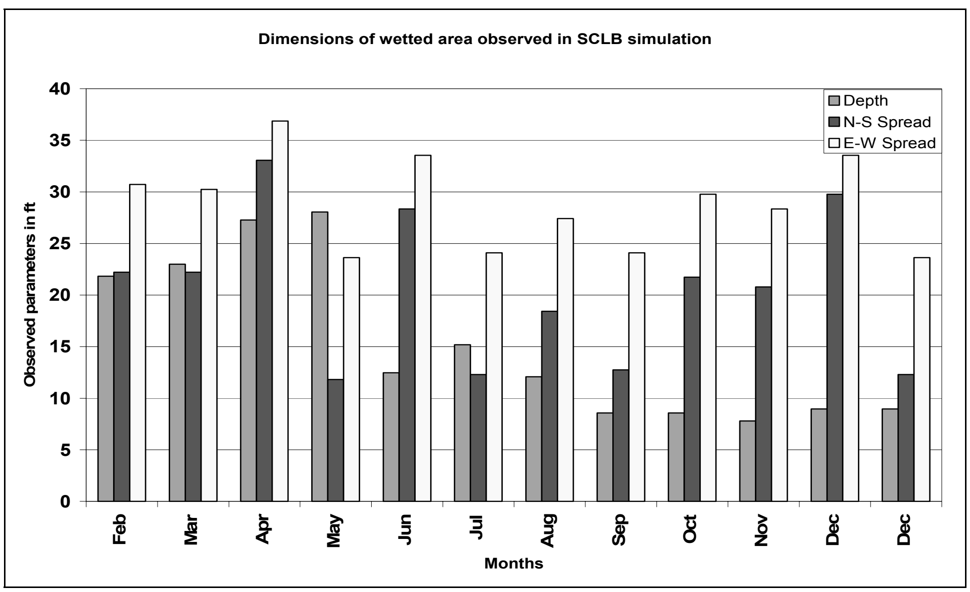

Figure 4.10 Variation of water saturation contour dimensions over the SCL-B simulation

4.2.6 Comparison of simulations

The following sections compare the infiltration depth and north-south lateral extent for particular months between different simulations. The differences between the observations are discussed relative to variations between the simulated conditions.

4.2.6.1 SL-A and SL-B simulations

The SL-A and SL-B simulations varied in the size of ET domains. Please refer to Figures 4.11 and 4.12 for comparison of infiltration depth, and north-south lateral extent of wetted area, respectively, between the two simulations. It can be observed from Figure 4.11 that the infiltration depth in case of the SL-B simulation is consistently larger as compared to the SL-A simulation. SL-B simulations were received much less ET than SL-A simulations, hence the trench in the SL-A simulations lost more of its water to ET while the trench in the SL-B simulation lost some water to ET and more to infiltration. It can be seen in Figure 4.12 that the north-south lateral extent was consistently higher in case of SL-B simulations as compared to SL-A simulations. The larger lateral extent of the wetted area in the SL-B simulation is mainly due to the fact that less water was evaporated from a smaller ET domain size in the SL-B simulation. Thus, it is speculated that the ET domain type B is more realistic in simulating weather conditions in an ETA drainfield model as compared to ET domain of type A.

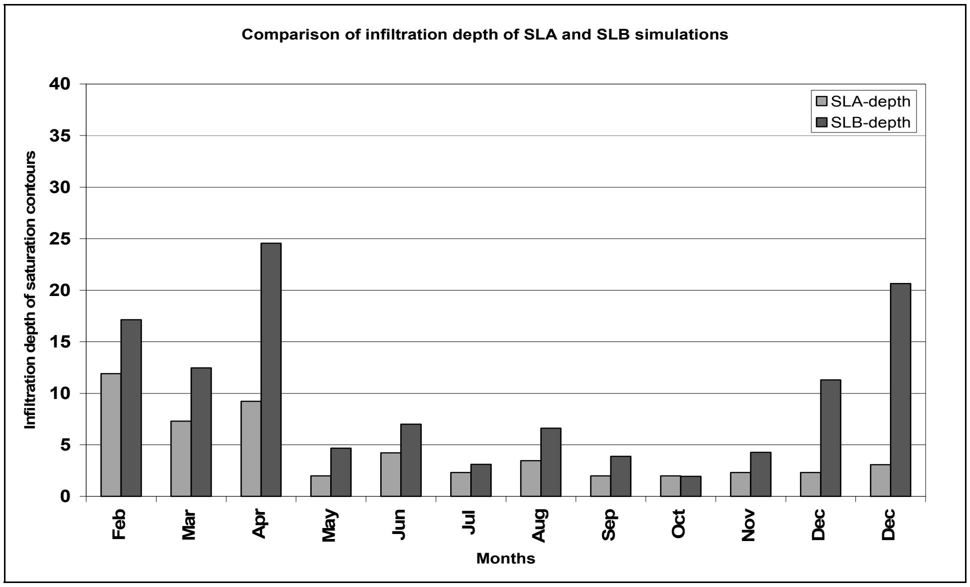

Figure 4.11 Comparison of the variation of infiltration depth over the SL-A and SL-B simulation runs

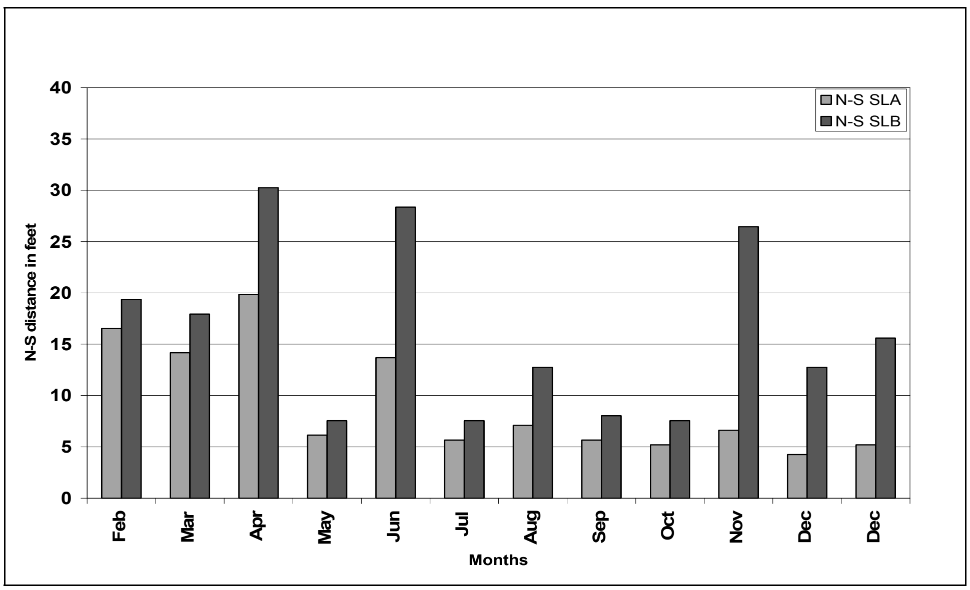

Figure 4.12 Comparison of variation of north-south lateral extent of wetted area in SL-A and SL-B simulation runs

4.2.6.2 SL-B and SCL-B simulations

The SL-B and SCL-B simulations differed in the type of local soil. Figures 4.13 and 4.14 show a comparison of infiltration depth and north-south lateral extent of wetted area, respectively, between the two simulations. It can be seen from Figure 4.13 that the infiltration depth in SCL-B was consistently higher than the infiltration depth in SL-B, except for the month of December. The larger infiltration depth in the SCL-B simulation can be explained by the fact that the sandy clay loam soil has a higher percentage of clay as compared to sandy loam soil, which results in higher capillary forces. Higher capillary forces help in retaining water in the soil at low pressure heads. Thus, water was retained in the sandy clay loam soil and infiltrated by capillary forces in the downward direction, while more water was removed due to ET from a sandy loam soil, which has lower capillary forces, and hence less capacity to retain water. Also, infiltration of water is faster in sandy loam soil than in sandy clay loam soil as pore diameters in sandy clay loam soil are smaller than in sandy loam soil. Differences in pore diameter and capillary forces results in higher infiltration of water in sandy loam soil during the wet months of December-1 and December-2. Figure 4.14 shows the north-south lateral extent of wetted area for SCL-B and SL-B simulations. It can be seen that the lateral extent of wetted area in SCL-B simulation was almost always greater than the SL-B simulations. The reason for the greater lateral extent of wetted area in SCL-B simulations was also due to the capacity of sandy clay loam soil to retain more water than sandy loam soil.

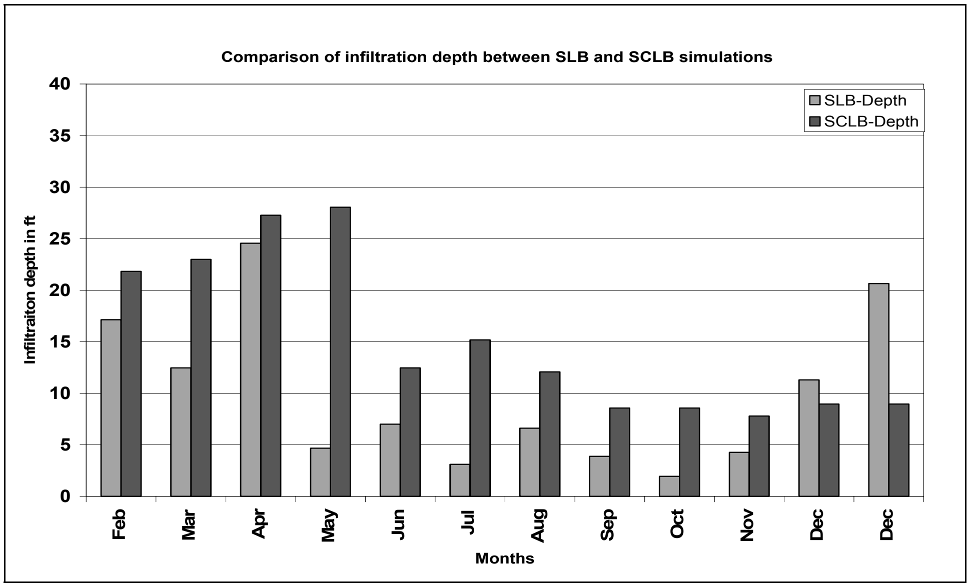

Figure 4.13 Comparison of the variation of the infiltration depth in SL-B and SCL-B simulation runs

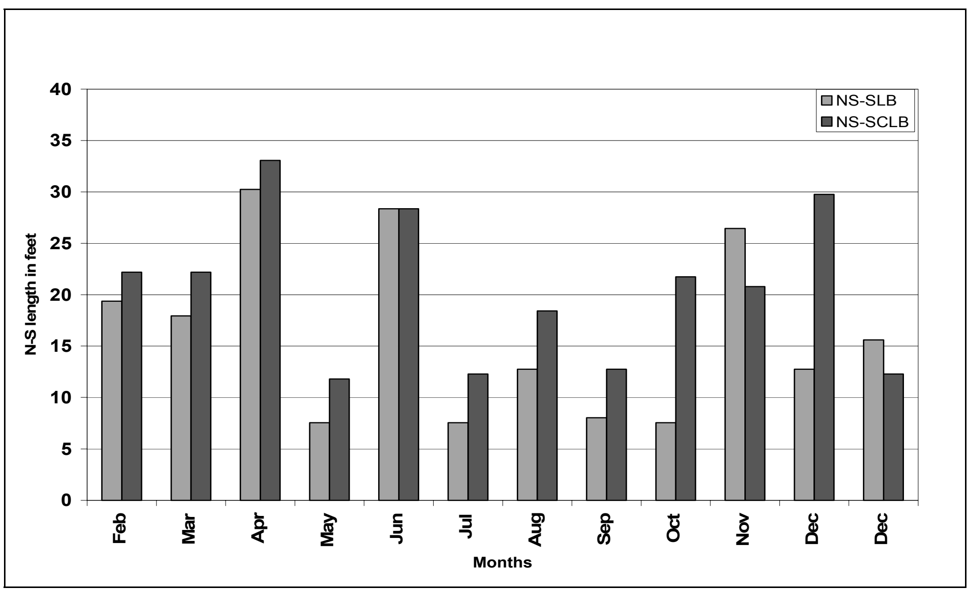

Figure 4.14 Comparison of the variation in north-south lateral extent of wetted area over the SL-B and SCL-B simulation runs

4.2.7 Implications

It can be seen from the above mentioned comparisons that sandy loam soil loses more water to ET per unit area as compared to sandy clay loam soil. This indicates that the ET area responsible for removing water from an ETA trench would have to be larger in case of sandy clay loam soil as compared to sandy loam soil for removal of the same amount of water by ET. Thus, it can be said that the ETA trenches in sandy clay loam soil will need greater set-back distances as compared to ETA trenches in sandy loam soils in order to make optimal use of the ET process.

4.3 FEMWATER Results

It was found that the steady-state simulation in FEMWATER did not converge. The spatial discretization of the model in the horizontal as well as in the vertical direction was made finer by reducing the spacing between the vertices used to create the finite element mesh. Spacing between vertices was initially entered as 5 ft and was successively reduced up to 0.5 ft. The layer thickness was initially set at 1 ft, which was further reduced to 0.5 ft. The residual error reduced as the mesh was made finer, and the time required for convergence for the first three time-steps also reduced to a certain extent. However, the mesh refinement had to be stopped after it was observed that the simulation began to blow up, i.e., residual errors to the order to 1×10^{37} and finally to -1.0 were observed.

In the transient simulation, similar problems with convergence were observed. In spite of a lowest constant time step of 1×10^{-4} day, the simulation converged only for the first three time-steps for the spatial discretization mentioned earlier and then began to blow up as mentioned in the case of the steady-state simulation. The initial time-step size was 1×10^{-4}.

It was observed that adjusting the material property curves resulted in faster convergence of the simulations. The material property curves were adjusted so as to have a smooth curve with fewer number of data points on them. Although this manipulation of material property curves resulted in convergence of the simulation, it was at the expense of accurate material property curves and resulted in inaccurate representation of soil properties. Thus, the reliability of the simulation results could not be discerned or quantified, and the FEMWATER code had to be abandoned for simulating the required ETA drainfield condition.

There were several suggestions from GMS-FEMWATER users that a trial-and-error approach be used to determine if the solutions converged by increasing the value of convergence criteria. Several attempts were made by increasing the steady-state and transient-state convergence criterion to significantly high values (10-100 ft) and see if the simulation converged. These attempts resulted in some converged time-steps initially, but eventually also failed at later times.

CHAPTER 5

CONCLUSIONS AND RECOMMENDATIONS

5.1 Conclusions

The goals of this thesis were to select and use a three-dimensional groundwater flow model capable of performing unsaturated zone flow simulations for modeling flow around an ETA drainfield trench. The goals were accomplished by performing simulations using the conceptual model of the ETA trench in MODFLOW-SURFACT and observed data from the Phase 1 study. Two types of soils (SL and SCL) with two different sizes of ET domain (A and B) were simulated by performing four separate simulation runs, and the following conclusions were reached.

- The finite element groundwater flow and transport modeling code GMS-FEMWATER was unable to provide numerical solutions for flow near an ETA trench due to convergence difficulties during simulations.
- The finite difference groundwater flow and transport modeling code MODFLOW-SURFACT was able to provide numerical solutions for flow near an ETA trench and was successfully used in this study.
- The negative recharge mechanism was used to simulate ET as the Evapotranspiration Package in MODFLOW-SURFACT does not remove moisture from the unsaturated zone.
- The total recharge and negative recharge rates were accurately processed by MODFLOW-SURFACT during the simulation of ET domain types A and B.

- The reduced ET domain size resulted in deeper infiltration of water into the soil and more lateral spread of water as compared to the simulation with bigger ET domain size.
- All four runs demonstrated that lateral movement of water was more predominant than downward movement, thus allowing removal by ET.
- The wetted area due to application of water to the ETA trench in the top layer of the model reduced significantly during dry periods in sandy loam soil.
- More water was lost to infiltration than to ET from the trench during wet periods in sandy loam and sandy clay loam soils.
- Infiltration and retention of water in sandy clay loam soil was more than that in sandy loam soil due to relatively higher capillary forces in sandy clay loam soil.
- It was demonstrated by the simulation runs that no water infiltrated to the full depth of the model, which indicates that the ETA trench simulated did not make a significant contribution to groundwater recharge.

5.2 Recommendations

Results presented in this thesis are more qualitative than quantitative due to several assumptions made in the study. First, it was assumed that the soil properties remain constant with time, which may not be the case, as the application of effluent wastewater to the ETA trench may reduce the hydraulic conductivity of soil immediately surrounding the trench due to clogging of pores by the microorganisms or organic matter present in the wastewater effluent. Second, the ET area may vary in size due to seasonal variation, which was not simulated in this study. Observations of the ET area in the field indicated by wet soil and vegetation surrounding the trench should be made with respect to seasonal changes and actual size of the ET area should be assigned in the ETA trench model. Third, the mechanism of negative recharge was used to simulate ET in the model. The mechanism of negative recharge draws water from the full depth of the model whereas ET is typically considered to remove water only down to a certain depth from the soil surface, which is limited by the depth of the root zone of the plants. Thus, modification of existing modules in MODFLOW-SURFACT or development of new modules that simulate ET appropriately in the unsaturated zone simulations needs to be done.

Field observations on the test site as part of the Phase 1 study indicate that the lateral spread of ET area for ETA trenches was greater than 3 ft. Model observations seen from simulation results of the ETA trench model in this study demonstrate that the lateral spread of moisture was typically more than 3 ft. Hence it is likely that the current TCEQ drainfield requirements for set-back distance of 3 ft between trenches would be inadequate for ETA trenches due to overlapping of ET areas between the trenches. The set-back distance in case of ETA trenches would be a function of the local soil type and needs to be revised depending on the soil conditions.

REFERENCES

Celia, M.A., Bouloutas, E.T., and Zarba, A. (1990). “A general mass-conservative numerical solution for the unsaturated flow equation,” *Water Resources Research,* 26(7), 1483-1496.

Chen, S-K., Liu, W.C., and Huang, H-C. (2002). “Analysis of water movement in paddy rice fields (II) simulation studies.” *Journal of Hydrology*, 268(1-4), 259-271.

Computational Science Educational Project (1996). “Physics 594, Computational Science, LU Decomposition.” http://csep1.phy.ornl.gov/guidry/phys594/lectures/linear_algebra/lanotes/node3.html [accessed 08/23/2003]

Domenico A. P. and Schwartz W. F., (1990). “Elastic Properties and Main Equations of Flow.” *Physical and Chemical Hydrogeology,* John Wiley and Sons, New York, N.Y., 99-136.

Donherty, J. (2001). “Improved calculations for dewatered cells in MODFLOW.” *Ground Water,* 39(6), 863-869.

Evans, A.R., Turnbull, J.S., and Richards, R.D. (1995). “Use of DoD groundwater modeling system GMS to model the hydrodynamics of Central O’ahu, Hawaii.” *Water Resources and Environmental Hazards*; Emphasis on Hydrologic and Cultural Insight in the Pacific Rim; Proceedings, American Water Resources. (1995), Honolulu, Oahu, Hawaii, 257-266.

Fetter, W.C, (2001). *Applied Hydrogeology*, 4th Edition, Prentice-Hall Inc., Englewood Cliffs, NJ.

Heinzer, D.M. (1998). “Dewatering Analysis of the Dura Avenue Landfill in Toledo, Ohio Using Three Dimensional FEMWATER Analysis,” Master of Science Thesis, University of Toledo, Toledo, OH.

Hung, C. Y. (2002). “Evaluation of application of one-dimensional groundwater transport model to PRESTO-EPA model.” *Practice Periodical of Hazardous, Toxic and Radioactive Waste Management,* 6(1), 49-55.

Hydrogeologic, Inc., (1996). MODFLOW-SURFACT Software (Version 2.2) Overview: Installation, Registration, and Running Procedures. Herndon, VA.

Krambis, C. Jr. (2002). “Stratigraphy and hydrogeology of Northwest Aiken County, South Carolina,” Master of Science Thesis, Clemson University, SC.

Lin, H, J., and Deliman, N.P. (1995). "Application of GMS-FEMWATER Model to Two Case Studies Involving Flow and Transport." *Groundwater Management: Proceedings of the International Symposium Sponsored by the Water Resources Engineering Division*, American Society of Civil Engineers, in conjunction with the ASCE's First International Conference on Water Resources Engineering in San Antonio, Texas, (1995). San Antonio, TX, 407-411.

Lin, H. J., Richards, D. R., Talbot, C. A., Yeh, G. T., Cheng, J., Cheng, H., and Jones, N. L. (1997). "FEMWATER: A Three-Dimensional Finite Element Computer Model for Simulating Density-Dependent Flow and Transport in Variably Saturated Media." Technical Report CHL-97-12, U.S. Army Corps of Engineers Waterways Experiment Station, Vicksburg, MS, Department of Civil and Environmental Engineering, Pennsylvania State University, University Park, PA, and Department of Civil Engineering, Engineering Computer Graphics Laboratory, Brigham Young University, Provo, UT.

Mualem, Y. 1976. A new model for predicting the hydraulic conductivity of unsaturated porous media. *Water Resources Research*, 12, 513-522.

McReynolds, Don (1995). "Hydrologic Atlas of Lubbock County, Texas." *High Plains Underground Water Conservation District No. 1*, Lubbock, TX.

Ng, C.W.W., Wang, B., and Tung, K.Y. (2001). "Three-dimensional numerical investigations of groundwater responses in an unsaturated slope subjected t various rainfall patterns." *Canadian Geotechnical Journal*, 38(5), 1049-1062.

Ouyang, Y., and Zheng, C. (1999). "Density-Driven Transport of Dissolved Chemicals Through Unsaturated Soil." *Soil Science*, 164(6), 376-390.

Peng, W.-S., Benegar, J. J., Hampton, D. R., Konikow, L. W., and Kambham, K. (2000). "Can contaminant transport models predict breakthrough?" *Ground Water Monitoring and Remediation*, 20(4), 104-113.

Ronayne, M. J., Blandford, T. N., Earley, D, III, Schmidt-Peterson, Rolf. (1999). "Simulation of mine pit lake recovery in a block-faulted porphyry copper deposit." *Geological Society of America, 1999 Annual Meeting, Abstracts with Programs*. 31(7), 85.

Uwiera, M.M.E., and Reeves, J.M. (2000). "Three dimensional coupled brine transport simulation studies." *Computational Methods in Water Resources*. 1 & 2, 353-356.

Williams, A.G., Miller, T.C., Kelley, T.C., and Tocci, D.M. (1996). "Approaches to Modeling Richard's Equation." *Center for Multiphase Research News*, 2(2), 2-8.

Wolfram Research "Eric Weinstein's World of Mathematics, Terminology, Quadrature." http://mathworld.wolfram.com/Quadrature.html [accessed 11/07/2003]

Yeh, G. T. (1987b). "3DFEMWATER: A three-dimensional finite element model of water flow through saturated-unsaturated media." ORNL-6368, Oak Ridge National Laboratory, Oak Ridge, TN.

Yeh, G. T. (1990). "3DLEWASTE: A hybrid Lagrangian-Eulerian finite element model of waste transport through saturated-unsaturated media." *PSU Technical Report*, Department of Civil Engineering, The Pennsylvania State University, University Park, PA.

APPENDIX A

PROCEDURE FOR SETTING UP A MODFLOW-SURFACT SIMULATION MODEL USING GROUNDWATER VISTAS

PROCEDURE FOR SETTING UP A MODFLOW-SURFACT SIMULATION MODEL

USING GROUNDWATER VISTAS

A.1 Initialization

1) Start Groundwater Vistas. The following screen will appear.

Figure A.1 Groundwater Vistas start-up dialog.

2) Click on "*File*" menu and click on "*New*." This opens a new simulation file.

3) The new simulation file automatically opens an "*Initialize Model Grid*" dialog.

4) The "*Initialize Model Grid*" dialog is made up of three sections. (1) Horizontal Grid Information, (2) Vertical Model Grid, and (3) Default Parameter Values.

A.1.1 Horizontal Grid Information

1) Enter a value of 60 for number of rows.
2) Enter a value of 60 for number of columns.
3) Enter a value of 1 ft for Uniform X Spacing.
4) Enter a value of 1 ft for Uniform Y Spacing.

A.1.2 Vertical Model Grid

1) Enter a value of 46 for number of layers.
2) Enter a value of 0 ft for Bottom Elevation.
3) Enter a value of 80 ft for Top Elevation.
4) Select the check box next to "*Layers are Flat*."

A.1.3 Default Parameters Values

The data regarding the hydraulic conductivity was used from the phase 1 study of the septic tank drainfield.

Enter a value of 0.5 ft/d for K_x, K_y and K_z. K_x, K_y and K_z stand for hydraulic conductivity in the X, Y and Z directions respectively in the local soil.

1) Enter a value of $6.04x10^5$ for the Storage Coefficient (S).
2) Enter a value of 0.345 for Specific Yield (S_y).
3) Enter a value of 0.41 for Porosity.

4) Enter a value of 30 for the "*Maximum Number of Stress Periods*."

5) Accept all other default values as they are not required for a flow simulation.

6) Make sure that the "*Initialize Model Grid*" dialog looks similar to the one shown in Figure A.2.

7) Now, click *OK* to close the dialog. A rectangular mesh as shown in Figure A.3 will appear in a few seconds.

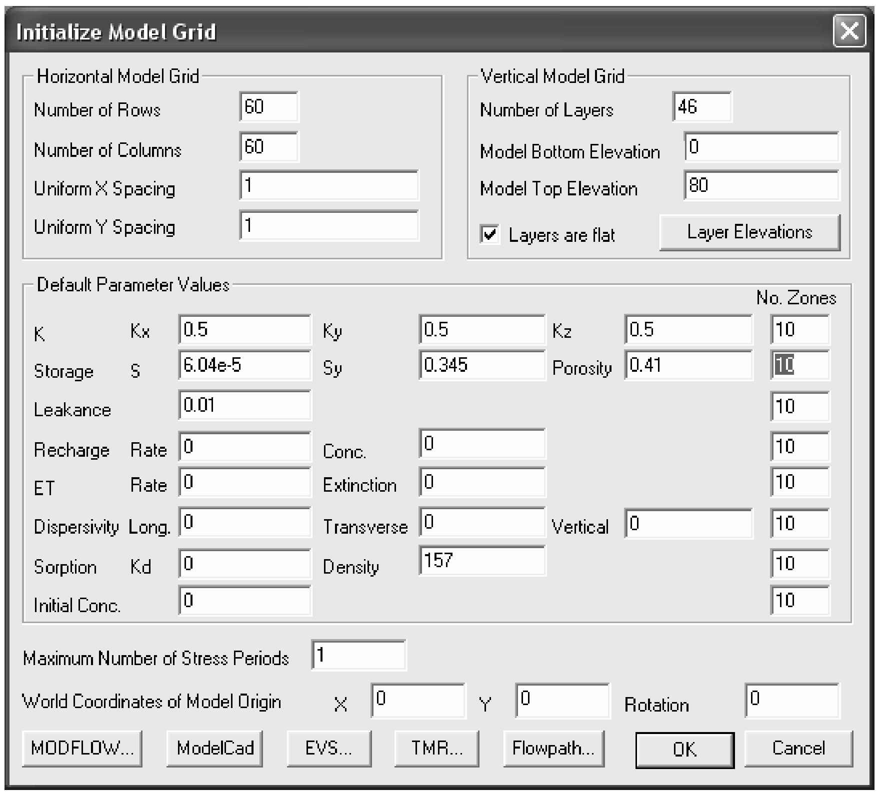

Figure A.2 GroundWater Vistas model grid initialization dialog.

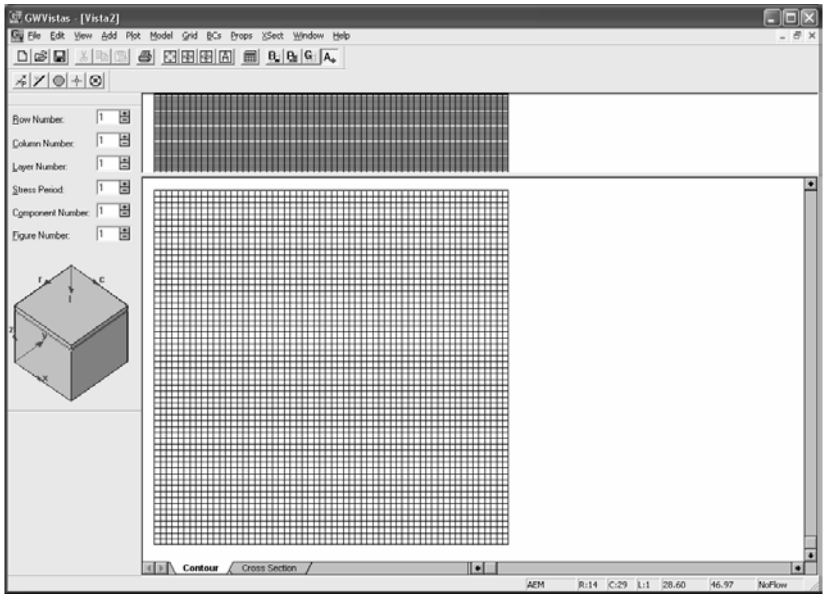

Figure A.3 Plan view of the model in GroundWater Vistas.

A.2 Setting Up Groundwater Vistas to Execute a Modflow-Surfact Simulation

1) Click on the "*Model*" menu and single click on "*Paths to Models*." A "*Path to Model Executables*" dialog opens.
2) Change the "*ModflowWin32*" option from "*Run-Execute*" to "*Do Not Use*."
3) Now change the "*Model information"* and "*Path and Code Name*" so that the MODFLOW-SURFACT numerical code executes the simulation when the run command is initiated in Groundwater Vistas.
4) Change the "*Path and Code Name*" for the "*model*" MODFLOW by browsing and selecting the MSFT.exe file. The default installation set up for MODFLOW-SURFACT creates a directory by the name MSVMS in the C drive of the

computer and saves the Msft.exe file in this directory. Thus the default "*Path and Code Name*" input is C:\MSVMS\Msft.exe.

5) Now, set up the working directory. The working directory is where all the files of the current simulation will be stored when created. Browse to the directory where you want the simulation files to be saved. The address to this directory is automatically input in the dialog.

6) Next, enter the command line in front of the space provided in the same line as the MODFLOW code and below the command line column. The command line was entered in the format 1<single space><filename>. The command line reads as 1 SepticSim, where SepticSim is the name of the file.

7) Make sure that the "*Path to Model Executables*" dialog looks exactly as the one shown in Figure A.4.

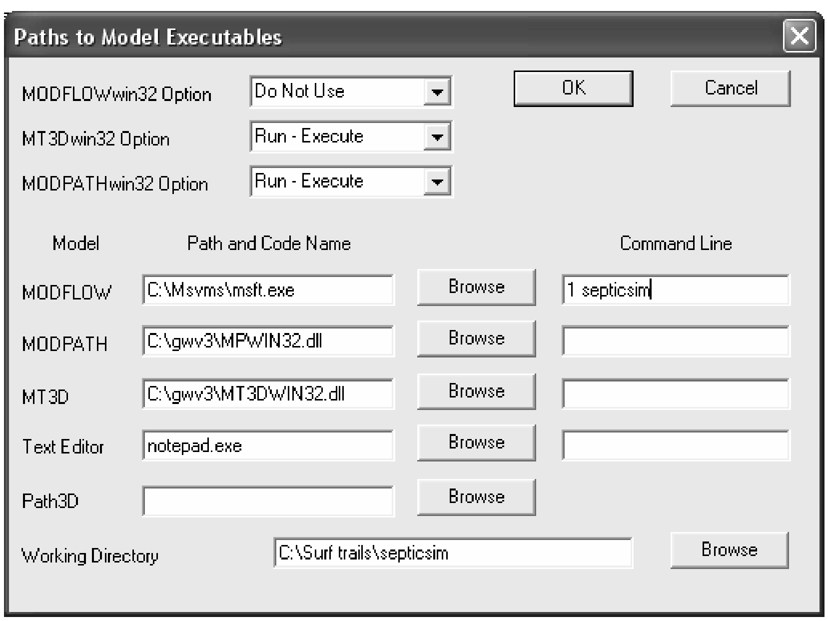

Figure A.4 Dialog showing input path to model executable files.

8) Click OK to close the dialog.

A.3 Selection of Modflow Packages for the Simulation

1) Click menu "Model"→ "*MODFLOW*" → "*Packages*". The "*Modflow Packages*" dialog opens up.
2) Enter the root file name in the top left corner of the dialog. The root file name is the file name of the simulation and in the present case is "SepticSim".
3) Change the *MODFLOW* version to *SURFACT*. This option is below the root filename input.
4) Assign a unit number, "*Unit No.,*" to the Modflow packages. Also, since we need to plot the vectors of various parameters in the results of the simulation, the "*cell-by-cell flow terms*" option should be selected for all the packages.
5) Click/Select the following packages and assign different values of Unit Number to them.
    a. Basic Package
    b. BCF Package
    c. Output Control Package
    d. Solver Package
    e. Drain Package
    f. Recharge Package
6) Next, select the type of solver that will be used to solve the differential equations in the simulation. The PCG4 solver is the most robust and efficient solver provided with the MODFLOW-SURFACT code and should be selected. The option for the PCG4 solver is in the same line as the Solver Package.

7) Make sure that the"*Modflow Packages*" dialog looks exactly like the one shown in Figure A.5.

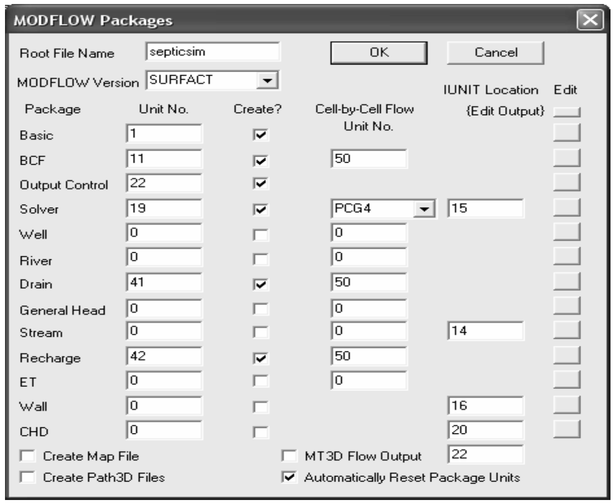

Figure A.5 Dialog showing the MODFLOW modules selected in the model.

8) Click OK to close the dialog.

A.3.1 Basic Package Input

1) Click menu "*Model*"→ "*MODFLOW*" → "*Basic Package*". The "Basic *Package*" dialog opens up.

2) The first two rows are used to input the details about the simulation like the type of simulation, the time being simulated and any special comments about the properties of the medium and other such details that would be useful in identifying the simulation for the user.

3) Since the current simulation is a transient state simulation the "*Steady State Simulation*" option, which is selected as a default, should be unselected for the present simulation.

4) Next, enter a value of 30 for the "*Number of Stress Periods*" in the simulation.

5) Select the check box next to the option of "*Save Starting Heads.*"

6) Select on the check box next to the option "*Print Commands in Dataset.*"

7) Select "*Days*" as the unit of time and select "*Feet*" as the unit of length. Leave all the other options at their default values. Make sure that the "*Basic Package*" dialog looks exactly similar to the one shown in the Figure A.6.

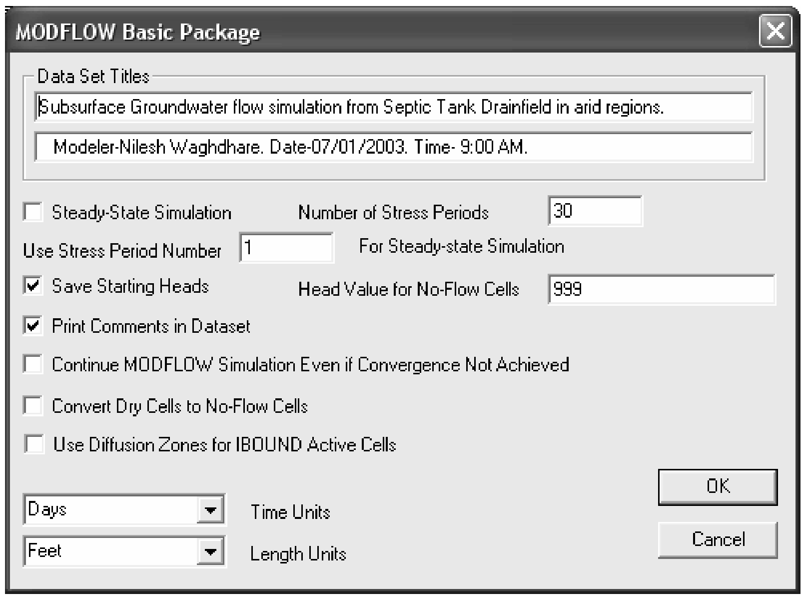

Figure A.6 Dialog showing the Basic Package input**.**

8) Click OK to close the dialog.

A.3.2 BCF Package

1) Click menu "*MODEL*" → "*MODFLOW*" → "*BCF Package*." The "*MODFLOW BCF Package*" dialog opens up.

2) Starting from the top, select the check box next to the option "*Compute Leakance (VCONT).*"

3) Select "*Leakance*" Option for "*Leakance Zone Represents*."

4) In the "*Layer Types*" section, choose the option "*3-Unconfined (T-varies)*" for all 46 layers in the model. Normally all the layers except the first would have this option by default.

5) Choose the "*Harmonic Averaging*" option under the "*BCF3/4 Averaging*" column for all 46 layers in the model. This option is selected by default. The harmonic averaging scheme carries out a more realist calculation of transmissivity/hydraulic conductivity than other options available.

6) Select the "*Use Variably Saturated Option [BCF4] in the Modflow-Surfact*" option to simulate the variably saturated groundwater flow for the current simulation.

7) Select the check box next to the option "*Update VCONT when transmissivity is updated for unconfined layers*."

8) Make sure that the "*MODFLOW BCF Package*" dialog looks exactly like the one shown in the Figure A.7.

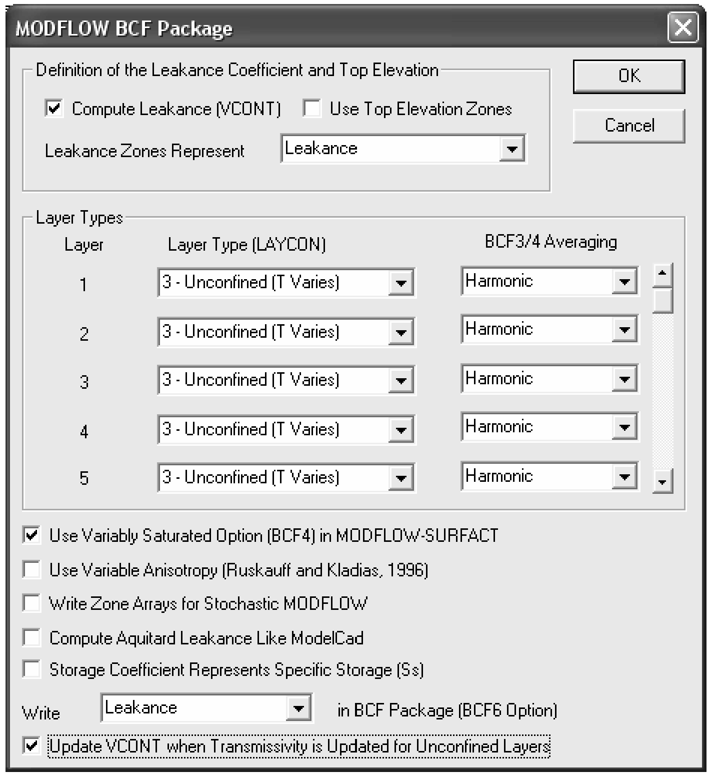

Figure A.7 Dialog showing input to the MODFLOW BCF Package.

9) Click OK to close the dialog.

<u>A.3.3 Output Control Package Input</u>

1) Click on menu "*MODEL*" → "*MODFLOW*" → "*OUTPUT CONTROL*." The "*Simplified Output Control Package*" dialog opens. One can change the format of the output by editing the parameters in this dialog. For the purpose of our simulation we need not change the setting and hence accept the default settings.

2) Make sure that the "*Simplified Output Control Package*" dialog looks exactly like the one shown in the Figure A.8.

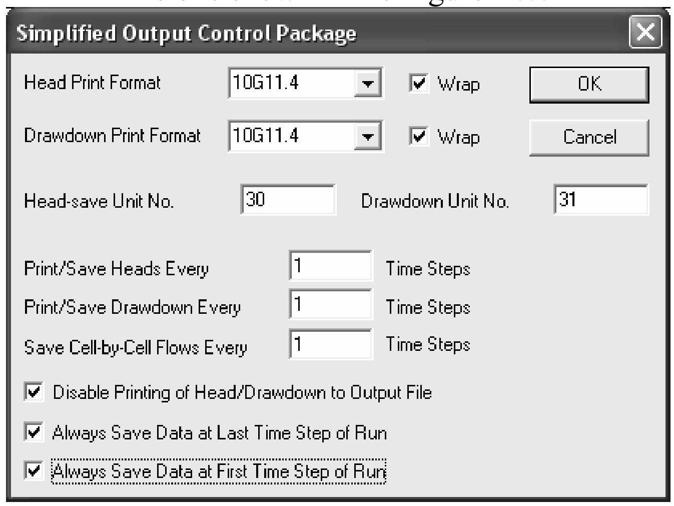

Figure A.8 Dialog showing input to the Output Control Package.

3) Click on OK to close the dialog.

A.3.4 Modflow Recharge/ET Package Input

1) Click on menu "*MODEL*" → "*MODFLOW*" → "*RECHARGE/ET*". The "*RECHARGE/ET Package*" dialog opens.

2) Select the "*Top Layer Only*" for the "*Recharge Applied To*" option. Accept all other default settings.

3) Make sure that the "*RECHARGE/ET Package*" dialog looks exactly like the one shown in Figure A.9.

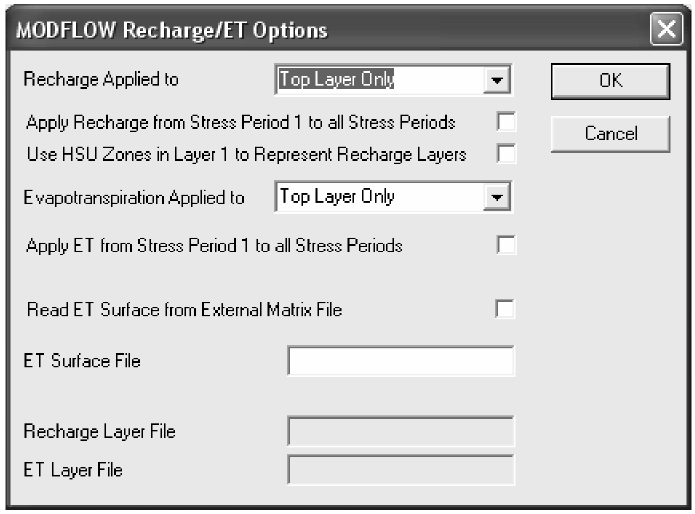

Figure A.9 Dialog showing the input to the Recharge Package options.

4) Click OK to close the dialog.

A.4 Stress Period Setup Input

1) Click on menu "*MODEL*"→ "*MODFLOW*" → "*Stress Period Setup….*" The "*Stress Period Setup Package*" dialog opens up.
2) For each stress period, enter a value of 1 d for "*Period Length*," enter a value of 1 for "*Number of Time Steps*," and enter a value of 1.2 for "*Time Step Multiplier*."
3) Enter the above-mentioned values for all the stress periods in the simulation. These values are only initialized here and would be later modified in the "*ATO4 Package.*"
4) Make sure that the "*Stress Period Setup Package*" dialog looks exactly like the one shown in Figure A.10.

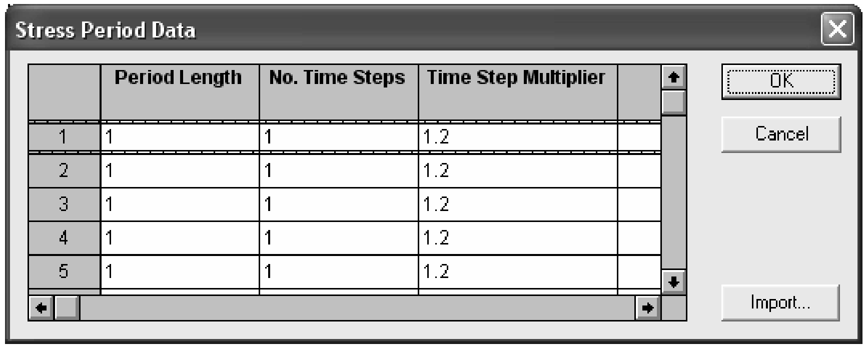

Figure A.10 Dialog showing the input of stress period data in MODFLOW.

5) Click OK to close the dialog.

A.4.1 Initial Heads Input

The initial heads setup for the first simulation in the series of simulations is different from the setup of intermediate simulations in the series.

A.4.1.1 Initial Heads Setup for the First Simulation in the Series

1) Click on menu "*MODEL*" → "*MODFLOW*" → "*INITIAL HEADS*." The "*Initial Head Setup*" dialog opens up.
2) The "*Initial Head Setup*" dialog is made up of two sections, (1) Head-Save File Options and (2) Default Heads in Each Layer. For setting up the first simulation in the series, input in the "*Default Heads in Each Layer*" option is required.
3) Enter a value of -1055 ft in the every row representing layers of the first column. The pressure head value of -1055 ft was selected as the saturation moisture content at a pressure head of -1055 ft is equal to 12 % gravimetric moisture content according to the Van Genutchen equation. Since the observed gravimetric moisture content at the field site was 12 % at the beginning to the field

experiment we have tried to simulate similar initial moisture content for the simulation.

4) Accept all other default values in the dialog and make sure that the dialog looks exactly like the one shown in Figure A.11.

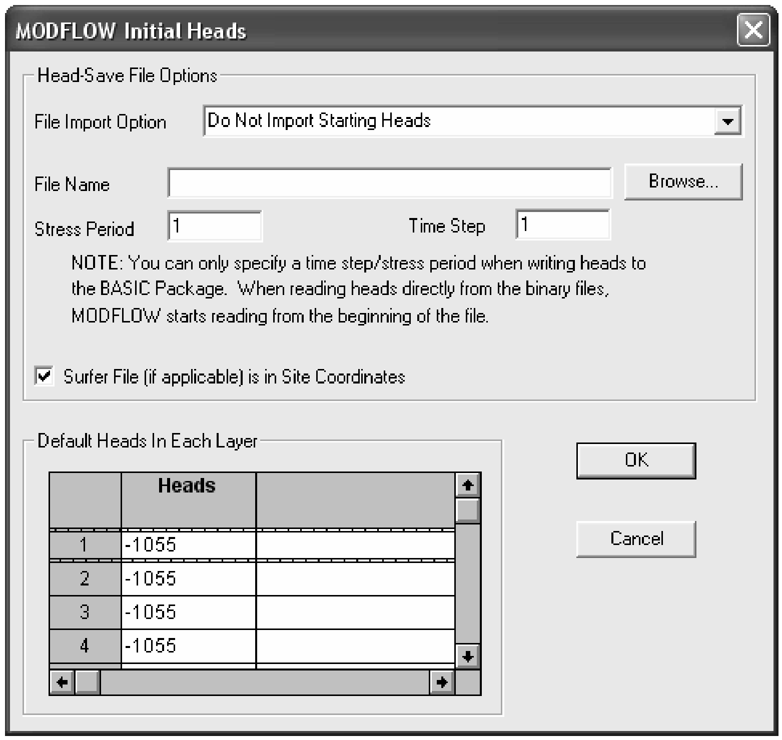

Figure A.11 Dialog showing input of the initial pressure head input for the first simulation.

5) Click OK to close the dialog.

A.4.1.2 Initial Heads Setup for the Second and Successive Simulations in the Series

1) Click on menu "*MODEL*" → "*MODFLOW*" → "*INITIAL HEADS*." The "*Initial Head Setup*" dialog opens up.

2) The "*Initial Head Setup*" dialog is made up of two sections, (1) Head-Save File Options and (2) Default Heads in Each Layer. For setting up the second and

successive simulations in the series input in the "*Head-Save File*" option is required.

3) Change the "*File Import Option*" from "*Do Not Import Starting Heads*" to "*Set Heads from File (Head-save, BASIC Package, SURFER, matrix).*"
4) Browse to the heads file (.HDS file where the final hydraulic head values in the simulation are stored) from the first or the previous simulation, as the case may be, and select the .HDS file.
5) Now, enter the last time-step number of the last stress period and the last stress period number of the previous simulation in the "*Time Step*" and "*Stress Period*" options, respectively. The last time-step number of the last stress period is selected so that the second simulation uses the final hydraulic heads of the first simulation as its initial condition thus making the simulations continuous.
6) Accept all other default values in the dialog and make sure that the dialog looks exactly like the one shown in Figure A.12.
7) Click OK to close the dialog.

A.5 Selection of Surfact Packages

1) Click on menu "*MODEL*" → "*MODFLOW-SURFACT*" → "*PACKAGES*." The "*Modflow-Surfact Packages*" dialog opens up.
2) Enter a value of 11 for "*Units No.,*" for the "*BCF4 Package*" and select the check box in the same row as the "*BCF4 Package*" option under the "*Create?*" column.

3) Enter a value of 33 for "*Units No.,*" for the "*ATO4 Package*" and select the check box in same row as the "*ATO4 Package*" option under the "*Create?*" column.

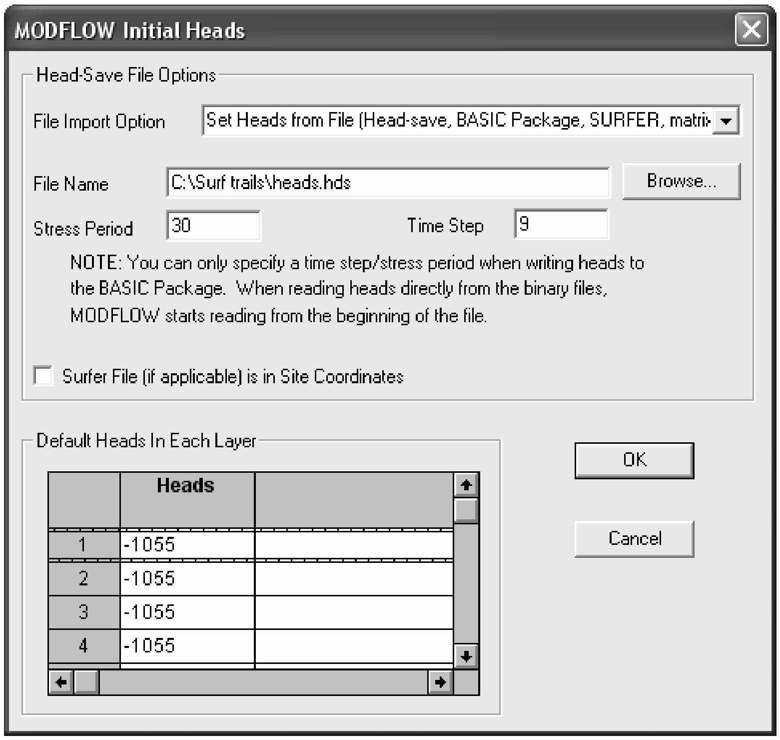

Figure A.12 Dialog showing input of pressure heads to maintain continuity between simulations.

4) Enter a value of 44 for "*Unit No.*" for the "*PCG4 Package*" and select on the check box in same row as the "*PCG4 Package*" option under the "*Create?*" column.

5) Enter a value of 18 for "*Units No.,*" for the "RSF*4 Package*" and select the check box in the same row as the "RSF*4 Package*" option under the "*Create?*" column.

6) Accept all other default values and make sure that the "*Modflow Surfact Packages*" dialog looks exactly like the one shown in Figure A.13.

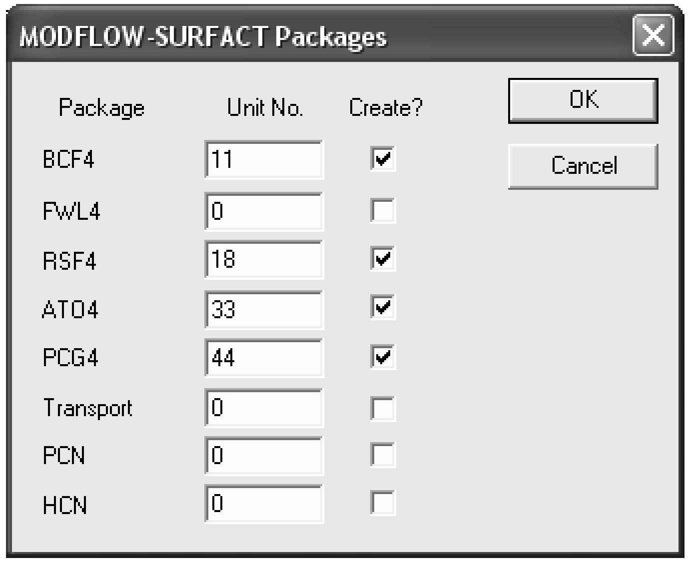

Figure A.13 Dialog showing the selected MODFLOW-SURFACT packages.

6) Click OK to close the dialog.

A.5.1 BCF Package Input

1) Click on menu "*MODEL*" → "*MODFLOW-SURFACT*" → "*BCF4 Package*." The "*BCF4 Parameters*" dialog opens up.
2) Select the check box next to the option "*Implement Variably Saturated Flow Option*."
3) Select the "*1-Van Genutchen for water flow*" option for the "*Unsaturated Modeling Option (IREALS)*."
4) Select the "*0-Upstream Weighting*" option for the "*Relative Permeability Option (ICNTRL)*."
5) Select on the check box for "*Unsaturated Zone Parameters are Variable*" option.
6) Accept all other default values and make sure that the "*BCF4 Parameters*" dialog looks exactly like the one in Figure A.14.

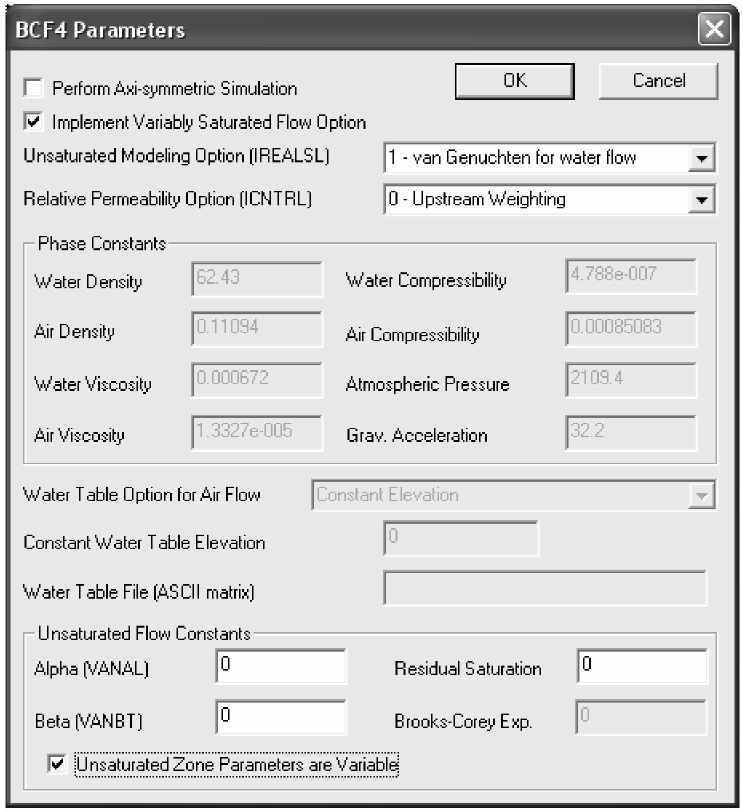

Figure A.14 Dialog showing input to the BCF4 package.

7) Click OK to close the dialog.

A.5.2 Automatic Time Stepping Package Input

1) The input to the "*ATO4 Package*" is done to edit the time-step values for individual stress periods in the simulation. Time-step values for each stress period have to be entered separately. Setup for the first stress period is shown below. The values for initial time-step size for different stress periods vary from 0.1 to 0.5 days. The values for the maximum time-step size for different stress periods vary from 1 to 0.5 day. The minimum time-step size, the time-step multiplier and the

time-step reduction factor remain constant for all stress periods. The values entered for remaining stress periods have been tabulated in the appendices.

2) Click on menu "*MODEL*" → "*MODFLOW-SURFACT*" → "*AUTO TIME STEPPING…*" The "*Automatic Time Stepping*" dialog opens up.

3) Enter a value of 1 as shown in Figure A.15 below and click OK.

Figure A.15 Dialog showing the selection of the stress period to edit in the ATO4 package in MODFLOW-SURFACT.

4) A new "*Automatic Time Stepping*" dialog opens up.

5) Enter a value of 0.5 day for "*Initial Time Step Size*." This value may be reduced successively if convergence is not achieved in the particular stress period.

6) Enter a value of 1 X 10^{-4} day for the "*Minimum Time Step Size*." This value is the lowest time-step that the "*ATO4 Package*" may use if convergence is not achieved for the stress period. This value may be further reduced if convergence is not readily achieved.

7) Enter a value of 1 day for "*Maximum Time Step Size*." This value is also reduced successively if convergence is not achieved in the particular stress period.

8) Enter a value of 1.2 for the "*Time Step Multiplier*." This value is used in increasing the successive time-step size by the "*ATO4 Package*" when convergence is achieved for a particular time-step.

9) Enter a value of 2.0 for the "*Time Step Reduction Factor*" or "*T.S. Reduction Factor*." This value is used by the "*ATO4 Package*" when reducing the successive time-step size when convergence is not achieved for a particular time-step.

10) Using the "*ATO4 Package*" the output from the simulation can be selected at desired predetermined intervals of time or a certain number of times in a particular stress period or after a certain number of time-steps in a particular stress period. We have used the option to print an output after every time-step in a given stress period.

11) Click on the "*Print Times*" button, the "Printout Times" dialog opens. Enter the values 0.5, 0.75 and 1.0 one below the other and click OK. Next enter a value of 3.0 in the "*Number of Printout Times*" box.

12) Accept all other default values and make sure that the "*ATO4 Parameters*" dialogs looks exactly like the one shown in Figure A.16.

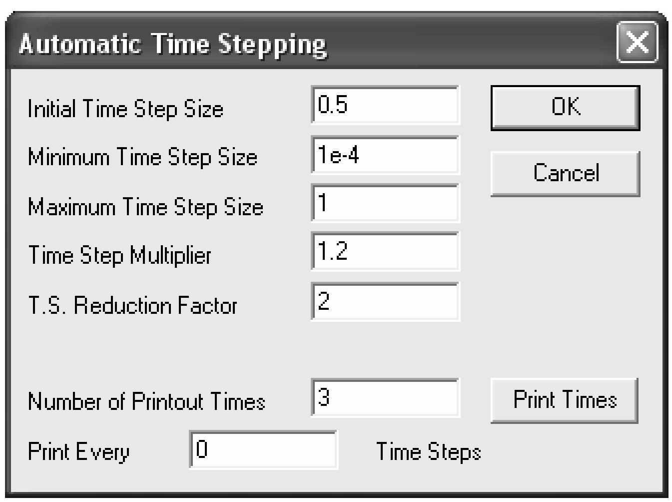

Figure A.16 Dialog showing the input of time stepping parameters in the ATO4 package.

13) Click OK to close the dialog.

A.5.3 PCG4 Solver Package Input

1) Click on menu "*MODEL*" → "*MODFLOW-SURFACT*" → "*PCG4 Package.*" The "*PCG4 Parameters*" dialog opens up.
2) The Newton-Raphson Linearization option selects a more robust method to solve the non-linear differential equations encountered in simulation of groundwater flow in the unsaturated/variably-saturated medium. In trial simulations it was observed that simulation did not converge for certain time-steps and hence the Newton-Raphson Linearization Option was included to achieve convergence during all time-steps of any particular stress period.
3) Click on the check box next to the option "*Use Newton-Raphson Linearization*" option.
4) Enter a value of 0.1 for the "*Backtracking Factor [BFACT]*" and enter a value of 1.0 for the "*Residual Reduction Factor [RESRED].*" These values were selected for robustness and efficiency of the Newton-Raphson Linearization Method solver and were used as per the instructions in the MODFLOW-SURFACT version 2.2 User's Manual (Hydrogeologic Inc., 1996).
5) Make sure that the "*PCG4 Parameters*" dialog looks exactly like the one shown in Figure A.17.

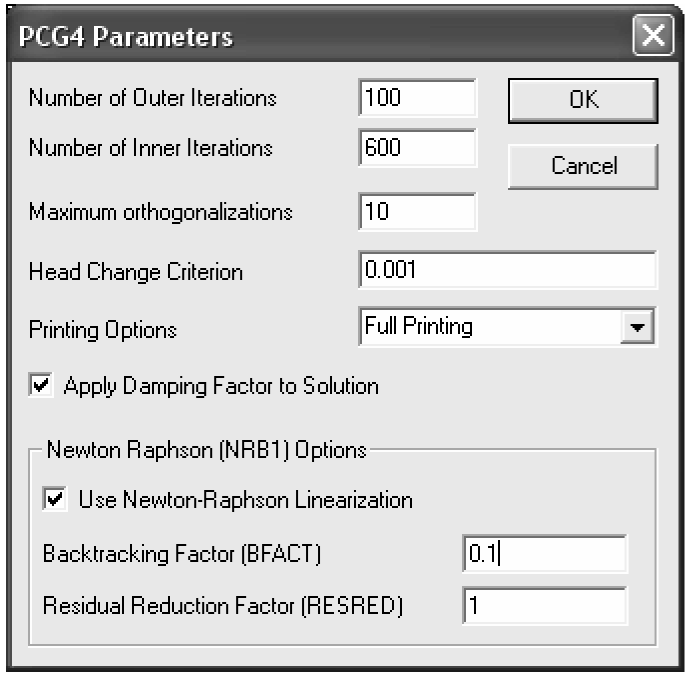

Figure A.17 Dialog showing the input to the PCG4 package.

6) Click OK to close the dialog.

A.6 Assigning Layer Elevations

A.6.1 Layer Top Elevations Input

1) Click menu "*Props*" → Select "*Top Elevations*."
2) Click menu "Props" → "Property *Values*" → "*Database.*" The "*Zone Database Information*" dialog opens up.
3) Enter the values given in Table 1 in the first column for the top elevations of each layer. Start by entering the top elevation of the top layer and work towards the bottom layer.
4) Accept all other default values and make sure that the "*Zone Database Information*" dialog looks exactly like the one shown in Figure A.18.

Table A.1 Top elevations of layers in the model in feet.

Layer Number	Top Elevation	Layer Number	Top
1	80.00	24	58.50
2	79.67	25	56.50
3	79.33	26	54.50
4	78.89	27	52.50
5	78.44	28	50.50
6	78.00	29	48.50
7	77.50	30	46.50
8	77.00	31	44.50
9	76.50	32	42.50
10	76.00	33	39.50
11	75.40	34	36.50
12	74.70	35	33.50
13	73.90	36	30.50
14	73.00	37	27.50
15	72.00	38	24.50
16	70.90	39	21.50
17	69.70	40	18.50
18	68.40	41	15.50
19	67.00	42	12.50
20	65.50	43	9.50
21	63.90	44	6.50
22	62.20	45	3.50
23	60.40	46	0.50

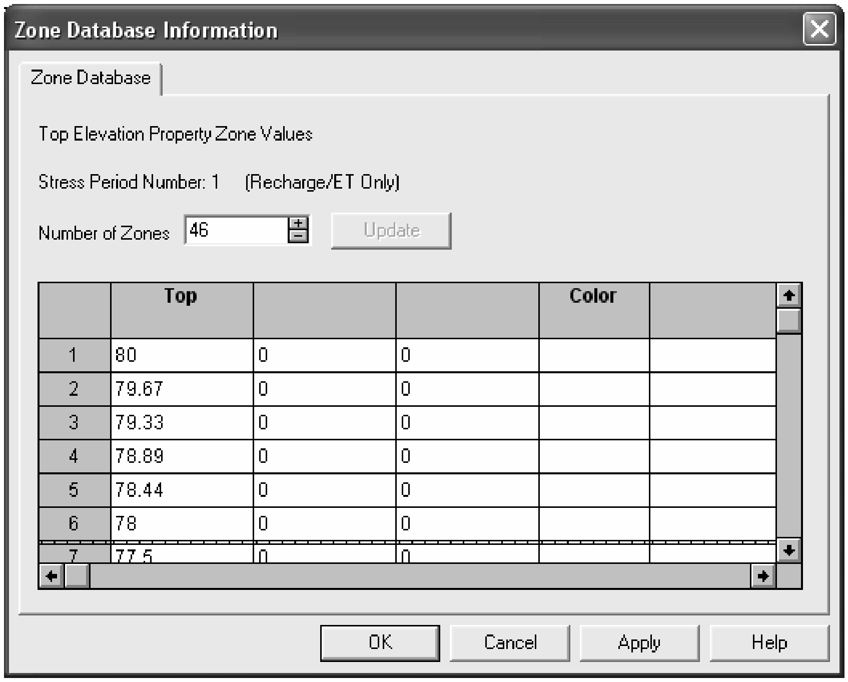

Figure A.18 Input dialog showing the input of the top elevation of layers in the model.

5) Click OK and close the dialog.

<u>A.6.2 Layer Bottom Elevations Input</u>

1) Click menu "*Props*" → Select "*Bottom Elevations*."
2) Click menu "*Props*" → "*Property Values*" → "*Database*." The "*Zone Database Information*" dialog opens up.
3) Enter the values given in Table 2 below in the first column for the bottom elevations of each respective layer. Start by entering the bottom elevation of the top layer and work towards the bottom layer.

Table A.2 Bottom elevations of layers in the model in feet.

Layer Number	Bottom Elevation	Layer Number	Bottom Elevation
1	79.67	24	56.50
2	79.33	25	54.50
3	78.89	26	52.50
4	78.44	27	50.50
5	78.00	28	48.50
6	77.50	29	46.50
7	77.00	30	44.50
8	76.50	31	42.50
9	76.00	32	39.50
10	75.40	33	36.50
11	74.70	34	33.50
12	73.90	35	30.50
13	73.00	36	27.50
14	72.00	37	24.50
15	70.90	38	21.50
16	69.70	39	18.50
17	68.40	40	15.50
18	67.00	41	12.50
19	65.50	42	9.50
20	63.90	43	6.50
21	62.20	44	3.50
22	60.40	45	56.50
23	58.50	46	0

4) Accept all other default values and make sure that the "*Zone Database Information*" dialog looks exactly like the one shown in Figure A.19 and click OK to close the dialog.

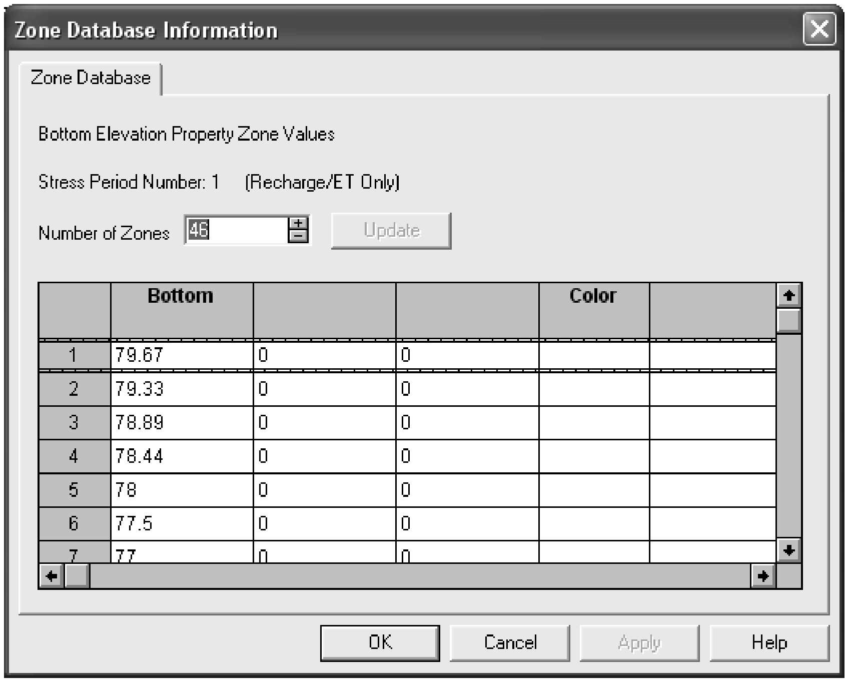

Figure A.19 Input dialog showing the input of bottom layer elevation in the model.

A.7 Assigning material property zones

A.7.1 Assigning Colors to Zones

1) The "*Zone Database Information*" dialog should be open before you start the assigning colors to respective zones.

2) Click on the box under "*Color*" that is in the same line as the zone number to be edited. A "*Zone Color Information*" dialog opens up.

3) Select "*Solid Type Color*" and the required color from the array of choices available.

4) Make sure the dialog looks similar to the one shown in Figure A.20 with the exception of the color being selected.

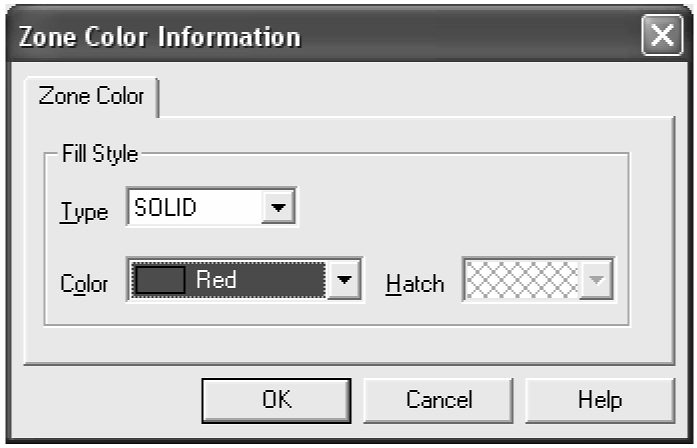

Figure A.20 Dialog showing the selection of the color zone.

5) Click “*Apply*” and then “*OK*” to close the dialog. The required color has now been selected and applied for the zone.

A.7.2 Assigning Hydraulic Conductivity

1) Click on menu “*Props*” → Select “*Hydraulic Conductivity*.”
2) Click on menu “*Props*” → “*Property Values*” → “*Database*.” The “*Zone Database Information*” dialog opens up.
3) Enter the hydraulic conductivity property zone values for the appropriate zone through the “*Zone Database Information*” dialog.
4) Enter the values of $K_x = K_y = K_z = 25$ ft/d for zone 2, values for zone 1 will be the default values as they have been entered through the “*Initialize Model Grid*” dialog. Select a blue color for zone 1 and green color for zone 2. See previous section for procedure to select color for zones.

5) Accept all other default values and make sure that the "*Zone Database Information*" dialog looks exactly like the one shown in the Figure A.21 and click OK to close the dialog.

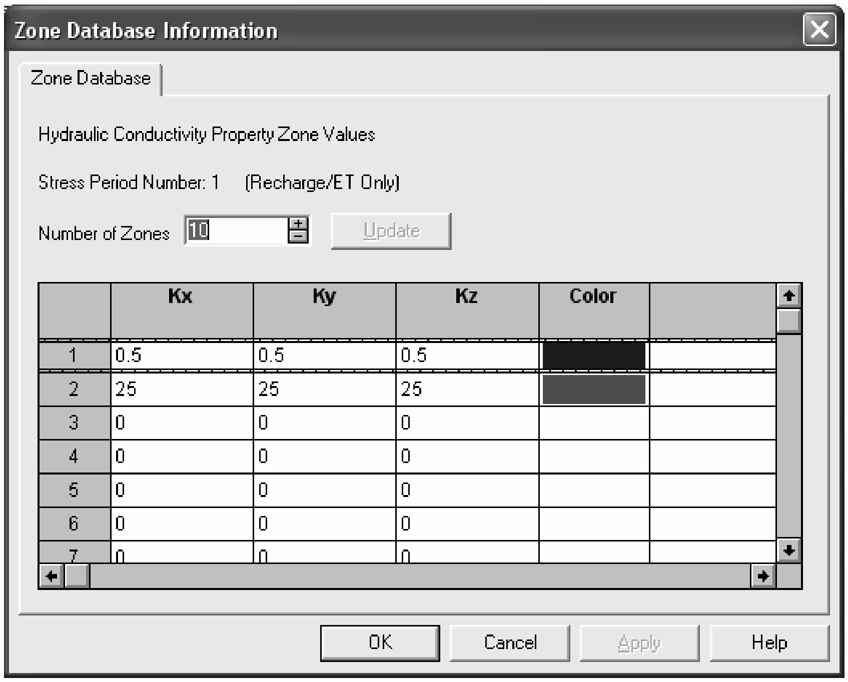

Figure A. 21 Input dialog showing the input of hydraulic conductivity for material zones in the model.

6) Next, Select on the "*Contour View*" if the contour view is not already selected, make sure that the "*Properties Tab*" in the top menu is selected.

7) Select or go to layer 2 using the options listed on the top left corner of the screen.

8) Next, click on the "*Zone Window*" button on the top left of the menu bar.

9) In order to modify the hydraulic conductivity property of the drainfield area, the area needs to be selected. Drag a rectangle while pressing the left mouse button, and then release the left mouse button.

10) A "*Map Window*" dialog opens up.

11) Enter 20 ft as the "*X Origin*" value, 28.5 ft as the "*Y Origin*" value, 3 ft as the "*Height*" value and 20 ft as the "*Width*" value. The above mentioned values are input as this positions the drainfield central to the model which is the ideal location for the drainfield.

12) Make sure that the "*Map Window*" dialog looks exactly like the one shown in the Figure A.22 and then click OK. The "*Map Window*" dialog closes and a new "*Set Zone Number*" dialog appears.

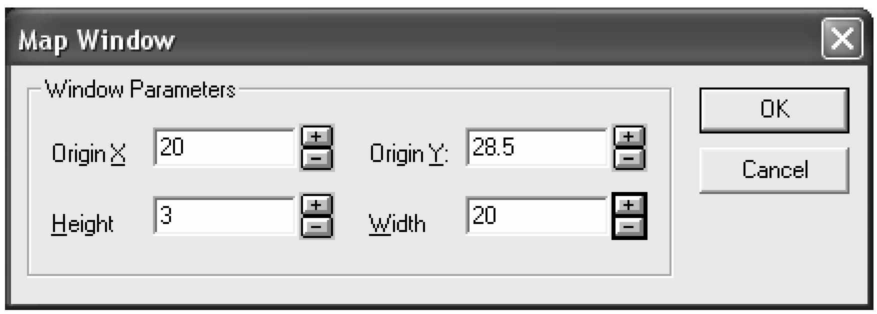

Figure A. 22 Dialog showing the input of coordinates for the selection of zone area in the model.

13) Enter a value of 2 as the zone number; make sure that the "*Set Zone Number*" dialog looks exactly like the one shown in the Figure A.23 and click OK to close the dialog.

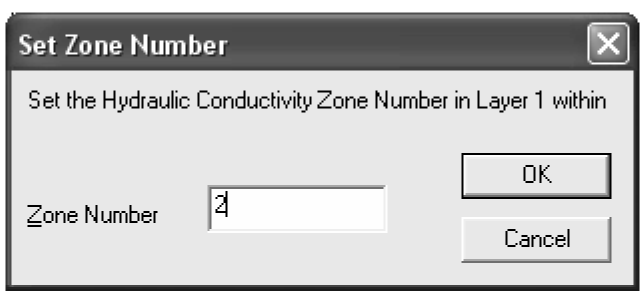

Figure A. 23 Dialog showing the selection of zone numbers for the zone area selected in the model.

14) It was found that this method selects an extra row and column in the model as GroundWater Vistas selects a whole row when decimal numbers for row or column numbers are used. To rectify this, the user is urged to modify the additional cells manually.

15) Follow the procedure from step 7 to step 14 above for assigning zone numbers to layers 3, 4 and 5.

16) Select layer 1 after the zone in layer 5 has been assigned.

A.7.3 Assigning Storage/Porosity

1) Click on menu "*Props*" → Select "*Storage/Porosity*."

2) Click on menu "Props" → "*Property Values*" → "*Database*." The "*Zone Database Information*" dialog opens up.

3) Enter the storage/porosity property zone values for the appropriate zone through the "*Zone Database Information*" dialog.

4) Enter the values of $S = 6.04x10^5$, $S_y = 0.385$ and Porosity = 0.43 for zone 2, values for zone 1 will be the default values as they have been entered through the "*Initialize Model Grid*" dialog. Select a blue color for zone 1 and green color for zone 2. See section on assigning zone colors for procedure to select color for zones.

5) Accept all other default values and make sure that the "*Zone Database Information*" dialog looks exactly like the one shown in the Figure A.24 and click OK to close the dialog.

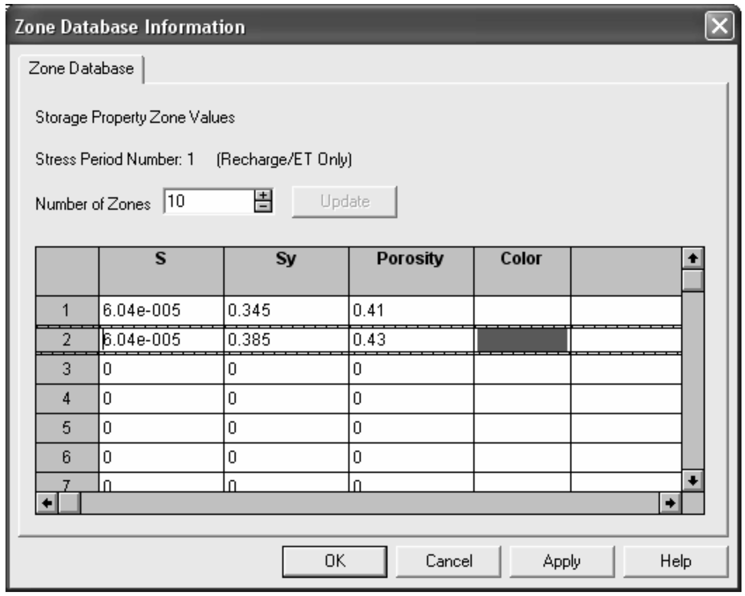

Figure A. 24 Input dialog showing input of soil properties for respective zones in the model.

6) Next, Select/Click on the "*Contour View*" if the contour view is not already selected, make sure that the "*Properties Tab*" in the top menu is selected.

7) Select or go to layer 2 using the options listed on the top left corner of the screen.

8) Next, click on the "*Zone Window*" tab/button on the top left of the menu.

9) In order to modify the storage/porosity property of the drainfield area, the area needs to be selected. Drag a rectangle pressing the left mouse button, and then release the left mouse button.

10) A "*Map Window*" dialog opens up.

11) Enter 20 ft as the "*Origin X"* value, 28.5 ft as the "*Origin Y*" value, 3 ft as the "*Height*" value and 20 ft as the "*Width*" value. The above mentioned values are input as this positions the drainfield central to the model which is the ideal location for the drainfield.

12) Make sure that the "*Map Window*" dialog looks exactly like the one shown in the Figure A.25 and then click OK. The "*Map Window*" dialog closes and a new "*Set Zone Number*" dialog appears.

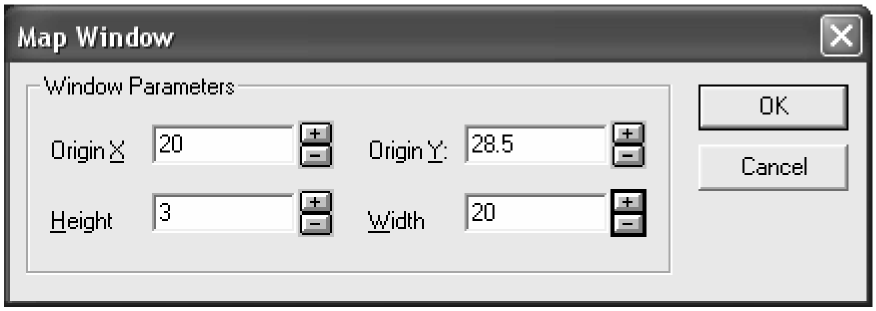

Figure A. 25 Dialog showing the input of coordinates for the selection of zone areas in the model.

13) Enter a value of 2 as the zone number, make sure that the "*Set Zone Number*" and click OK to close the dialog.

14) It was found that this method selects an extra row and column in the model as GroundWater Vistas selects a whole row when decimal numbers for row or column numbers are used. To rectify this, the user is urged to modify the additional cells manually.

15) Follow the procedure mentioned from step 7 to step 14 above for assigning zone numbers to layers 3, 4 and 5.

16) Select layer 1 after the zone in layer 5 has been assigned.

A.7.4 Assigning Interbed Storage

1) Click on menu "*Props*" → "*Interbed Storage*."

2) Click on menu "*Props*" → "*Property Values*" → "*Database*." The "*Zone Database Information*" dialog opens up.

3) Enter the Interbed Storage property zone values for the appropriate zone through the "*Zone Database Information*" dialog.

4) Enter the values of Alpha = 0.00246 /ft, Beta = 1.89, and Residual Saturation = 0.1585 for zone 1 and enter the values of Alpha = 0.004756 /ft, Beta = 2.68, and Residual Saturation = 0.10465 for zone 2. Select a blue color for zone 1 and green color for zone 2. See section assigning zone colors for procedure to select color for zones.

5) Accept all other default values and make sure that the "*Zone Database Information*" dialog looks exactly like the one shown in the Figure A.26 below and click APPLY and OK to close the dialog.

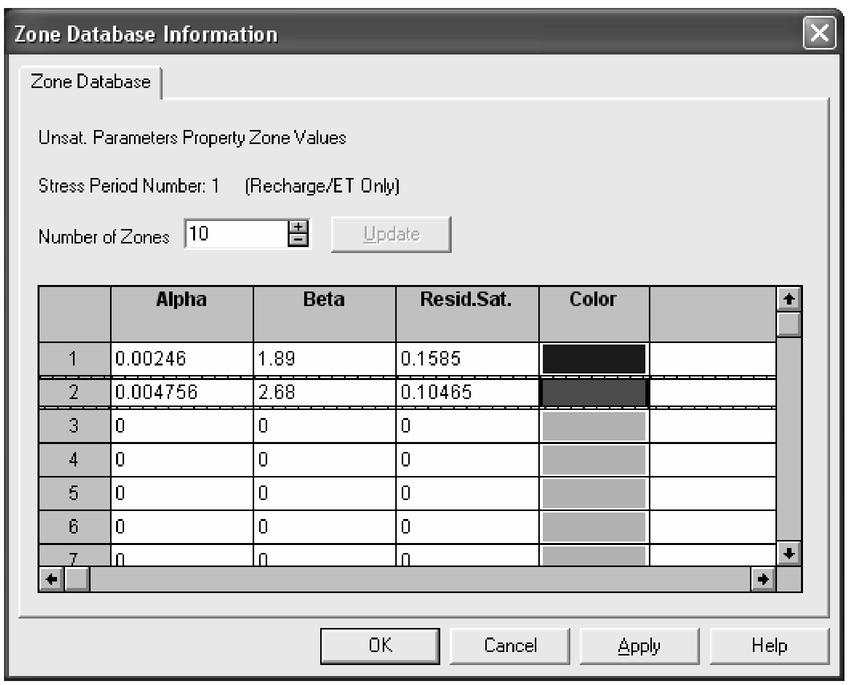

Figure A. 26 Input dialog showing the input of Van Genuchten parameters and residual saturation in the model for respective zones.

6) Next, Select/Click on the contour view if the "*Contour View*" is not selected, make sure that the "*Properties Tab*" in the top menu is selected.

7) Select or go to layer 2 using the options listed on the top left corner of the screen.

8) Next, click on the "*Zone Window*" tab/button on the top left of the menu.

9) In order to modify the storage/porosity property of the drainfield area, the area needs to be selected. Drag a rectangle pressing the left mouse button, and then release the left mouse button.

10) A "*Map Window*" dialog opens up.

11) Enter 20 ft as the "*Origin X*" value, 28.5 ft as the "*Origin Y*" value, 3 ft as the "*Height*" value and 20 ft as the "*Width*" value. The above mentioned values are input as this positions the drainfield central to the model which is the ideal location for the drainfield.

12) Make sure that the "*Map Window*" dialog looks exactly like the one shown in Figure A.27 and then click OK. The "*Map Window*" dialog closes and a new "Set Zone Number" dialog appears.

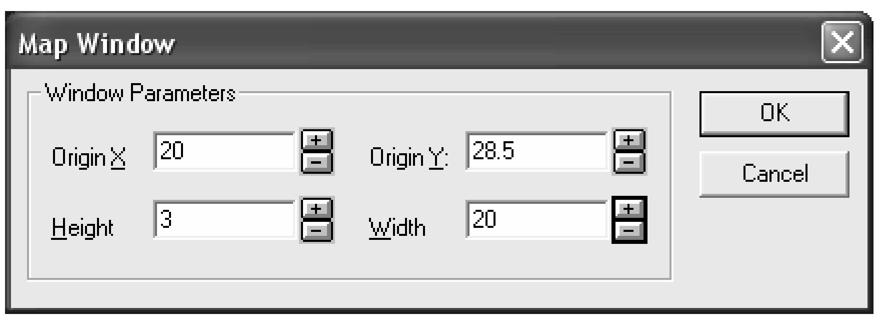

Figure A. 27 Dialog showing the input of coordinates for the selection of zone area in the model.

13) Enter a value of 2 as the zone number and click OK to close the dialog.

14) It was found that this method selects an extra row and column in the model as GroundWater Vistas selects a whole row when decimal numbers for row or

column numbers are used. To rectify this, the user is urged to modify the additional cells manually.

15) Follow the procedure mentioned from step 7 to step 14 above for assigning zone number to layers 3, 4 and 5.

16) Select layer 1 after the zone in layer 5 has been assigned.

A.8 Assigning Recharge

1) Click on menu "*Props*" → Select "*Recharge*."

2) Click on menu "*Props*" → "*Property Values*" → "*Database*." The "*Zone Database Information*" dialog opens up.

3) Enter the Recharge property zone values for the appropriate zone through the "*Zone Database Information*" dialog.

4) Enter the values of –0.02 ft/d for zone 1, and 0.45 ft/d for zone 2. Select a blue color for zone 1 and green color for zone 2. See section on assigning zone colors for procedure to select color for zones.

5) Accept all other default values and make sure that the "*Zone Database Information*" dialog looks exactly like the one shown in Figure A.28 and click OK to close the dialog.

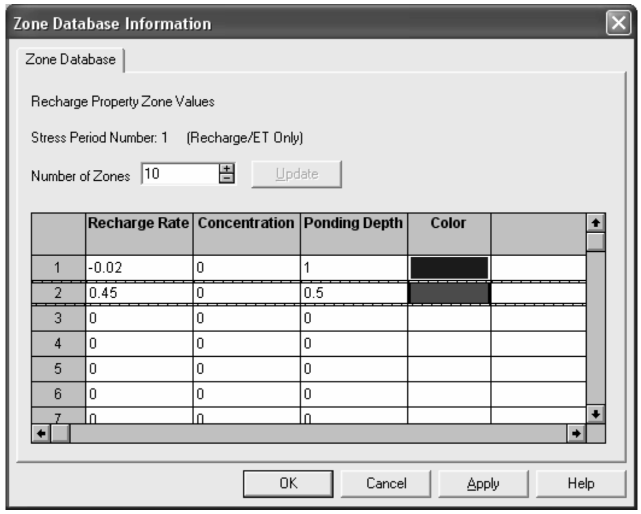

Figure A. 28 Dialog showing the input of positive and negative recharge values for respective zones in the model.

6) Next, Select on the contour view if the "*Contour View*" is not already selected, make sure that the "*Properties Tab*" in the top menu is selected.

7) Select or go to layer 2 using the options listed on the top left corner of the screen.

8) Next, click on the "*Zone Window*" tab/button on the top left of the menu bar.

9) In order to modify the storage/porosity property of the drainfield area, the area needs to be selected. Drag a rectangle pressing the left mouse button, then release the left mouse button.

10) A "*Map Window*" dialog opens up.

11) Enter 20 ft as the "*Origin X*" value, 28.5 ft as the "*Origin Y*" value, 3 ft as the "*Height*" value and 20 ft as the "*Width*" value. The above mentioned values are input as this positions the drainfield central to the model which is the ideal location for the drainfield.

12) Make sure that the "*Map Window*" dialog looks exactly like the one shown in the Figure A.29 and then click OK. The "*Map Window*" dialog closes and a new "*Set Zone Number*" dialog appears.

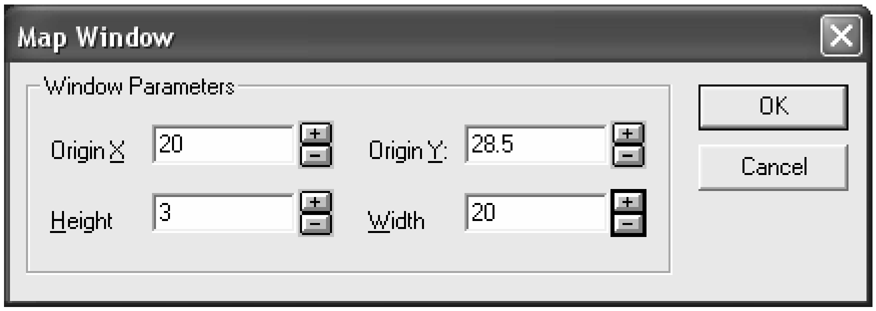

Figure A. 29 Dialog showing the input of coordinates for the selection of zone area in the model.

13) Enter a value of 2 as the zone number and click OK to close the dialog.

14) It was found that this method selects an extra row and column in the model as GroundWater Vistas selects a whole row when decimal numbers for row or column numbers are used. To rectify this, the user is urged to modify the additional cells manually.

15) Follow the procedure mentioned from step 7 to step 14 above for assigning zone number to layers 3, 4 and 5.

16) Select layer 1 after the zones in layer 5 have been assigned.

A.9 Assigning Drains

The drain type boundary condition is useful in simulating a boundary that only removes water from the model. If the head in the model cell drops below the drain elevation, the drain will not inject water into the model. Under these conditions the drain becomes inactive. The drain type of boundary condition was used in the simulation to determine the quantity of water that infiltrated from the drainfield and reached the water table, which was assumed to exist at 80 ft below the surface.

1) Click on menu “BC’s” → Select “Drain.”
2) Select or go to layer 46 using the options listed on the top left corner of the screen.
3) Next, click on the “*Zone Window*” tab/button on the top left of the menu bar.
4) Drag a rectangle pressing the left mouse button, then release the left mouse button.
5) A “*Map Window*” dialog opens up.
6) Enter 0 ft as the “*Origin X*” value, 0 ft as the “*Origin Y*” value, 60 ft as the “*Height*” value and 60 ft as the “*Width*” value.
7) Make sure that the “*Map Window*” dialog looks exactly like the one shown in the Figure A.30 and then click OK. The “*Map Window*” dialog closes and a new “*Drain Boundary Condition*” dialog appears.

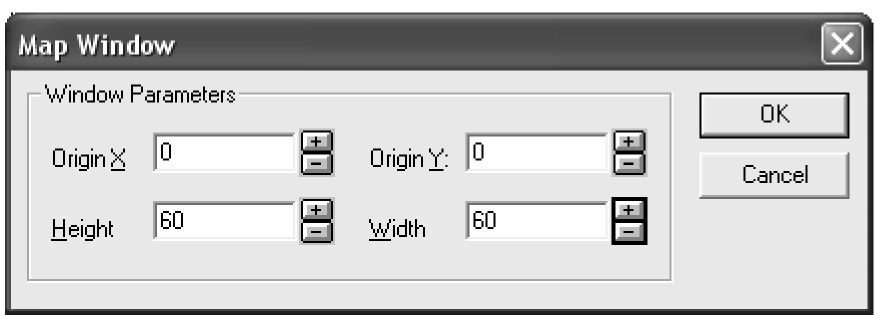

Figure A.30 Dialog showing the input of coordinates for the selection of zone area in the model.

8) Enter a value of 0.5 ft/d for the “*Hydraulic Conductivity*,” enter a value of 1.2 ft for the “*Thickness of Drainbed*.” The thickness of the drainbed was assigned a value of 1.2 ft as this was the thickness of 46th layer of the model.

9) Accept all other default settings and make sure that the "*Drain Boundary Condition*" dialog looks exactly like the one shown in Figure A.31.

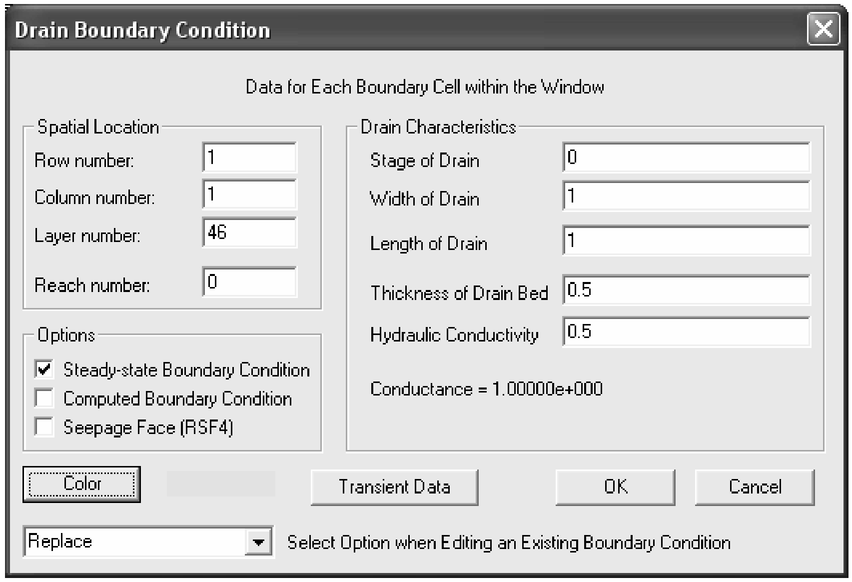

Figure A.31 Dialog showing the input of the drain boundary condition in the model.

A.10 Saving the Model

1) Click on menu "*File*" → "*Save As*".
2) Make sure to save the simulation with the file name "*SepticSim*."

A.11 Running the Model

1) Click on menu "*MODEL*" → "*MODFLOW*" → "*CREATE DATASETS*". A "*Display Error/Warning File*" dialog as shown in Figure A.32, will open up, click on "*Yes*" in this dialog to show the error/warning file. On making sure that there are no errors or warnings in the file proceed execute the "*Run*" command.

Figure A.32 Dialog to choose the display of the error/warning file on creation of data files in MODFLOW-SURFACT.

2) Click on menu "*MODEL*" → "*MODFLOW*" → "*Run Modflow*". The MSFT.exe graphic window opens in a few seconds. The progress of the simulation can be viewed as the simulation is executed.

A.12 Importing Model Results

The results of a simulation can be imported into Groundwater Vistas either automatically or manually. The results can be imported automatically at the end of a simulation.

A.12.1 Automatic Import of Results

1) After the end of a simulation run, Groundwater Vistas opens a dialog as shown in Figure A.33 to inform the user that the simulation has finished and if the results of the simulation should be processed/ imported in Groundwater Vistas.
2) Select "*Yes*" to import the results.

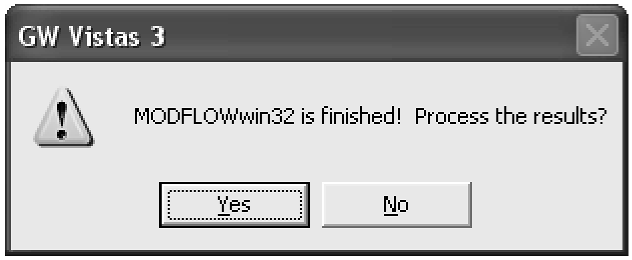

Figure A.33 Dialog showing the completion of model simulation and prompt for the user to select display of result

3) On clicking on "*Yes*" the "Import Model Results" dialog opens up.

4) Enter the required "Stress Period" and "Time Step" of the simulation executed that are to be viewed. For the current simulation we will select stress period number 30 and a time-step number 9.

5) There are three different types of data that can be imported either separately or combined. These are the hydraulic head distribution, the saturated moisture content (a.k.a. drawdown) and the cell-by-cell flow terms. The cell-by-cell flow terms help in plotting velocity vectors of groundwater flow in the particular stress period of the simulation. The Hydraulic Head distribution is imported by default. The Drawdown and the cell-by-cell flow terms have to be imported by clicking/ selecting the check box in front of the options "Drawdown File" and "Cell-By-Cell Flow File."

6) Make sure that the "Import Model Results" dialog looks exactly like the one shown in Figure A.34. The file path names shown in the illustration may not be the same as the ones seen on your dialog and should be ignored. Click OK to close the dialog and import the results. The results take anywhere from the a few seconds to a few minutes to be imported.

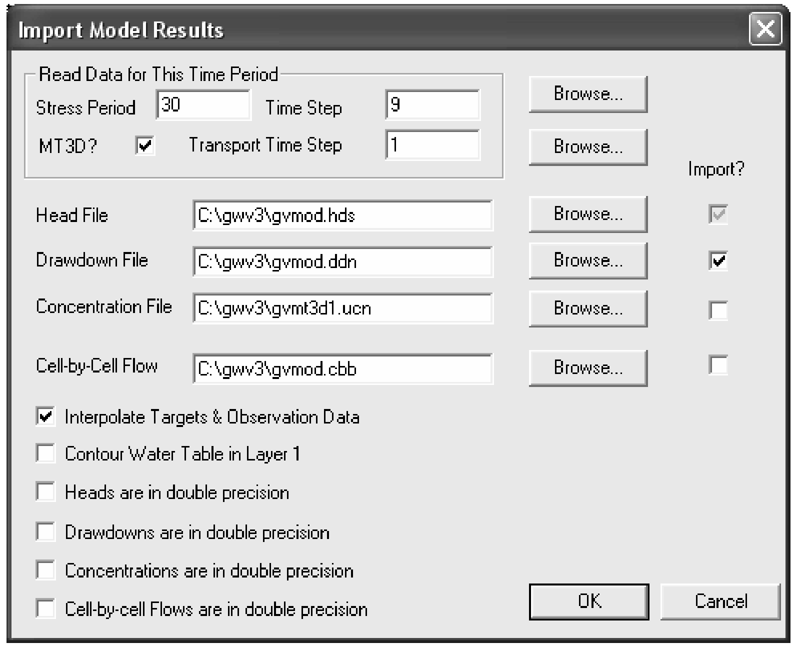

Figure A.34 Dialog showing the selected options for processing of simulated results.

The results of the simulation can be viewed in the form of contour displays, color floods, velocity vector maps, mass balance analysis and mass balance data. The reader is referred to the GroundWater Vistas manual for more information on procedure to view the output results of the simulation.

APPENDIX B

DAILY VALUES OF LOADING RATE,

WASTEWATER ET RATE, AND

RAINFALL RATE IN FT/DAY

FROM PHASE-1

STUDY

Table B.1 Daily values of loading rate, Wastewater ET rate, and Rainfall Rate in ft/d from Phase 1 study.

Date	Field	WW-Avg-ET	Rainfall	Actual Application
	Application	Rate	Rate	Rate
	Rate ft/d (1)	ft/d (2)	ft/d (3)	ft/d (4)
	9	9	9	(4) =(1)-(2)+(3)
1/15/2000	1.04	1.31E-02	0.0E+00	1.03E+00
1/16/2000	0.98	1.29E-02	0.0E+00	9.70E-01
1/17/2000	0.96	1.43E-02	0.0E+00	9.48E-01
1/18/2000	0.88	1.53E-02	0.0E+00	8.69E-01
1/19/2000	0.86	1.50E-02	0.0E+00	8.41E-01
1/20/2000	0.85	1.98E-02	0.0E+00	8.27E-01
1/21/2000	0.31	5.79E-03	0.0E+00	2.99E-01
1/22/2000	1.04	2.09E-02	0.0E+00	1.02E+00
1/23/2000	0.75	1.14E-02	0.0E+00	7.37E-01
1/24/2000	0.74	1.30E-02	0.0E+00	7.31E-01
1/25/2000	0.70	1.33E-02	0.0E+00	6.86E-01
1/26/2000	0.69	1.28E-02	0.0E+00	6.80E-01
1/27/2000	0.64	1.46E-02	0.0E+00	6.20E-01
1/28/2000	0.62	8.39E-03	0.0E+00	6.13E-01
1/29/2000	0.60	1.15E-02	0.0E+00	5.88E-01
1/30/2000	0.56	1.18E-02	0.0E+00	5.47E-01
1/31/2000	0.53	8.84E-03	0.0E+00	5.26E-01
2/1/2000	0.52	0.00E+00	7.5E-03	5.31E-01
2/2/2000	0.51	0.00E+00	8.3E-04	5.16E-01
2/3/2000	0.49	9.58E-03	0.0E+00	4.76E-01
2/4/2000	0.49	1.66E-02	0.0E+00	4.74E-01
2/5/2000	0.49	1.25E-02	0.0E+00	4.82E-01
2/6/2000	0.42	1.18E-02	0.0E+00	4.09E-01
2/7/2000	0.45	1.44E-02	0.0E+00	4.33E-01
2/8/2000	0.44	1.42E-02	0.0E+00	4.25E-01
2/9/2000	0.43	1.49E-02	0.0E+00	4.20E-01
2/10/2000	0.42	1.72E-02	0.0E+00	4.02E-01
2/11/2000	0.42	1.72E-02	0.0E+00	4.02E-01
2/12/2000	0.41	1.41E-02	0.0E+00	3.91E-01
2/13/2000	0.41	1.66E-02	0.0E+00	3.91E-01
2/14/2000	0.40	1.88E-02	0.0E+00	3.85E-01
2/15/2000	0.41	1.77E-02	0.0E+00	3.95E-01
2/16/2000	0.41	2.15E-02	0.0E+00	3.86E-01
2/17/2000	0.41	1.49E-02	0.0E+00	3.91E-01

Table B.1 continued

Date	Field	WW-Avg-ET	Rainfall	Actual Application
	Application	Rate	Rate	Rate
	Rate ft/d (1)	ft/d (2)	ft/d (3)	ft/d (4)
	9	9	9	(4) =(1)-(2)+(3)
2/18/2000	0.41	2.21E-02	0.0E+00	3.92E-01
2/19/2000	0.41	1.66E-02	0.0E+00	3.93E-01
2/20/2000	0.42	1.41E-02	0.0E+00	4.07E-01
2/21/2000	0.40	1.49E-02	0.0E+00	3.88E-01
2/22/2000	0.41	0.00E+00	3.3E-03	4.13E-01
2/23/2000	0.42	1.63E-02	0.0E+00	4.05E-01
2/24/2000	0.42	1.93E-02	0.0E+00	4.02E-01
2/25/2000	0.43	2.10E-02	0.0E+00	4.11E-01
2/26/2000	0.44	2.34E-02	0.0E+00	4.18E-01
2/27/2000	0.44	2.22E-02	0.0E+00	4.17E-01
2/28/2000	0.46	1.76E-02	0.0E+00	4.41E-01
2/29/2000	0.45	2.11E-02	0.0E+00	4.33E-01
3/1/2000	0.46	2.00E-02	0.0E+00	4.39E-01
3/2/2000	0.48	0.00E+00	5.0E-03	4.82E-01
3/3/2000	0.46	1.96E-02	0.0E+00	4.44E-01
3/4/2000	0.49	1.66E-02	0.0E+00	4.76E-01
3/5/2000	0.50	1.78E-02	0.0E+00	4.86E-01
3/6/2000	0.48	2.18E-02	0.0E+00	4.57E-01
3/7/2000	0.50	0.00E+00	1.7E-03	5.03E-01
3/8/2000	0.51	2.10E-02	0.0E+00	4.85E-01
3/9/2000	0.54	2.58E-02	0.0E+00	5.11E-01
3/10/2000	0.53	1.83E-02	0.0E+00	5.16E-01
3/11/2000	0.56	2.44E-02	0.0E+00	5.37E-01
3/12/2000	0.53	1.94E-02	0.0E+00	5.15E-01
3/13/2000	0.55	2.16E-02	0.0E+00	5.24E-01
3/14/2000	0.55	1.57E-02	0.0E+00	5.39E-01
3/15/2000	0.55	1.82E-02	0.0E+00	5.30E-01
3/16/2000	0.56	2.74E-02	0.0E+00	5.32E-01
3/17/2000	0.57	1.70E-02	0.0E+00	5.49E-01
3/18/2000	0.58	1.49E-02	0.0E+00	5.69E-01
3/19/2000	0.63	2.18E-02	0.0E+00	6.09E-01
3/20/2000	0.64	2.06E-02	0.0E+00	6.14E-01
3/21/2000	0.64	0.00E+00	1.3E-02	6.50E-01
3/22/2000	0.58	0.00E+00	7.3E-02	6.53E-01
3/23/2000	0.49	0.00E+00	2.5E-02	5.15E-01

Table B.1 continued

Date	Field	WW-Avg-ET	Rainfall	Actual Application
	Application	Rate	Rate	Rate
	Rate ft/d (1)	ft/d (2)	ft/d (3)	ft/d (4)
	9	9	9	(4) =(1)-(2)+(3)
3/24/2000	0.55	2.53E-03	0.0E+00	5.50E-01
3/25/2000	0.63	1.09E-02	0.0E+00	6.22E-01
3/26/2000	0.62	0.00E+00	8.3E-04	6.25E-01
3/27/2000	0.66	2.97E-02	0.0E+00	6.25E-01
3/28/2000	0.65	2.61E-02	0.0E+00	6.22E-01
3/29/2000	0.65	3.34E-02	0.0E+00	6.17E-01
3/30/2000	0.64	2.83E-02	0.0E+00	6.16E-01
3/31/2000	0.64	0.00E+00	1.7E-02	6.56E-01
4/1/2000	0.56	0.00E+00	7.0E-02	6.27E-01
4/2/2000	0.55	0.00E+00	8.3E-04	5.49E-01
4/3/2000	0.48	7.06E-03	0.0E+00	4.72E-01
4/4/2000	0.61	1.81E-02	0.0E+00	5.97E-01
4/5/2000	0.61	2.50E-02	0.0E+00	5.86E-01
4/6/2000	0.62	3.74E-02	0.0E+00	5.84E-01
4/7/2000	0.64	4.17E-02	0.0E+00	5.96E-01
4/8/2000	0.69	3.75E-02	0.0E+00	6.51E-01
4/9/2000	0.60	2.68E-02	0.0E+00	5.75E-01
4/10/2000	0.63	3.48E-02	0.0E+00	5.91E-01
4/11/2000	0.64	0.00E+00	1.2E-02	6.49E-01
4/12/2000	0.61	1.08E-02	0.0E+00	5.95E-01
4/13/2000	0.60	0.00E+00	8.3E-04	6.00E-01
4/14/2000	0.60	2.96E-02	0.0E+00	5.68E-01
4/15/2000	0.64	4.61E-02	0.0E+00	5.96E-01
4/16/2000	0.59	4.52E-02	0.0E+00	5.50E-01
4/17/2000	0.62	3.62E-02	0.0E+00	5.88E-01
4/18/2000	0.62	3.81E-02	0.0E+00	5.81E-01
4/19/2000	0.62	5.12E-02	0.0E+00	5.66E-01
4/20/2000	0.64	5.66E-02	0.0E+00	5.81E-01
4/21/2000	0.60	4.40E-02	0.0E+00	5.60E-01
4/22/2000	0.60	5.01E-02	0.0E+00	5.54E-01
4/23/2000	0.57	5.22E-02	0.0E+00	5.16E-01
4/24/2000	0.58	5.29E-02	0.0E+00	5.24E-01
4/25/2000	0.54	4.41E-02	0.0E+00	4.97E-01
4/26/2000	0.54	4.81E-02	0.0E+00	4.91E-01
4/27/2000	0.54	5.75E-02	0.0E+00	4.79E-01

Table B.1 continued

Date	Field	WW-Avg-ET	Rainfall	Actual Application
	Application	Rate	Rate	Rate
	Rate ft/d (1)	ft/d (2)	ft/d (3)	ft/d (4)
	9	9	9	(4) =(1)-(2)+(3)
4/28/2000	0.51	2.94E-02	0.0E+00	4.79E-01
4/29/2000	0.50	0.00E+00	4.3E-02	5.47E-01
4/30/2000	0.42	1.20E-02	0.0E+00	4.11E-01
5/1/2000	0.46	3.42E-02	0.0E+00	4.26E-01
5/2/2000	0.45	0.00E+00	4.2E-03	4.59E-01
5/3/2000	0.42	2.42E-02	0.0E+00	3.95E-01
5/4/2000	0.45	3.12E-02	0.0E+00	4.14E-01
5/5/2000	0.42	2.98E-02	0.0E+00	3.93E-01
5/6/2000	0.43	4.17E-02	0.0E+00	3.84E-01
5/7/2000	0.43	5.62E-02	0.0E+00	3.77E-01
5/8/2000	0.45	5.67E-02	0.0E+00	3.98E-01
5/9/2000	0.45	5.33E-02	0.0E+00	3.98E-01
5/10/2000	0.45	3.76E-02	0.0E+00	4.10E-01
5/11/2000	0.46	5.50E-02	0.0E+00	4.07E-01
5/12/2000	0.47	7.09E-02	0.0E+00	3.99E-01
5/13/2000	0.48	3.80E-02	0.0E+00	4.47E-01
5/14/2000	0.48	4.08E-02	0.0E+00	4.36E-01
5/15/2000	0.47	0.00E+00	1.7E-03	4.76E-01
5/16/2000	0.46	3.26E-02	0.0E+00	4.29E-01
5/17/2000	0.43	3.52E-02	0.0E+00	3.99E-01
5/18/2000	0.47	4.08E-02	0.0E+00	4.29E-01
5/19/2000	0.44	0.00E+00	4.2E-03	4.43E-01
5/20/2000	0.47	0.00E+00	8.3E-04	4.67E-01
5/21/2000	0.43	1.86E-02	0.0E+00	4.15E-01
5/22/2000	0.42	3.00E-02	0.0E+00	3.92E-01
5/23/2000	0.46	4.21E-02	0.0E+00	4.15E-01
5/24/2000	0.46	5.32E-02	0.0E+00	4.06E-01
5/25/2000	0.48	4.36E-02	0.0E+00	4.33E-01
5/26/2000	0.44	3.11E-02	0.0E+00	4.12E-01
5/27/2000	0.47	4.17E-02	0.0E+00	4.25E-01
5/28/2000	0.47	4.18E-02	0.0E+00	4.28E-01
5/29/2000	0.49	3.97E-02	0.0E+00	4.46E-01
5/30/2000	0.50	4.96E-02	0.0E+00	4.48E-01
5/31/2000	0.49	5.22E-02	0.0E+00	4.34E-01
6/1/2000	0.52	0.00E+00	2.3E-01	7.50E-01

Table B.1 continued

Date	Field	WW-Avg-ET	Rainfall	Actual Application
	Application	Rate	Rate	Rate
	Rate ft/d (1)	ft/d (2)	ft/d (3)	ft/d (4)
	9	9	9	(4) =(1)-(2)+(3)
6/2/2000	0.39	0.00E+00	1.7E-02	4.03E-01
6/3/2000	0.48	0.00E+00	8.3E-04	4.78E-01
6/4/2000	0.45	1.55E-02	0.0E+00	4.39E-01
6/5/2000	0.47	3.34E-02	0.0E+00	4.32E-01
6/6/2000	0.49	3.84E-02	0.0E+00	4.51E-01
6/7/2000	0.50	3.88E-02	0.0E+00	4.65E-01
6/8/2000	0.51	4.87E-02	0.0E+00	4.66E-01
6/9/2000	0.49	0.00E+00	4.3E-02	5.29E-01
6/10/2000	0.50	0.00E+00	8.3E-04	5.05E-01
6/11/2000	0.46	0.00E+00	1.4E-01	6.00E-01
6/12/2000	0.41	2.06E-02	0.0E+00	3.86E-01
6/13/2000	0.44	7.65E-03	0.0E+00	4.30E-01
6/14/2000	0.47	4.51E-02	0.0E+00	4.23E-01
6/15/2000	0.47	4.15E-02	0.0E+00	4.32E-01
6/16/2000	0.47	5.18E-02	0.0E+00	4.15E-01
6/17/2000	0.44	0.00E+00	9.4E-02	5.38E-01
6/18/2000	0.36	0.00E+00	2.7E-02	3.89E-01
6/19/2000	0.36	0.00E+00	2.3E-02	3.87E-01
6/20/2000	0.36	0.00E+00	4.2E-03	3.60E-01
6/21/2000	0.39	3.39E-02	0.0E+00	3.59E-01
6/22/2000	0.42	0.00E+00	8.3E-04	4.18E-01
6/23/2000	0.39	3.85E-02	0.0E+00	3.55E-01
6/24/2000	0.40	4.17E-02	0.0E+00	3.55E-01
6/25/2000	0.40	0.00E+00	6.7E-03	4.03E-01
6/26/2000	0.41	4.44E-02	0.0E+00	3.61E-01
6/27/2000	0.38	2.41E-02	0.0E+00	3.56E-01
6/28/2000	0.37	0.00E+00	7.8E-02	4.49E-01
6/29/2000	0.36	0.00E+00	2.0E-02	3.76E-01
6/30/2000	0.32	0.00E+00	2.5E-03	3.18E-01
7/1/2000	0.33	0.00E+00	5.0E-03	3.37E-01
7/2/2000	0.34	9.43E-03	0.0E+00	3.28E-01
7/3/2000	0.35	6.70E-02	0.0E+00	2.78E-01
7/4/2000	0.37	2.68E-02	0.0E+00	3.44E-01
7/5/2000	0.36	4.78E-02	0.0E+00	3.09E-01
7/6/2000	0.37	5.87E-02	0.0E+00	3.13E-01

Table B.1 continued

Date	Field	WW-Avg-ET	Rainfall	Actual Application
	Application	Rate	Rate	Rate
	Rate ft/d (1)	ft/d (2)	ft/d (3)	ft/d (4)
	9	9	9	(4) =(1)-(2)+(3)
7/7/2000	0.39	5.96E-02	0.0E+00	3.29E-01
7/8/2000	0.37	5.90E-02	0.0E+00	3.11E-01
7/9/2000	0.39	6.64E-02	0.0E+00	3.22E-01
7/10/2000	0.38	7.00E-02	0.0E+00	3.07E-01
7/11/2000	0.39	7.36E-02	0.0E+00	3.16E-01
7/12/2000	0.41	0.00E+00	1.7E-03	4.11E-01
7/13/2000	0.36	0.00E+00	1.9E-02	3.79E-01
7/14/2000	0.35	1.04E-03	0.0E+00	3.52E-01
7/15/2000	0.37	1.32E-02	0.0E+00	3.54E-01
7/16/2000	0.38	1.12E-02	0.0E+00	3.73E-01
7/17/2000	0.39	1.25E-02	0.0E+00	3.73E-01
7/18/2000	0.40	1.46E-02	0.0E+00	3.83E-01
7/19/2000	0.40	1.26E-02	0.0E+00	3.92E-01
7/20/2000	0.42	1.25E-02	0.0E+00	4.11E-01
7/21/2000	0.42	1.29E-02	0.0E+00	4.12E-01
7/22/2000	0.41	1.09E-02	0.0E+00	4.04E-01
7/23/2000	0.43	0.00E+00	2.4E-02	4.58E-01
7/24/2000	0.42	2.45E-03	0.0E+00	4.19E-01
7/25/2000	0.43	1.54E-02	0.0E+00	4.13E-01
7/26/2000	0.42	1.95E-02	0.0E+00	3.99E-01
7/27/2000	0.43	2.24E-02	0.0E+00	4.11E-01
7/28/2000	0.42	1.81E-02	0.0E+00	4.05E-01
7/29/2000	0.43	0.00E+00	1.1E-02	4.43E-01
7/30/2000	0.40	9.58E-03	0.0E+00	3.90E-01
7/31/2000	0.42	0.00E+00	2.5E-03	4.25E-01
8/1/2000	0.41	1.25E-02	0.0E+00	3.99E-01
8/2/2000	0.41	1.94E-02	0.0E+00	3.94E-01
8/3/2000	0.42	1.98E-02	0.0E+00	4.01E-01
8/4/2000	0.40	2.13E-02	0.0E+00	3.77E-01
8/5/2000	0.41	2.15E-02	0.0E+00	3.93E-01
8/6/2000	0.40	1.97E-02	0.0E+00	3.85E-01
8/7/2000	0.40	1.88E-02	0.0E+00	3.81E-01
8/8/2000	0.41	0.00E+00	1.5E-02	4.23E-01
8/9/2000	0.39	8.39E-03	0.0E+00	3.78E-01
8/10/2000	0.41	2.18E-02	0.0E+00	3.85E-01

Table B.1 continued

Date	Field	WW-Avg-ET	Rainfall	Actual Application
	Application	Rate	Rate	Rate
	Rate ft/d (1)	ft/d (2)	ft/d (3)	ft/d (4)
	9	9	9	(4) =(1)-(2)+(3)
8/11/2000	0.40	2.44E-02	0.0E+00	3.80E-01
8/12/2000	0.40	2.53E-02	0.0E+00	3.77E-01
8/13/2000	0.41	2.61E-02	0.0E+00	3.79E-01
8/14/2000	0.40	2.67E-02	0.0E+00	3.71E-01
8/15/2000	0.39	2.90E-02	0.0E+00	3.66E-01
8/16/2000	0.39	2.66E-02	0.0E+00	3.67E-01
8/17/2000	0.38	2.06E-02	0.0E+00	3.64E-01
8/18/2000	0.37	1.96E-02	0.0E+00	3.46E-01
8/19/2000	0.37	1.94E-02	0.0E+00	3.53E-01
8/20/2000	0.37	2.29E-02	0.0E+00	3.43E-01
8/21/2000	0.38	2.41E-02	0.0E+00	3.54E-01
8/22/2000	0.37	2.13E-02	0.0E+00	3.49E-01
8/23/2000	0.37	2.15E-02	0.0E+00	3.53E-01
8/24/2000	0.37	2.19E-02	0.0E+00	3.47E-01
8/25/2000	0.36	2.19E-02	0.0E+00	3.43E-01
8/26/2000	0.36	2.26E-02	0.0E+00	3.37E-01
8/27/2000	0.37	2.47E-02	0.0E+00	3.47E-01
8/28/2000	0.36	2.32E-02	0.0E+00	3.36E-01
8/29/2000	0.20	1.78E-02	0.0E+00	1.86E-01
8/30/2000	0.35	1.65E-02	0.0E+00	3.31E-01
8/31/2000	0.38	1.53E-02	0.0E+00	3.61E-01
9/1/2000	0.37	2.34E-02	0.0E+00	3.49E-01
9/2/2000	0.38	2.49E-02	0.0E+00	3.53E-01
9/3/2000	0.37	2.95E-02	0.0E+00	3.45E-01
9/4/2000	0.37	2.58E-02	0.0E+00	3.42E-01
9/5/2000	0.38	2.82E-02	0.0E+00	3.51E-01
9/6/2000	0.37	2.30E-02	0.0E+00	3.48E-01
9/7/2000	0.36	3.39E-02	0.0E+00	3.24E-01
9/8/2000	0.35	2.61E-02	0.0E+00	3.27E-01
9/9/2000	0.35	2.35E-02	0.0E+00	3.25E-01
9/10/2000	0.36	1.90E-02	0.0E+00	3.36E-01
9/11/2000	0.35	2.09E-02	0.0E+00	3.33E-01
9/12/2000	0.36	3.08E-02	0.0E+00	3.31E-01
9/13/2000	0.37	4.95E-02	0.0E+00	3.24E-01
9/14/2000	0.34	2.38E-02	0.0E+00	3.21E-01

Table B.1 continued

Date	Field	WW-Avg-ET	Rainfall	Actual Application
	Application	Rate	Rate	Rate
	Rate ft/d (1)	ft/d (2)	ft/d (3)	ft/d (4)
	9	9	9	(4) =(1)-(2)+(3)
9/15/2000	0.34	2.81E-02	0.0E+00	3.17E-01
9/16/2000	0.34	2.47E-02	0.0E+00	3.16E-01
9/17/2000	0.34	2.73E-02	0.0E+00	3.17E-01
9/18/2000	0.34	2.90E-02	0.0E+00	3.08E-01
9/19/2000	0.33	3.06E-02	0.0E+00	3.04E-01
9/20/2000	0.34	2.79E-02	0.0E+00	3.07E-01
9/21/2000	0.33	2.30E-02	0.0E+00	3.10E-01
9/22/2000	0.30	2.04E-02	0.0E+00	2.80E-01
9/23/2000	0.32	2.87E-02	0.0E+00	2.91E-01
9/24/2000	0.31	1.81E-02	0.0E+00	2.94E-01
9/25/2000	0.31	1.69E-02	0.0E+00	2.94E-01
9/26/2000	0.30	1.70E-02	0.0E+00	2.88E-01
9/27/2000	0.31	2.04E-02	0.0E+00	2.85E-01
9/28/2000	0.30	1.86E-02	0.0E+00	2.78E-01
9/29/2000	0.31	2.24E-02	0.0E+00	2.88E-01
9/30/2000	0.30	2.30E-02	0.0E+00	2.81E-01
10/1/2000	0.32	2.68E-02	0.0E+00	2.95E-01
10/2/2000	0.30	2.69E-02	0.0E+00	2.78E-01
10/3/2000	0.31	2.96E-02	0.0E+00	2.80E-01
10/4/2000	0.31	2.78E-02	0.0E+00	2.85E-01
10/5/2000	0.29	2.54E-02	0.0E+00	2.64E-01
10/6/2000	0.33	0.00E+00	8.3E-04	3.29E-01
10/7/2000	0.30	0.00E+00	8.3E-04	3.01E-01
10/8/2000	0.30	1.03E-02	0.0E+00	2.86E-01
10/9/2000	0.29	9.43E-03	0.0E+00	2.83E-01
10/10/2000	0.28	1.13E-02	0.0E+00	2.69E-01
10/11/2000	0.26	1.20E-02	0.0E+00	2.47E-01
10/12/2000	0.26	9.80E-03	0.0E+00	2.53E-01
10/13/2000	0.28	1.37E-02	0.0E+00	2.63E-01
10/14/2000	0.28	1.64E-02	0.0E+00	2.60E-01
10/15/2000	0.27	0.00E+00	6.7E-03	2.72E-01
10/16/2000	0.25	0.00E+00	8.3E-04	2.54E-01
10/17/2000	0.25	0.00E+00	6.5E-02	3.15E-01
10/18/2000	0.24	0.00E+00	8.3E-04	2.40E-01
10/19/2000	0.26	0.00E+00	8.3E-04	2.57E-01

Table B.1 continued

Date	Field	WW-Avg-ET	Rainfall	Actual Application
	Application	Rate	Rate	Rate
	Rate ft/d (1)	ft/d (2)	ft/d (3)	ft/d (4)
	9	9	9	(4) =(1)-(2)+(3)
10/20/2000	0.27	0.00E+00	8.3E-04	2.68E-01
10/21/2000	0.25	0.00E+00	2.5E-03	2.51E-01
10/22/2000	0.23	7.13E-03	0.0E+00	2.24E-01
10/23/2000	0.25	0.00E+00	1.5E-02	2.61E-01
10/24/2000	0.23	0.00E+00	1.5E-02	2.45E-01
10/25/2000	0.18	0.00E+00	1.1E-02	1.89E-01
10/26/2000	0.21	0.00E+00	8.3E-03	2.23E-01
10/27/2000	0.25	0.00E+00	5.8E-03	2.56E-01
10/28/2000	0.26	0.00E+00	5.8E-03	2.62E-01
10/29/2000	0.22	0.00E+00	4.2E-03	2.23E-01
10/30/2000	0.24	0.00E+00	4.2E-03	2.45E-01
10/31/2000	0.24	0.00E+00	5.0E-03	2.40E-01
11/1/2000	0.22	0.00E+00	3.3E-03	2.25E-01
11/2/2000	0.22	0.00E+00	2.5E-03	2.26E-01
11/3/2000	0.22	0.00E+00	2.5E-03	2.23E-01
11/4/2000	0.24	0.00E+00	1.7E-03	2.37E-01
11/5/2000	0.20	0.00E+00	2.5E-03	2.03E-01
11/6/2000	0.17	0.00E+00	1.7E-03	1.73E-01
11/7/2000	0.22	0.00E+00	8.3E-04	2.25E-01
11/8/2000	0.22	0.00E+00	1.8E-02	2.36E-01
11/9/2000	0.19	0.00E+00	2.8E-02	2.21E-01
11/10/2000	0.15	0.00E+00	8.3E-04	1.49E-01
11/11/2000	0.19	0.00E+00	0.0E+00	1.93E-01
11/12/2000	0.09	1.19E-03	0.0E+00	9.13E-02
11/13/2000	0.16	2.60E-03	0.0E+00	1.59E-01
11/14/2000	0.22	2.67E-03	0.0E+00	2.17E-01
11/15/2000	0.19	2.15E-03	0.0E+00	1.90E-01
11/16/2000	0.21	2.38E-03	0.0E+00	2.08E-01
11/17/2000	0.20	3.94E-03	0.0E+00	1.99E-01
11/18/2000	0.20	0.00E+00	1.7E-03	2.06E-01
11/19/2000	0.23	0.00E+00	1.7E-03	2.30E-01
11/20/2000	0.19	2.30E-03	0.0E+00	1.89E-01
11/21/2000	0.20	5.20E-03	0.0E+00	2.00E-01
11/22/2000	0.20	3.64E-03	0.0E+00	2.01E-01
11/23/2000	0.19	0.00E+00	1.6E-02	2.10E-01

Table B.1 continued

Date	Field	WW-Avg-ET	Rainfall	Actual Application
	Application	Rate	Rate	Rate
	Rate ft/d (1)	ft/d (2)	ft/d (3)	ft/d (4)
	9	9	9	(4) =(1)-(2)+(3)
11/24/2000	0.20	0.00E+00	1.7E-03	2.02E-01
11/25/2000	0.18	0.00E+00	8.3E-04	1.77E-01
11/26/2000	0.19	3.27E-03	0.0E+00	1.84E-01
11/27/2000	0.20	2.60E-03	0.0E+00	1.95E-01
11/28/2000	0.20	3.57E-03	0.0E+00	1.95E-01
11/29/2000	0.19	5.79E-03	0.0E+00	1.88E-01
11/30/2000	0.21	4.01E-03	0.0E+00	2.09E-01
12/1/2000	0.19	3.27E-03	0.0E+00	1.88E-01
12/2/2000	0.20	5.50E-03	0.0E+00	1.93E-01
12/3/2000	0.20	0.00E+00	1.7E-03	2.00E-01
12/4/2000	0.19	1.11E-03	0.0E+00	1.92E-01
12/5/2000	0.20	0.00E+00	8.3E-04	1.99E-01
12/6/2000	0.19	3.05E-03	0.0E+00	1.88E-01
12/7/2000	0.19	3.49E-03	0.0E+00	1.91E-01
12/8/2000	0.20	3.19E-03	0.0E+00	1.95E-01
12/9/2000	0.20	3.19E-03	0.0E+00	1.96E-01
12/10/2000	0.19	3.49E-03	0.0E+00	1.84E-01
12/11/2000	0.18	2.67E-03	0.0E+00	1.77E-01
12/12/2000	0.21	8.17E-03	0.0E+00	2.02E-01
12/13/2000	0.19	0.00E+00	8.3E-04	1.92E-01
12/14/2000	0.20	1.93E-03	0.0E+00	1.95E-01
12/15/2000	0.20	0.00E+00	8.3E-04	2.02E-01
12/16/2000	0.20	3.49E-03	0.0E+00	1.93E-01
12/17/2000	0.21	4.01E-03	0.0E+00	2.06E-01
12/18/2000	0.20	4.68E-03	0.0E+00	1.99E-01
12/19/2000	0.23	6.91E-03	0.0E+00	2.23E-01
12/20/2000	0.22	2.97E-03	0.0E+00	2.18E-01
12/21/2000	0.22	5.27E-03	0.0E+00	2.19E-01
12/22/2000	0.24	5.27E-03	0.0E+00	2.36E-01
12/23/2000	0.23	3.19E-03	0.0E+00	2.28E-01
12/24/2000	0.25	1.86E-03	0.0E+00	2.48E-01
12/25/2000	0.25	7.13E-03	0.0E+00	2.46E-01
12/26/2000	0.00	0.00E+00	0.0E+00	0.00E+00
12/27/2000	0.00	0.00E+00	2.5E-03	2.50E-03
12/28/2000	0.26	4.23E-03	0.0E+00	2.60E-01

Table B.1 continued

Date	Field	WW-Avg-ET	Rainfall	Actual Application
	Application	Rate	Rate	Rate
	Rate ft/d (1)	ft/d (2)	ft/d (3)	ft/d (4)
	9	9	9	(4) =(1)-(2)+(3)
12/29/2000	0.42	7.43E-05	0.0E+00	4.23E-01
12/30/2000	0.20	8.17E-04	0.0E+00	1.94E-01
12/31/2000	0.24	0.00E+00	8.3E-04	2.41E-01

APPENDIX C

CALCULATION OF ERROR FOR 30-DAY EVT TRIAL AND 1000-DAY EVT TRIAL

CALCULATION OF ERROR FOR 30-DAY EVT TRIAL AND 1000-DAY EVT TRIAL

C.1 Calculation of error for a 30-day EVT trial

Data Used:

1) Negative recharge rate applied- 0.02 ft/day
2) Duration of application- 30 days
3) Dimensions of model 60 ft X 60 ft X 80 ft
4) Number of layers in model 3
5) Types of soil used Sandy loam
6) Soil Properties
   a. Porosity 0.41
   b. Storativity 6×10^{-5}
   c. Residual water saturation 0.1585
   d. Van Genuchten alpha 2.46×10^{-3}
   e. Van Genuchten beta 1.89
7) Area over which negative recharge applied- 3600 ft^2

Calculations:

Layer elevations used for computation of initial water saturation

Layer 1	80 ft
Layer 2	53.33 ft
Layer 3	26.67 ft

Initial water saturation

Layer 1	0.595
Layer 2	0.606
Layer 3	0.618

Final water saturation

Layer 1	0.558
Layer 2	0.594
Layer 3	0.613

Water removed from each layer after simulation period

Layer 1	1456.502
Layer 2	472.38 ft^3
Layer 3	196.82 ft^3
Total water loss	2125.71 ft^3

Water loss value from MODFLOW-SURFACT diagnostic output- 2160 ft^3

Percentage error 1.59 %

C.2 Calculation of error for a 1000-day EVT trial

Data Used:

1) Negative recharge rate applied- 0.02 ft/day
2) Duration of application- 1000 days
3) Dimensions of model 60 ft X 60 ft X 80 ft
4) Number of layers in model 3
5) Types of soil used Sandy loam
6) Soil Properties
   a. Porosity 0.41
   b. Storativity 6×10^{-5}
   c. Residual water saturation 0.1585
   d. Van Genuchten alpha 2.46×10^{-3}
   e. Van Genuchten beta 1.89
7) Area over which negative recharge applied- 3600 ft^2

Calculations:

Layer elevations used for computation of initial water saturation

Layer 1	80 ft
Layer 2	53.33 ft
Layer 3	26.67 ft

Initial water saturation

Layer 1	0.595
Layer 2	0.606
Layer 3	0.618

Final water saturation

Layer 1	0.159
Layer 2	0.195
Layer 3	0.245

Water removed from each layer after simulation period

Layer 1	17,163.11 ft^3
Layer 2	16,178.98 ft^3
Layer 3	14,683.12 ft^3

Total water loss 48,025.2 ft^3

Water loss value from MODFLOW-SURFACT diagnostic output- 72,000 ft^3

Percentage error 33.3 %

Numerical Simulation of Unsaturated Flow Near a Septic System Drainfield

Volume II. Appendix D

By

Nilesh Waghdare, M.S.,
Ken Rainwater, Ph.D., P.E., DEE, and
Andrew Jackson, Ph.D., P.E.
Texas Tech University Water Resources Center
Box 41022
Lubbock, TX 79409-1022

Submitted to

Texas On-Site Wastewater Treatment Research Council
Texas Commission on Environmental Quality
OSSF Program MC-178
P.O. Box 13087
Austin, TX 78711-3087

December, 2003

APPENDIX D

CONTOUR AND VECTORS PLOTS

GENERATED FROM THE

SIMULATIONS

RUN

Simulation-SLA1-Sandy Loam soil with ET domain type A
Time -30 days after beginning of simulation
Date-2/13/2000

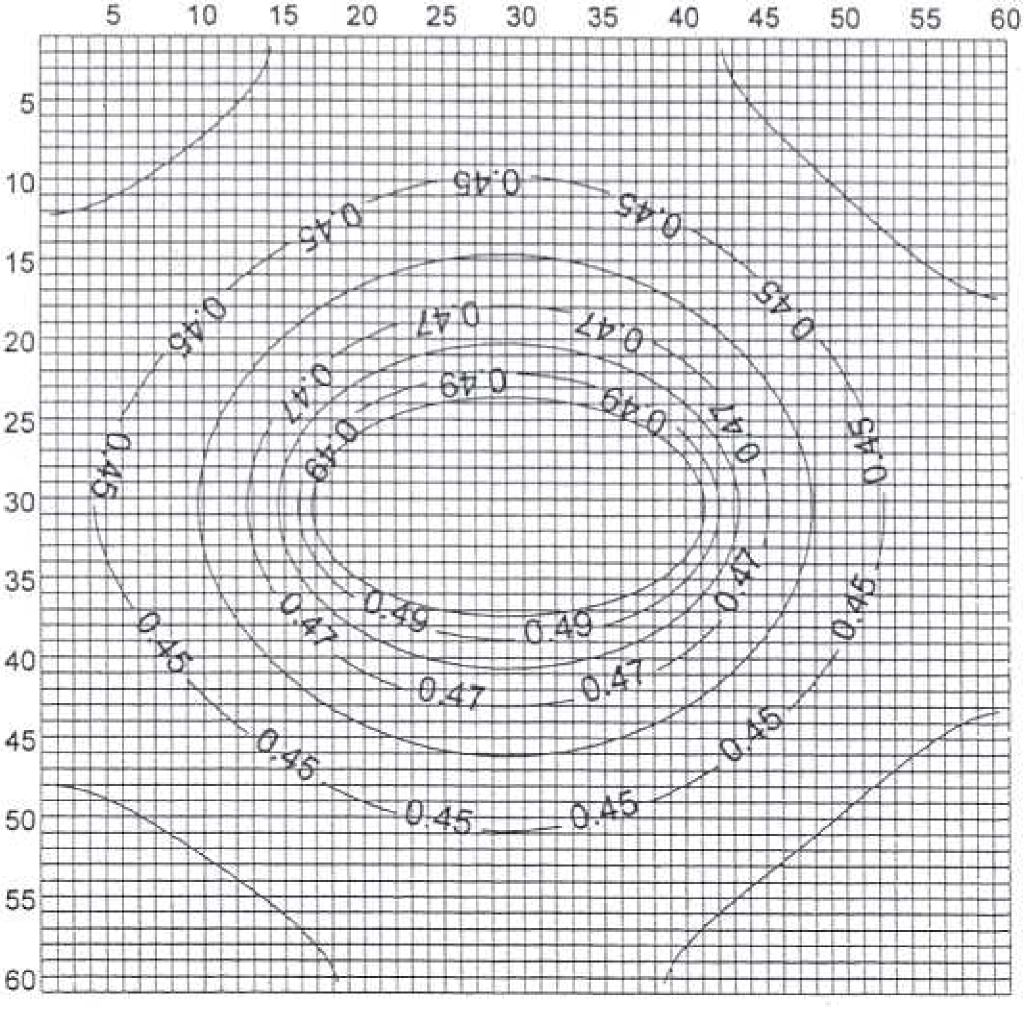

Figure D.1 Water saturation contours in plan view for SLA1

Simulation-SLA2-Sandy Loam soil with ET domain type A
Time -60 days after beginning of simulation
Date-3/14/2000

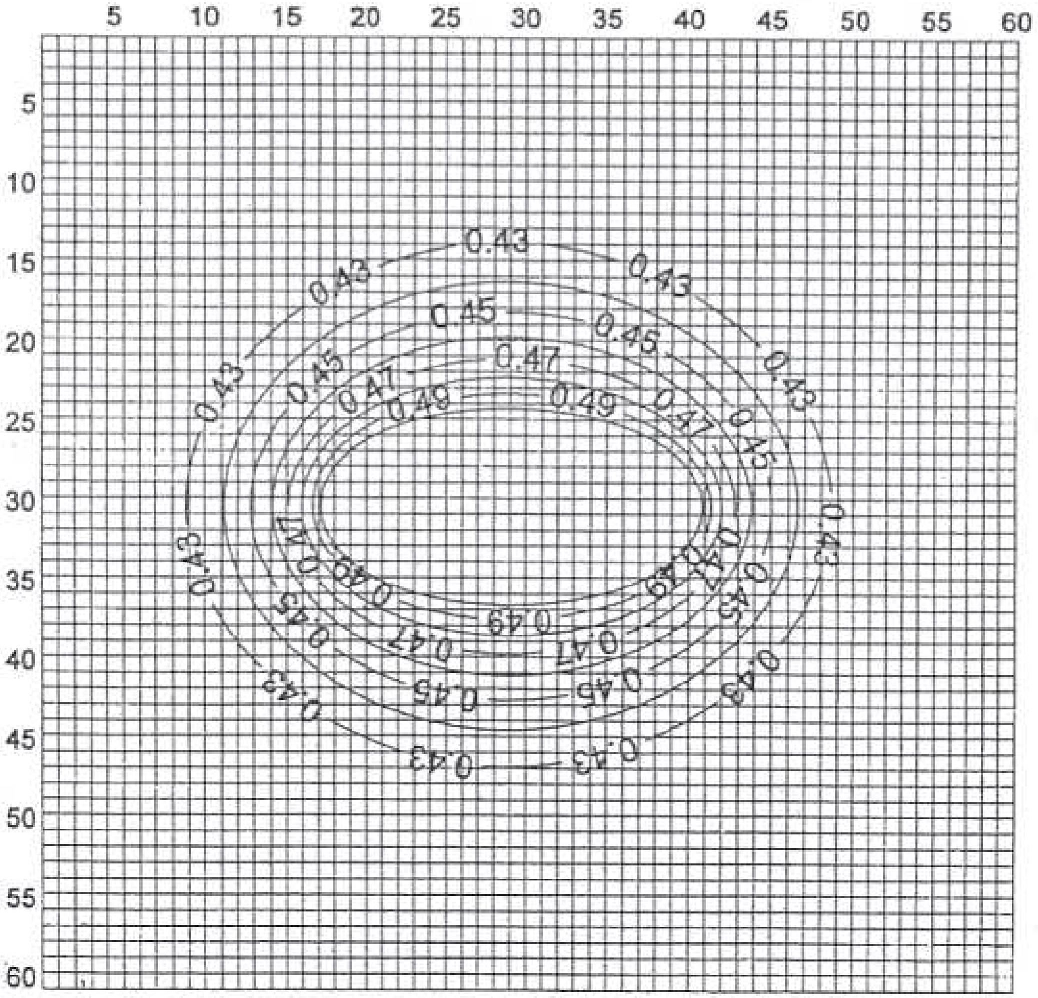

Figure D.2 Water saturation contours in plan view for SLA2

Simulation-SLA3-Sandy Loam soil with ET domain type A
Time -90 days after beginning of simulation
Date-4/13/2000

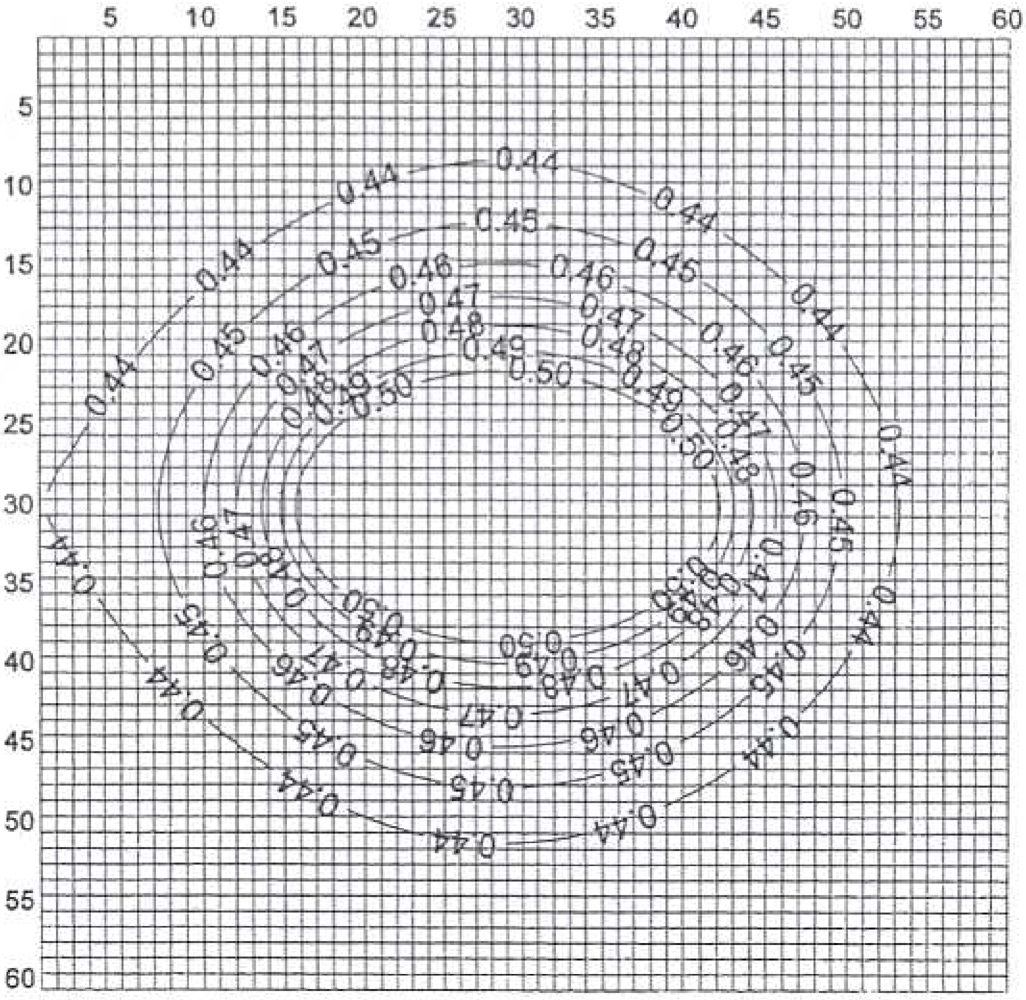

Figure D.3 Water saturation contours in plan view for SLA3

Simulation-SLA4-Sandy Loam soil with ET domain type A
Time -120 days after beginning of simulation
Date-5/13/2000

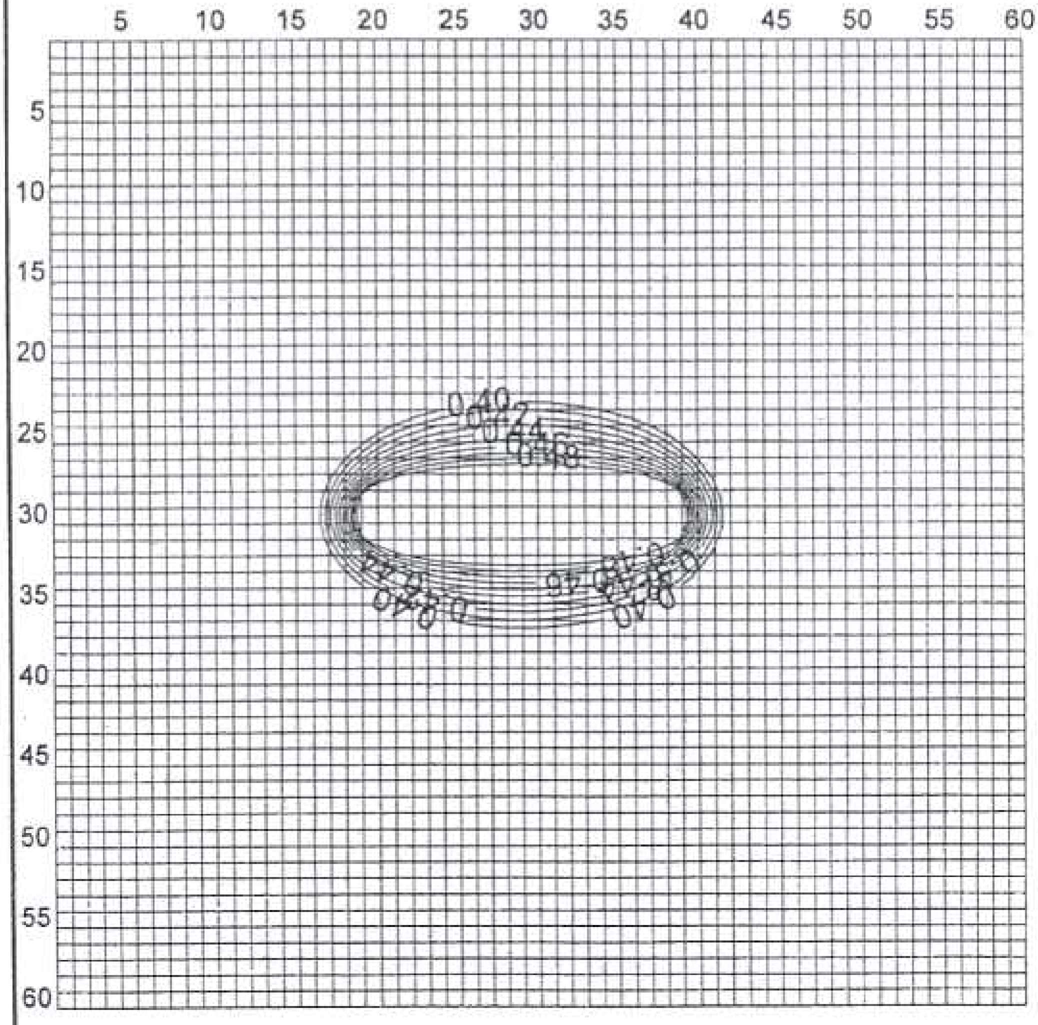

Figure D.4 Water saturation contours in plan view for SLA4

Simulation-SLA5-Sandy Loam soil with ET domain type A
Time -150 days after beginning of simulation
Date-6/12//2000

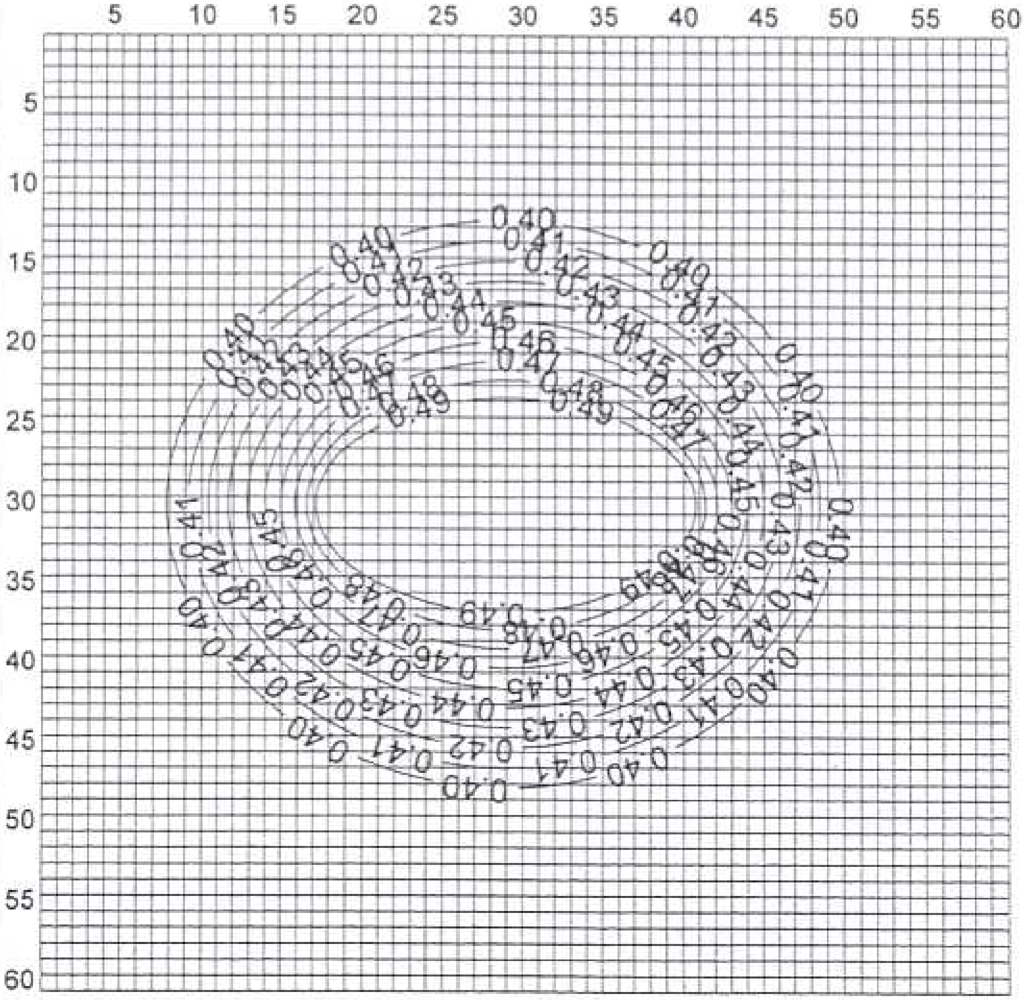

Figure D.5 Water saturation contours in plan view for SLA5

Simulation-SLA6-Sandy Loam soil with ET domain type A
Time -180 days after beginning of simulation
Date-7/12/2000

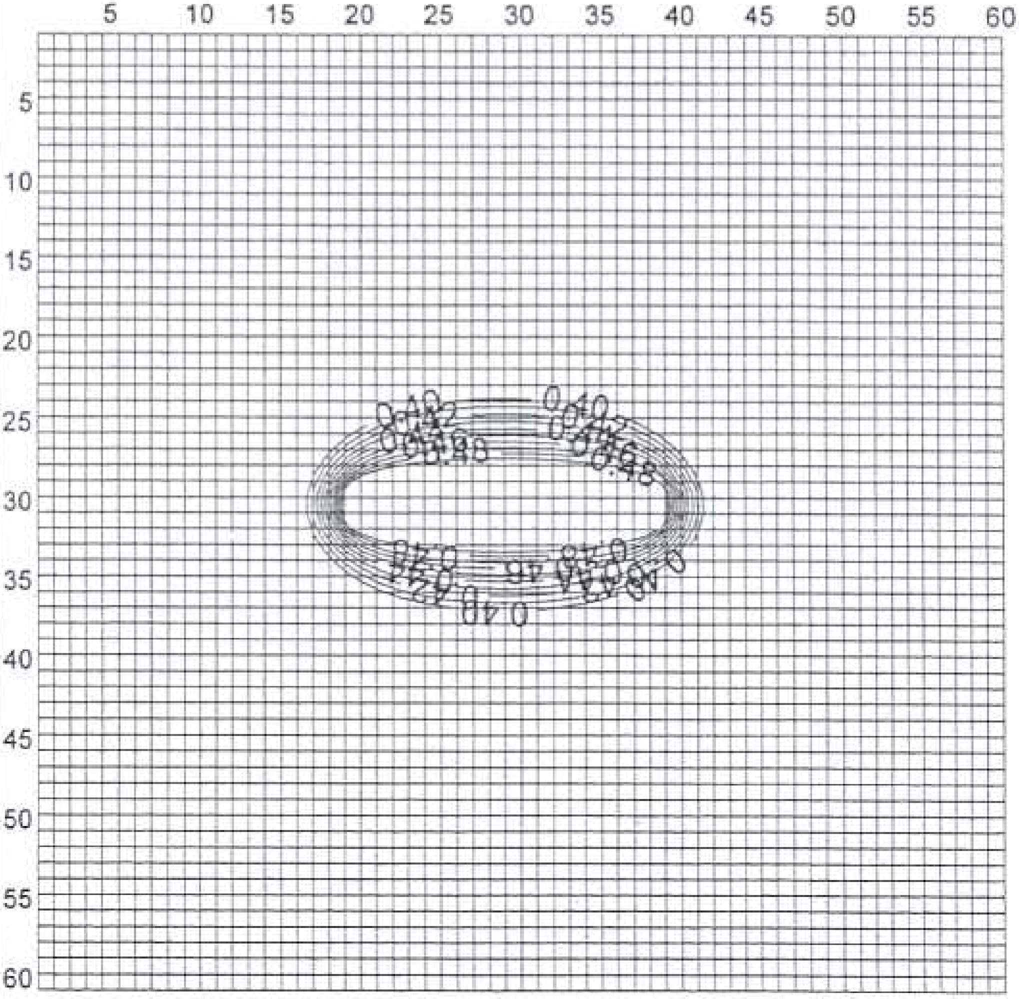

Figure D.6 Water saturation contours in plan view for SLA6

Simulation-SLA7-Sandy Loam soil with ET domain type A
Time -210 days after beginning of simulation
Date-8/11/2000

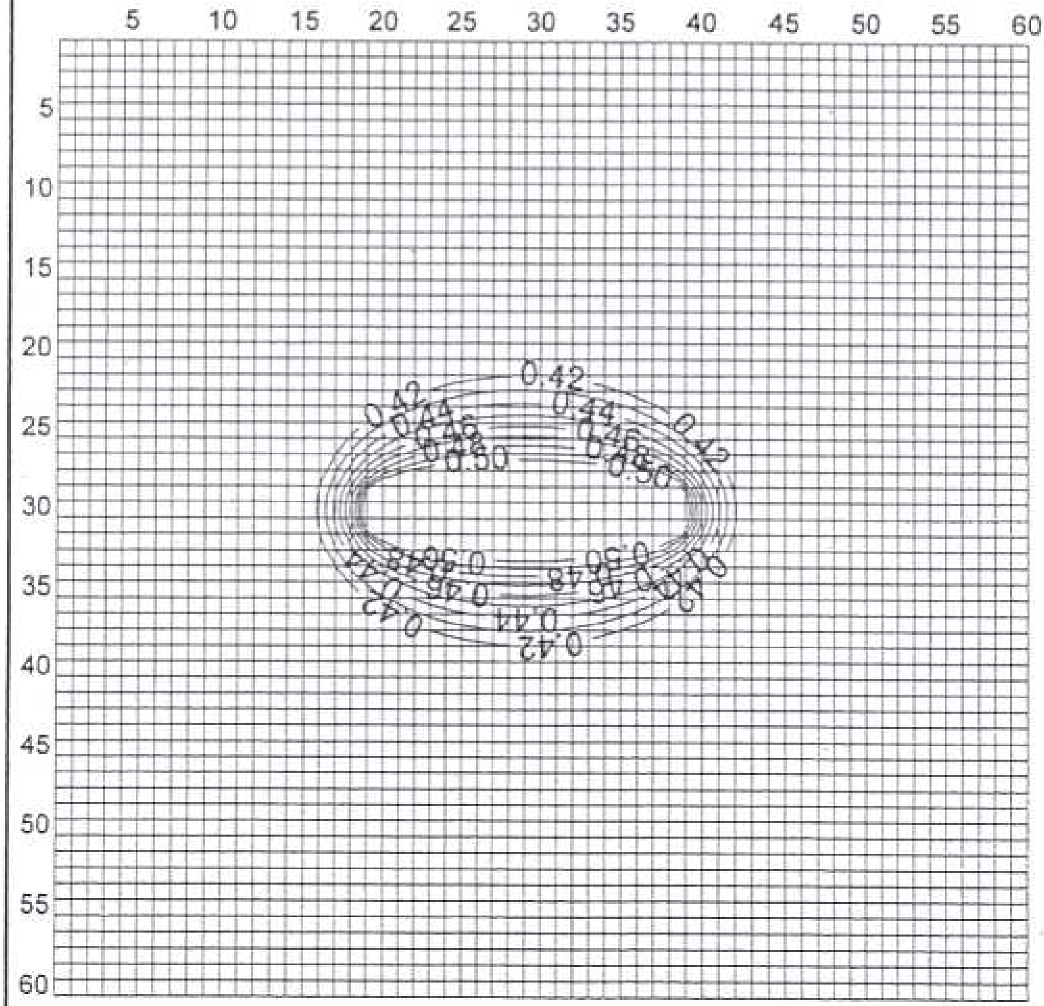

Figure D.7 Water saturation contours in plan view for SLA7

Simulation-SLA8-Sandy Loam soil with ET domain type A
Time -240 days after beginning of simulation
Date-9/10/2000

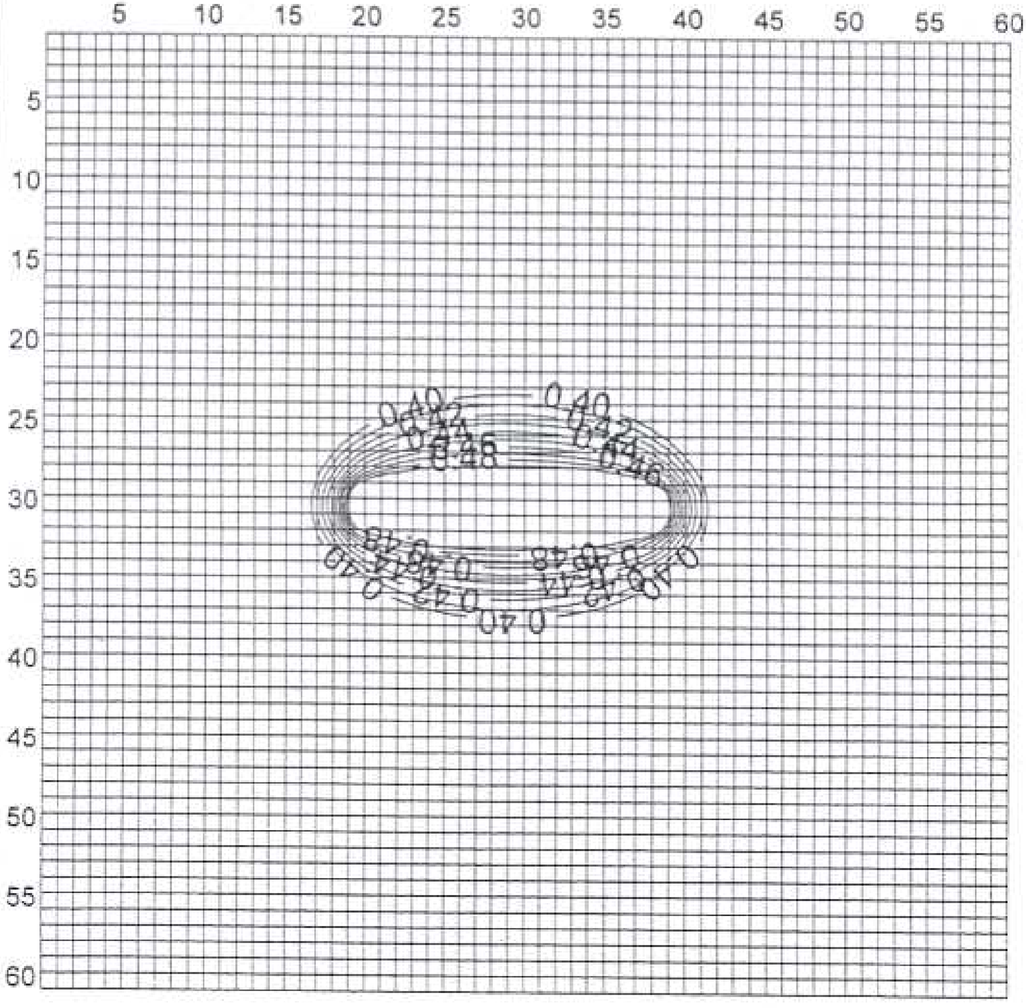

Figure D.8 Water saturation contours in plan view for SLA8

Simulation-SLA9-Sandy Loam soil with ET domain type A
Time -270 days after beginning of simulation
Date-10/10/2000

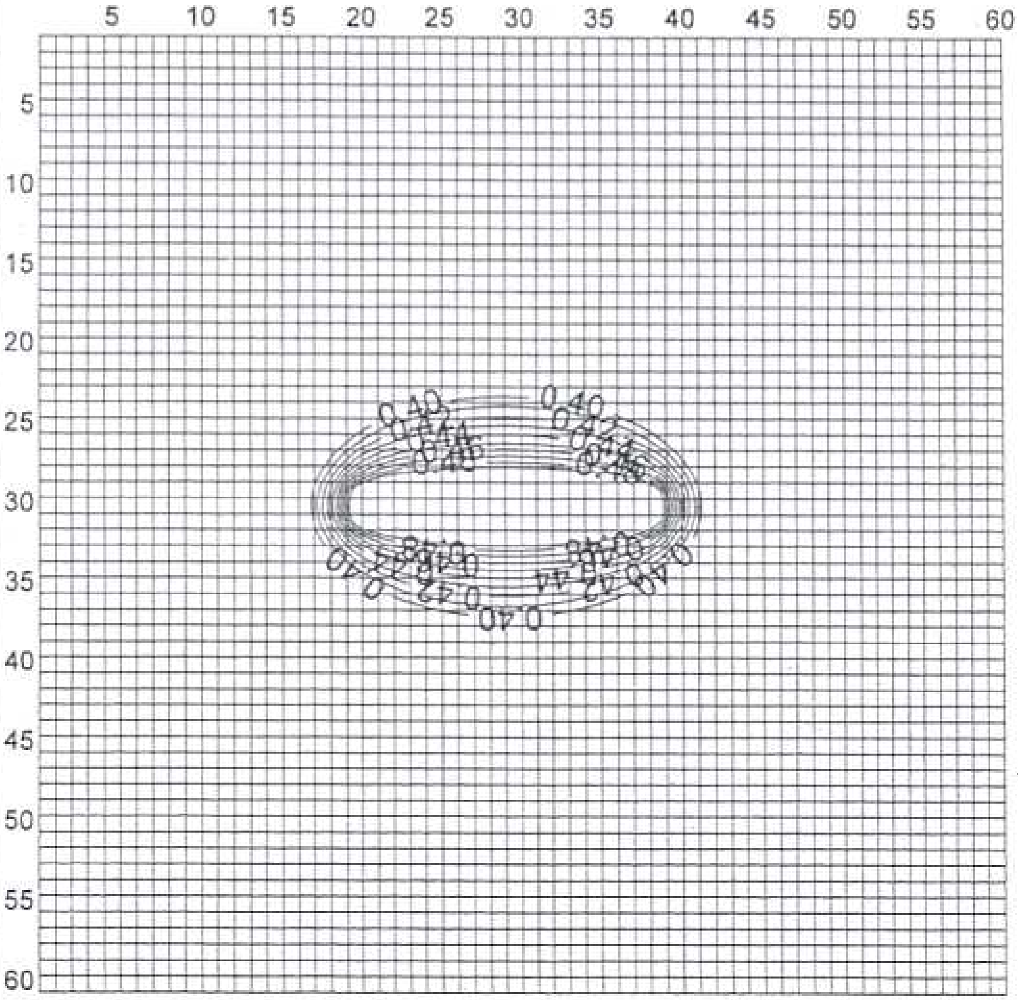

Figure D.9 Water saturation contours in plan view for SLA9

Simulation-SLA10-Sandy Loam soil with ET domain type A
Time -300 days after beginning of simulation
Date-11/9/2000

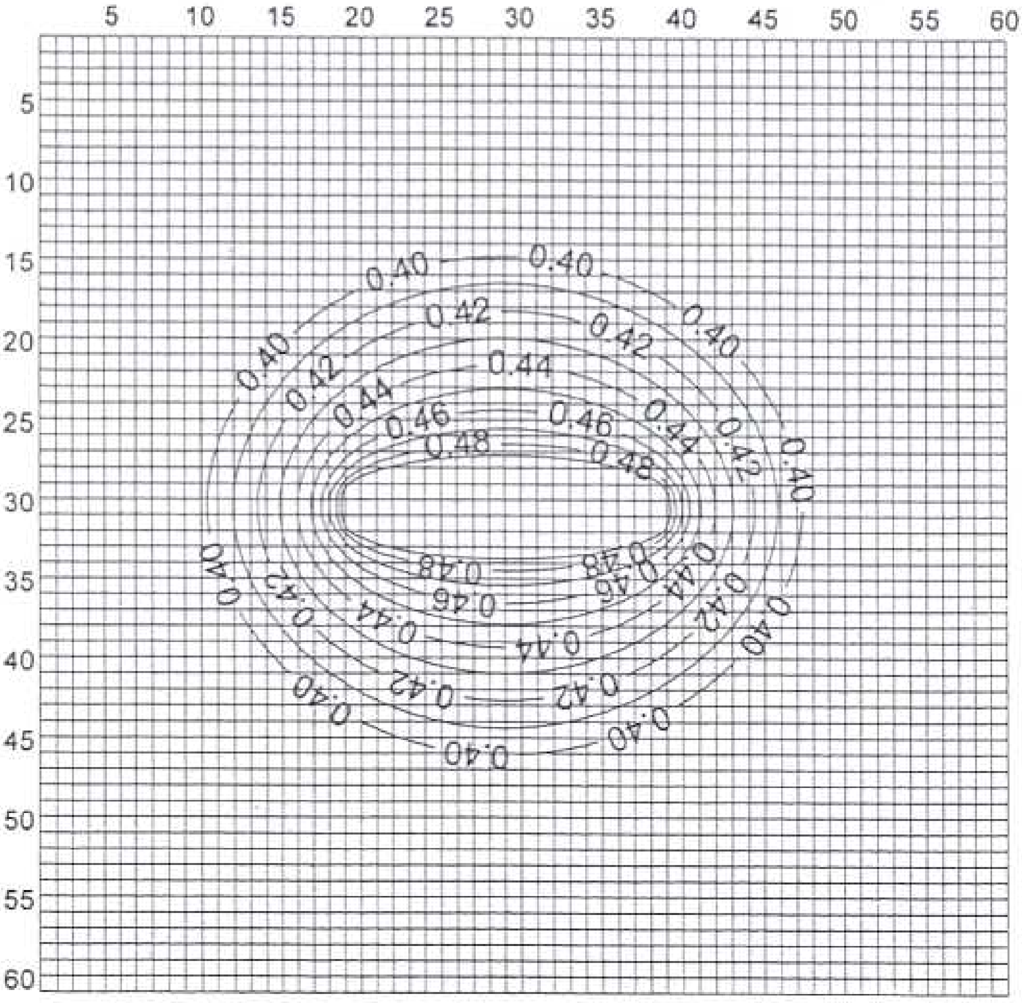

Figure D.10 Water saturation contours in plan view for SLA10

Simulation-SLA11-Sandy Loam soil with ET domain type A
Time -330 days after beginning of simulation
Date-12/9/2000

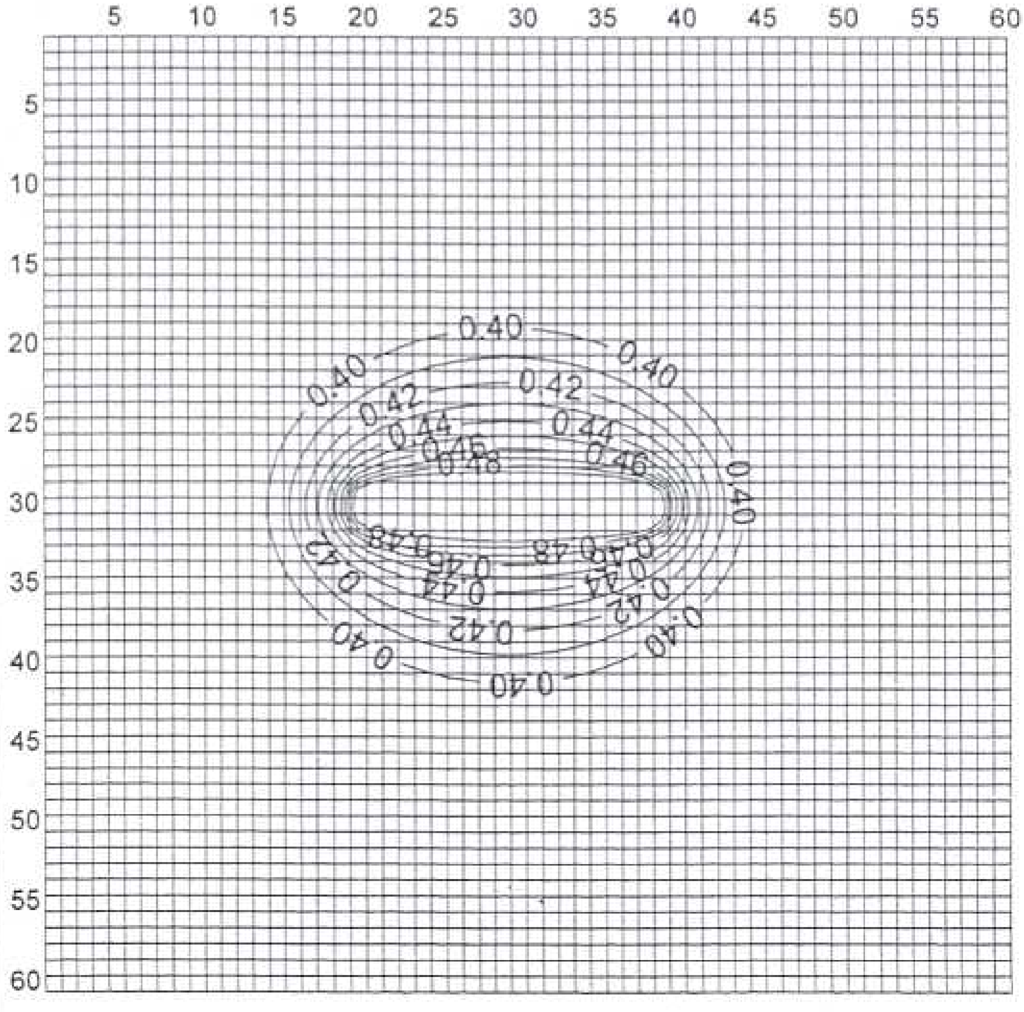

Figure D.11 Water saturation contours in plan view for SLA11

Simulation-SLA12-Sandy Loam soil with ET domain type A
Time -352 days after beginning of simulation
Date-12/31/2000

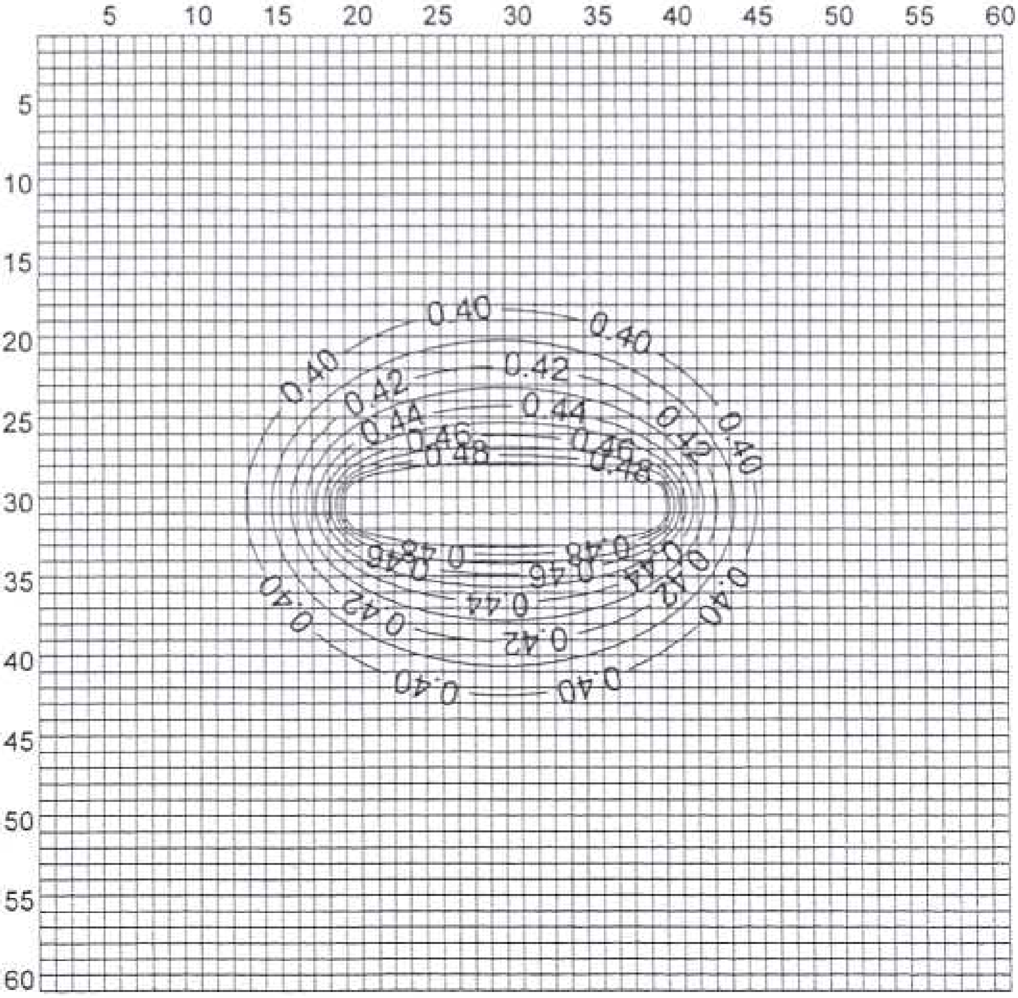

Figure D.12 Water saturation contours in plan view for SLA12

Simulation-SLA1-Sandy Loam soil with ET domain type A
Time -30 days after beginning of simulation
Date-2/13/2000

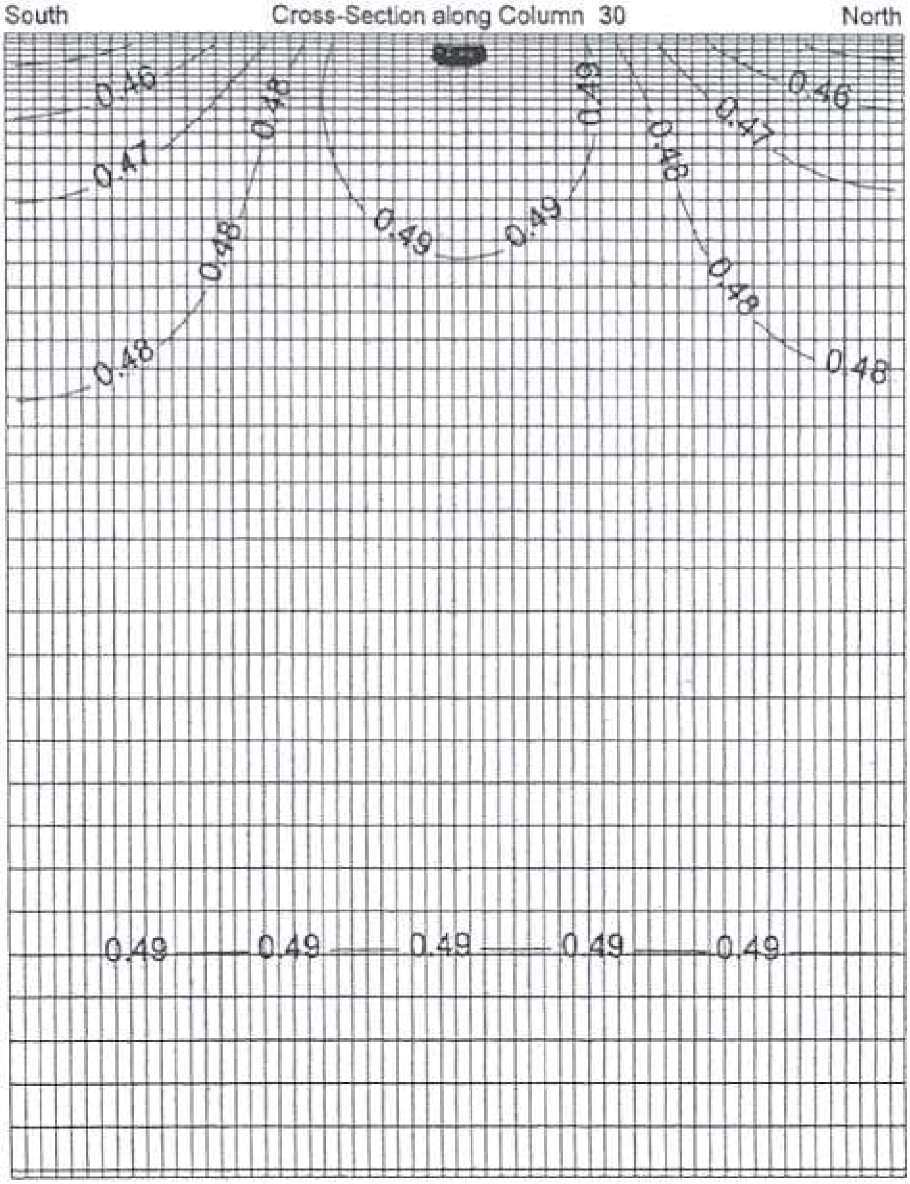

Figure D.13 Water saturation contours in cross-section for SLA1

Simulation-SLA2-Sandy Loam soil with ET domain type A
Time -60 days after beginning of simulation
Date-3/14/2000

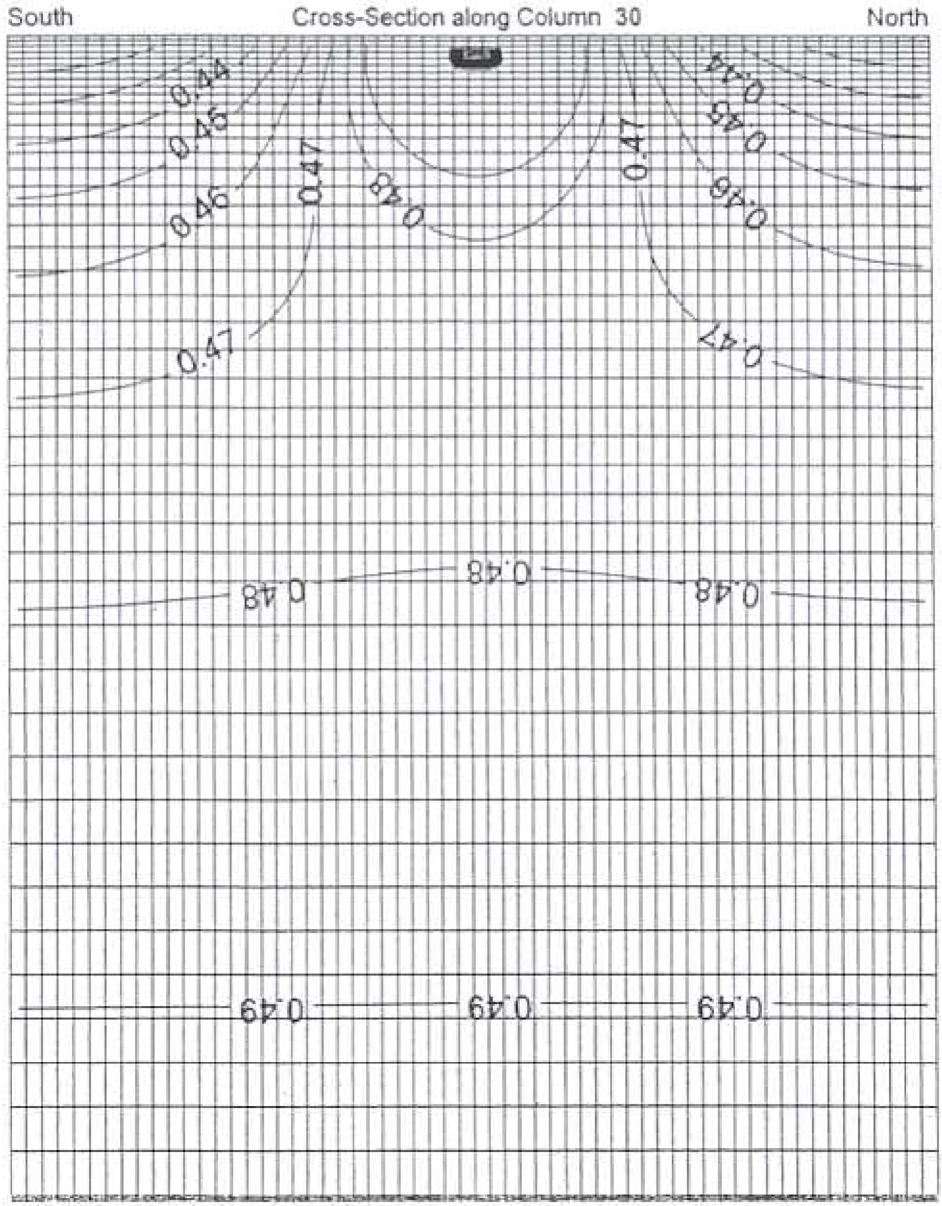

Figure D.14 Water saturation contours in cross-section for SLA2

Simulation-SLA3-Sandy Loam soil with ET domain type A
Time -90 days after beginning of simulation
Date-4/13/2000

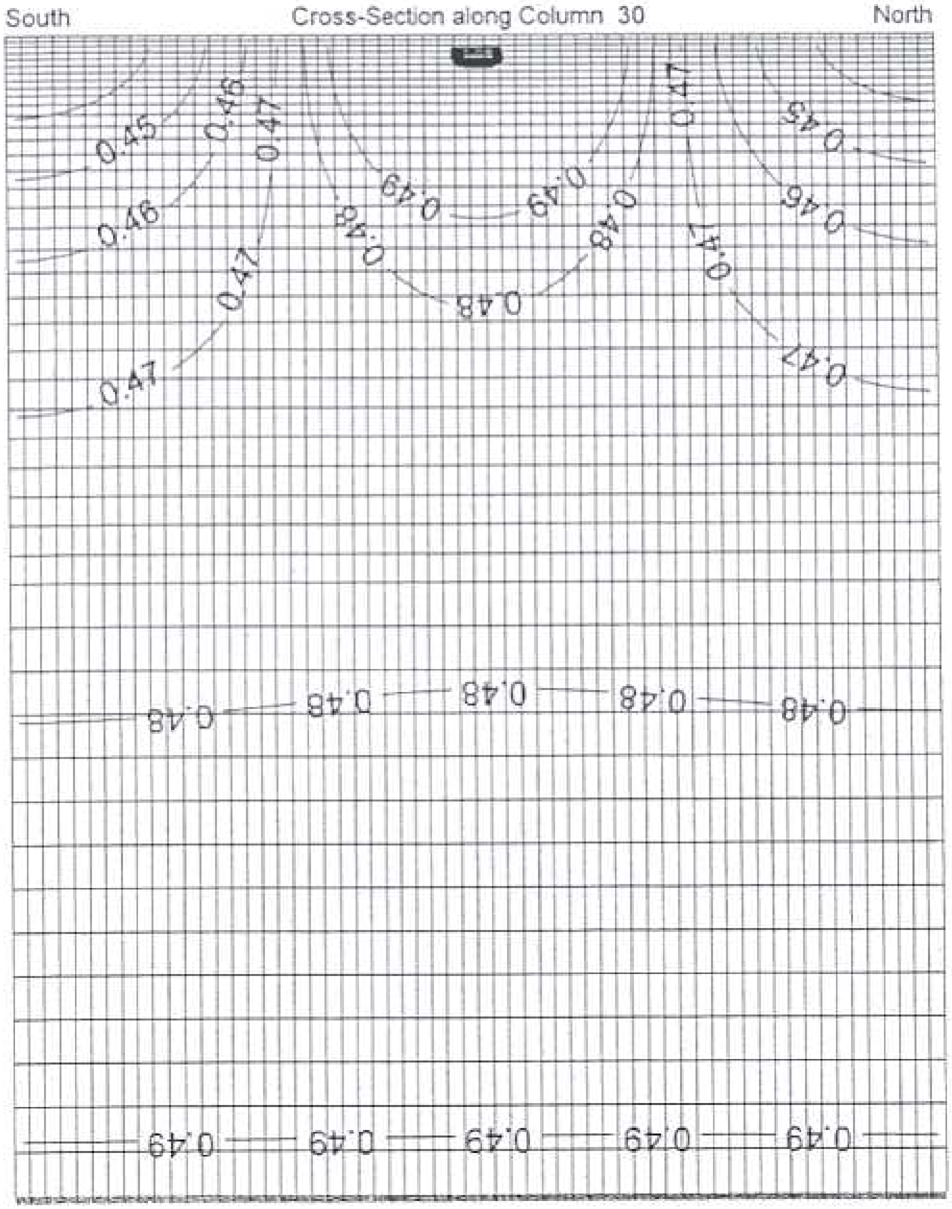

Figure D.15 Water saturation contours in cross-section for SLA3

Simulation-SLA4-Sandy Loam soil with ET domain type A
Time -120 days after beginning of simulation
Date-5/13/2000

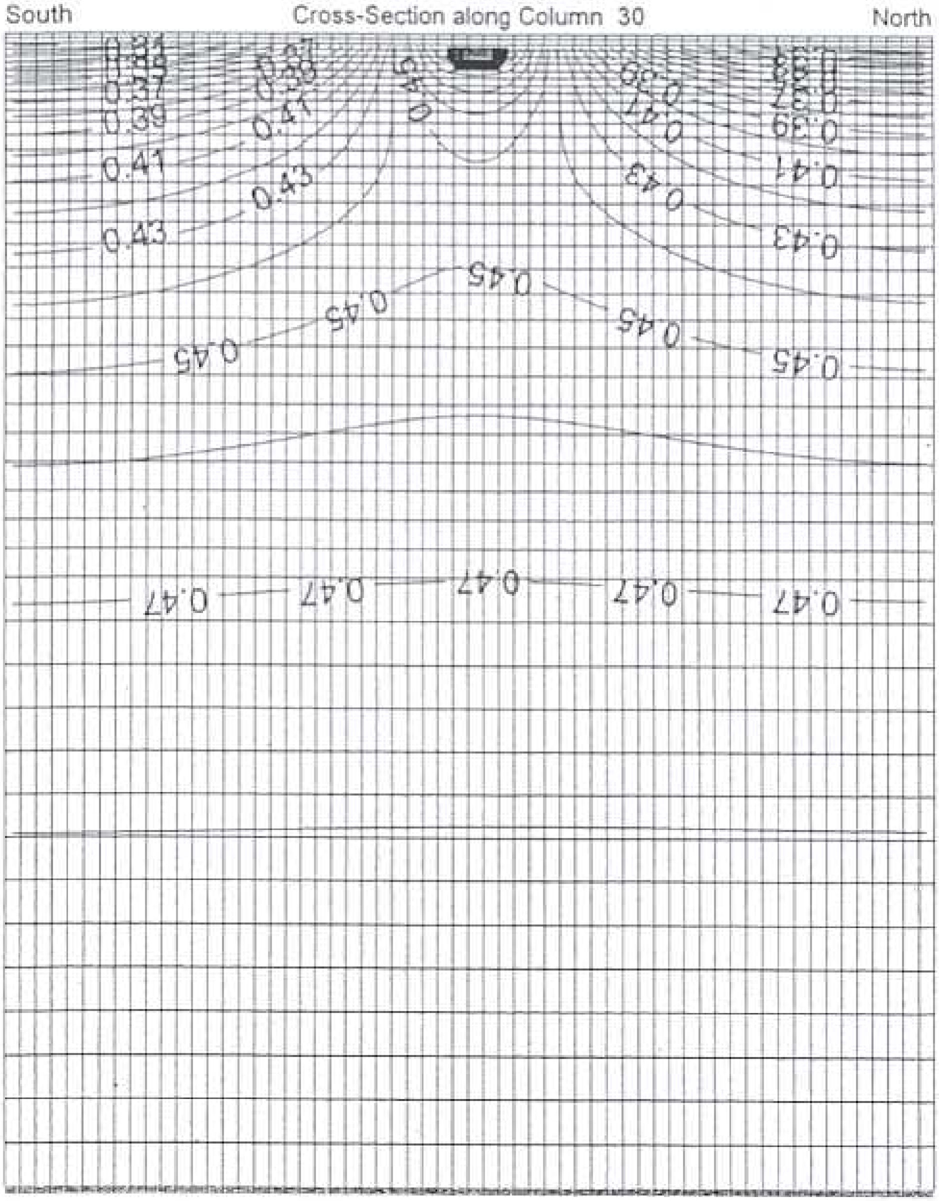

Figure D.16 Water saturation contours in cross-section for SLA4

Simulation-SLA5-Sandy Loam soil with ET domain type A
Time -150 days after beginning of simulation
Date-6/12//2000

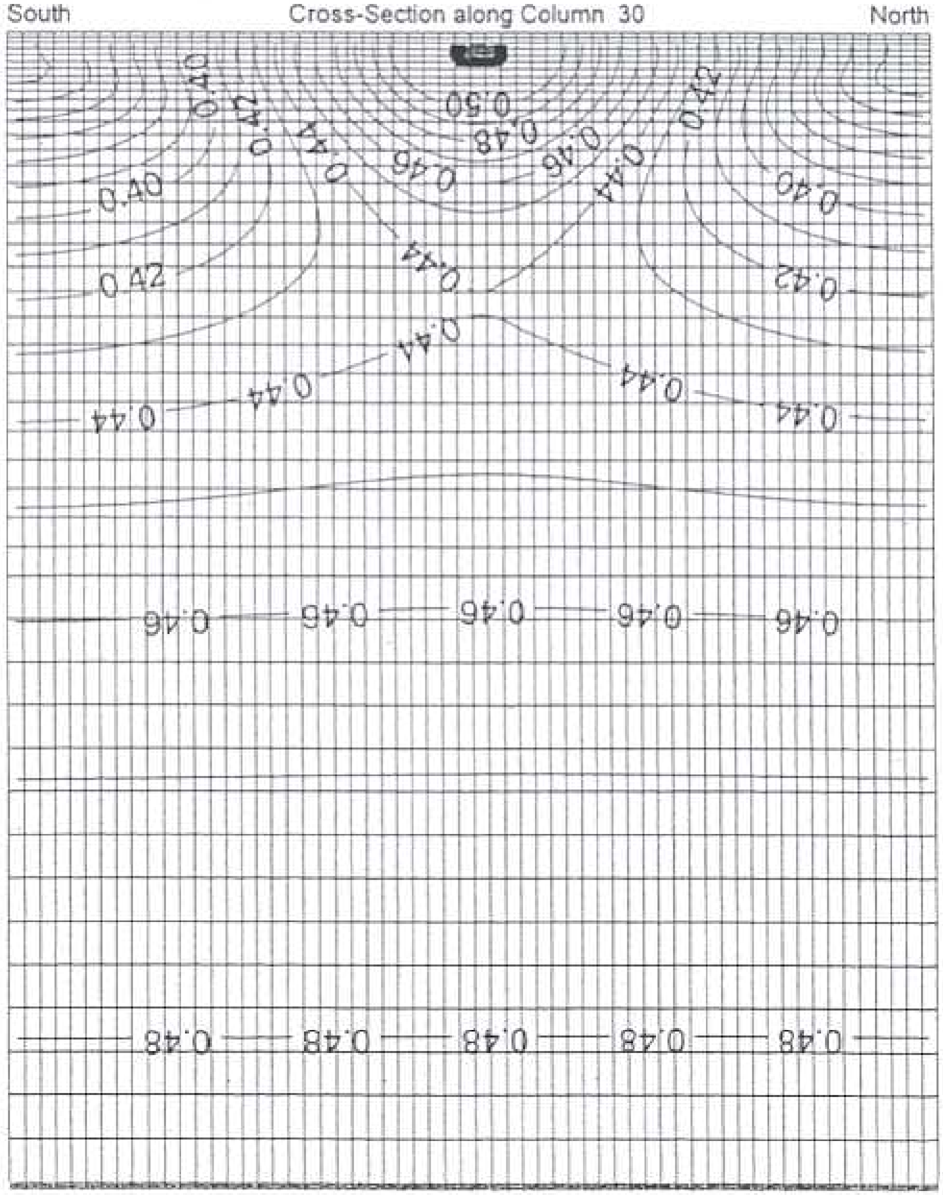

Figure D.17 Water saturation contours in cross-section for SLA5

Simulation-SLA6-Sandy Loam soil with ET domain type A
Time -180 days after beginning of simulation
Date-7/12/2000

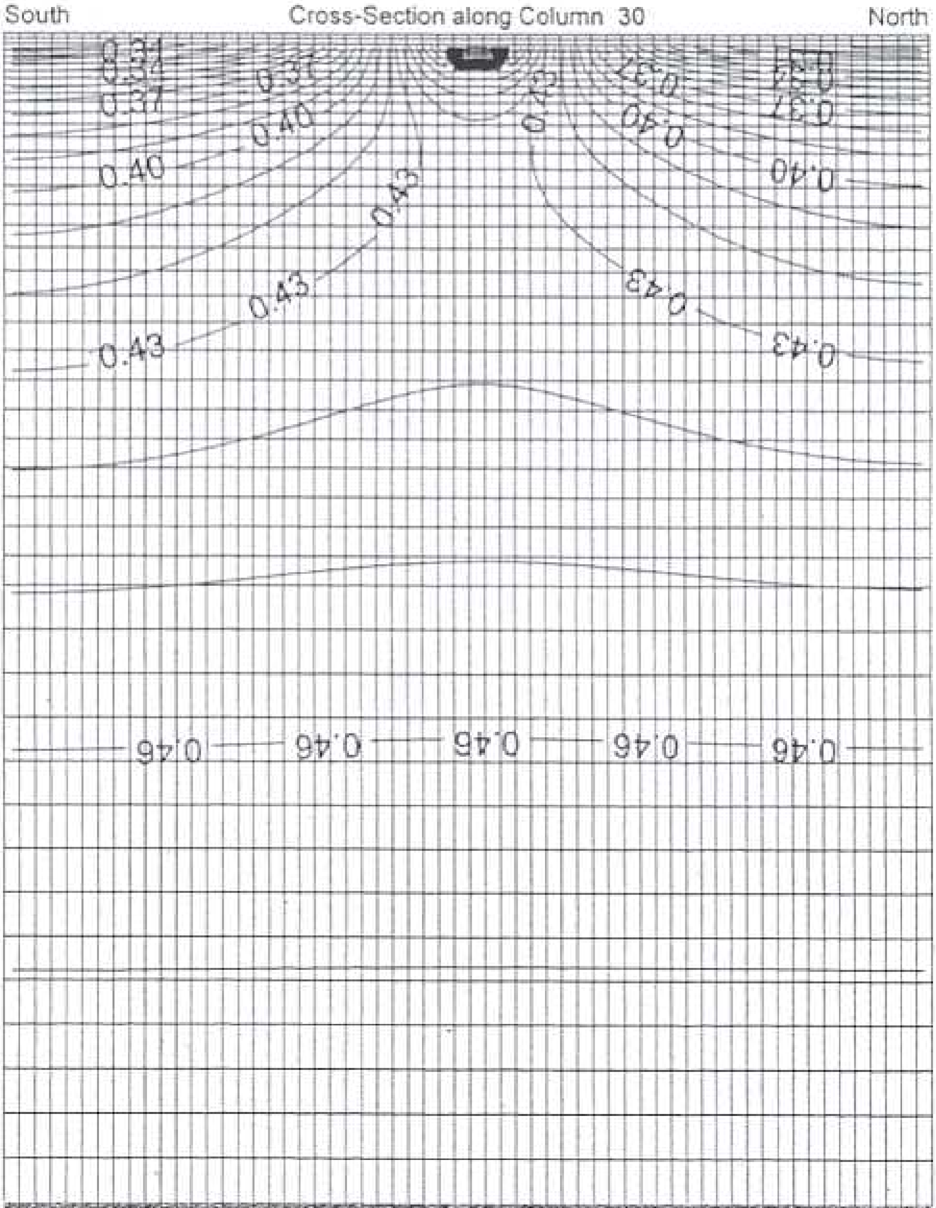

Figure D.18 Water saturation contours in cross-section for SLA6

Simulation-SLA7-Sandy Loam soil with ET domain type A
Time -210 days after beginning of simulation
Date-8/11/2000

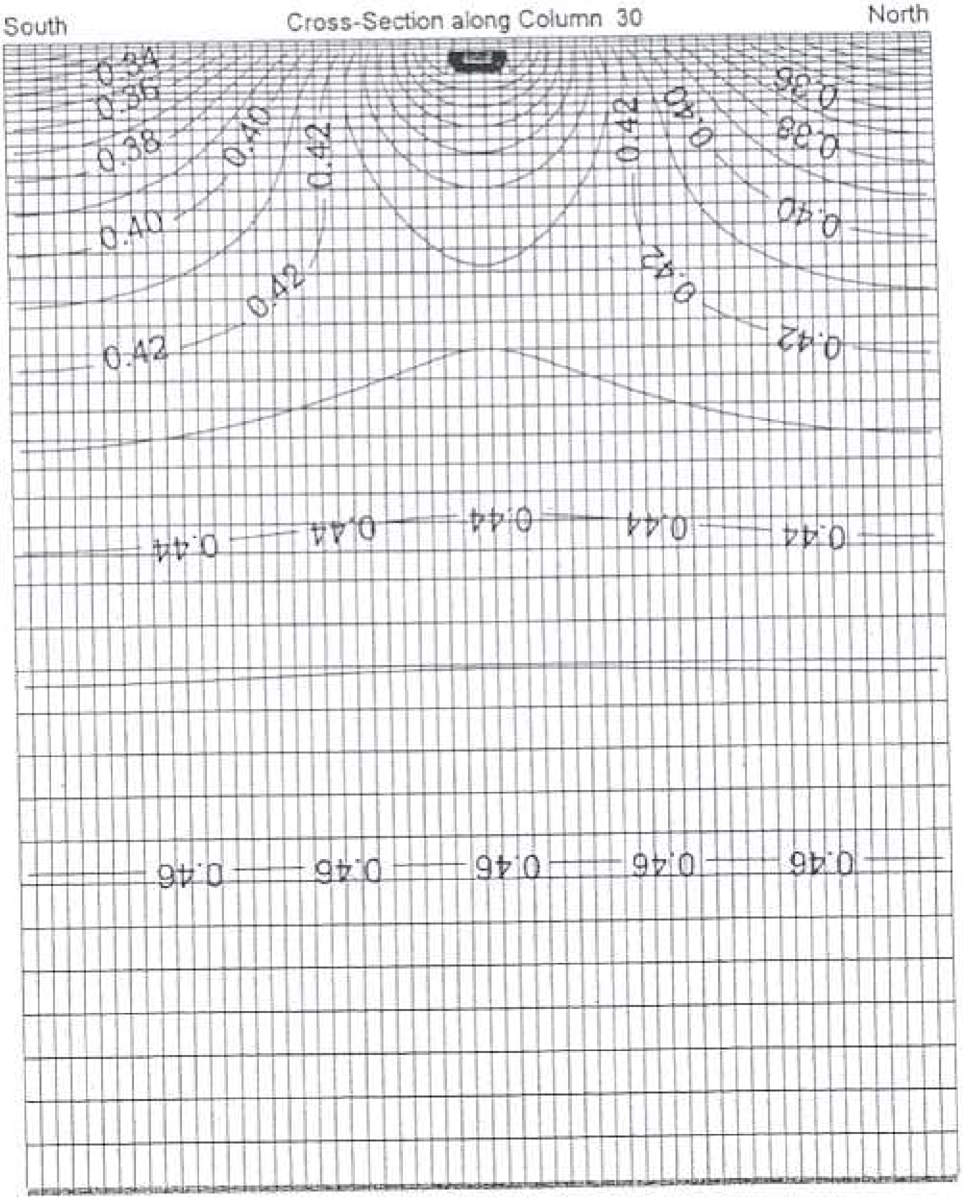

Figure D.19 Water saturation contours in cross-section for SLA7

Simulation-SLA8-Sandy Loam soil with ET domain type A
Time -240 days after beginning of simulation
Date-9/10/2000

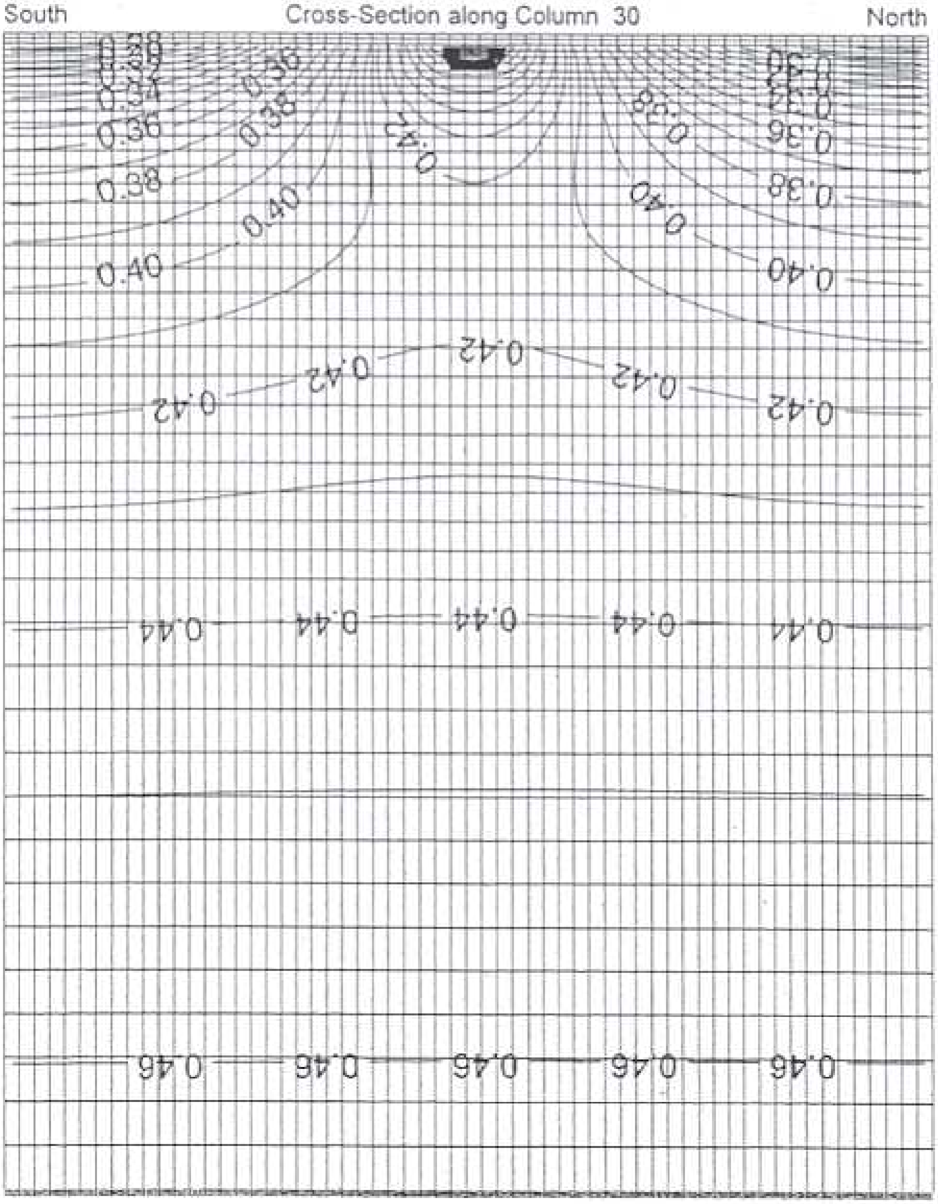

Figure D.20 Water saturation contours in cross-section for SLA8

Simulation-SLA9-Sandy Loam soil with ET domain type A
Time -270 days after beginning of simulation
Date-10/10/2000

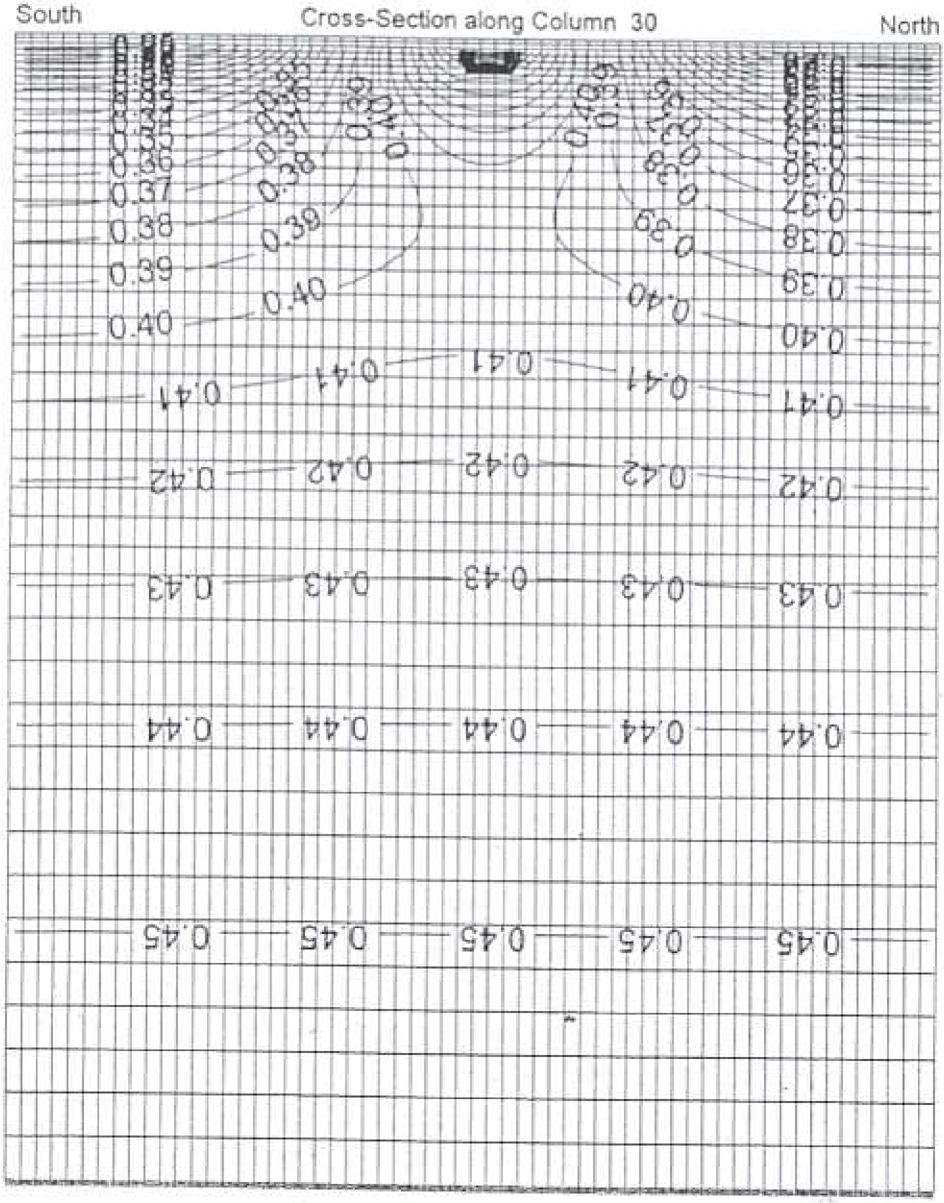

Figure D.21 Water saturation contours in cross-section for SLA9

Simulation-SLA10-Sandy Loam soil with ET domain type A
Time -300 days after beginning of simulation
Date-11/9/2000

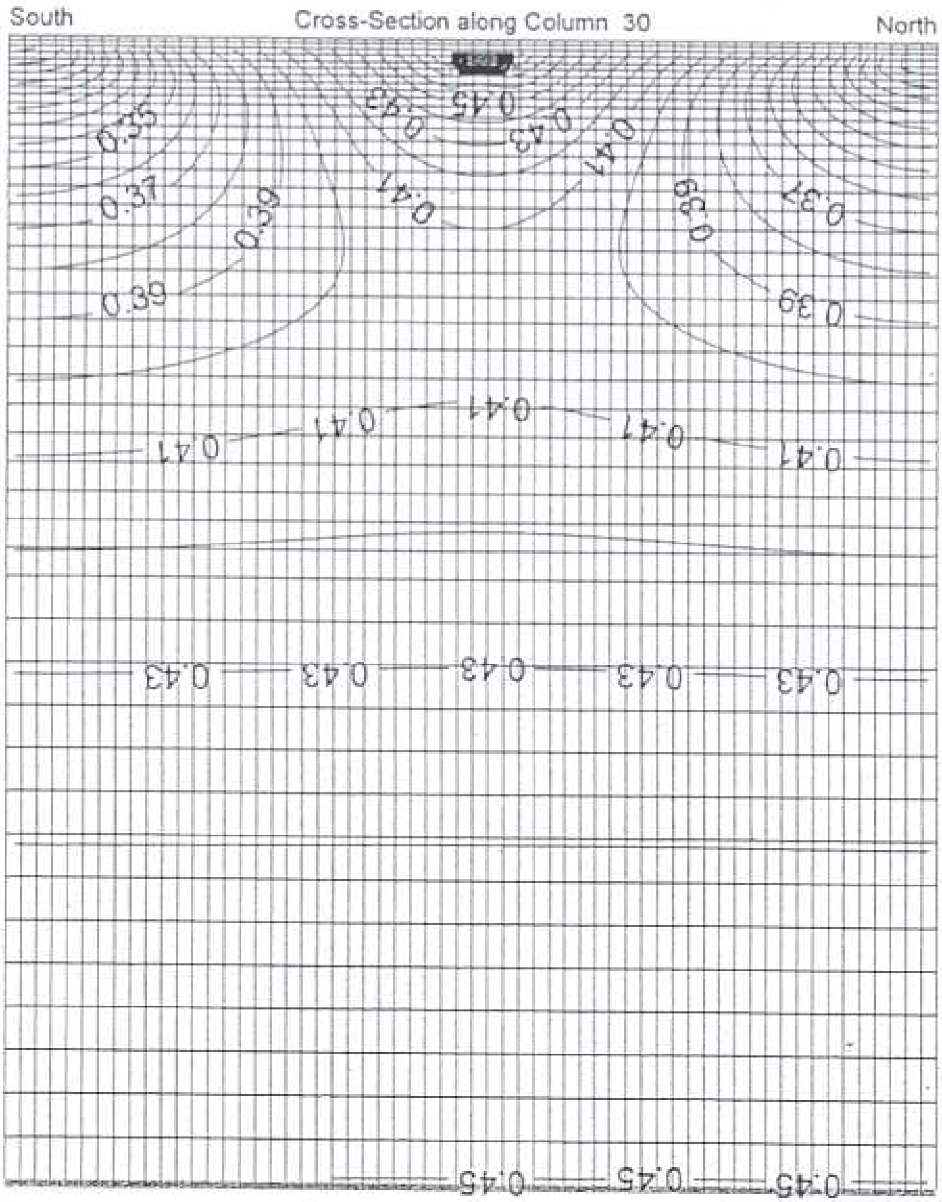

Figure D.22 Water saturation contours in cross-section for SLA10

Simulation-SLA11-Sandy Loam soil with ET domain type A
Time -330 days after beginning of simulation
Date-12/9/2000

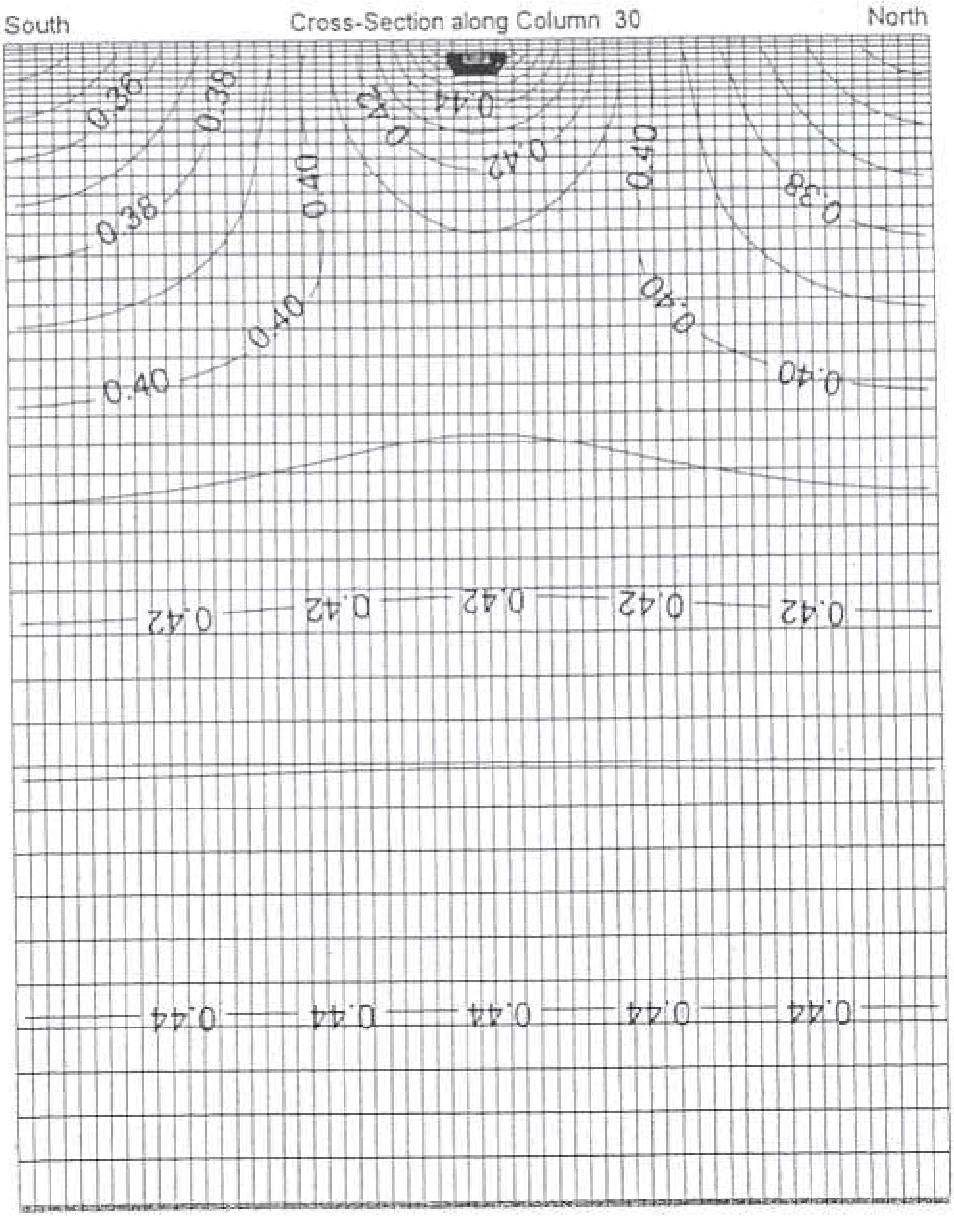

Figure D.23 Water saturation contours in cross-section for SLA11

Simulation-SLA12-Sandy Loam soil with ET domain type A
Time -352 days after beginning of simulation
Date-12/31/2000

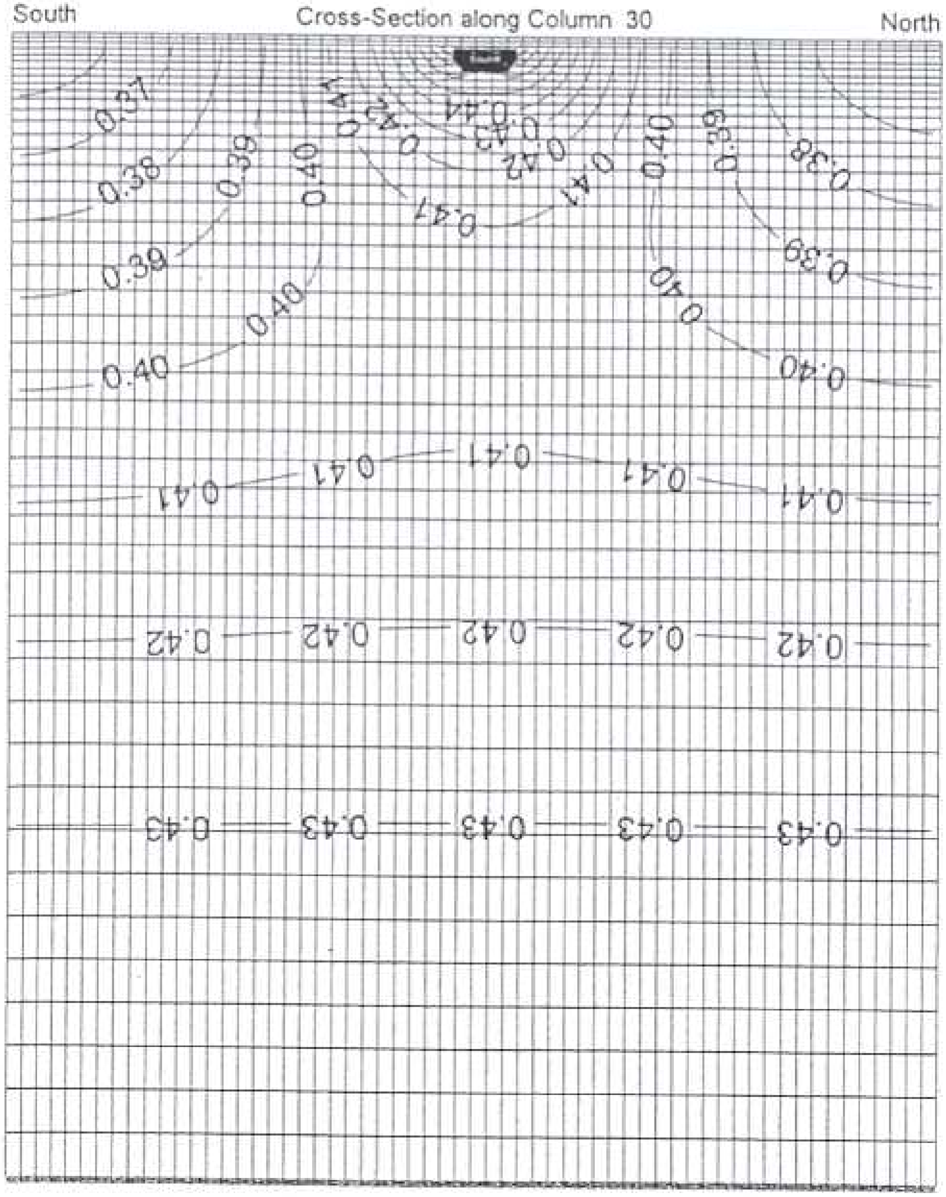

Figure D.24 Water saturation contours in cross-section for SLA12

Simulation-SLA1-Sandy Loam soil with ET domain type A
Time -30 days after beginning of simulation
Date-2/13/2000

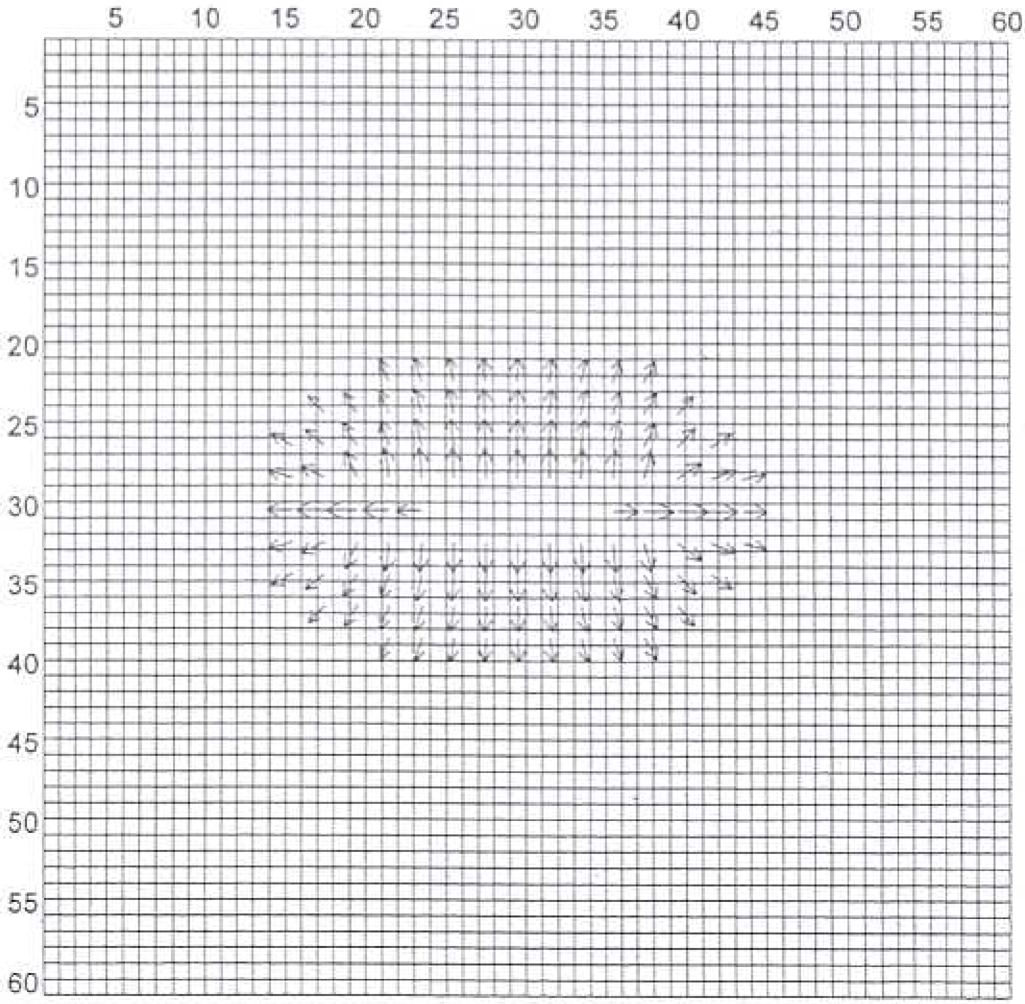

Figure D.25 Moisture movement vectors in plan view for SLA1

Simulation-SLA4-Sandy Loam soil with ET domain type A
Time -120 days after beginning of simulation
Date-5/13/2000

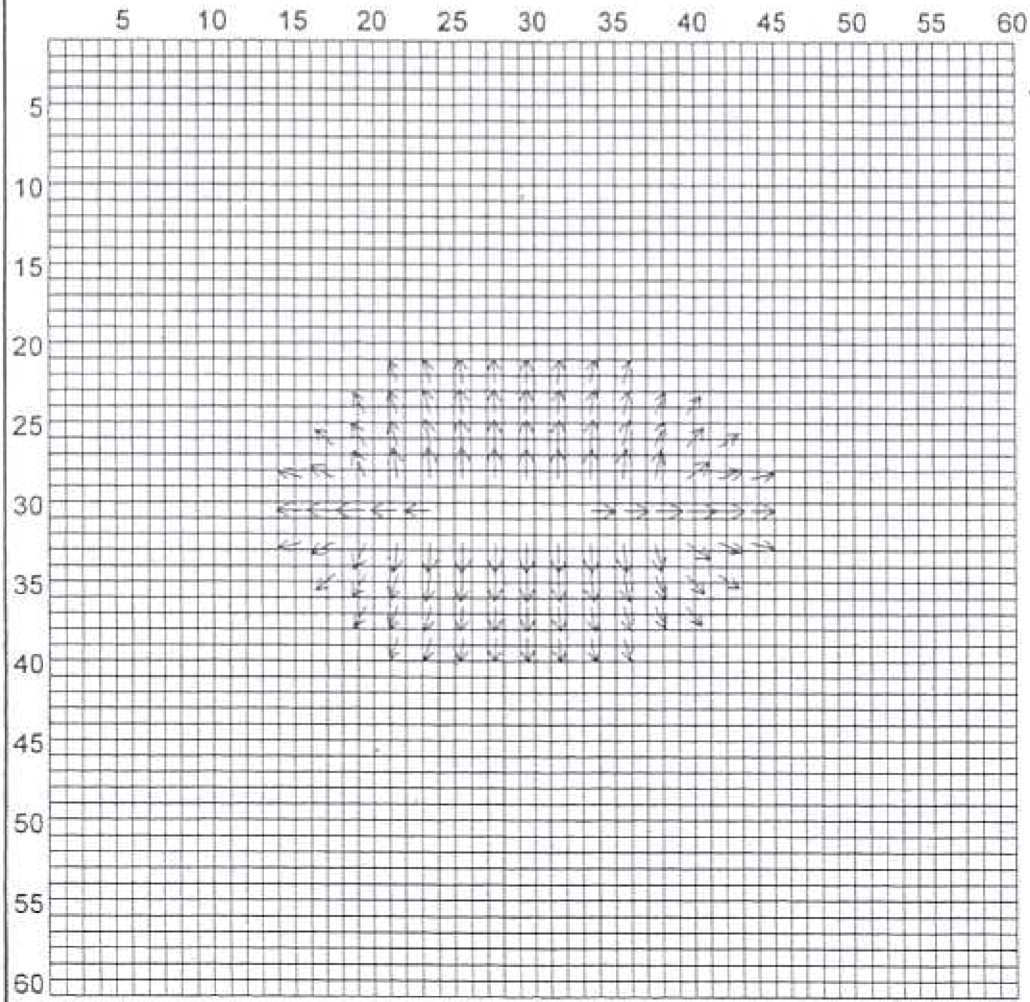

Figure D.26 Moisture movement vectors in plan view for SLA4

Simulation-SLA8-Sandy Loam soil with ET domain type A
Time -240 days after beginning of simulation
Date-9/10/2000

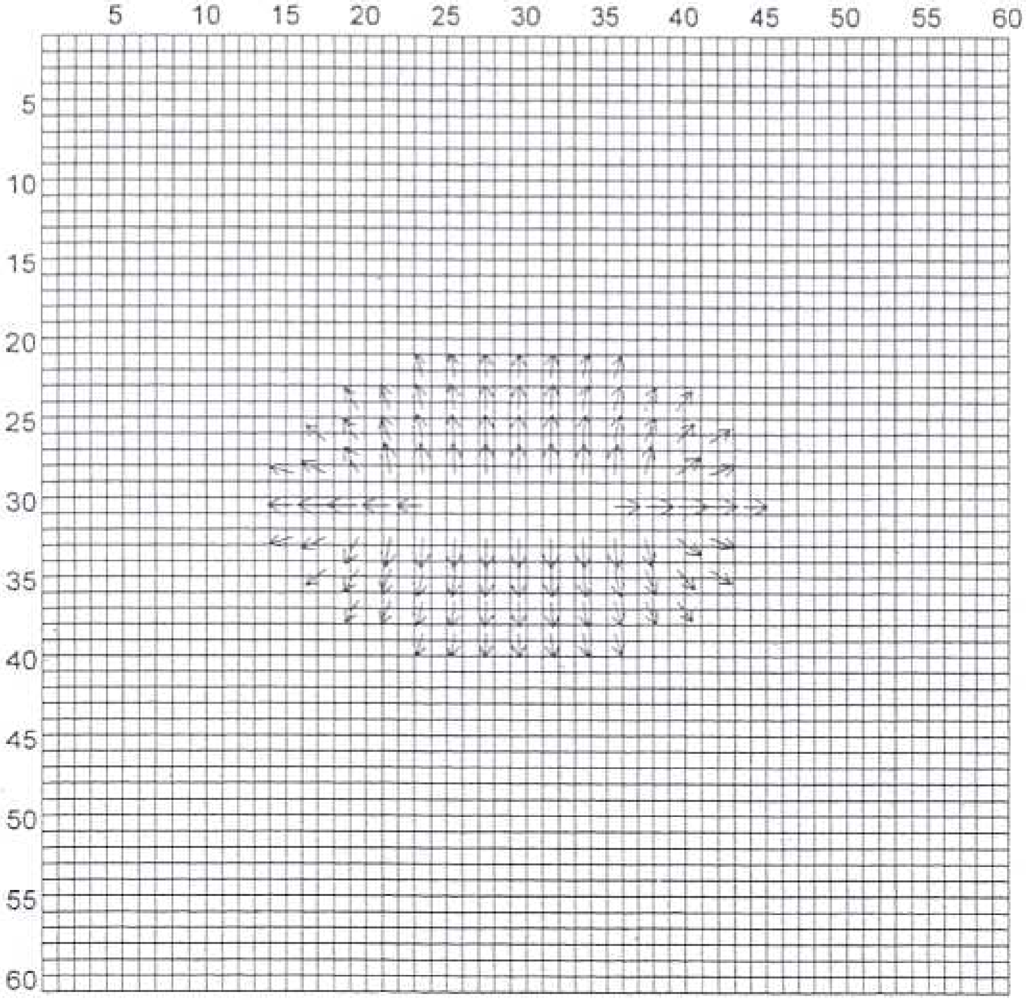

Figure D.27 Moisture movement vectors in plan view for SLA8

Simulation-SLA12-Sandy Loam soil with ET domain type A
Time -352 days after beginning of simulation
Date-12/31/2000

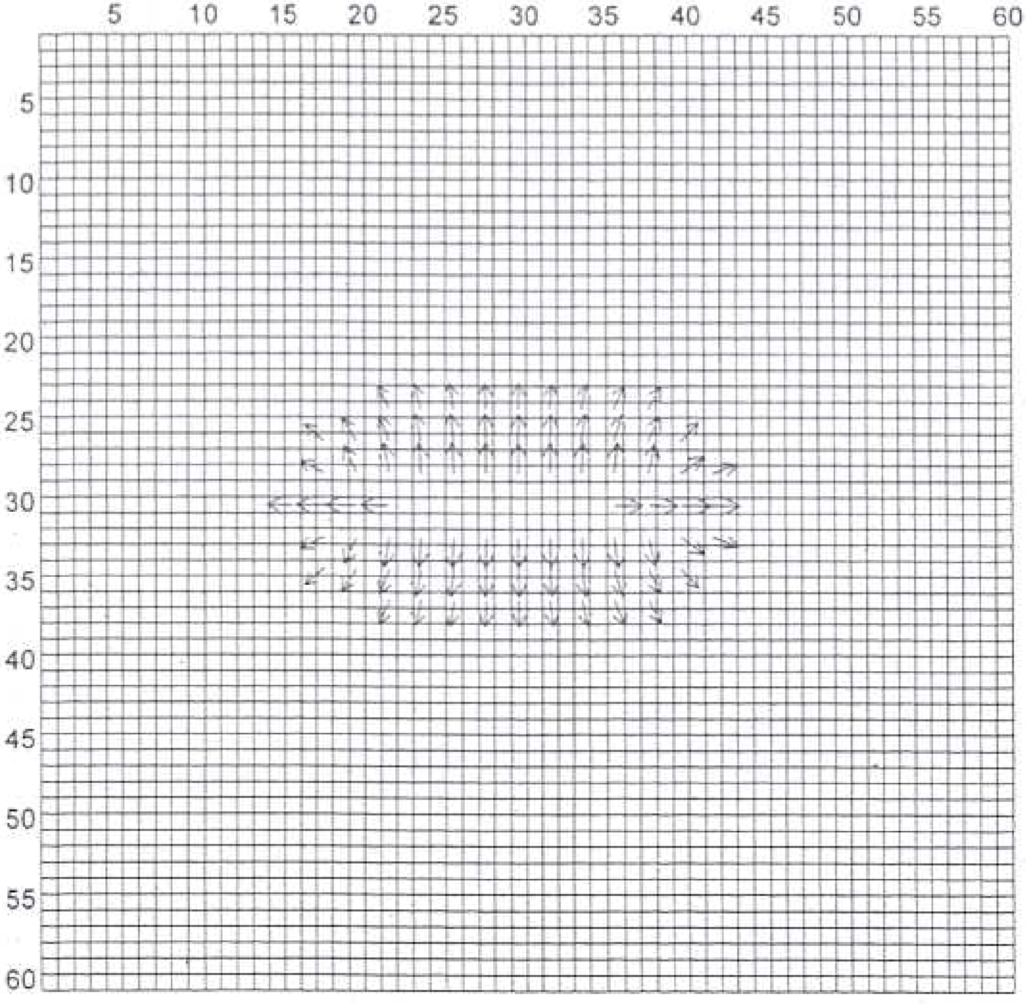

Figure D.28 Moisture movement vectors in plan view for SLA12

Simulation-SLA1-Sandy Loam soil with ET domain type A
Time -30 days after beginning of simulation
Date-2/13/2000

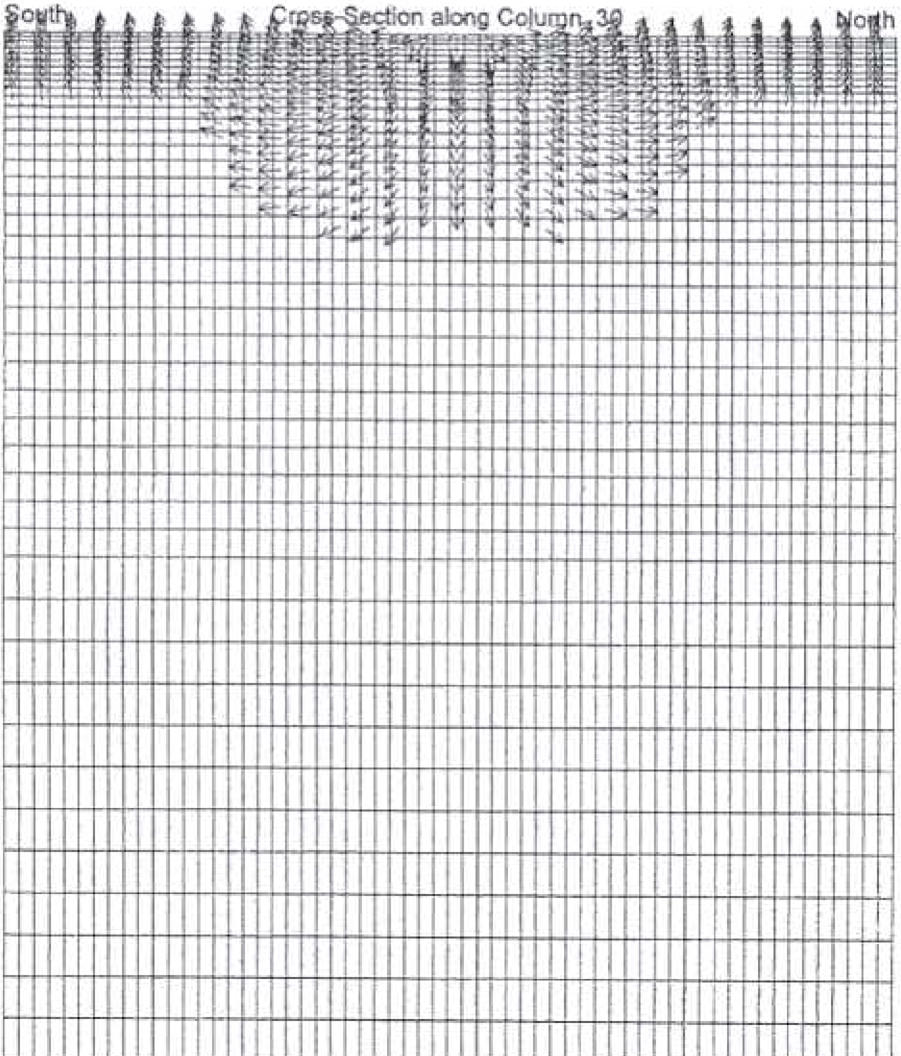

Figure D.29 Moisture movement vectors along C-30 for SLA1

Simulation-SLA4-Sandy Loam soil with ET domain type A
Time -120 days after beginning of simulation
Date-5/13/2000

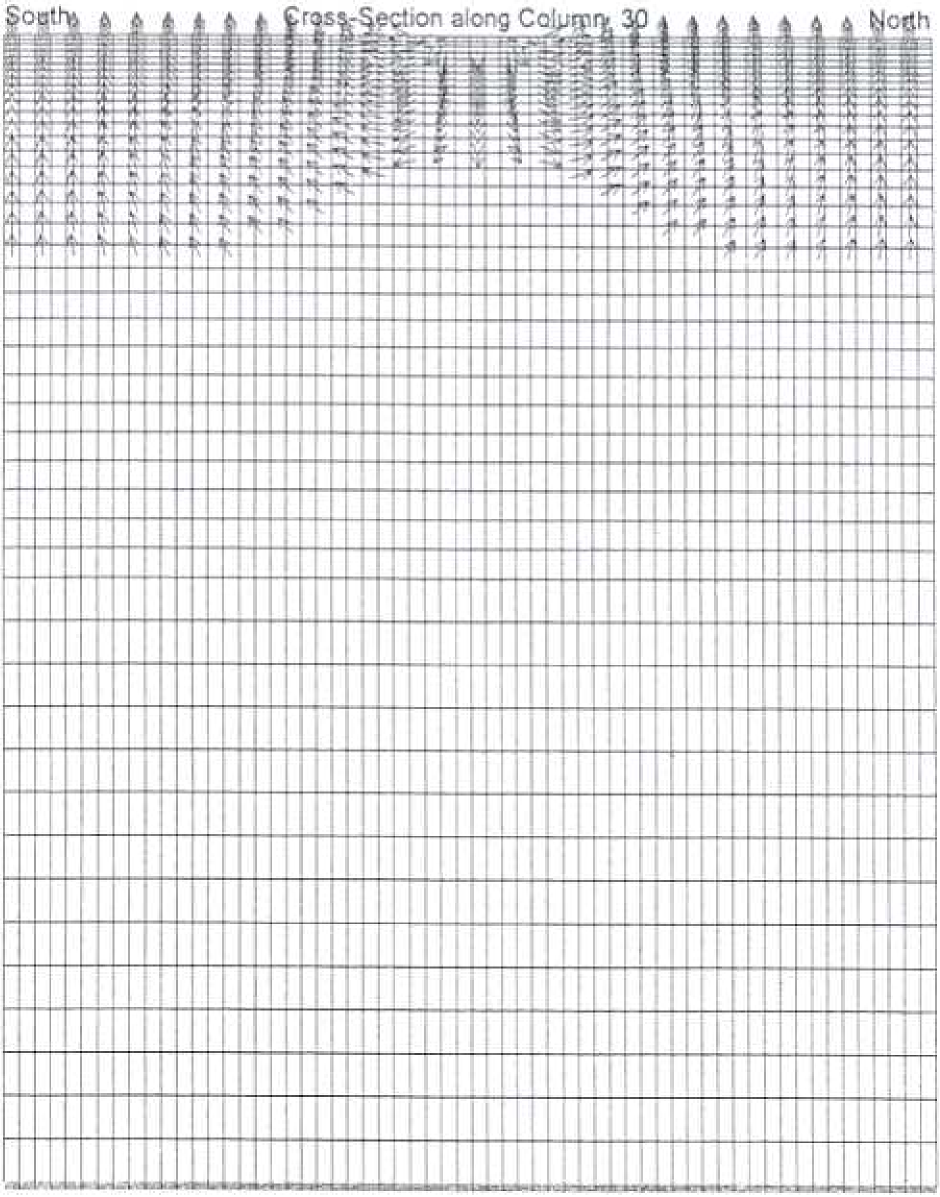

Figure D.30 Moisture movement vectors along C-30 for SLA4

Simulation-SLA8-Sandy Loam soil with ET domain type A
Time -240 days after beginning of simulation
Date-9/10/2000

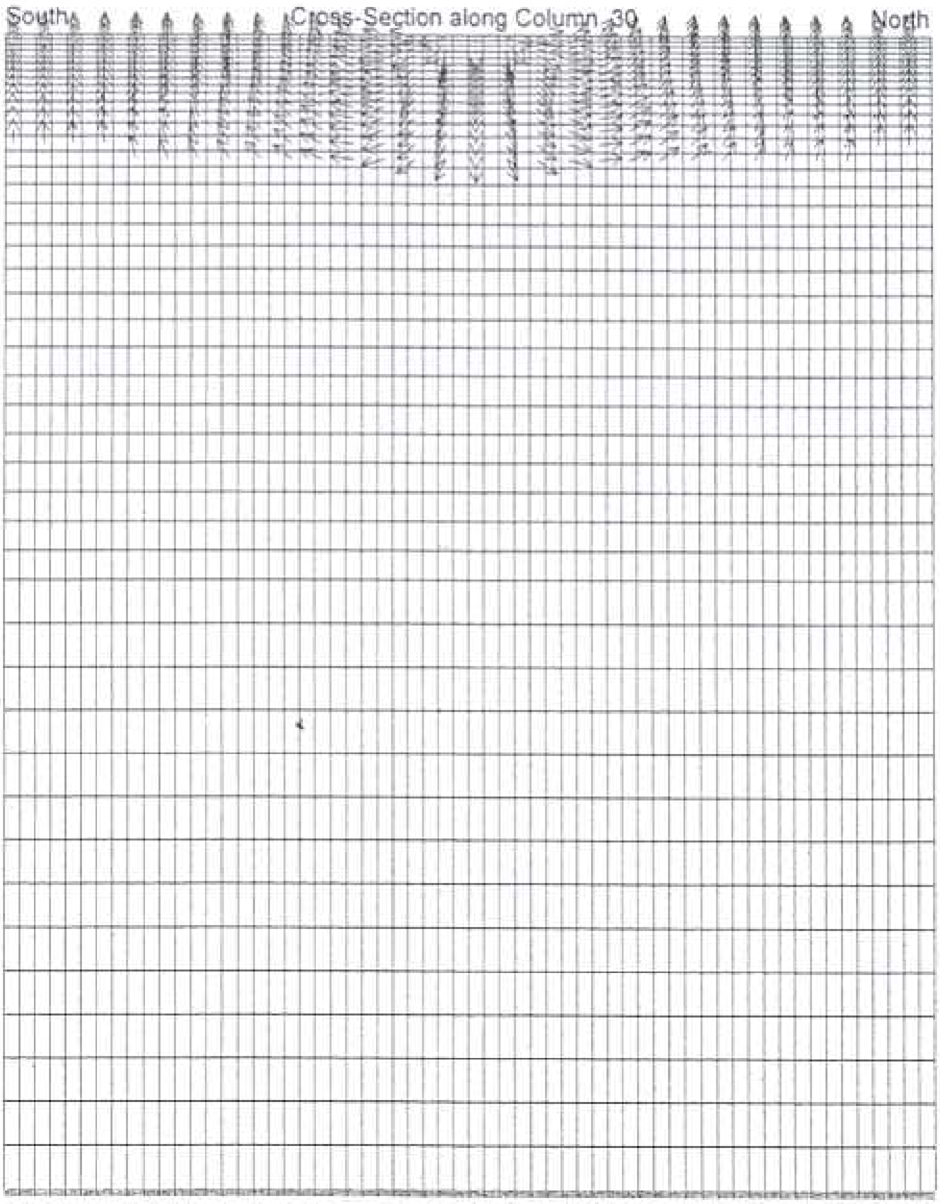

Figure D.31 Moisture movement vectors along C-30 for SLA8

Simulation-SLA12-Sandy Loam soil with ET domain type A
Time -352 days after beginning of simulation
Date-12/31/2000

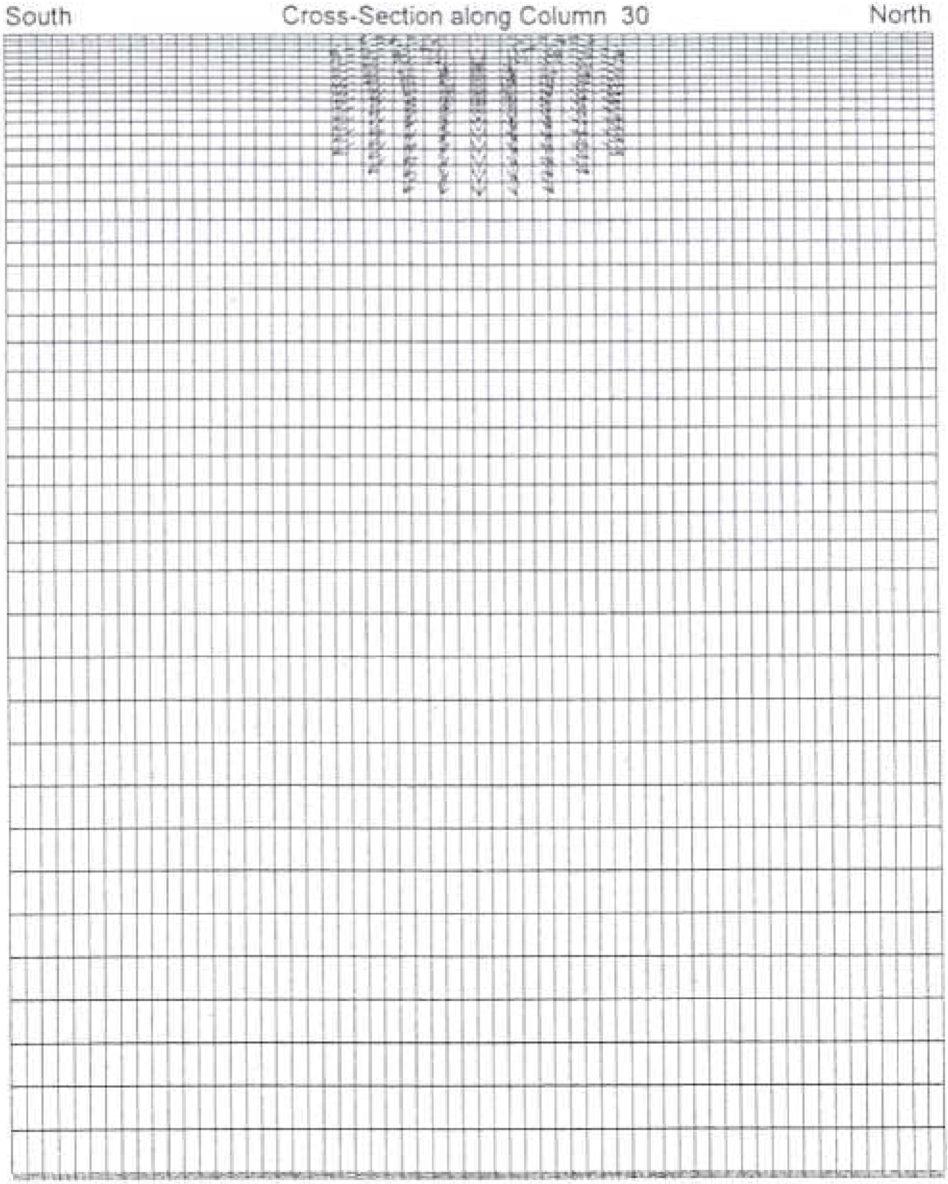

Figure D.32 Moisture movement vectors along C-30 for SLA12

Simulation-SLA1-Sandy Loam soil with ET domain type A
Time -30 days after beginning of simulation
Date-2/13/2000

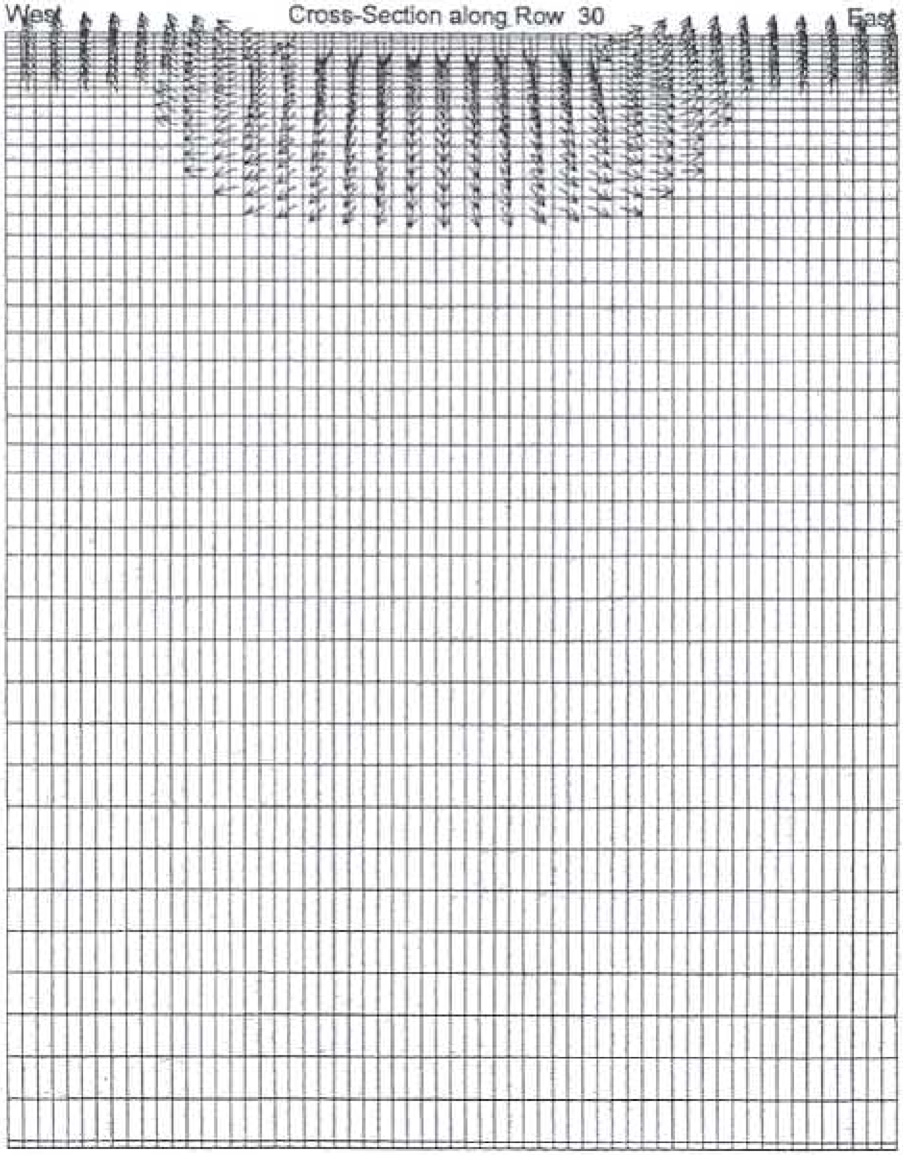

Figure D.33 Moisture movement vectors along R-30 for SLA1

Simulation-SLA4-Sandy Loam soil with ET domain type A
Time -120 days after beginning of simulation
Date-5/13/2000

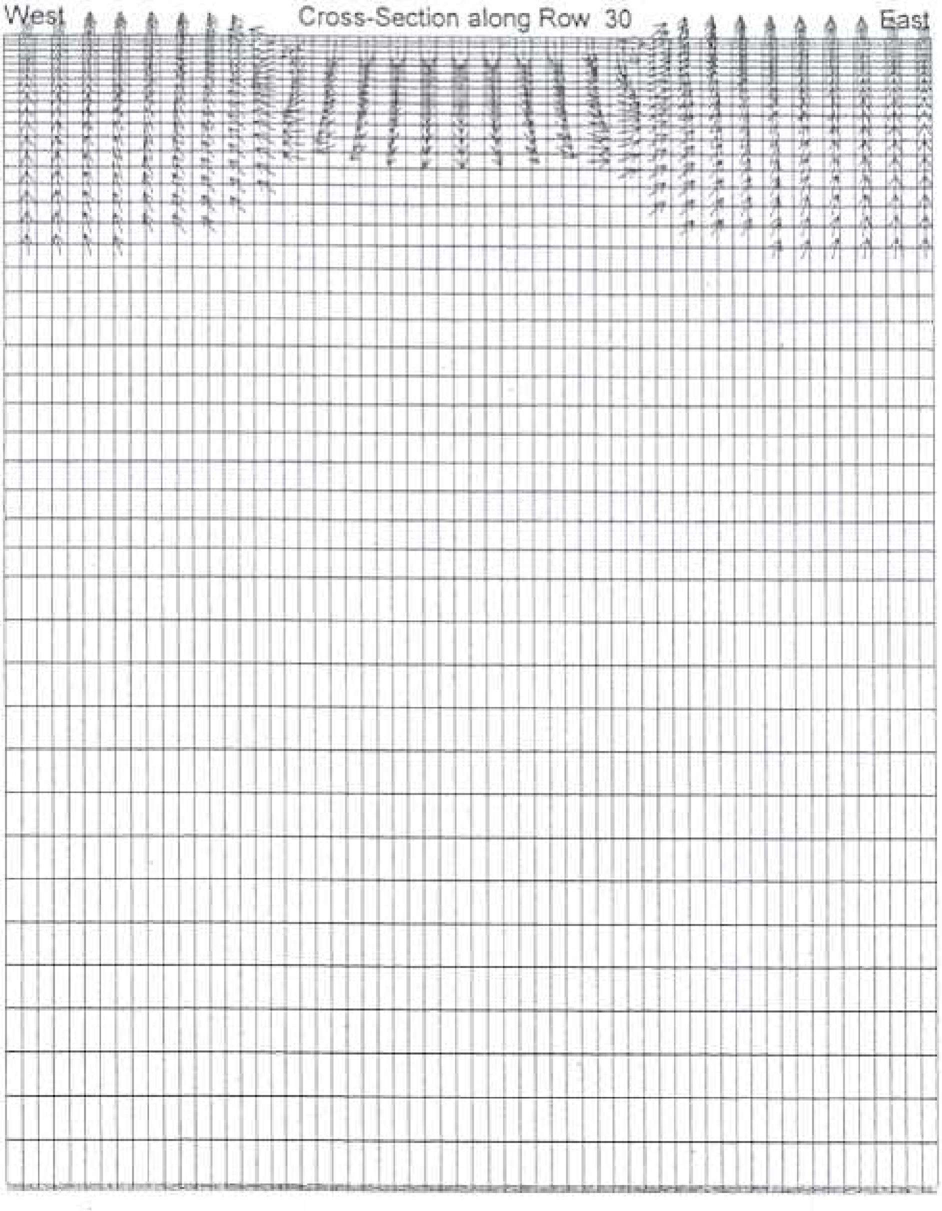

Figure D.34 Moisture movement vectors along R-30 for SLA4

Simulation-SLA8-Sandy Loam soil with ET domain type A
Time -240 days after beginning of simulation
Date-9/10/2000

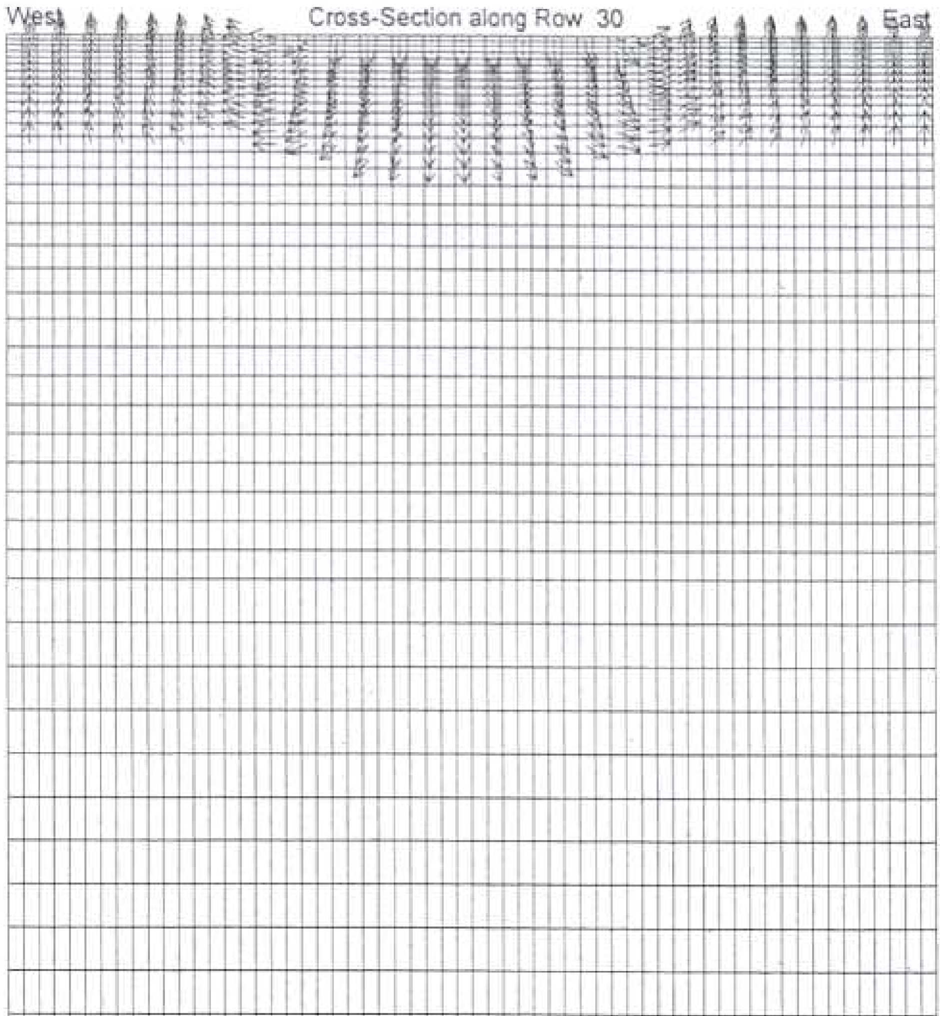

Figure D.35 Moisture movement vectors along R-30 for SLA8

Simulation-SLA12-Sandy Loam soil with ET domain type A
Time -352 days after beginning of simulation
Date-12/31/2000

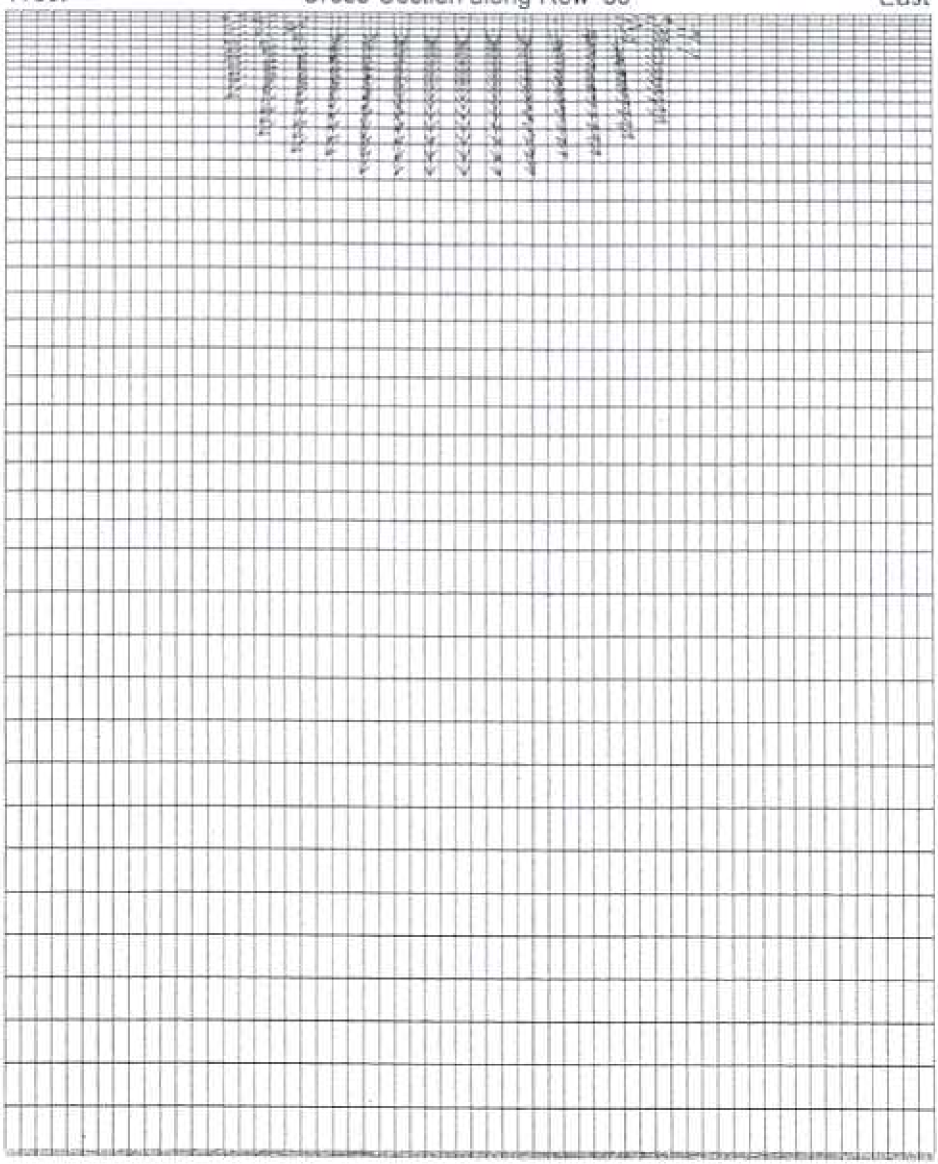

Figure D.36 Moisture movement vectors along R-30 for SLA12

Simulation-SLB1-Sandy Loam soil with ET domain type B
Time -30 days after beginning of simulation
Date-2/13/2000

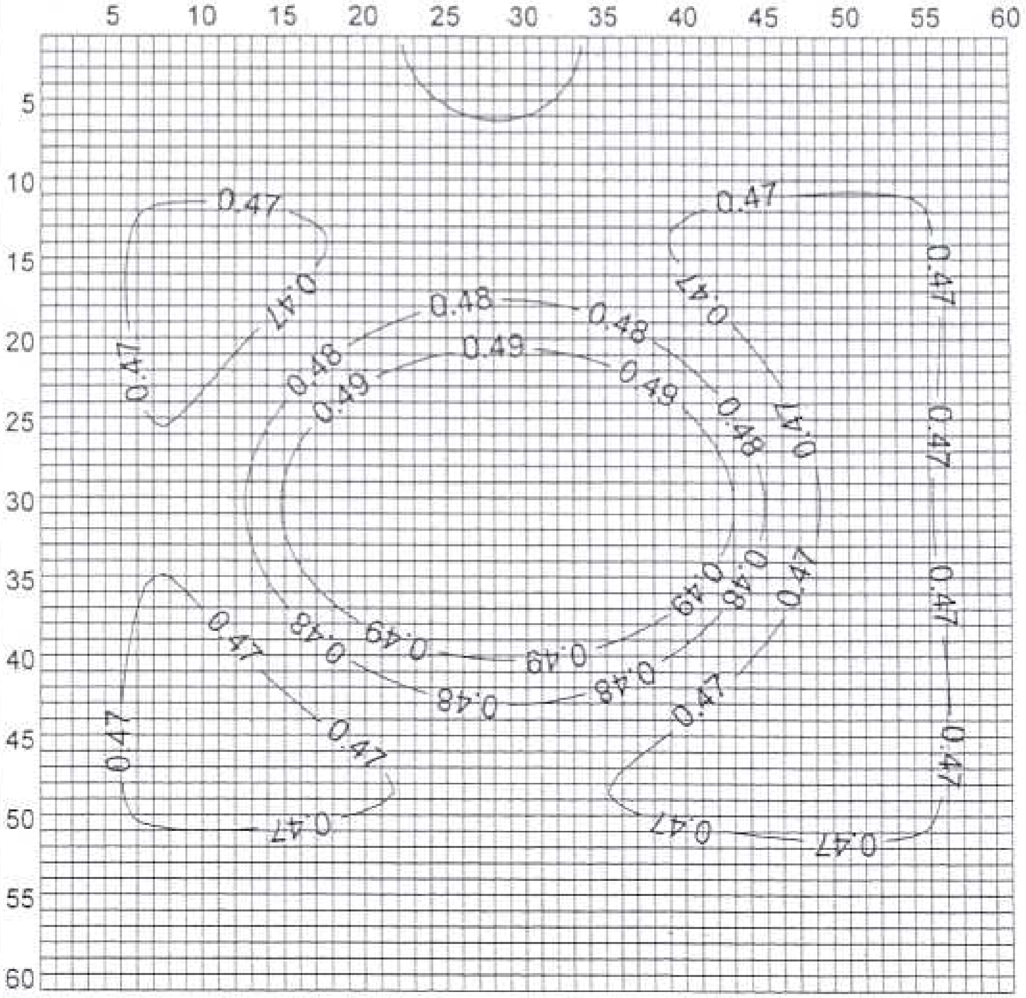

Figure D.37 Water saturation contours in plan view for SLB1

Simulation-SLB2-Sandy Loam soil with ET domain type B
Time -60 days after beginning of simulation
Date-3/14/2000

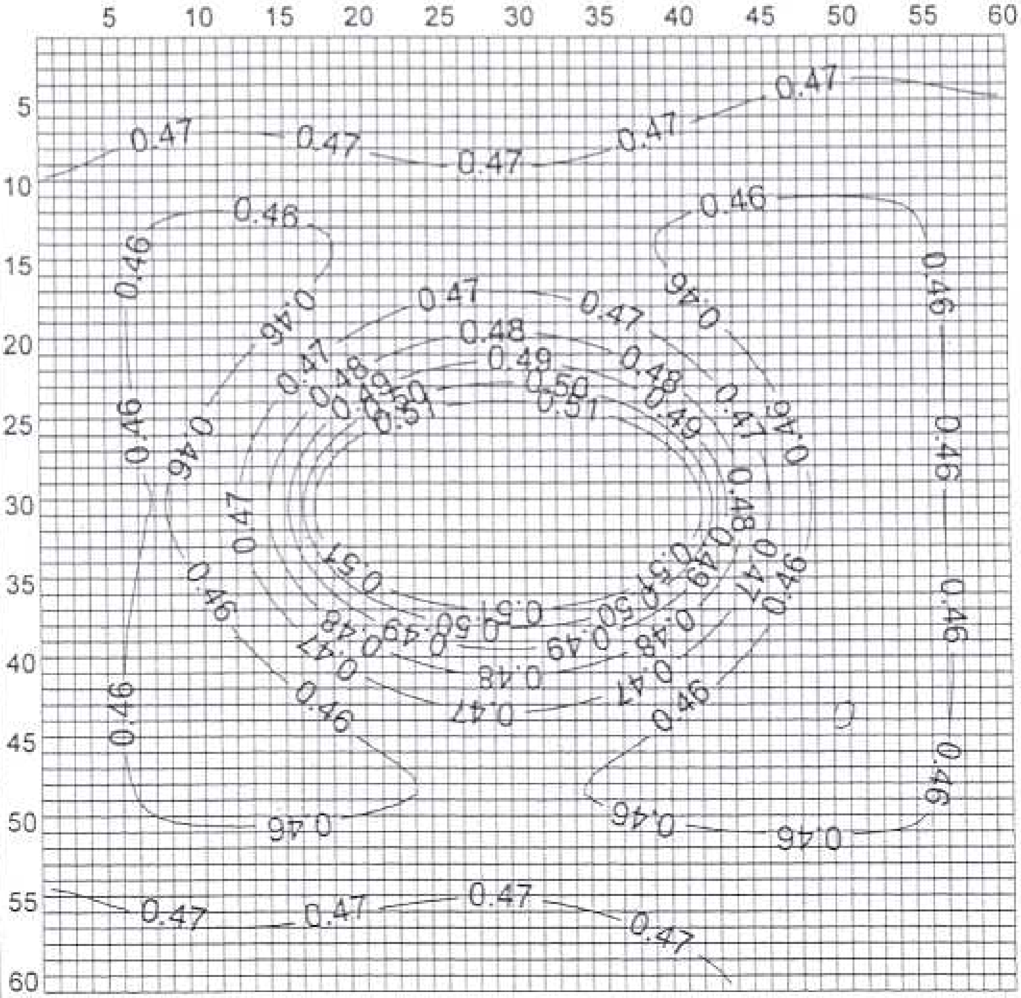

Figure D.38 Water saturation contours in plan view for SLB2

Simulation-SLB3-Sandy Loam soil with ET domain type B
Time -90 days after beginning of simulation
Date-4/13/2000

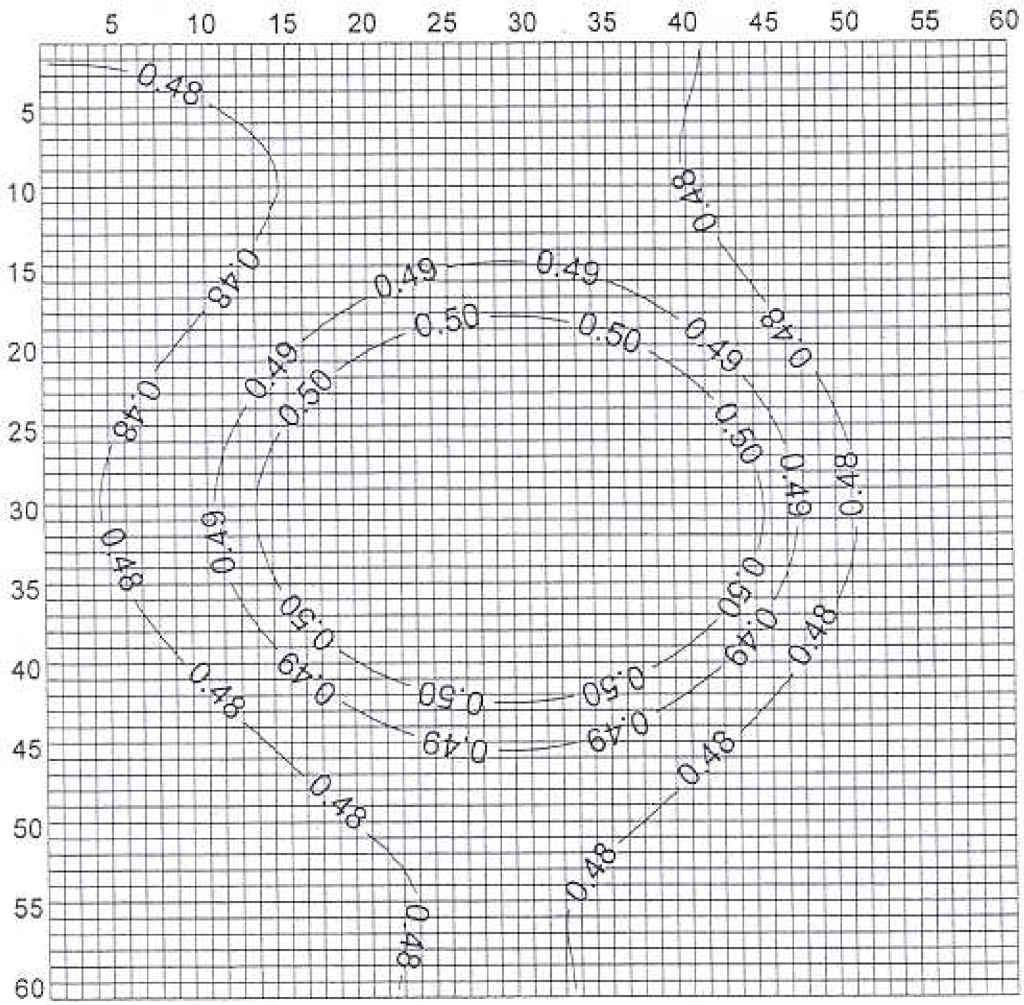

Figure D.39 Water saturation contours in plan view for SLB3

Simulation-SLB4-Sandy Loam soil with ET domain type B
Time -120 days after beginning of simulation
Date-5/13/2000

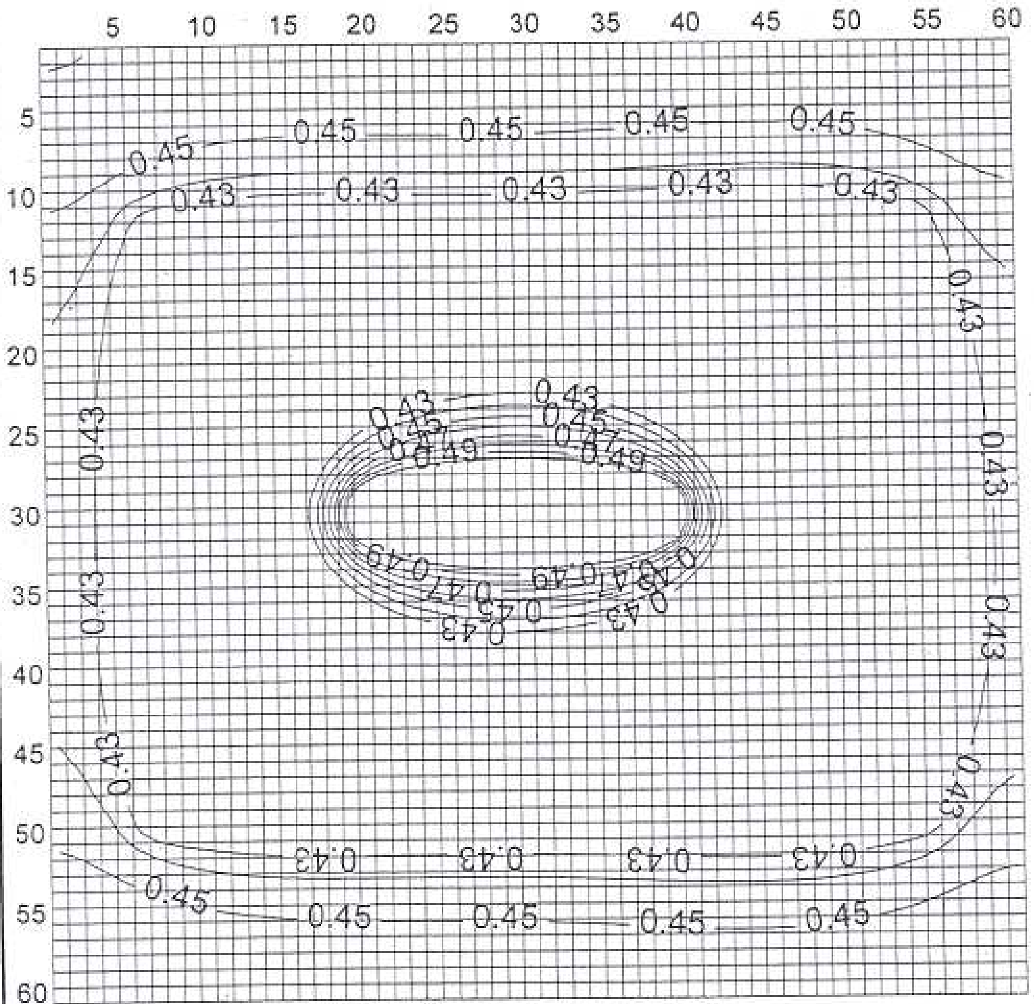

Figure D.40 Water saturation contours in plan view for SLB4

Simulation-SLB5-Sandy Loam soil with ET domain type B
Time -150 days after beginning of simulation
Date-6/12//2000

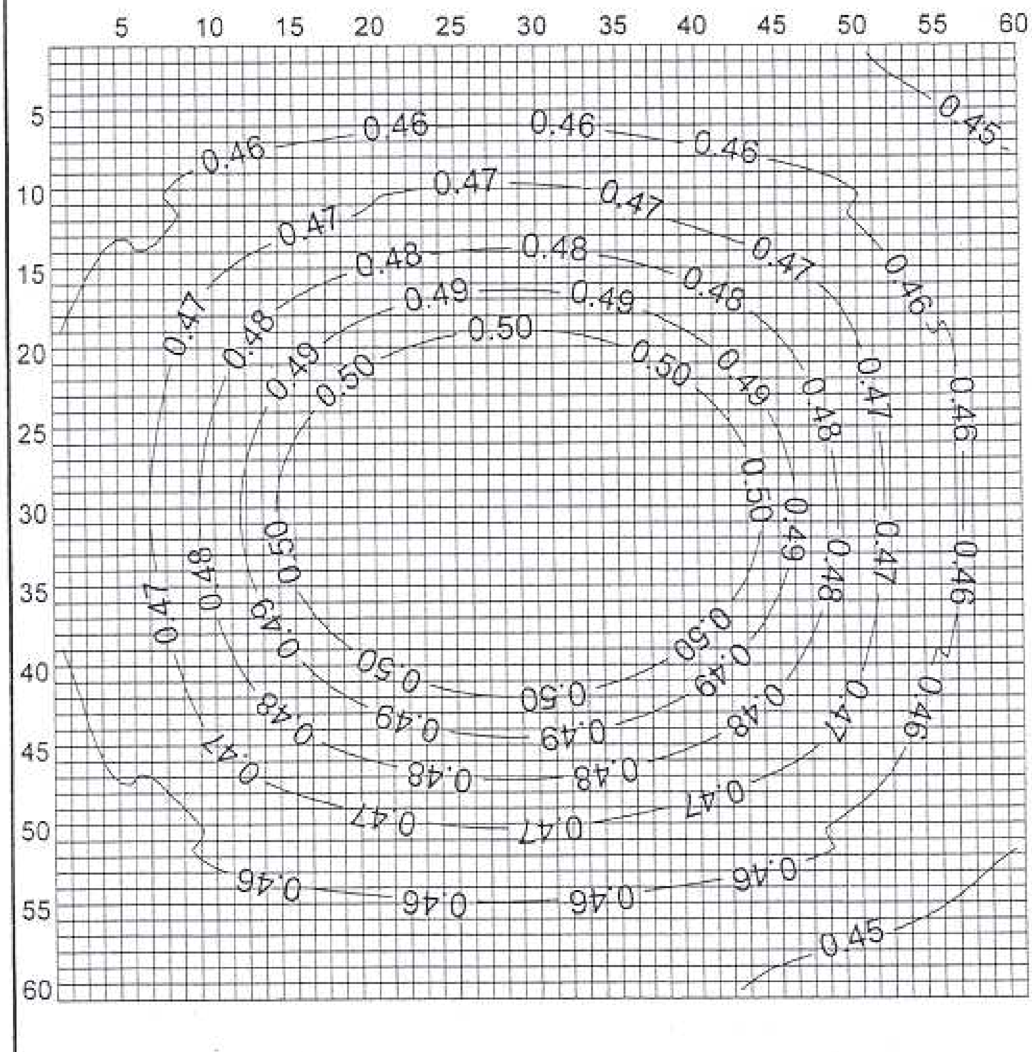

Figure D.41 Water saturation contours in plan view for SLB5

Simulation-SLB6-Sandy Loam soil with ET domain type B
Time -180 days after beginning of simulation
Date-7/12/2000

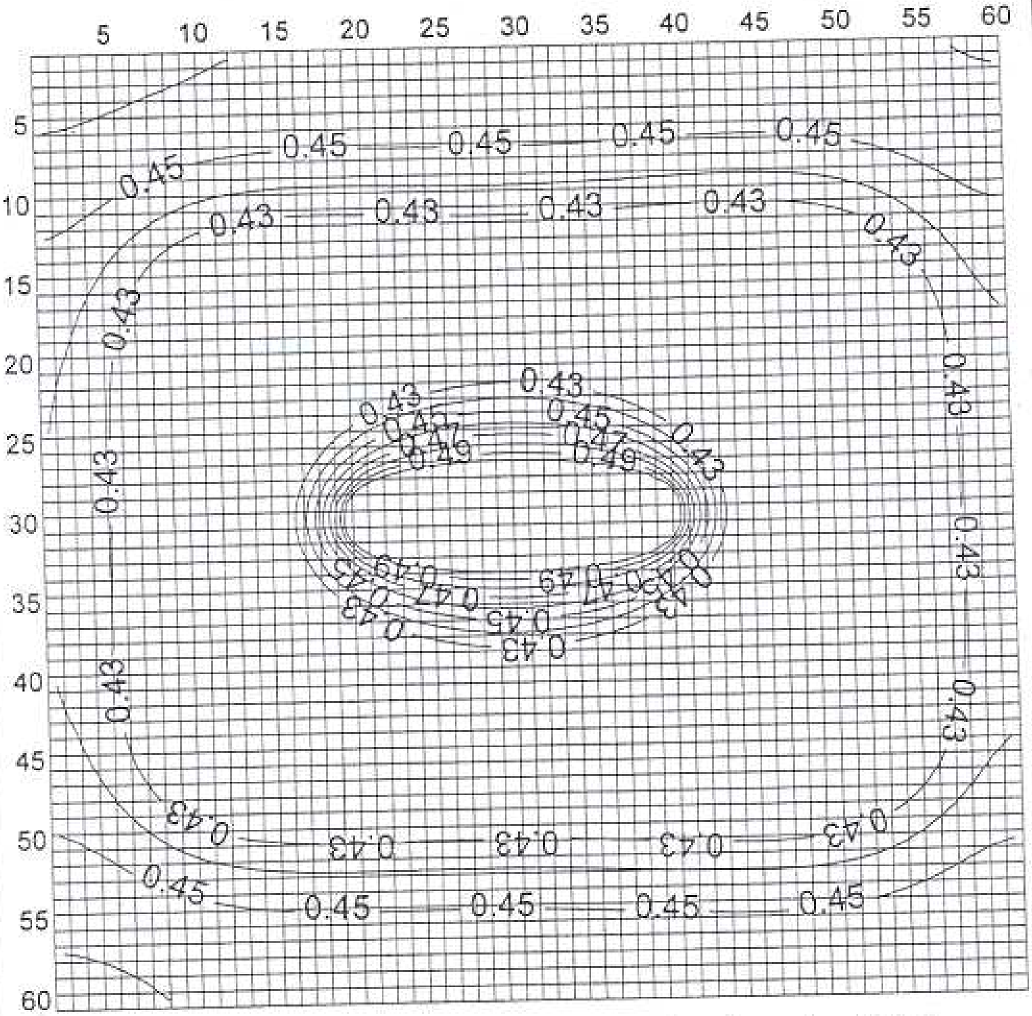

Figure D.42 Water saturation contours in plan view for SLB6

Simulation-SLB7-Sandy Loam soil with ET domain type B
Time -210 days after beginning of simulation
Date-8/11/2000

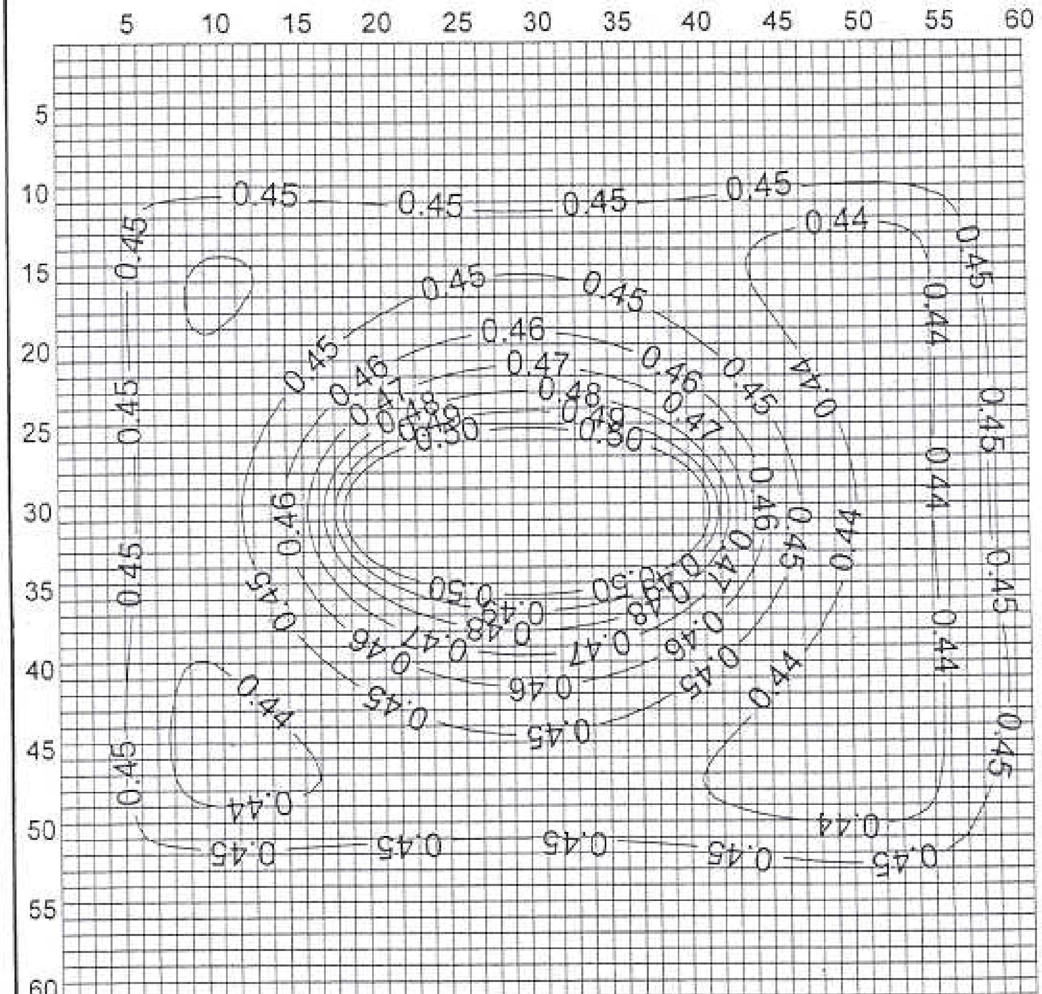

Figure D.43 Water saturation contours in plan view for SLB7

Simulation-SLB8-Sandy Loam soil with ET domain type B
Time -240 days after beginning of simulation
Date-9/10/2000

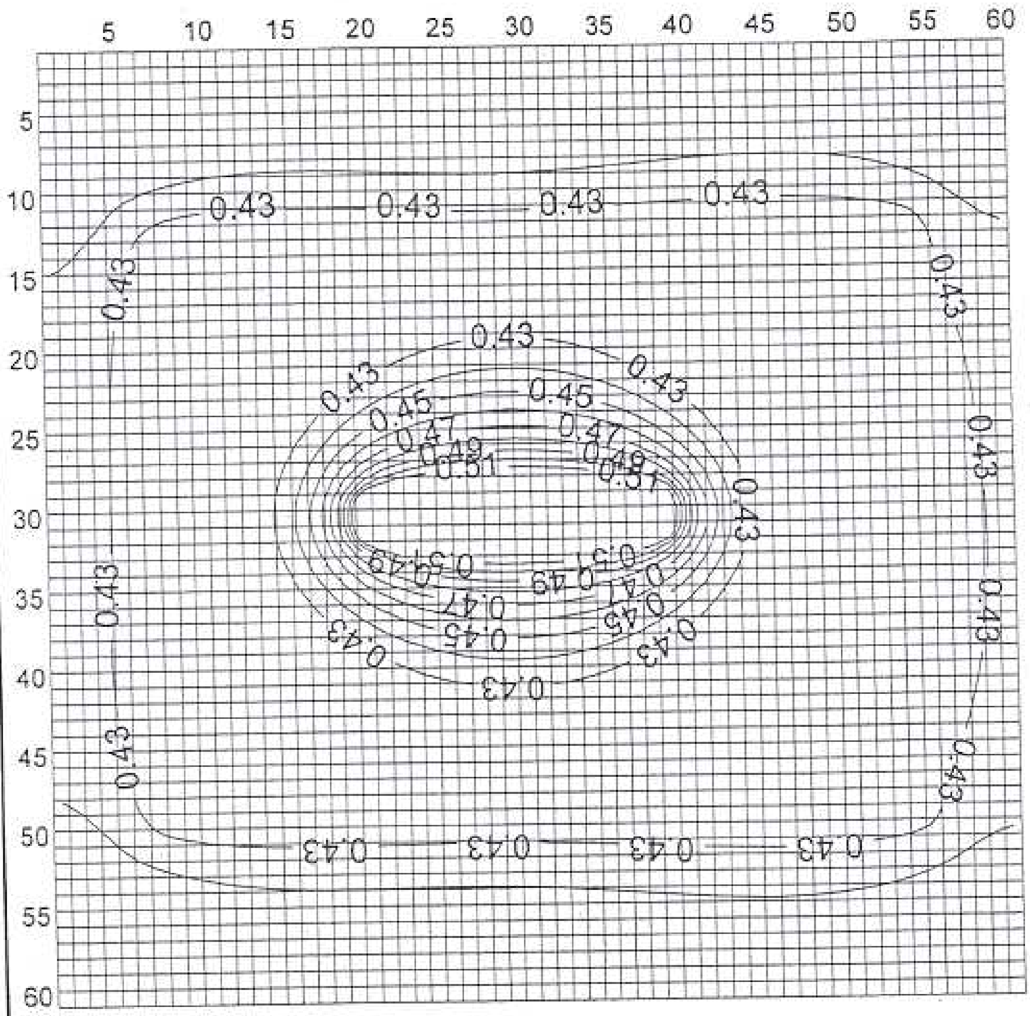

Figure D.44 Water saturation contours in plan view for SLB8

Simulation-SLB9-Sandy Loam soil with ET domain type B
Time -270 days after beginning of simulation
Date-10/10/2000

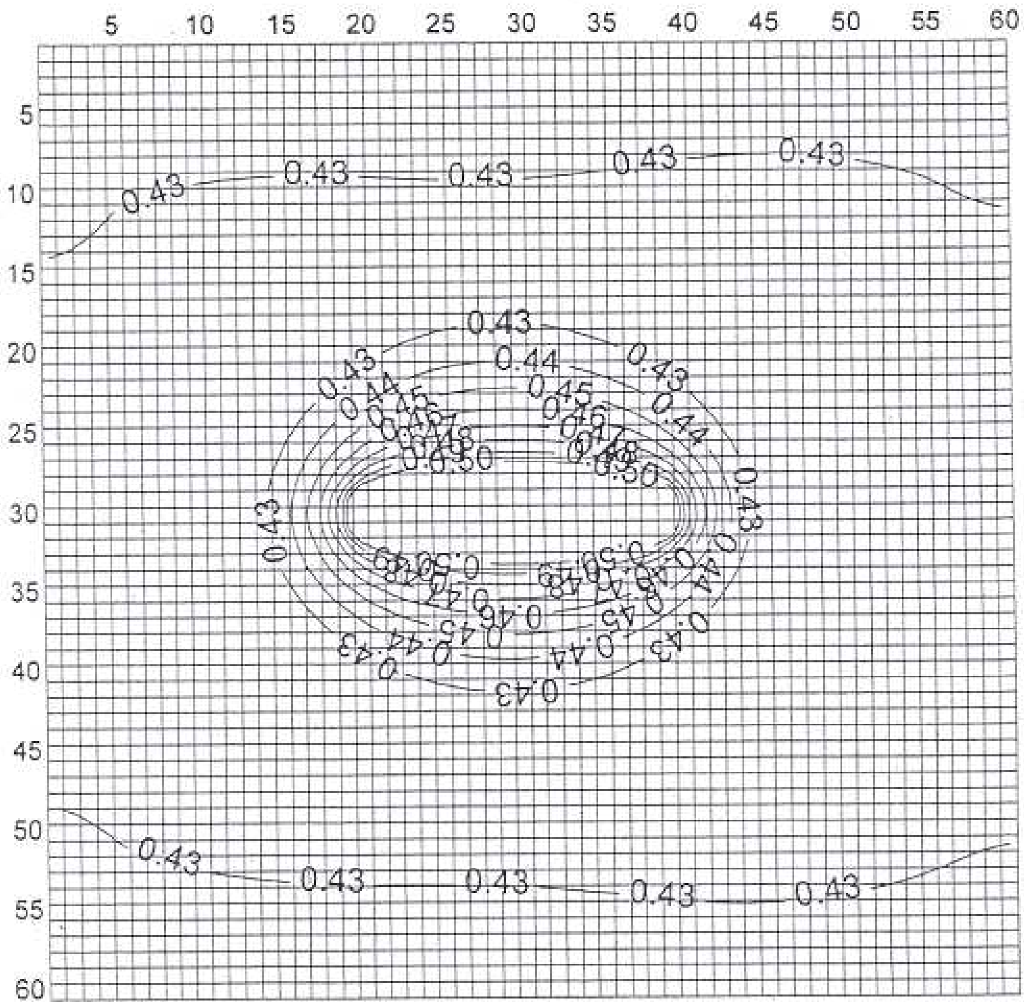

Figure D.45 Water saturation contours in plan view for SLB9

Simulation-SLB10-Sandy Loam soil with ET domain type B
Time -300 days after beginning of simulation
Date-11/9/2000

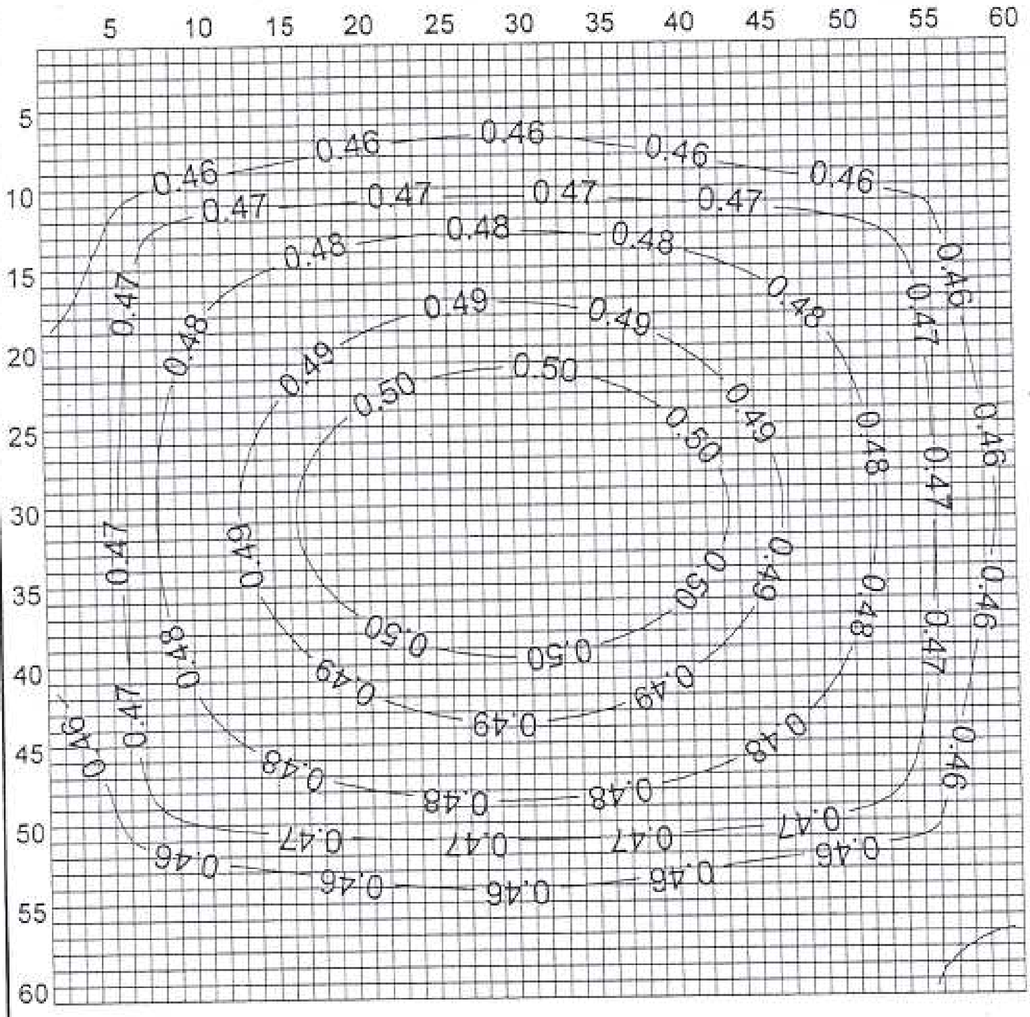

Figure D.46 Water saturation contours in plan view for SLB10

Simulation-SLB11-Sandy Loam soil with ET domain type B
Time -330 days after beginning of simulation
Date-12/9/2000

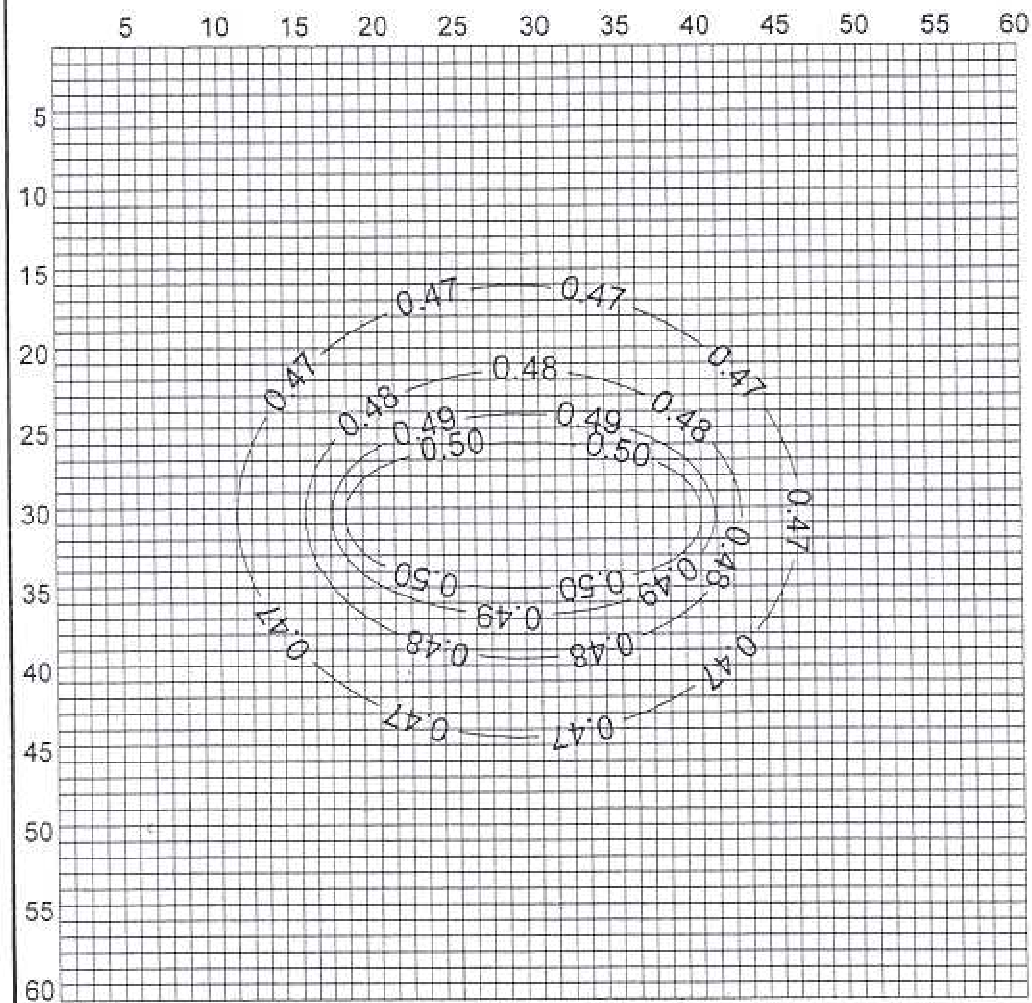

Figure D.47 Water saturation contours in plan view for SLB11

Simulation-SLB12-Sandy Loam soil with ET domain type B
Time -352 days after beginning of simulation
Date-12/31/2000

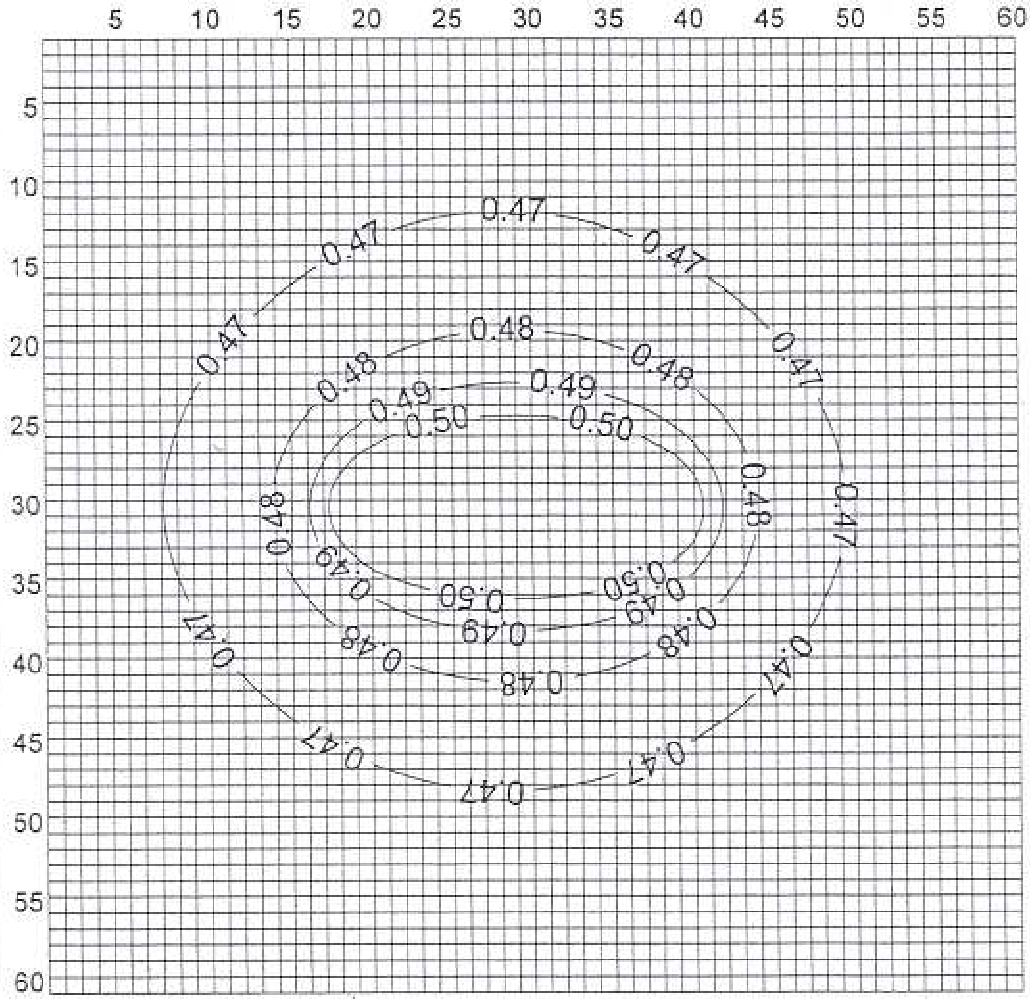

Figure D.48 Water saturation contours in plan view for SLB12

Simulation-SLB1-Sandy Loam soil with ET domain type B
Time -30 days after beginning of simulation
Date-2/13/2000

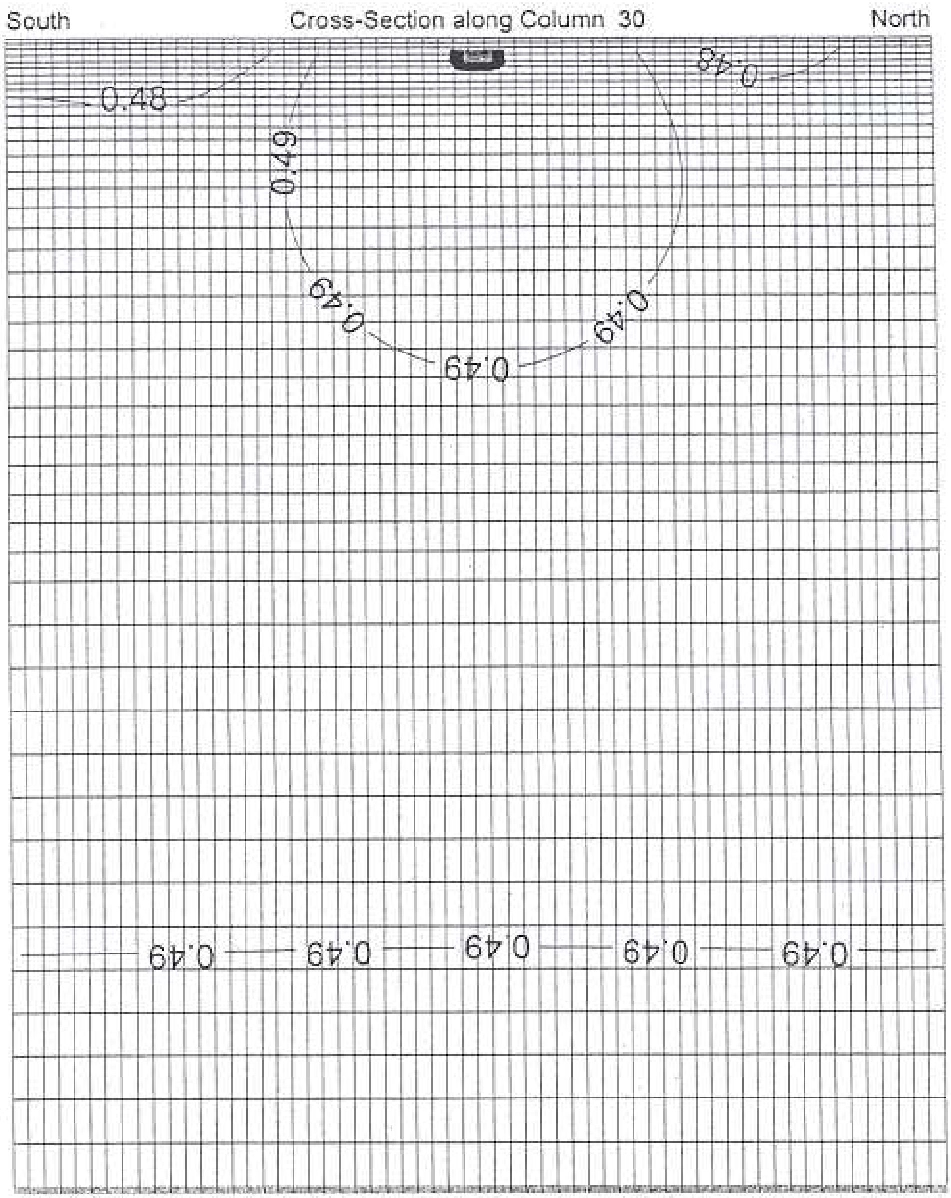

Figure D.49 Water saturation contours in cross-section for SLB1

Simulation-SLB2-Sandy Loam soil with ET domain type B
Time -60 days after beginning of simulation
Date-3/14/2000

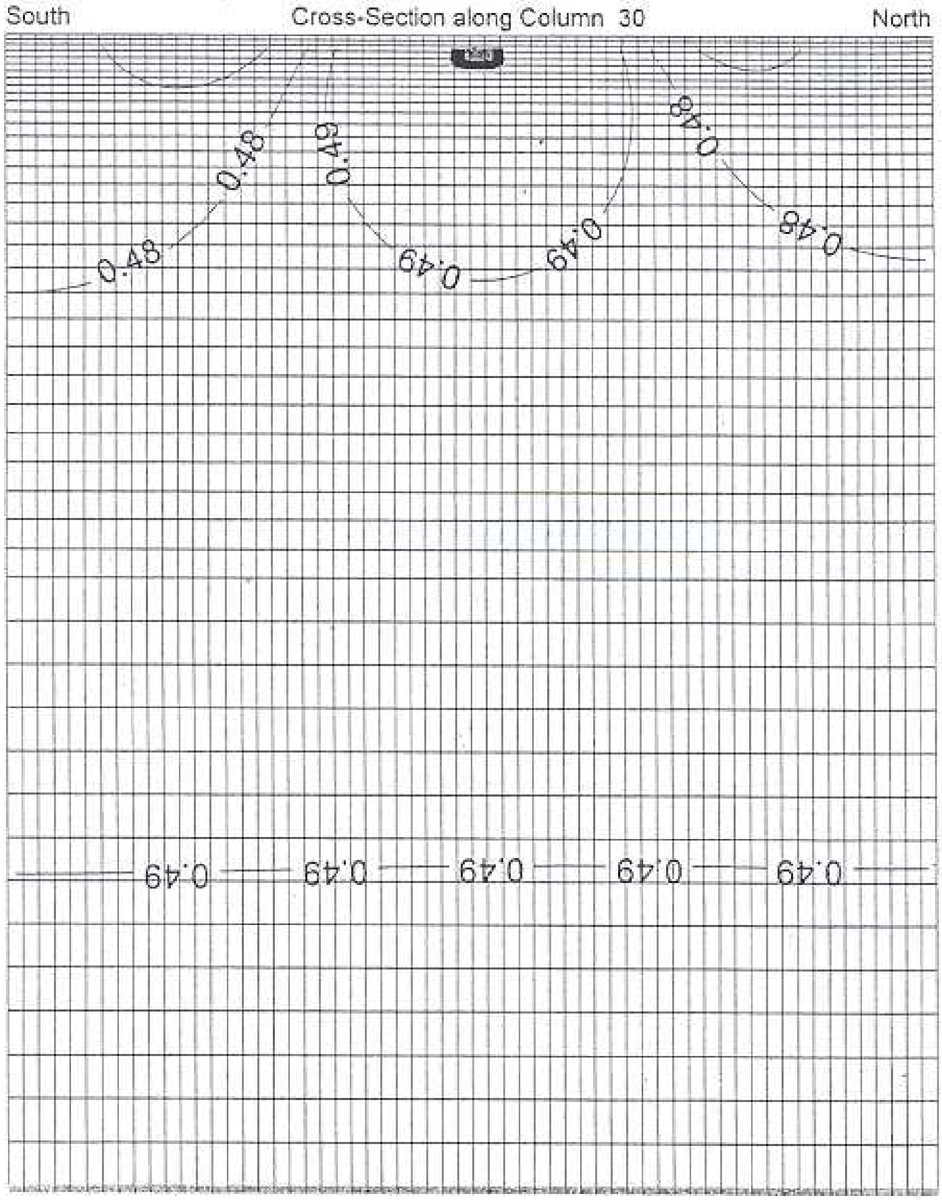

Figure D.50 Water saturation contours in cross-section for SLB2

Simulation-SLB3-Sandy Loam soil with ET domain type B
Time -90 days after beginning of simulation
Date-4/13/2000

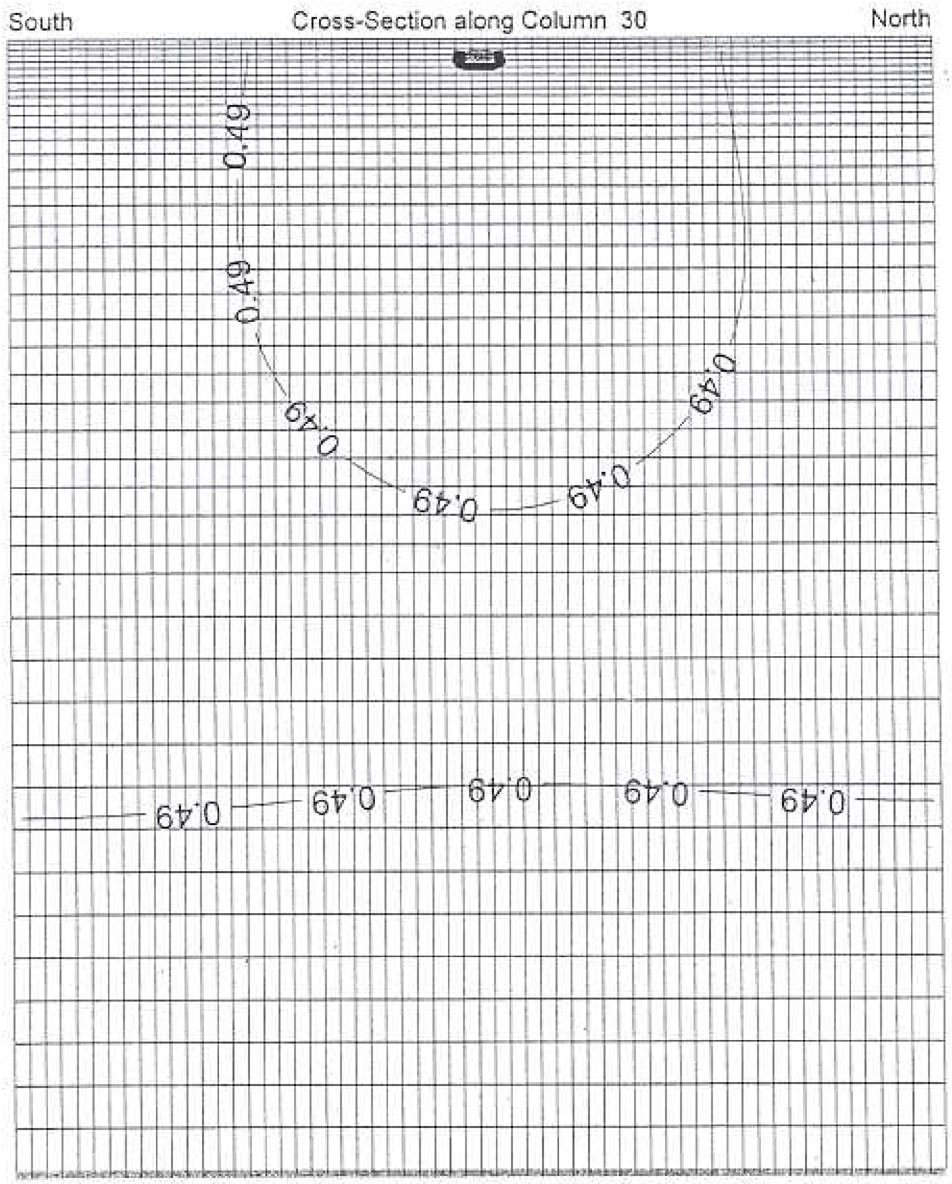

Figure D.51 Water saturation contours in cross-section for SLB3

Simulation-SLB4-Sandy Loam soil with ET domain type B
Time -120 days after beginning of simulation
Date-5/13/2000

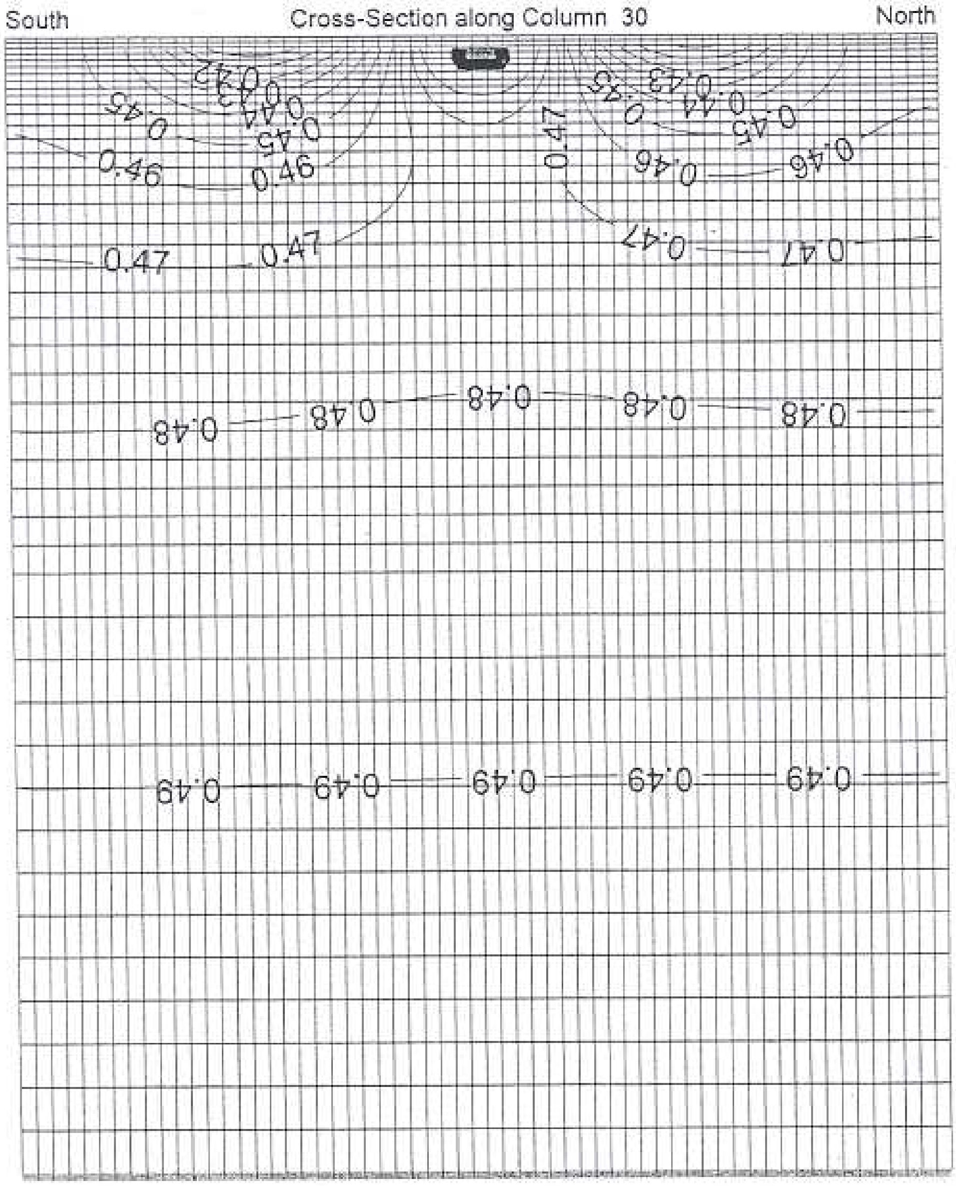

Figure D.52 Water saturation contours in cross-section for SLB4

Simulation-SLB5-Sandy Loam soil with ET domain type B
Time -150 days after beginning of simulation
Date-6/12//2000

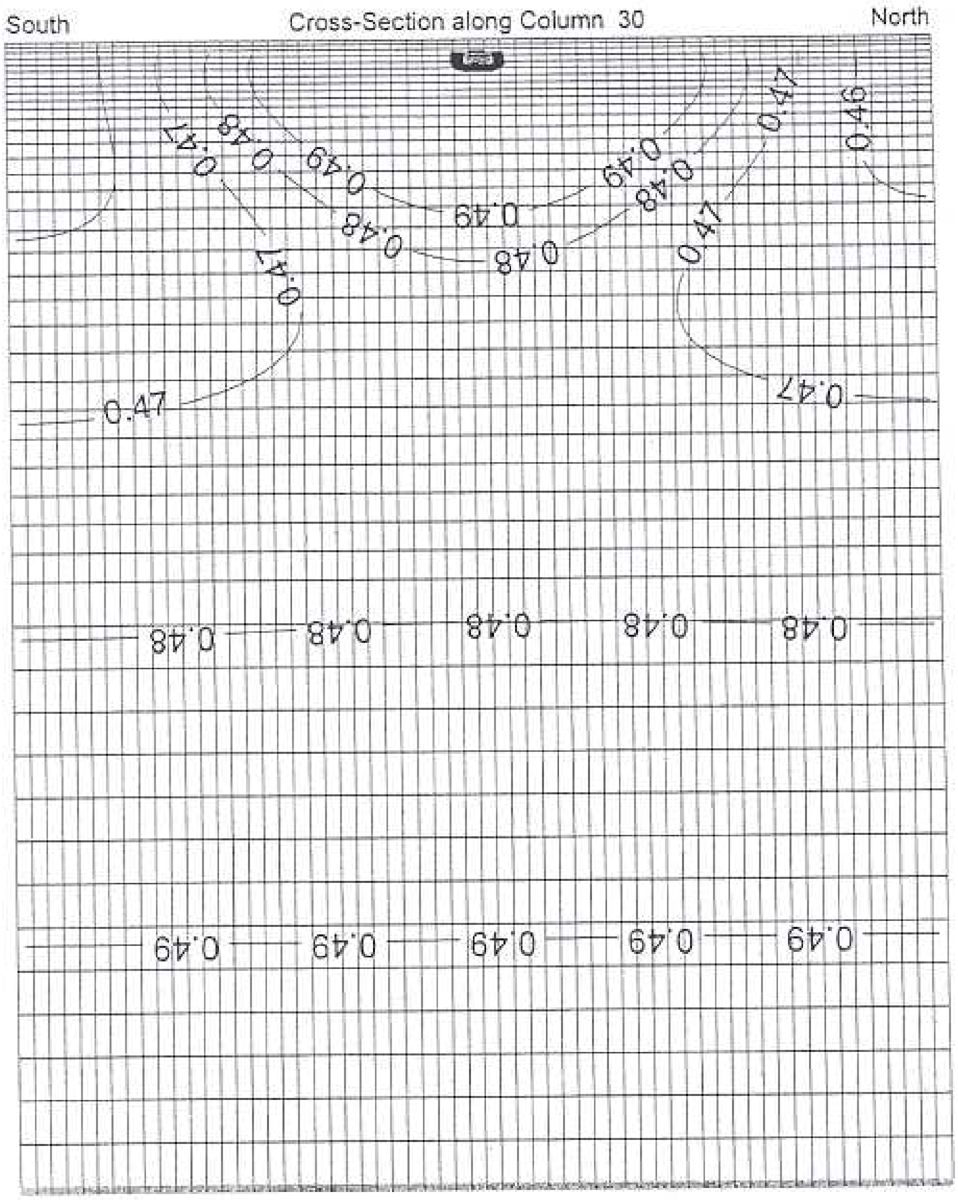

Figure D.53 Water saturation contours in cross-section for SLB5

Simulation-SLB6-Sandy Loam soil with ET domain type B
Time -180 days after beginning of simulation
Date-7/12/2000

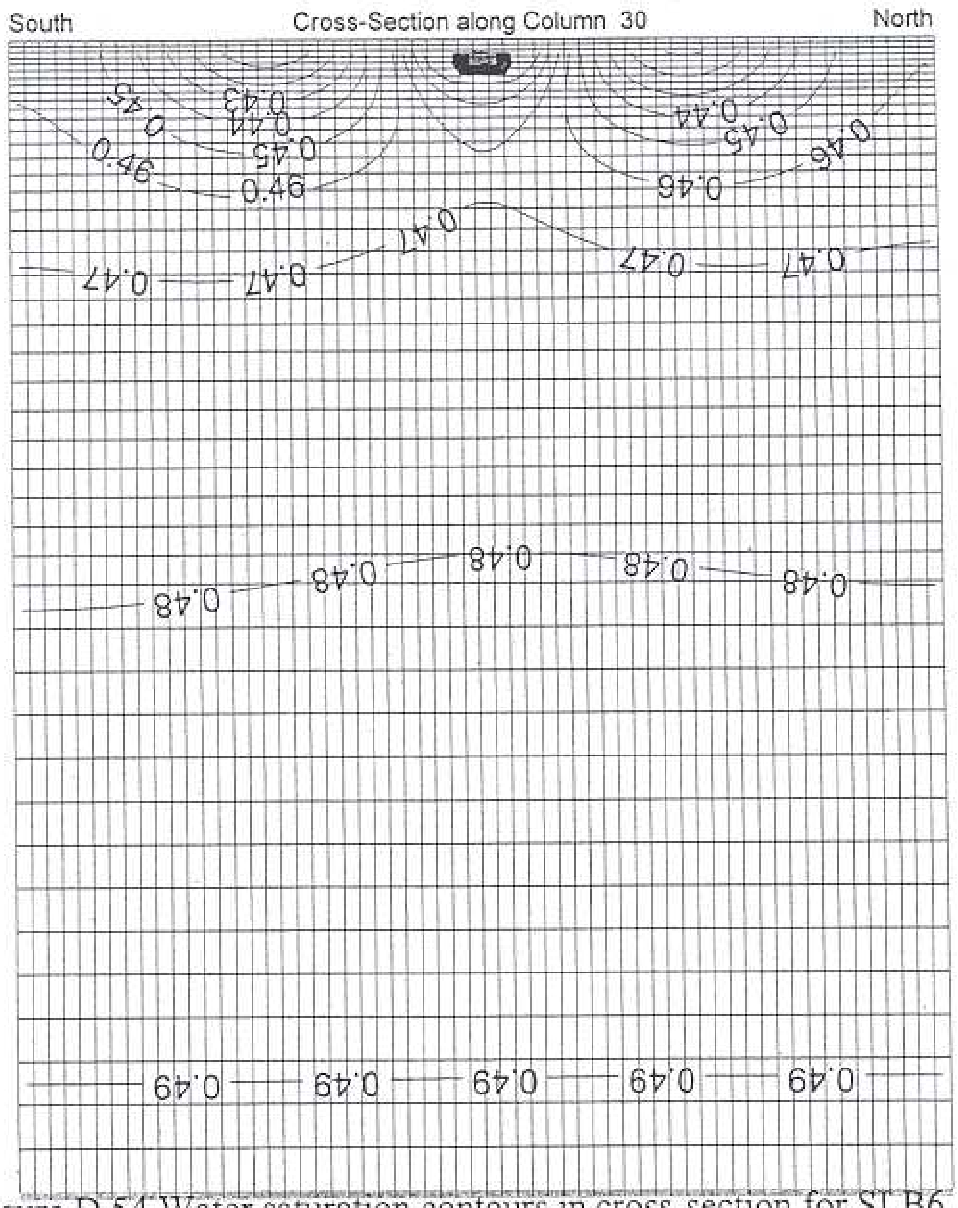

Figure D.54 Water saturation contours in cross-section for SLB6

Simulation-SLB7-Sandy Loam soil with ET domain type B
Time -210 days after beginning of simulation
Date-8/11/2000

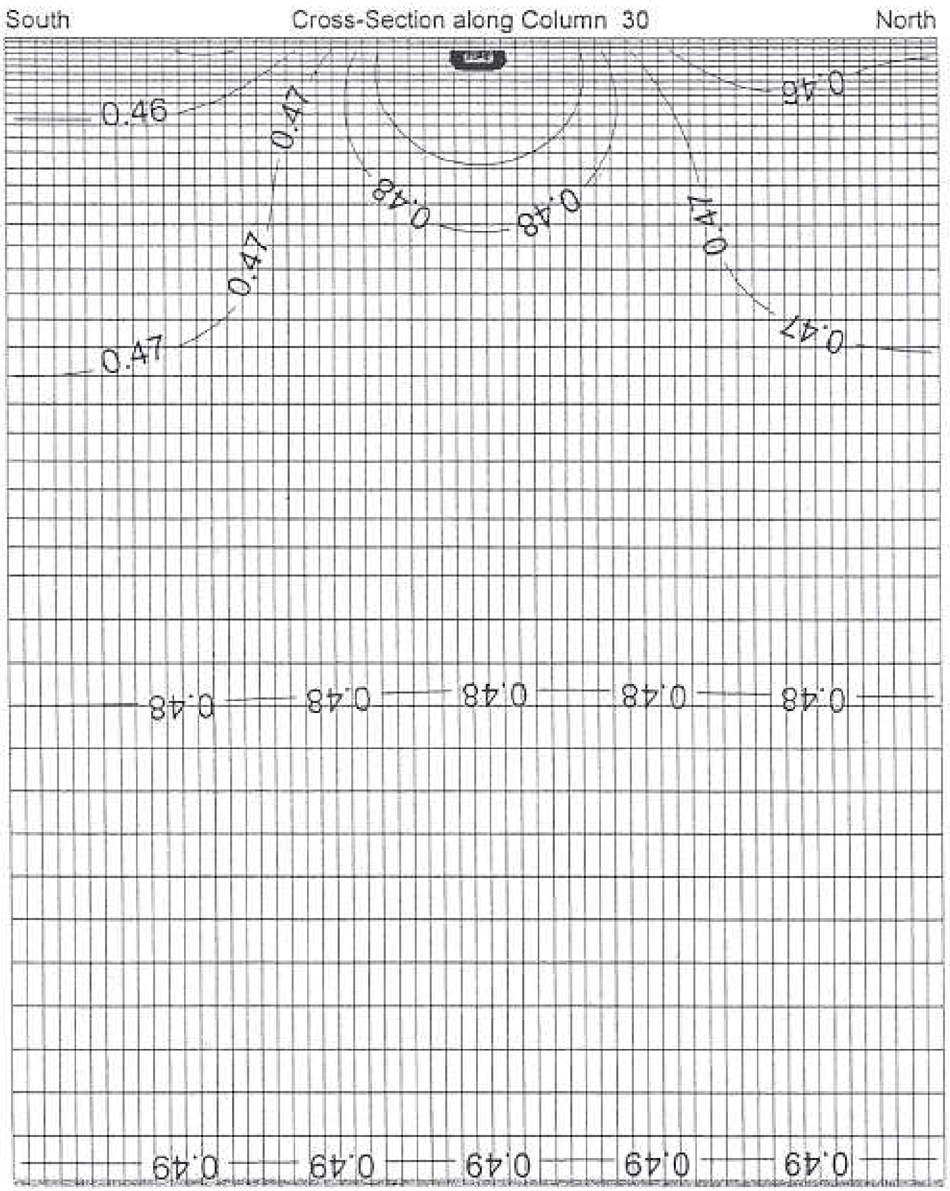

Figure D.55 Water saturation contours in cross-section for SLB7

Simulation-SLB8-Sandy Loam soil with ET domain type B
Time -240 days after beginning of simulation
Date-9/10/2000

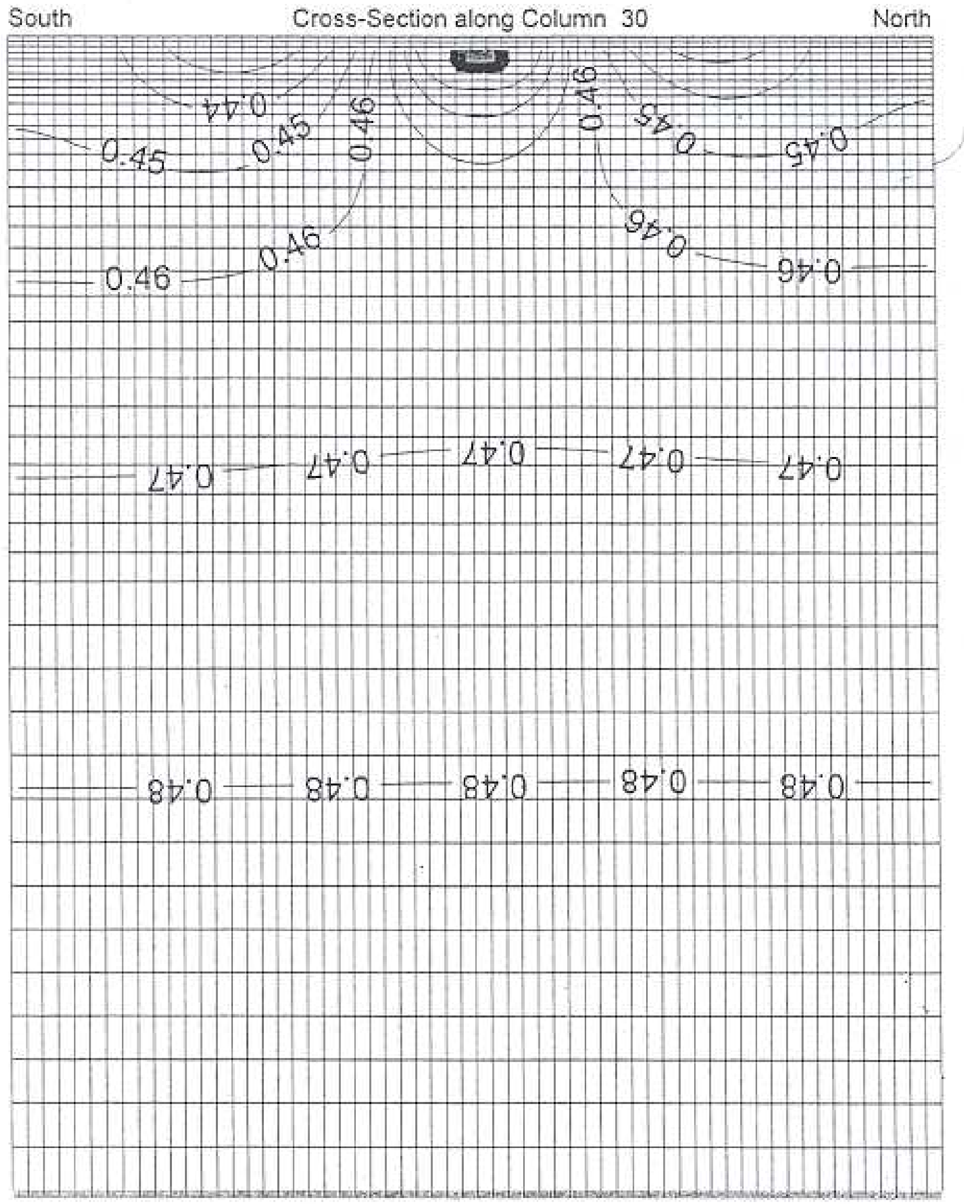

Figure D.56 Water saturation contours in cross-section for SLB8

Simulation-SLB9-Sandy Loam soil with ET domain type B
Time -270 days after beginning of simulation
Date-10/10/2000

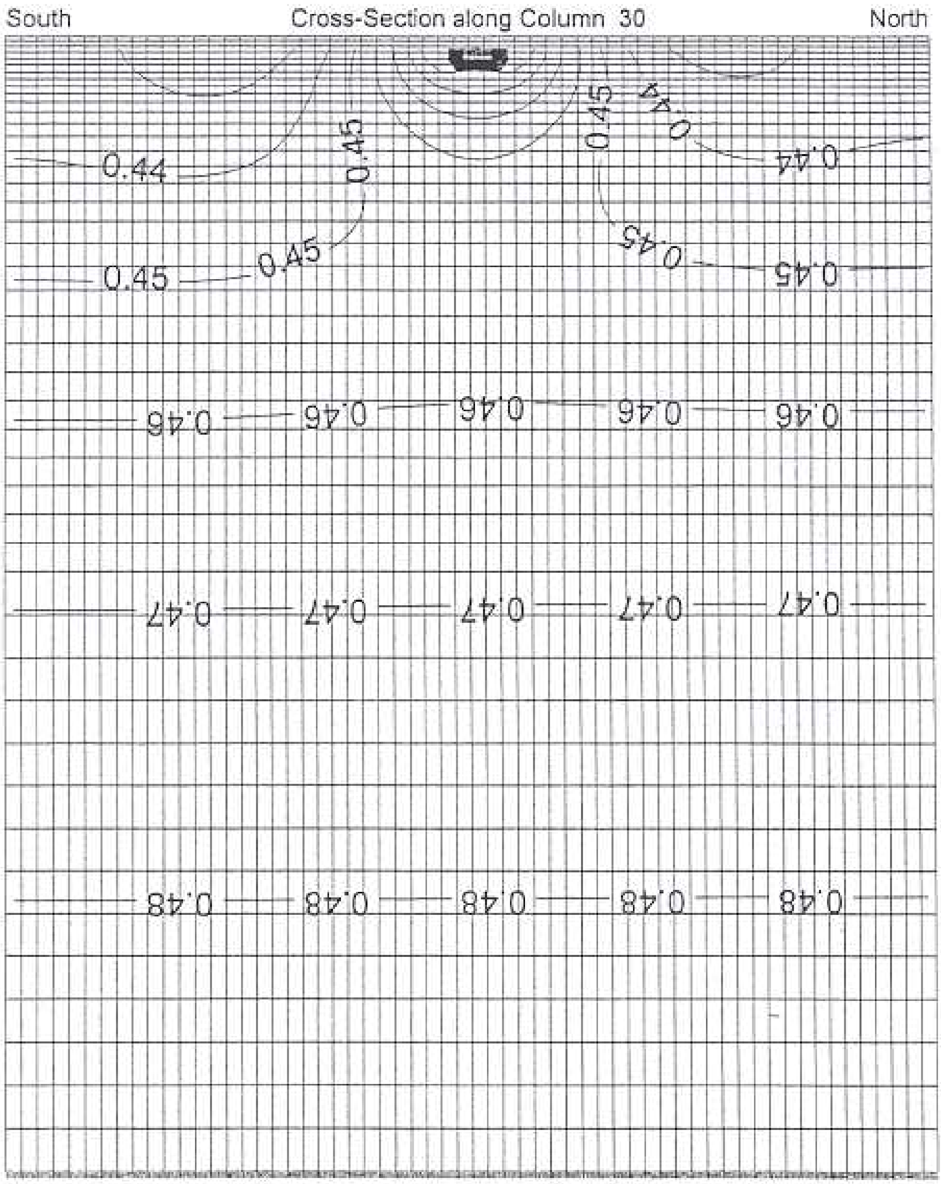

Figure D.57 Water saturation contours in cross-section for SLB9

Simulation-SLB10-Sandy Loam soil with ET domain type B
Time -300 days after beginning of simulation
Date-11/9/2000

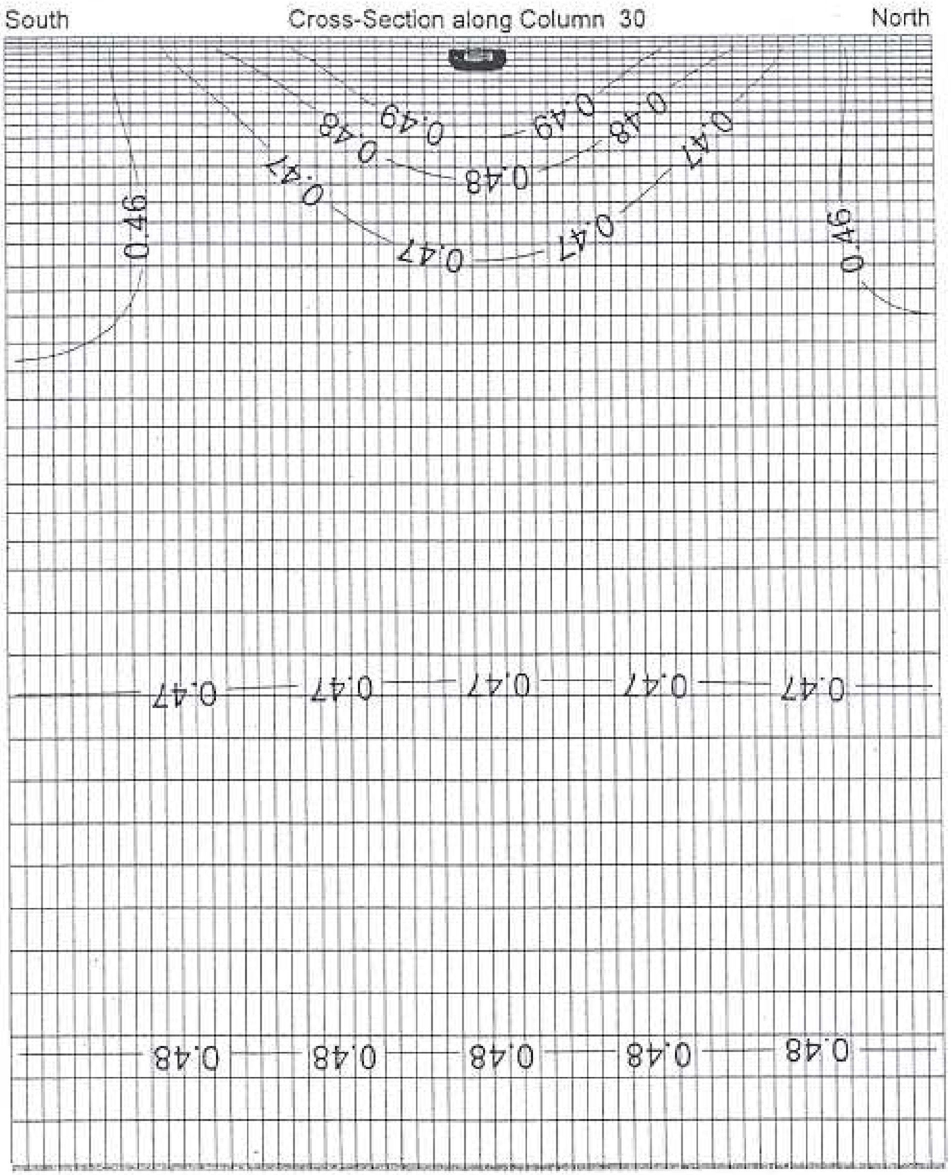

Figure D.58 Water saturation contours in cross-section for SLB10

Simulation-SLB11-Sandy Loam soil with ET domain type B
Time -330 days after beginning of simulation
Date-12/9/2000

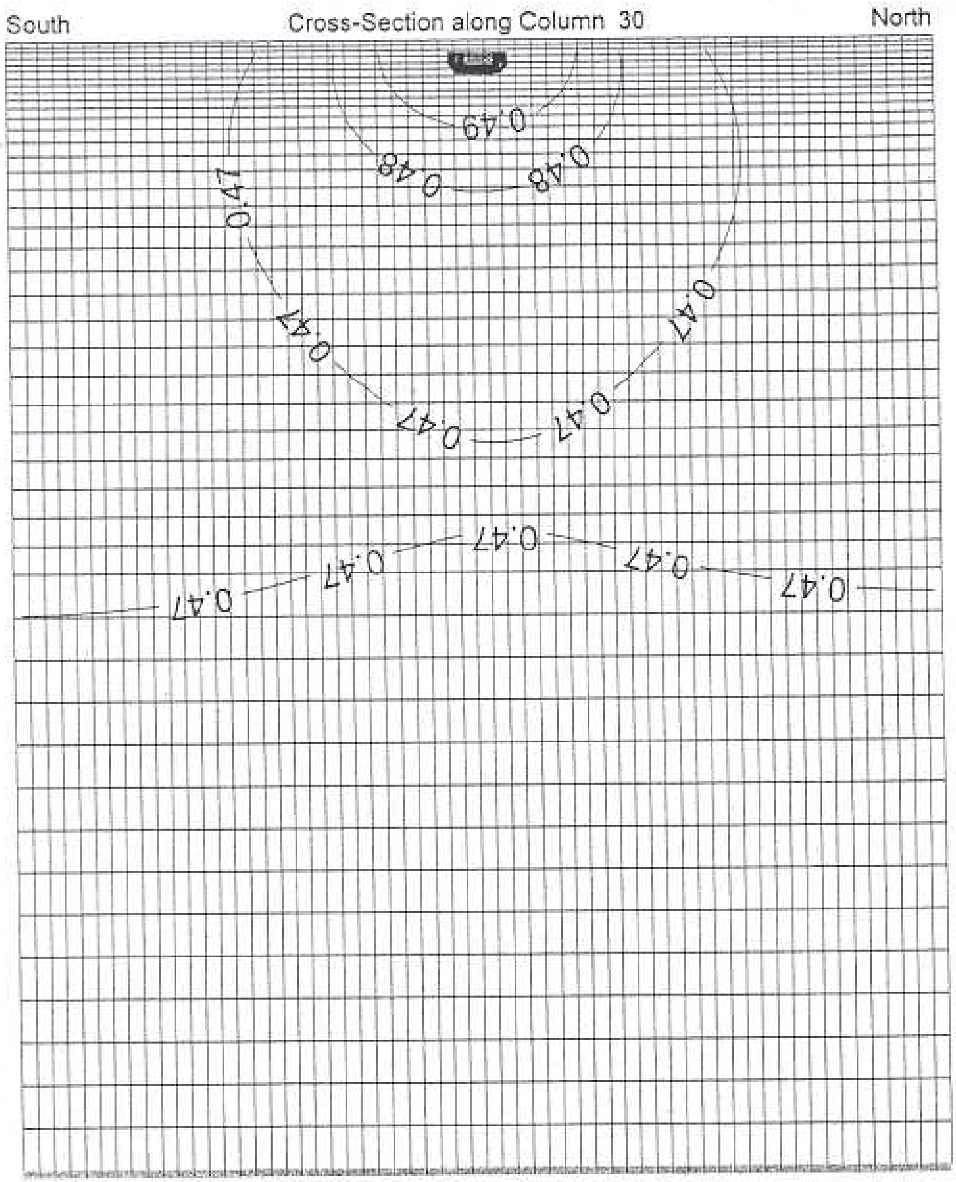

Figure D.59 Water saturation contours in cross-section for SLB11

Simulation-SLB12-Sandy Loam soil with ET domain type B
Time -352 days after beginning of simulation
Date-12/31/2000

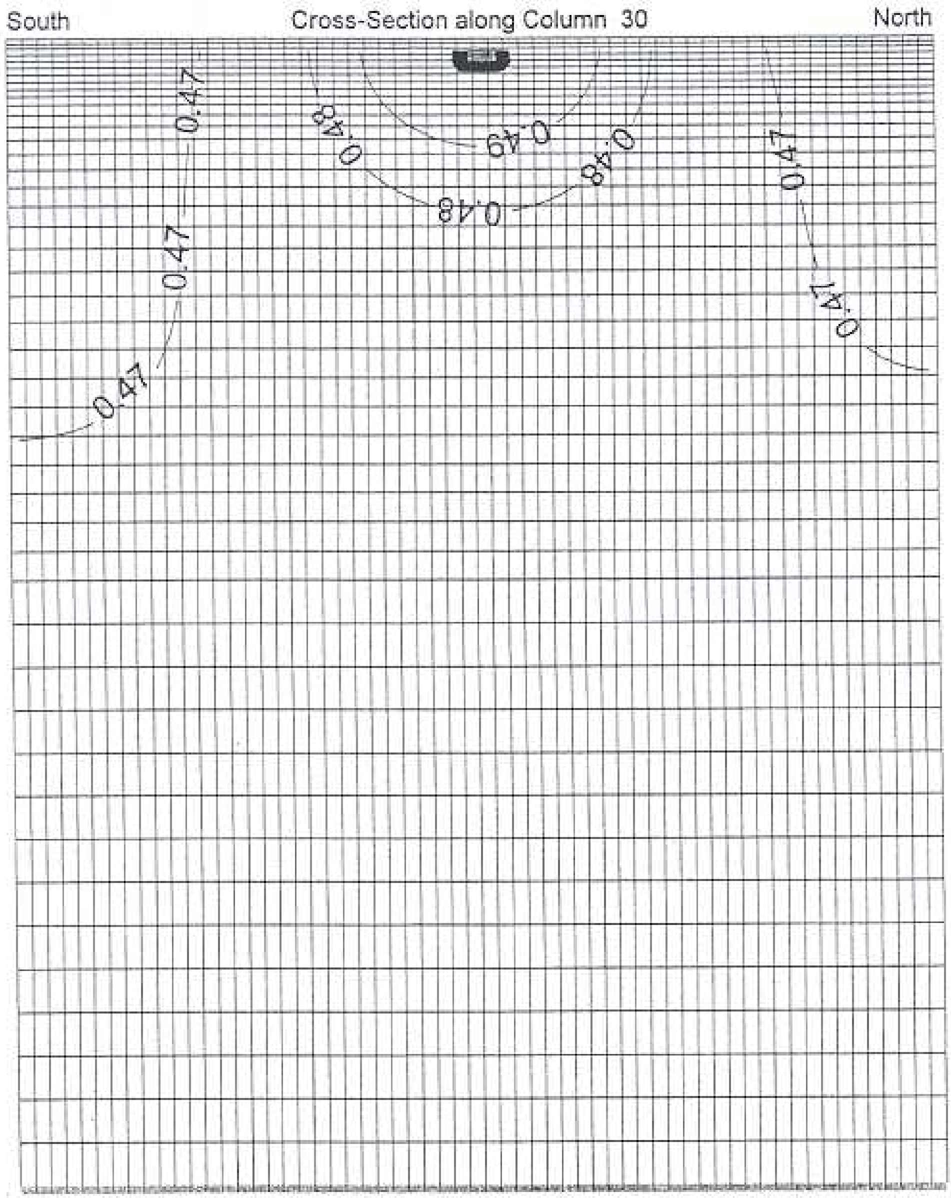

Figure D.60 Water saturation contours in cross-section for SLB12

Simulation-SLB1-Sandy Loam soil with ET domain type B
Time -30 days after beginning of simulation
Date-2/13/2000

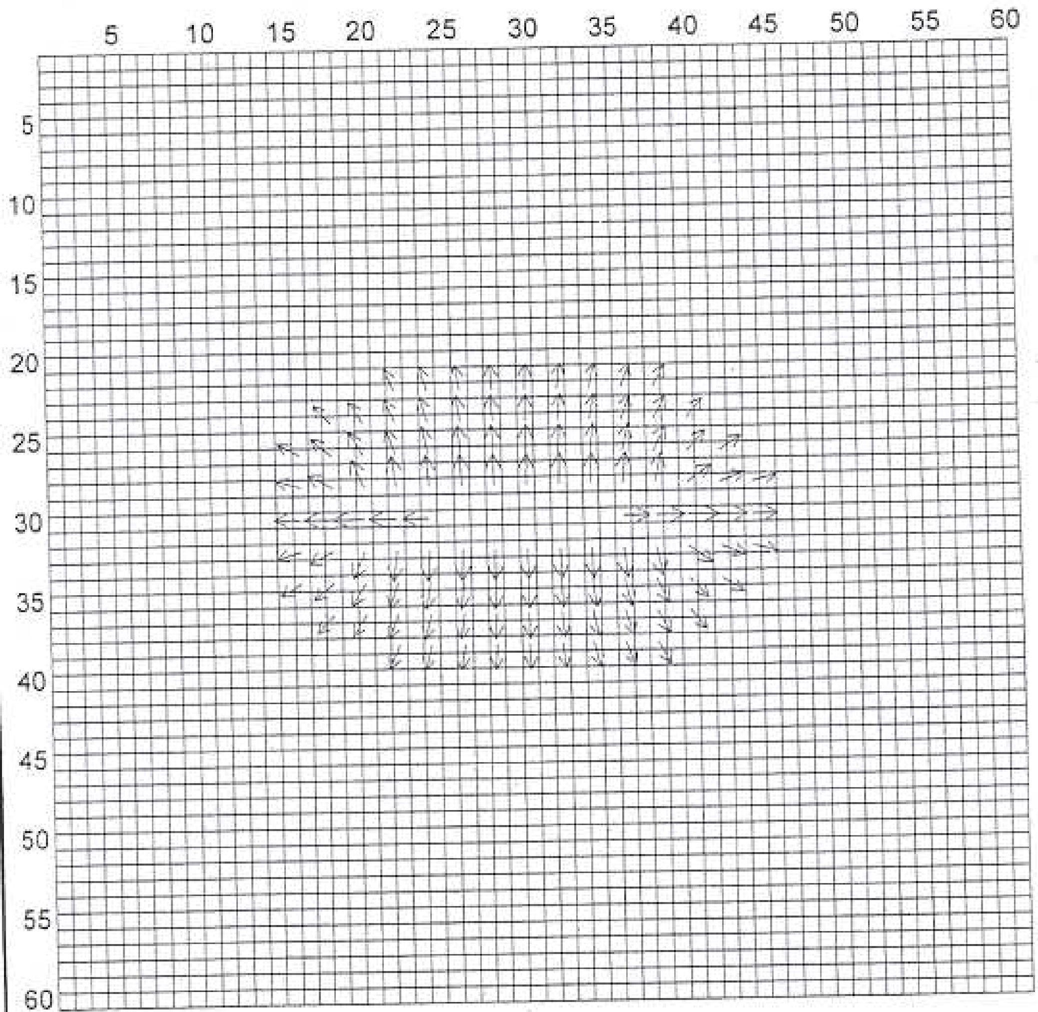

Figure D.61 Moisture movement vectors in plan view for SLB1

Simulation-SLB4-Sandy Loam soil with ET domain type B
Time -120 days after beginning of simulation
Date-5/13/2000

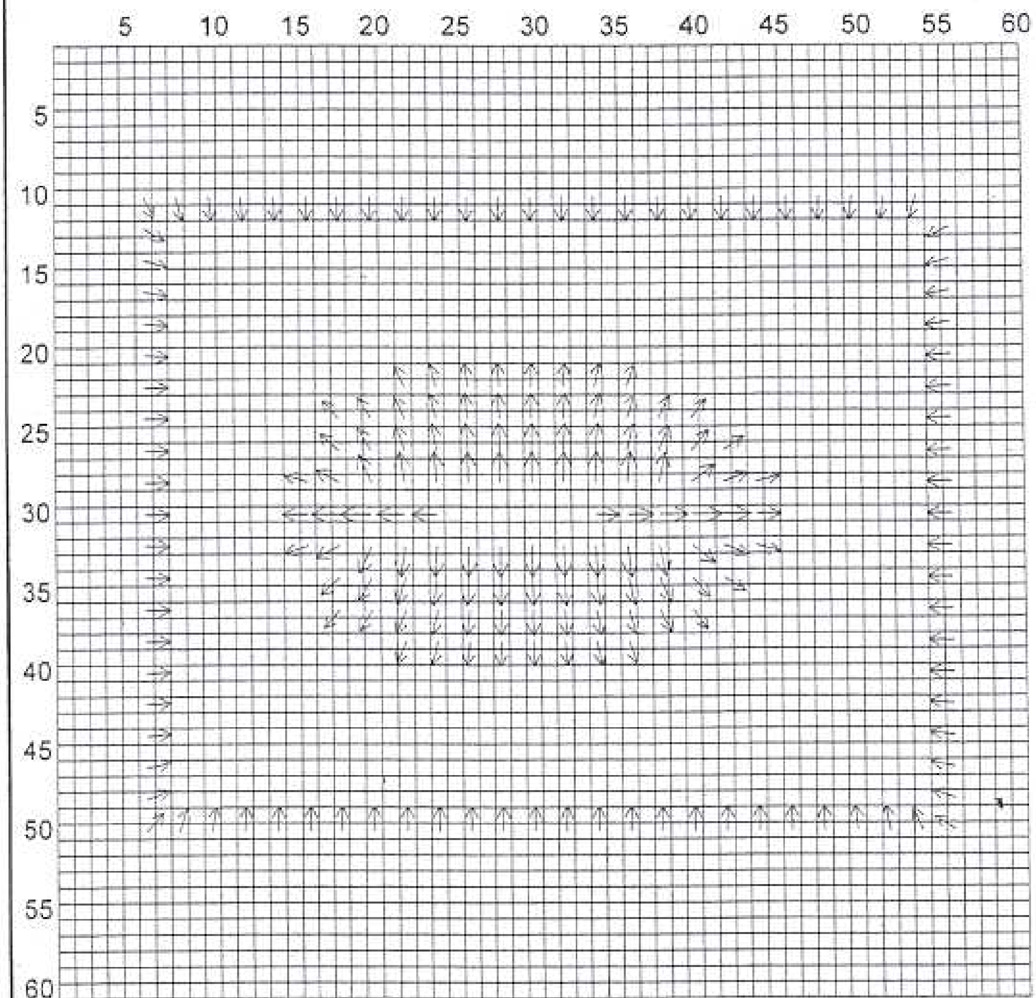

Figure D.62 Moisture movement vectors in plan view for SLB4

Simulation-SLB8-Sandy Loam soil with ET domain type B
Time -240 days after beginning of simulation
Date-9/10/2000

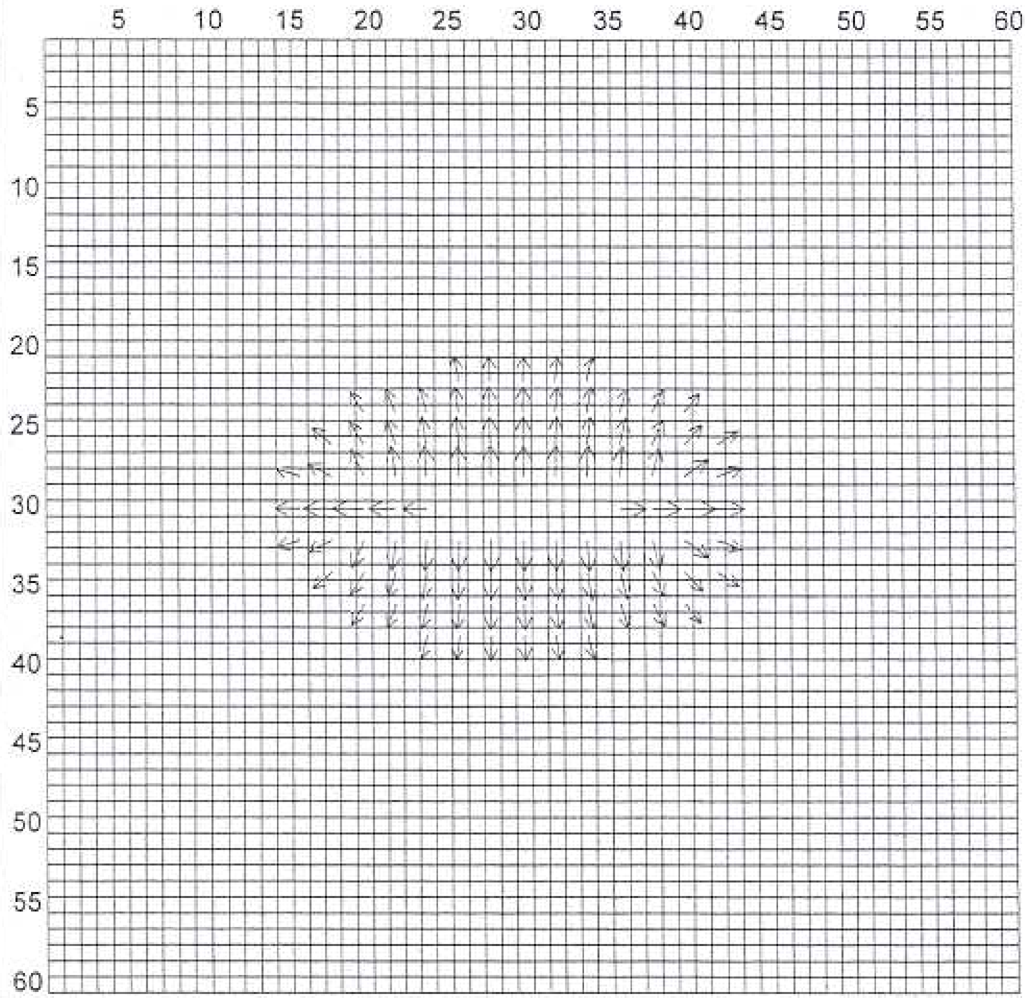

Figure D.63 Moisture movement vectors in plan view for SLB8

Simulation-SLB12-Sandy Loam soil with ET domain type B
Time -352 days after beginning of simulation
Date-12/31/2000

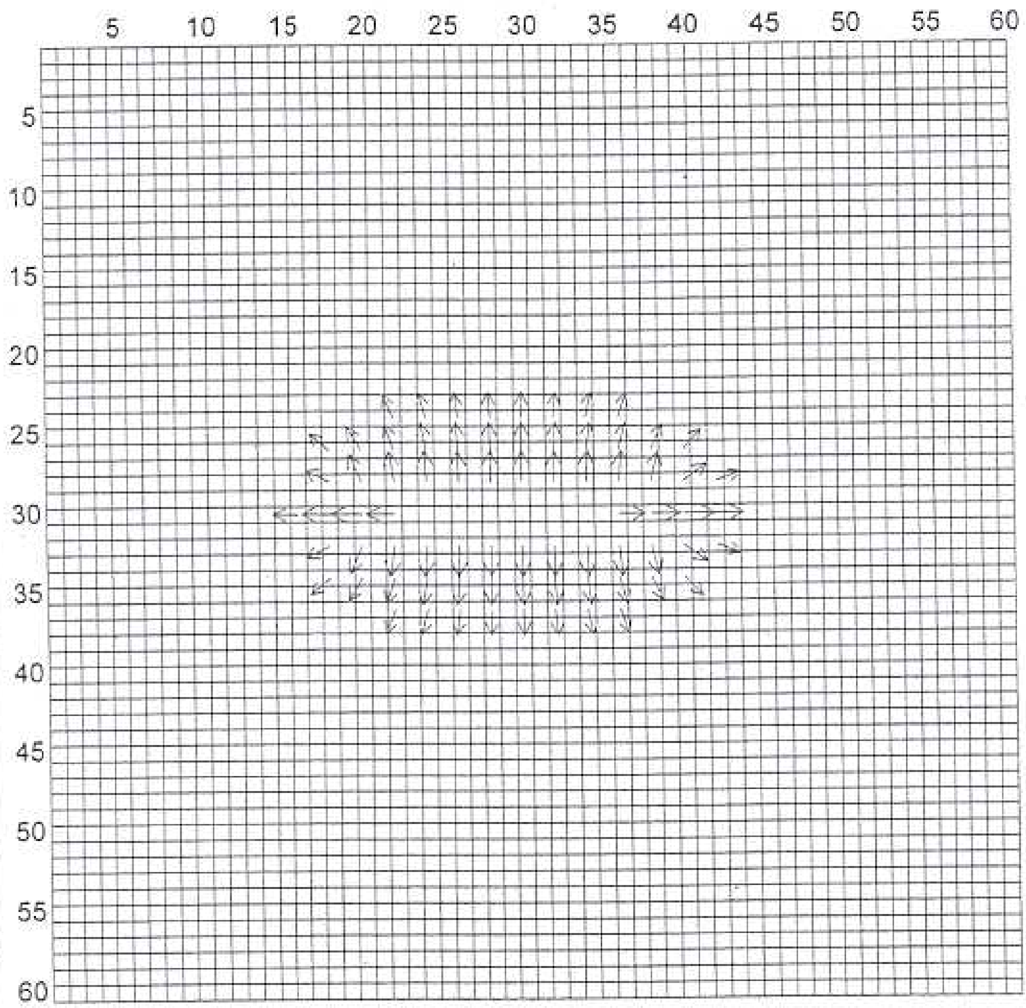

Figure D.64 Moisture movement vectors in plan view for SLB12

Simulation-SLB1-Sandy Loam soil with ET domain type B
Time -30 days after beginning of simulation
Date-2/13/2000

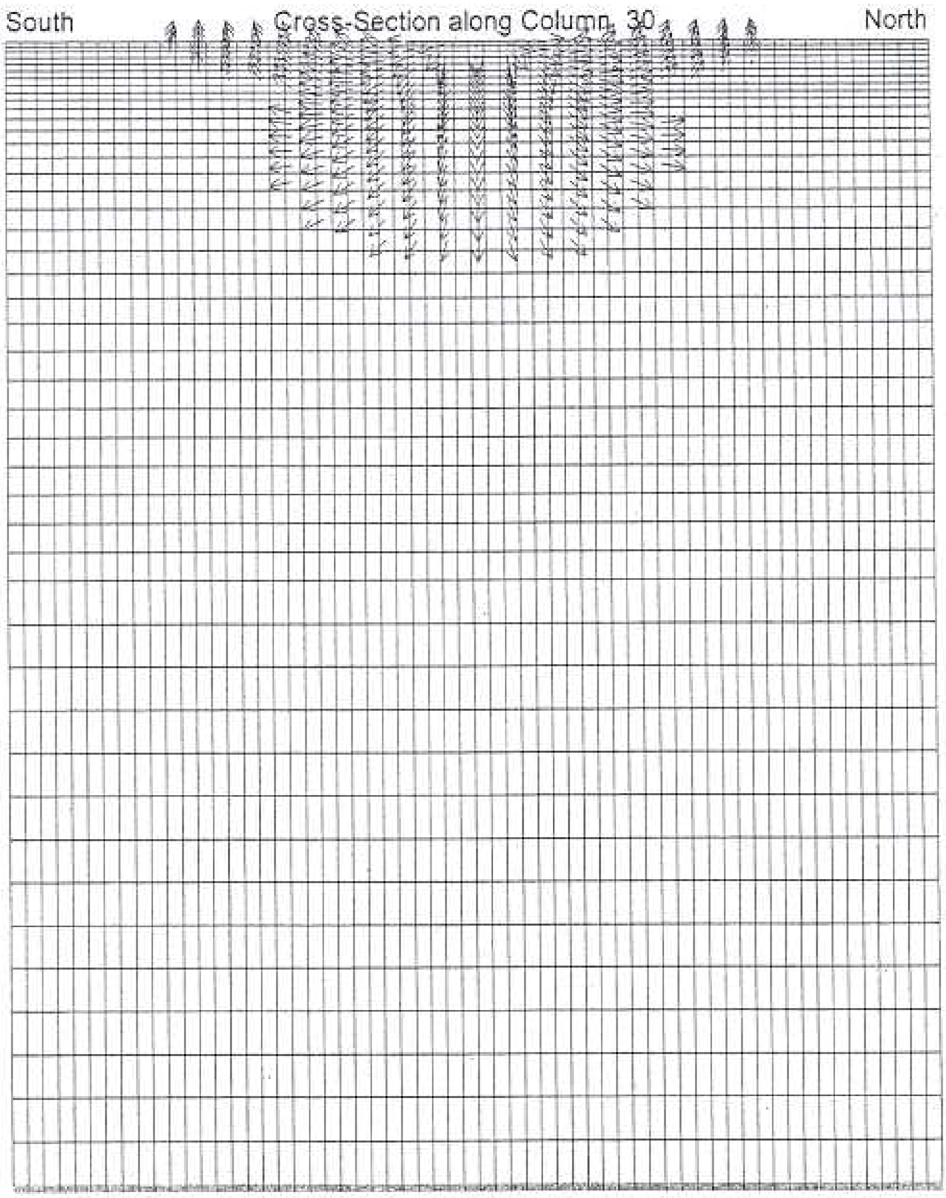

Figure D.65 Moisture movement vectors along C-30 for SLB1

Simulation-SLB4-Sandy Loam soil with ET domain type B
Time -120 days after beginning of simulation
Date-5/13/2000

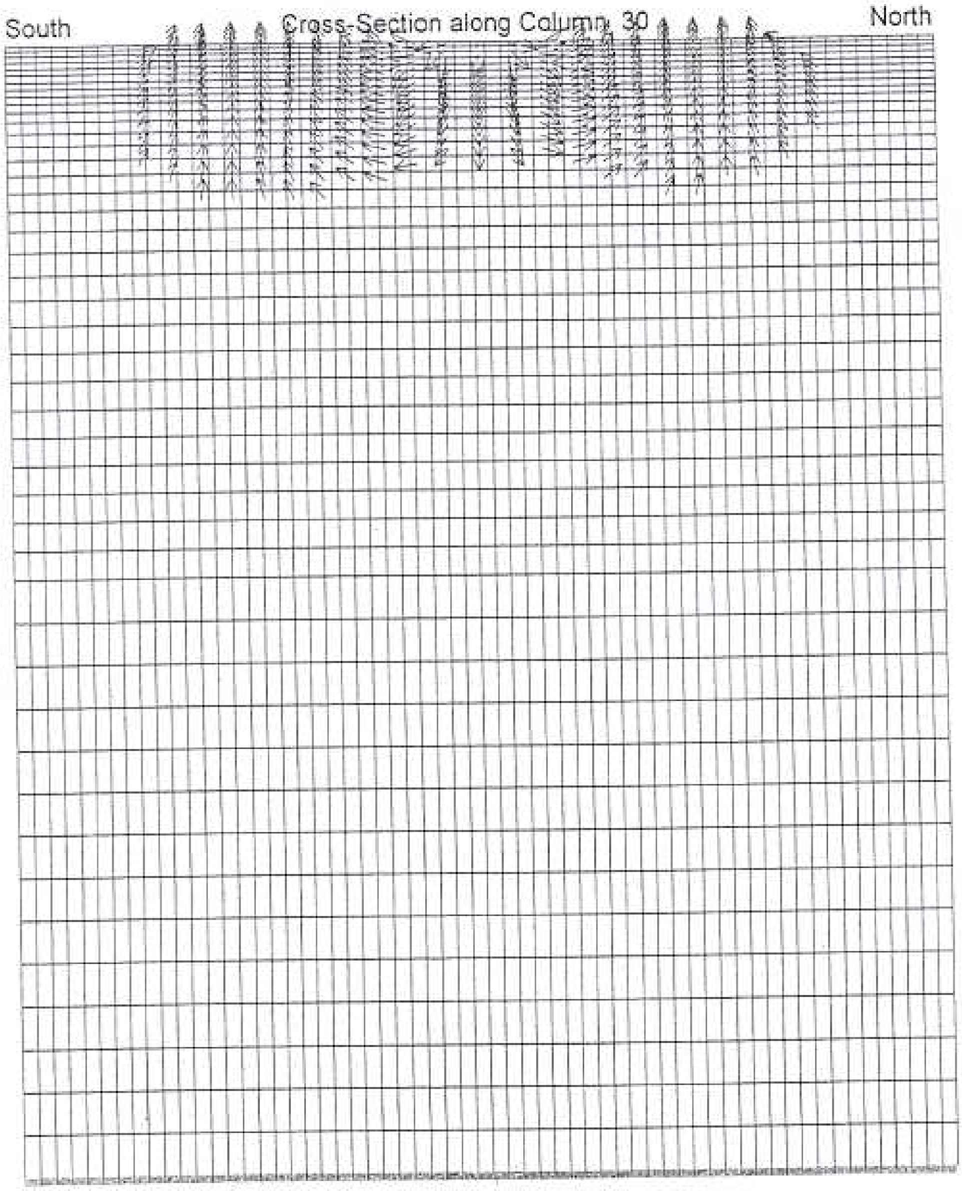

Figure D.66 Moisture movement vectors along C-30 for SLB4

Simulation-SLB8-Sandy Loam soil with ET domain type B
Time -240 days after beginning of simulation
Date-9/10/2000

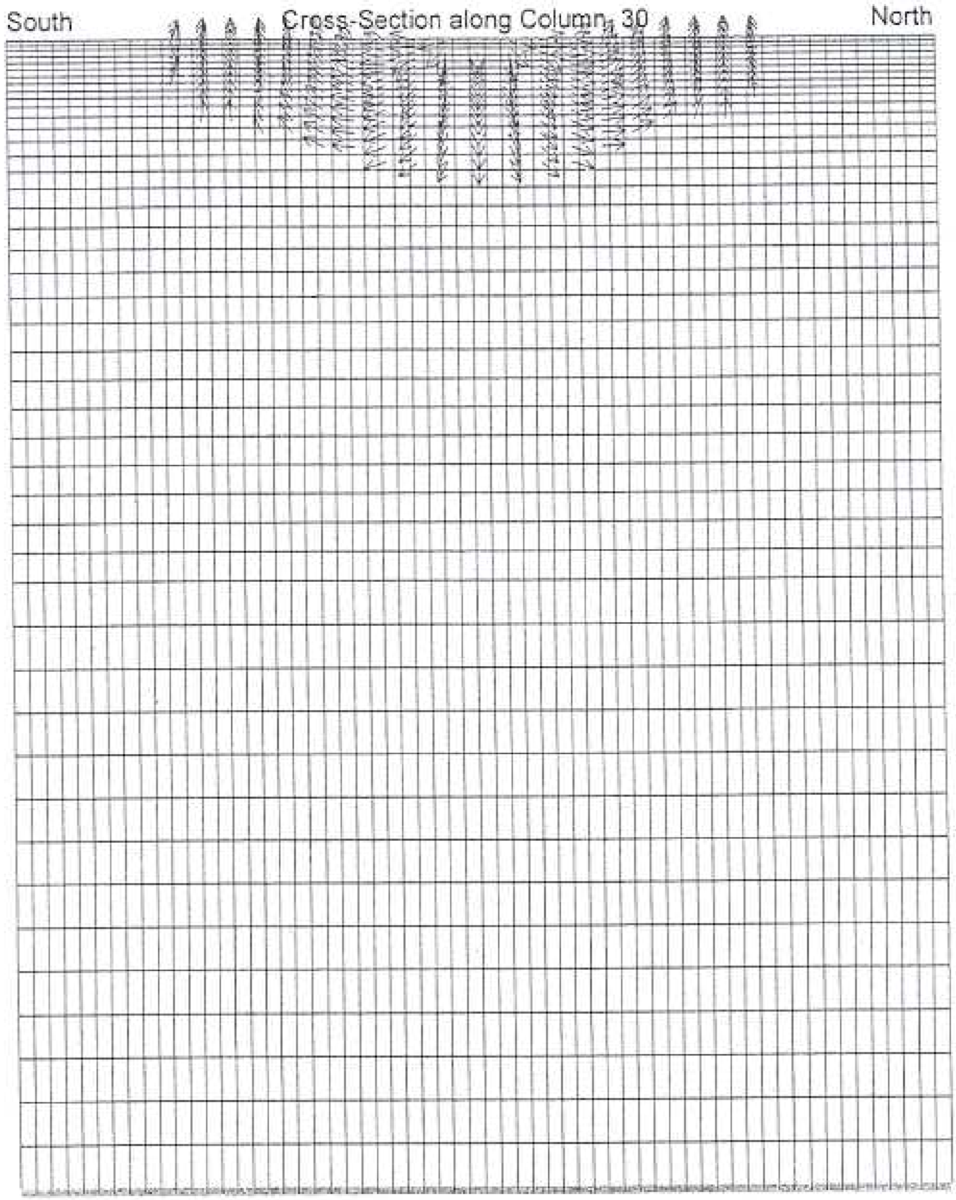

Figure D.67 Moisture movement vectors along C-30 for SLB8

Simulation-SLB12-Sandy Loam soil with ET domain type B
Time -352 days after beginning of simulation
Date-12/31/2000

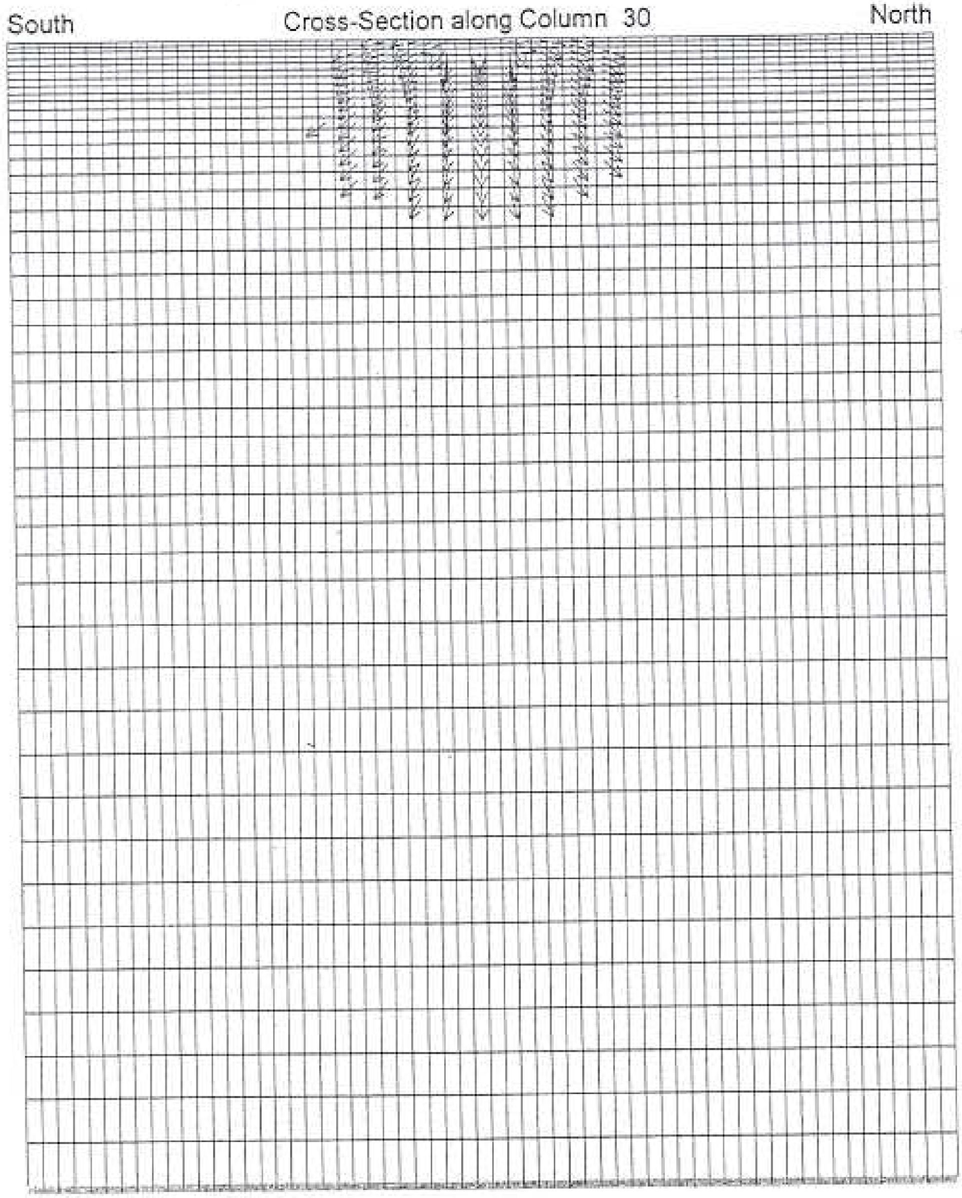

Figure D.68 Moisture movement vectors along C-30 for SLB12

Simulation-SLB1-Sandy Loam soil with ET domain type B
Time -30 days after beginning of simulation
Date-2/13/2000

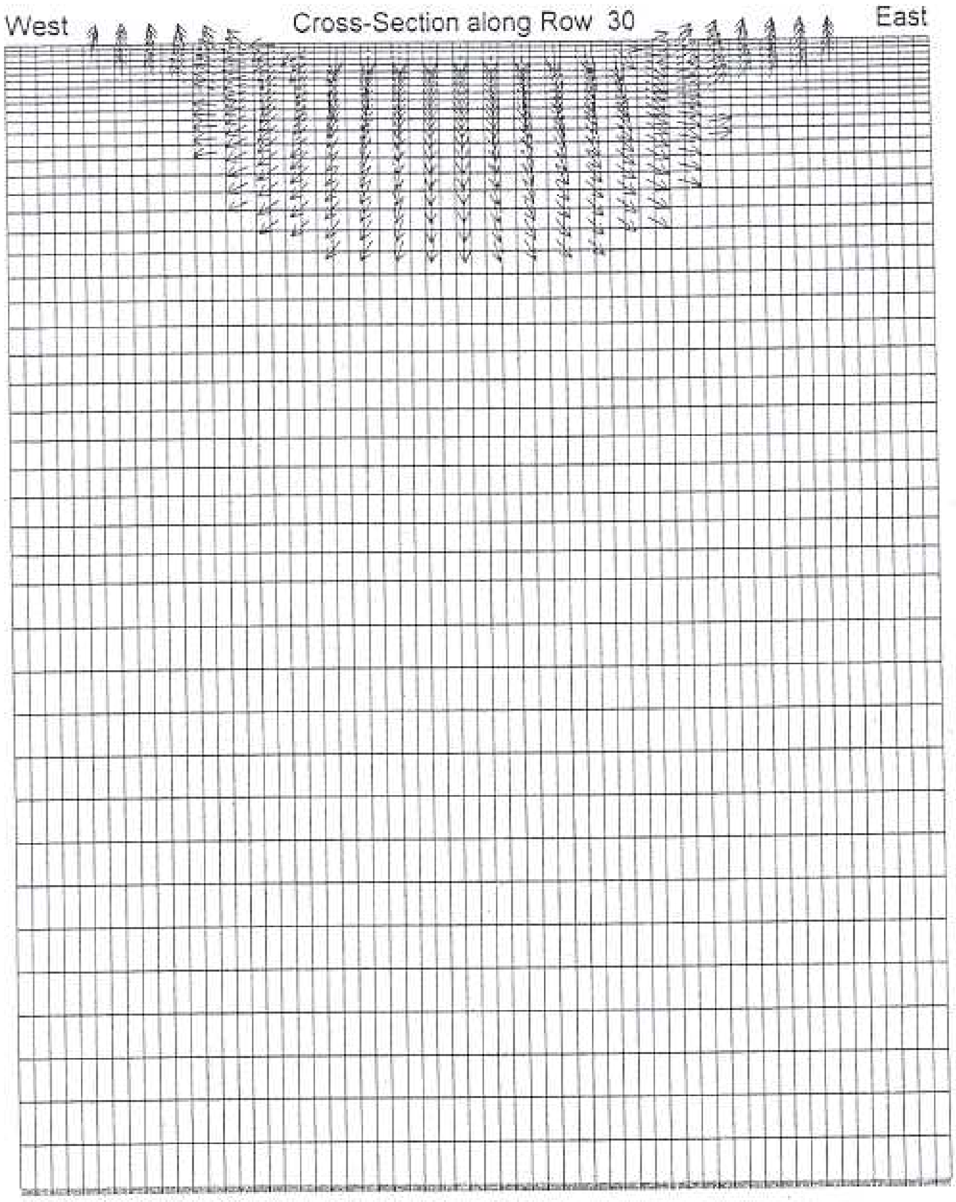

Figure D.69 Moisture movement vectors along R-30 for SLB1

Simulation-SLB4-Sandy Loam soil with ET domain type B
Time -120 days after beginning of simulation
Date-5/13/2000

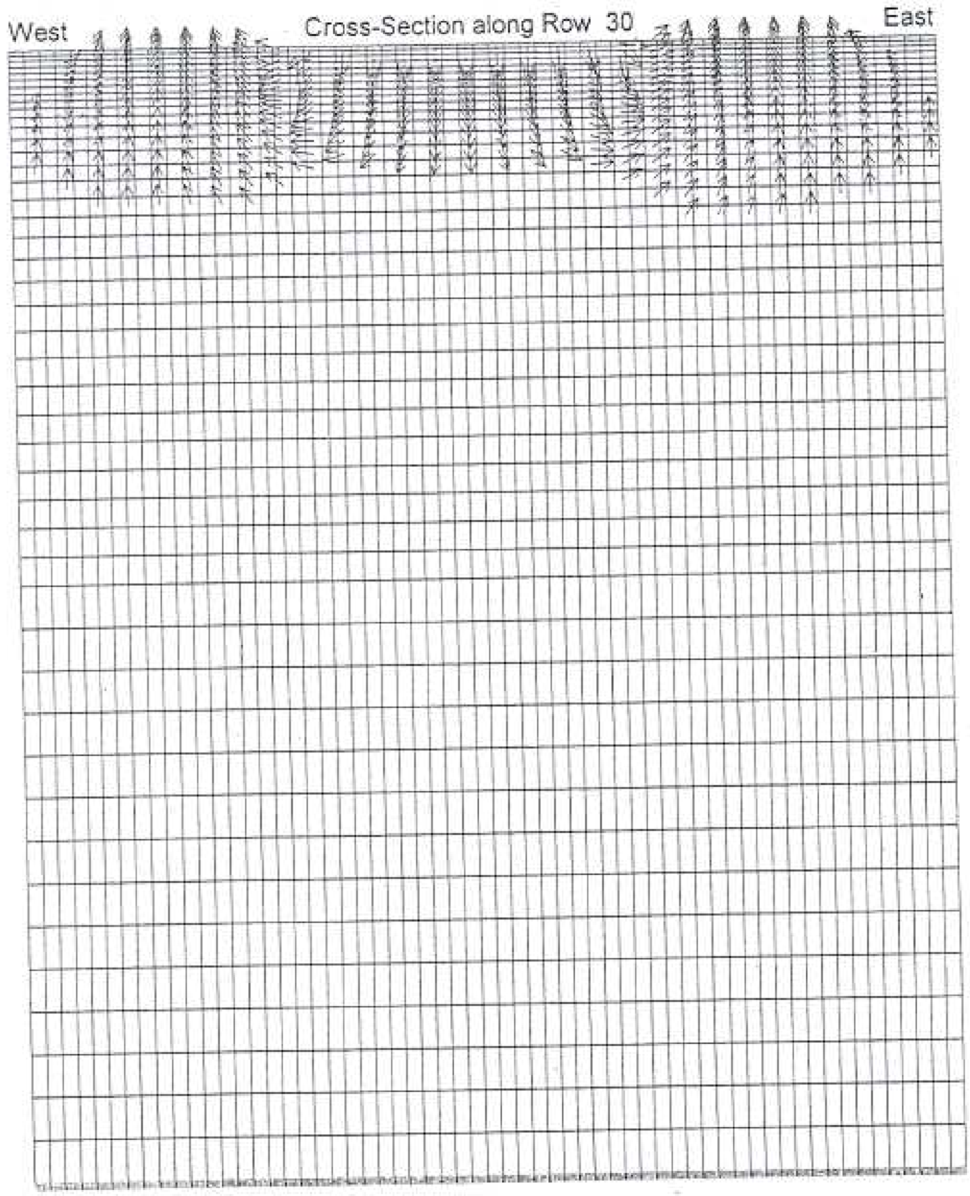

Figure D.70 Moisture movement vectors along R-30 for SLB4

Simulation-SLB8-Sandy Loam soil with ET domain type B
Time -240 days after beginning of simulation
Date-9/10/2000

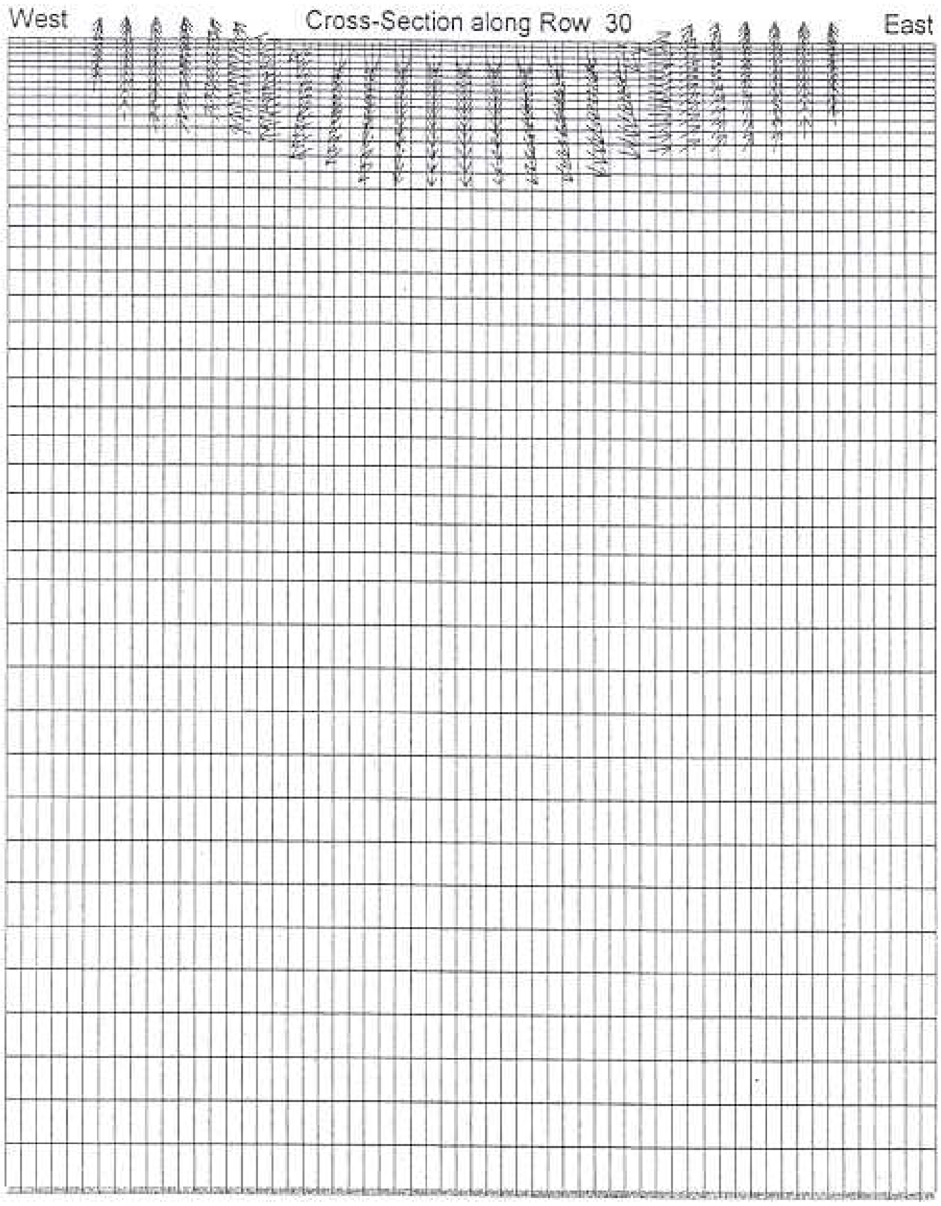

Figure D.71 Moisture movement vectors along R-30 for SLB8

Simulation-SLB12-Sandy Loam soil with ET domain type B
Time -352 days after beginning of simulation
Date-12/31/2000

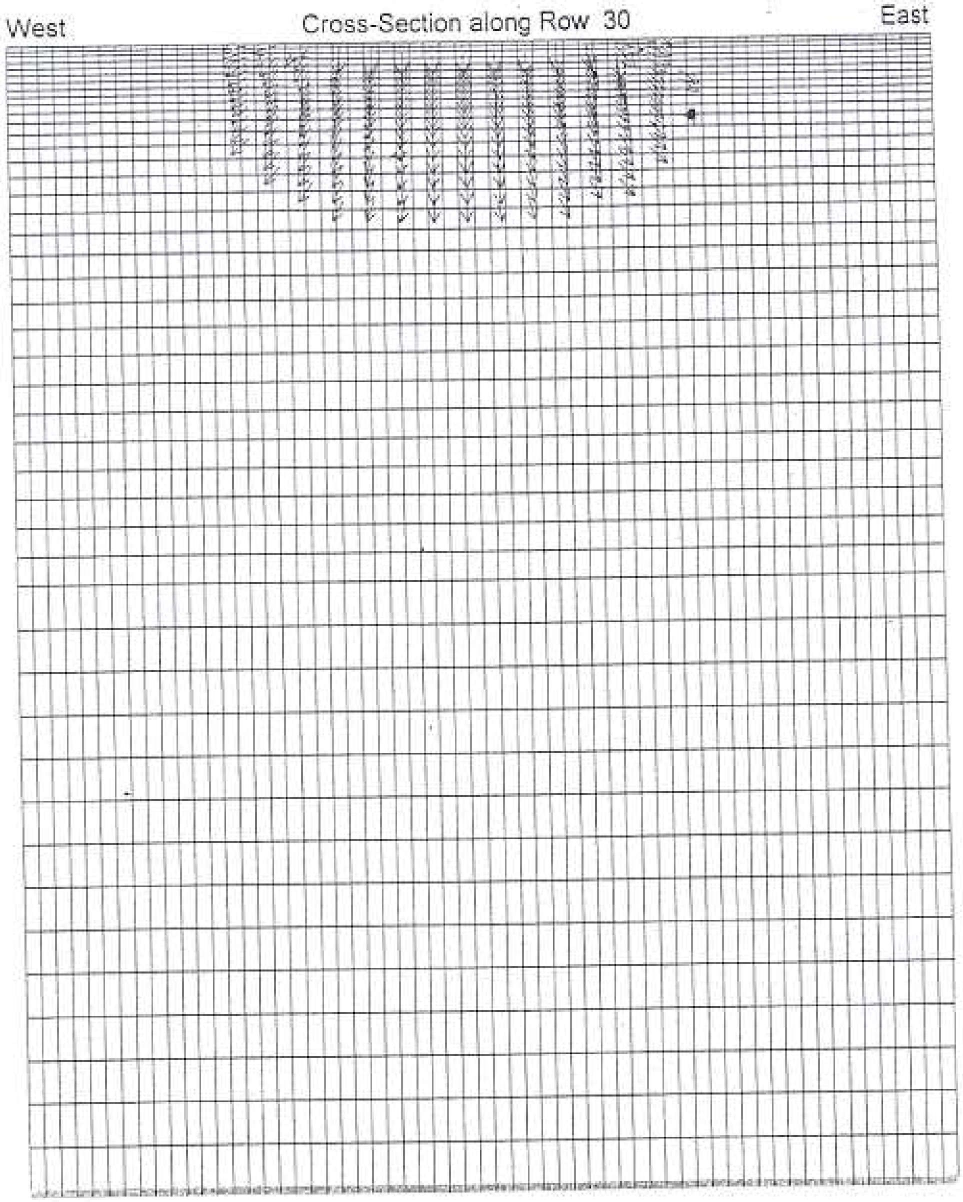

Figure D.72 Moisture movement vectors along R-30 for SLB12

Simulation-SCLA1-Sandy Clay Loam soil with ET domain type A
Time -30 days after beginning of simulation
Date-2/13/2000

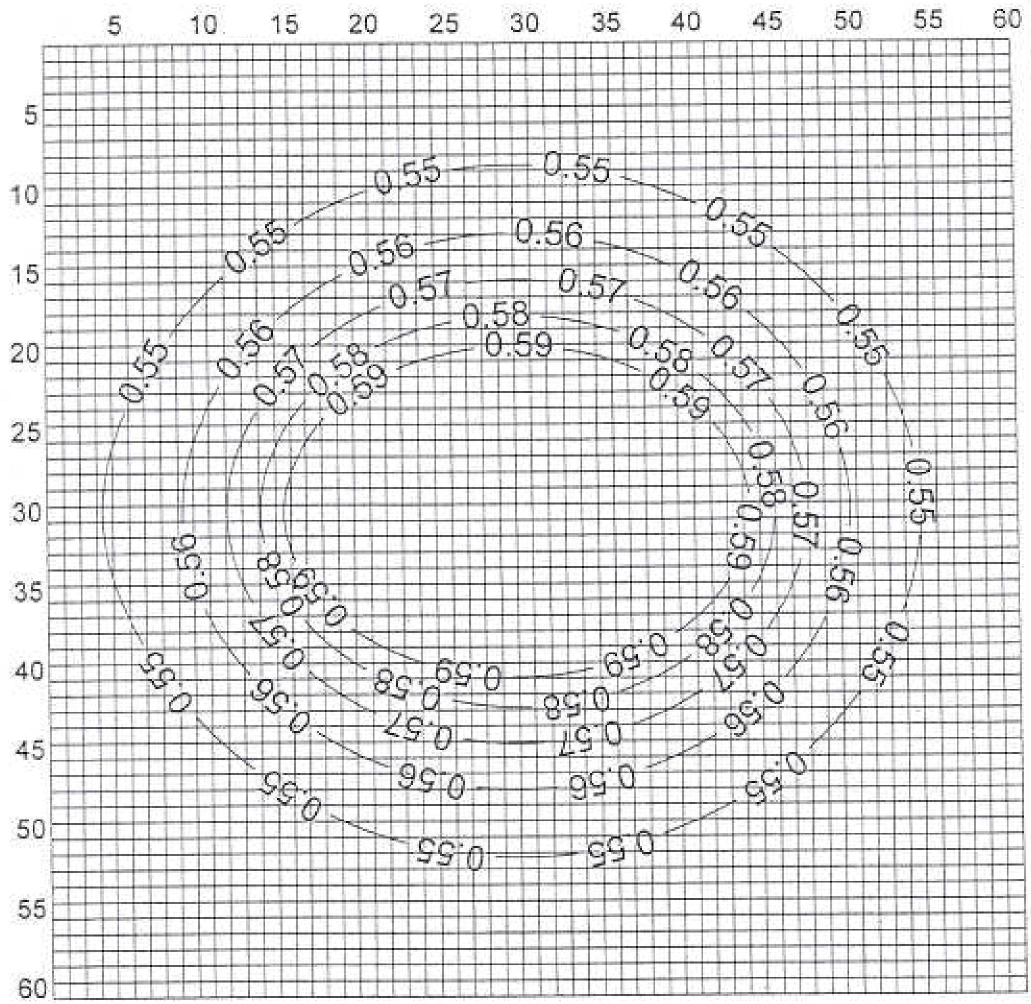

Figure D.73 Water saturation contours in plan view for SCLA1

Simulation-SCLA2-Sandy Clay Loam soil with ET domain type A
Time -60 days after beginning of simulation
Date-3/14/2000

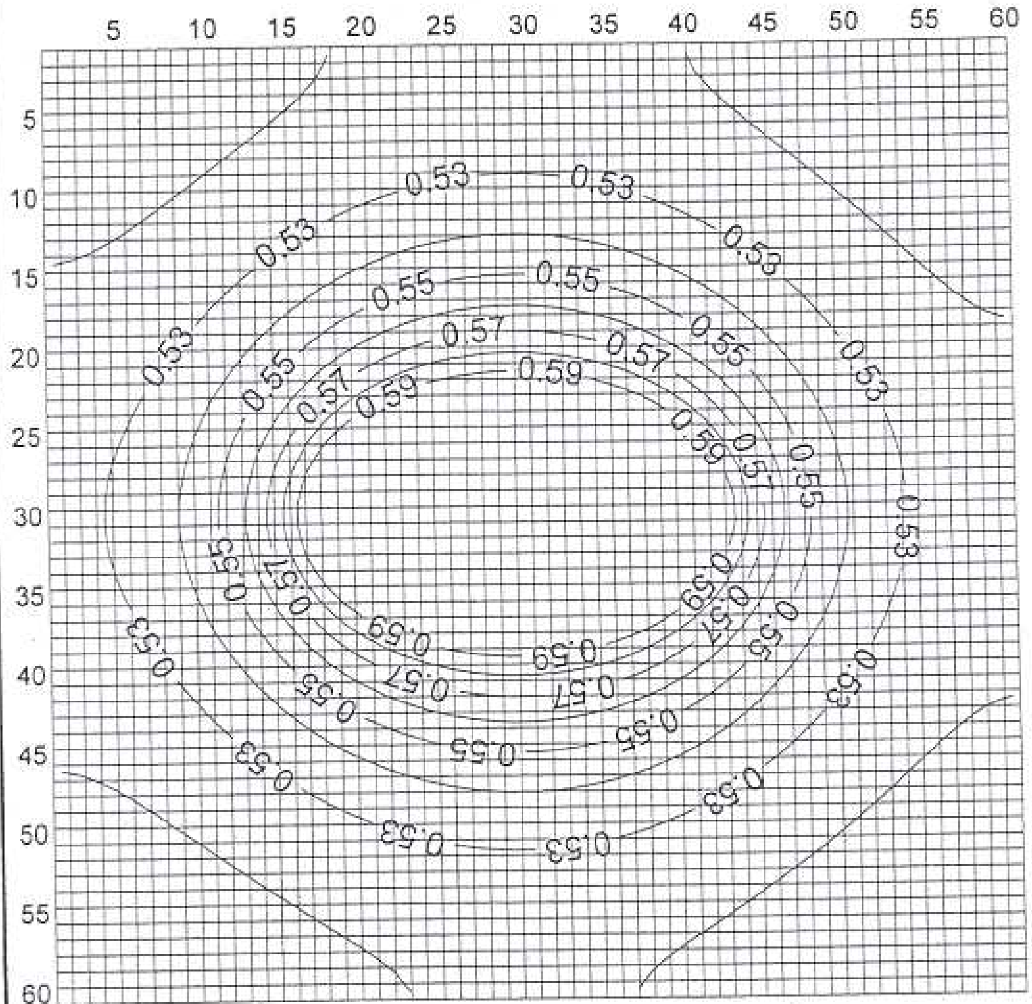

Figure D.74 Water saturation contours in plan view for SCLA2

Simulation-SCLA3-Sandy Clay Loam soil with ET domain type A
Time -90 days after beginning of simulation
Date-4/13/2000

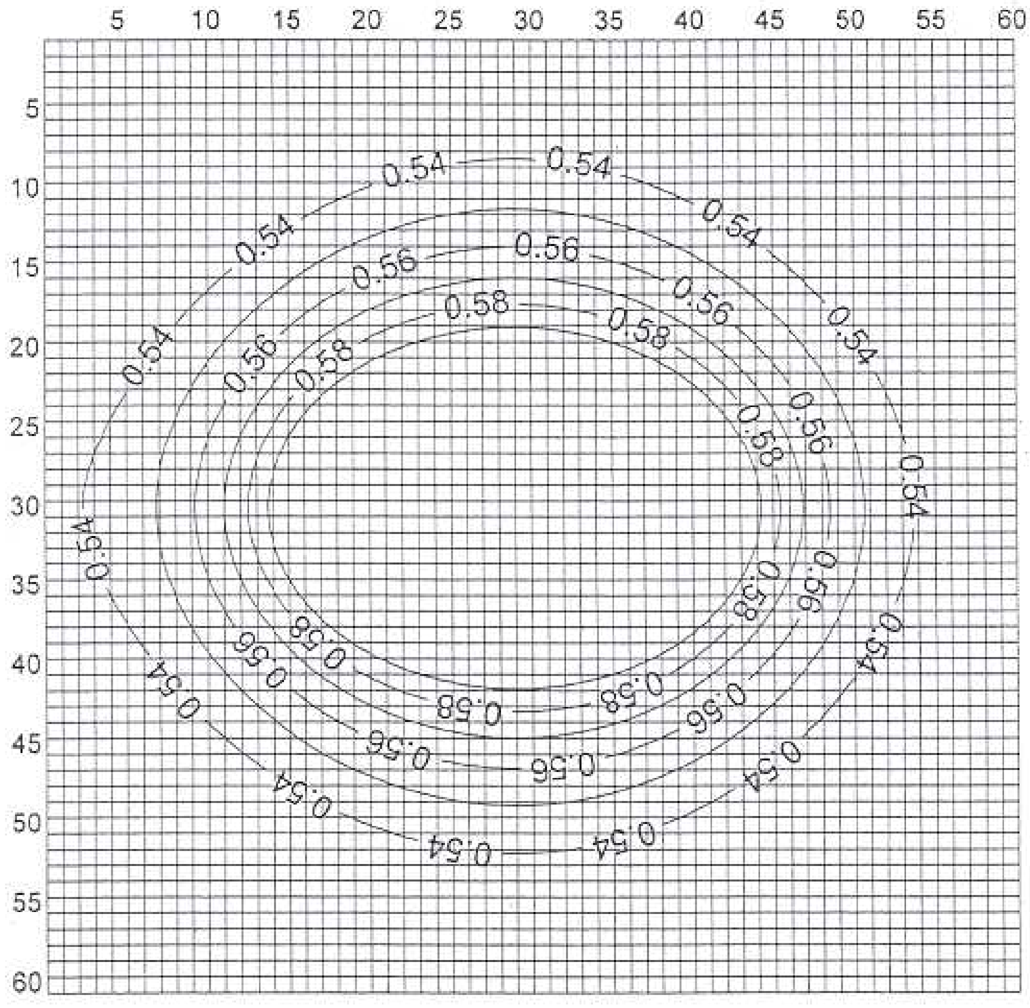

Figure D.75 Water saturation contours in plan view for SCLA3

Simulation-SCLA4-Sandy Clay Loam soil with ET domain type A
Time -120 days after beginning of simulation
Date-5/13/2000

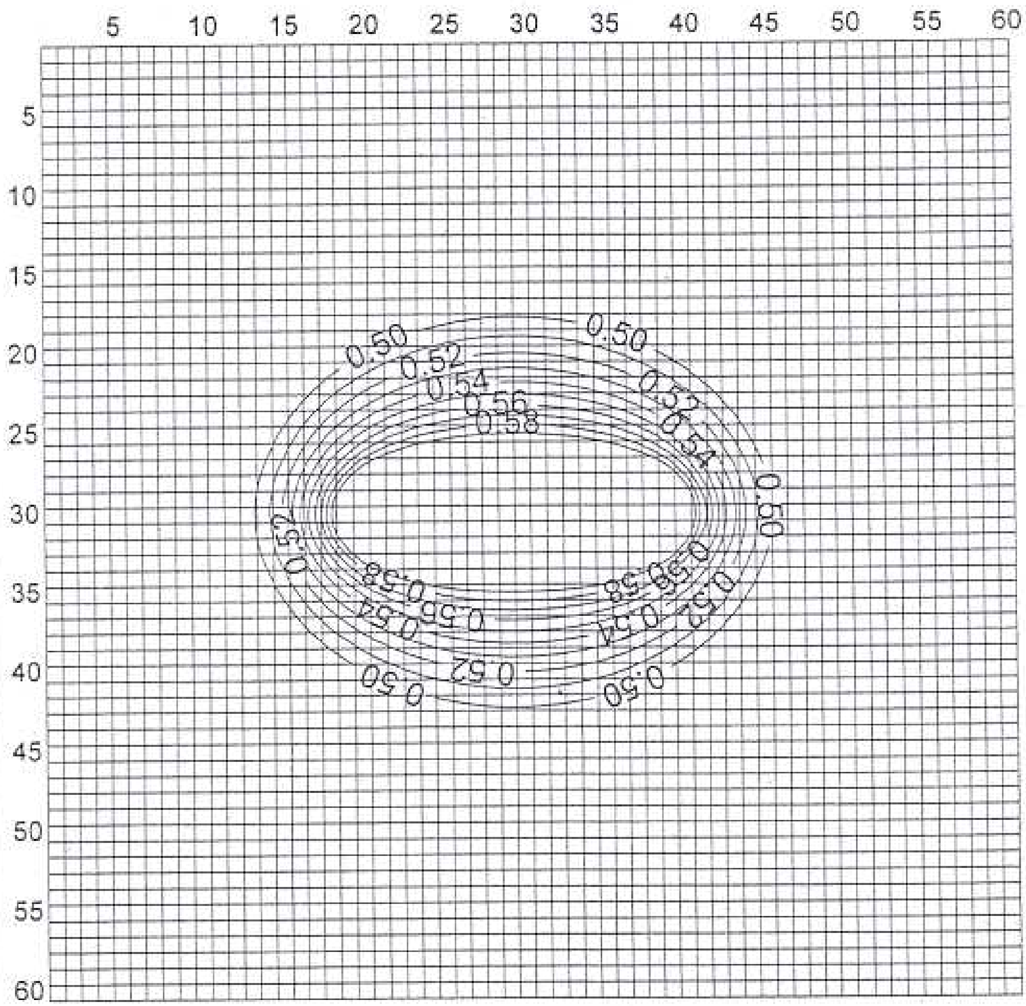

Figure D.76 Water saturation contours in plan view for SCLA4

Simulation-SCLA5-Sandy Clay Loam soil with ET domain type A
Time -150 days after beginning of simulation
Date-6/12//2000

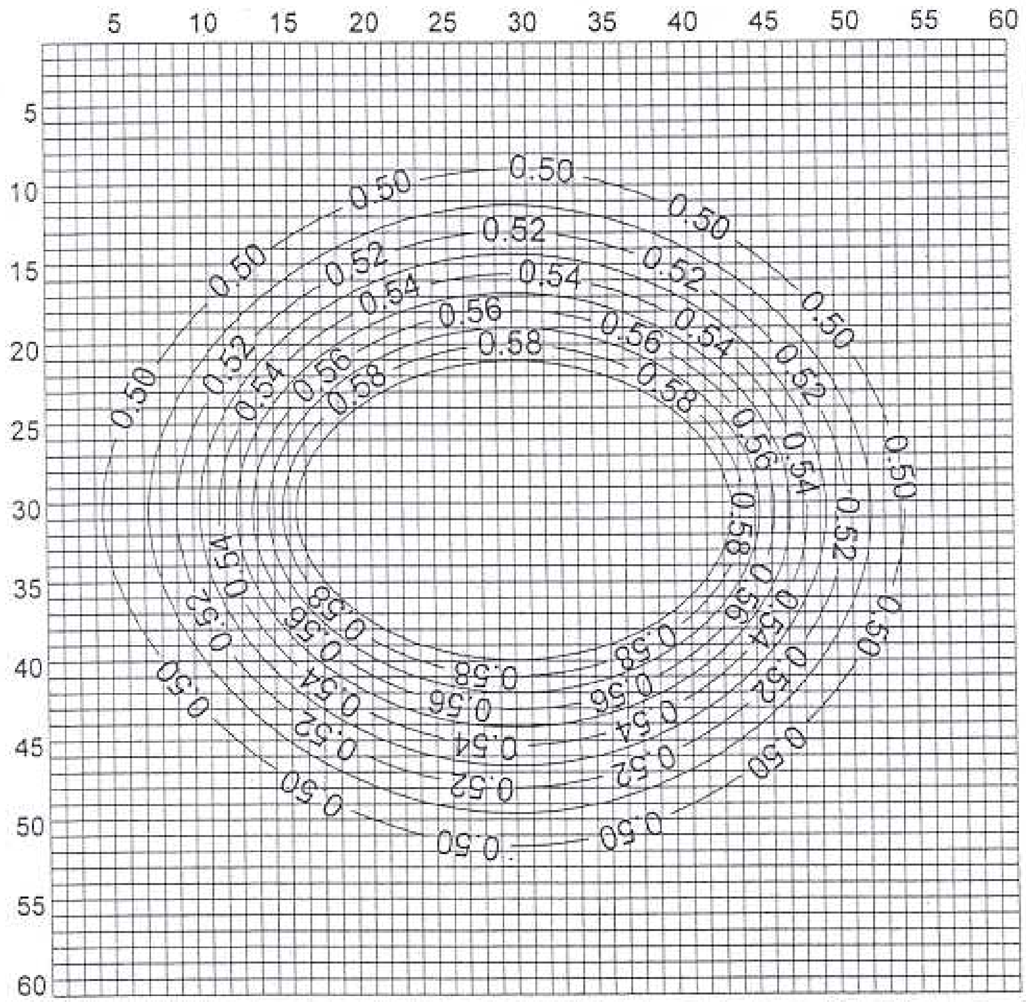

Figure D.77 Water saturation contours in plan view for SCLA5

Simulation-SCLA6-Sandy Clay Loam soil with ET domain type A
Time -180 days after beginning of simulation
Date-7/12/2000

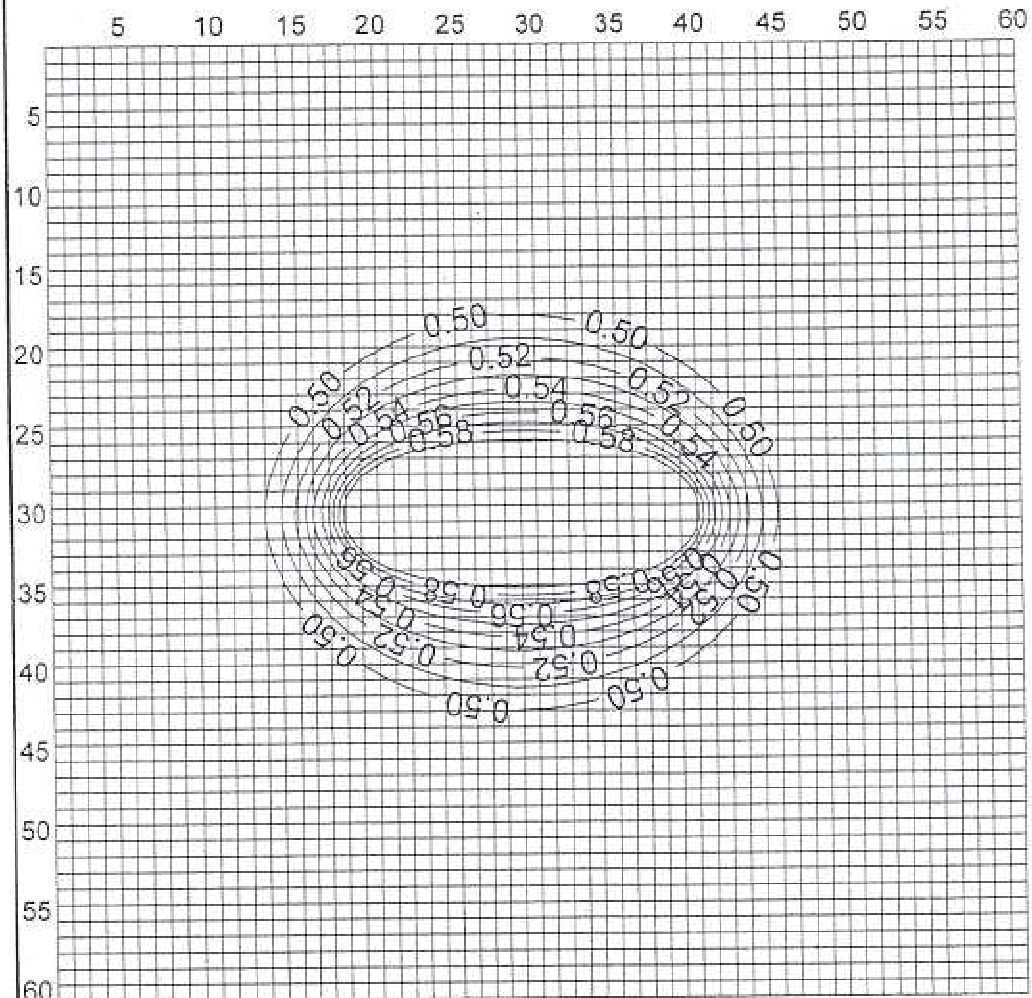

Figure D.78 Water saturation contours in plan view for SCLA6

Simulation-SCLA7-Sandy Clay Loam soil with ET domain type A
Time -210 days after beginning of simulation
Date-8/11/2000

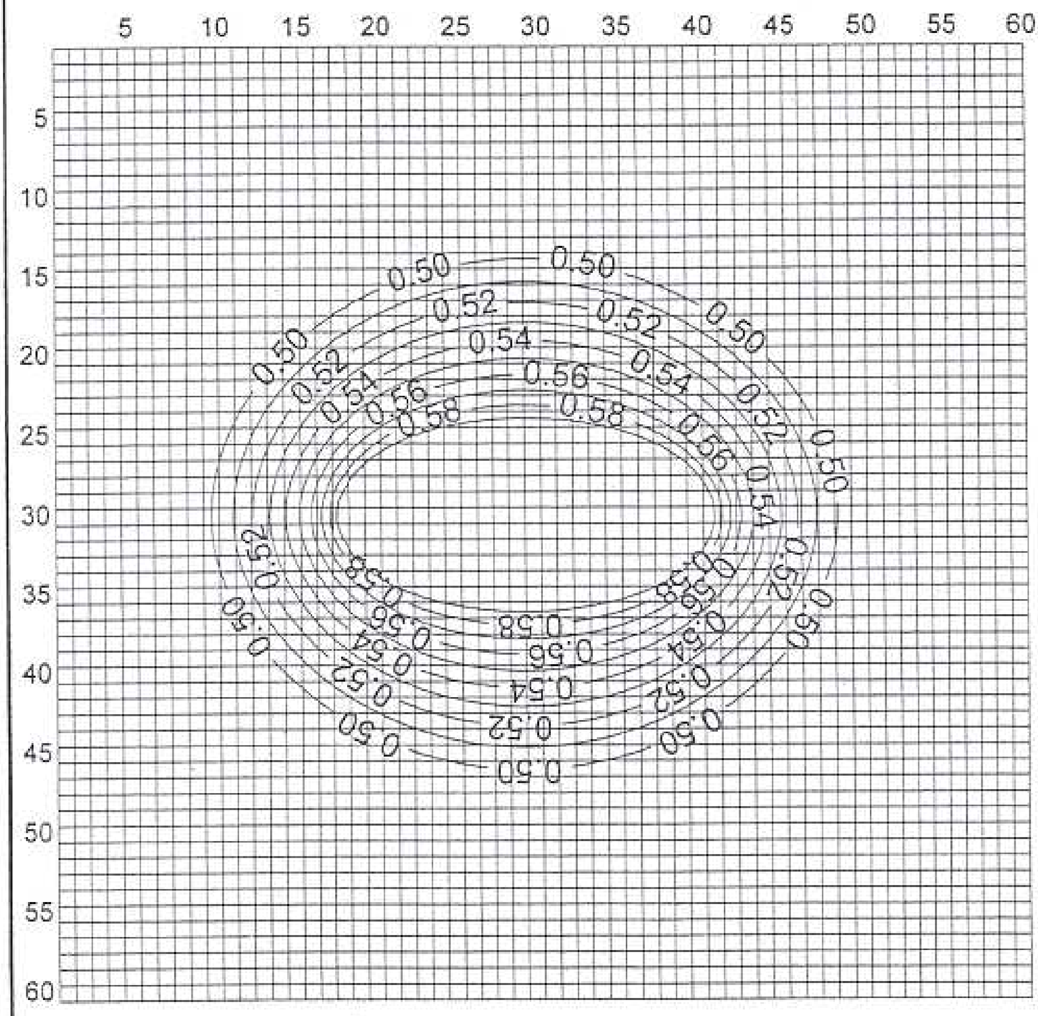

Figure D.79 Water saturation contours in plan view for SCLA7

Simulation-SCLA8-Sandy Clay Loam soil with ET domain type A
Time -240 days after beginning of simulation
Date-9/10/2000

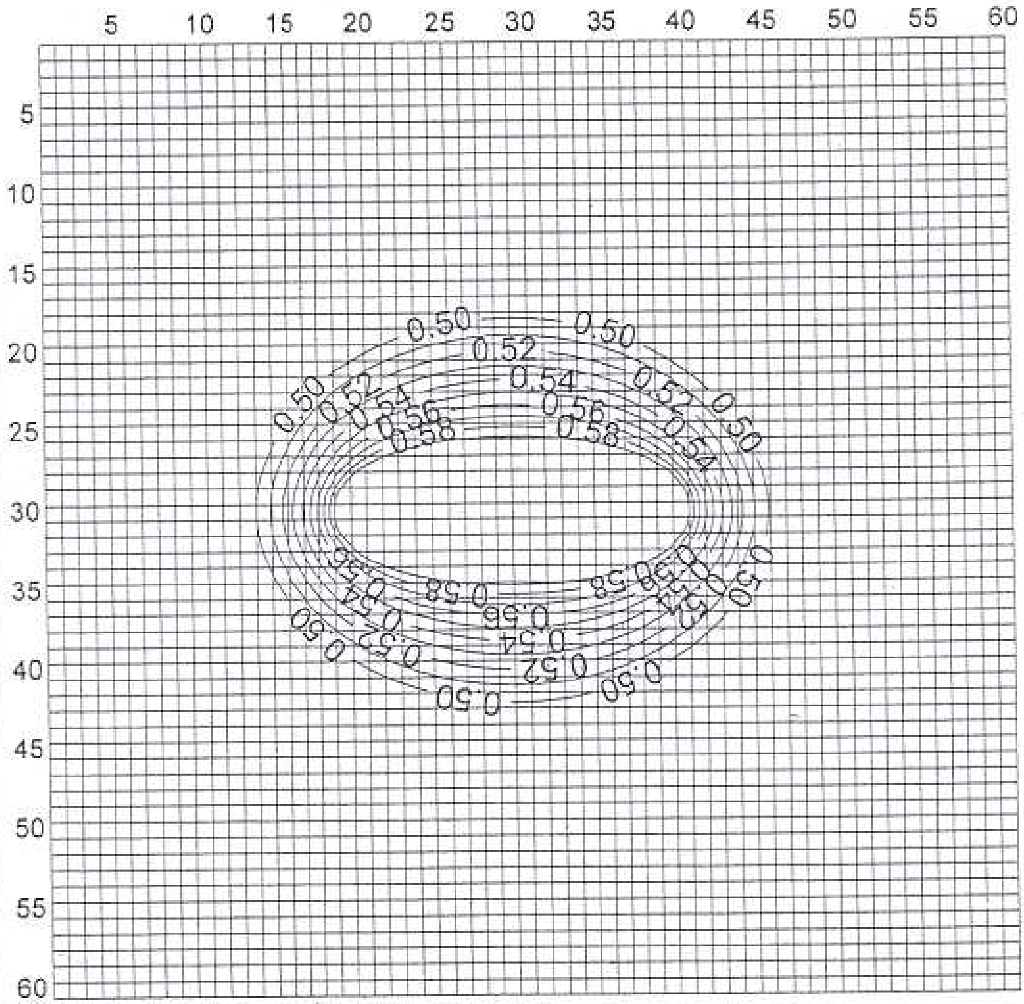

Figure D.80 Water saturation contours in plan view for SCLA8

Simulation-SCLA9-Sandy Clay Loam soil with ET domain type A
Time -270 days after beginning of simulation
Date-10/10/2000

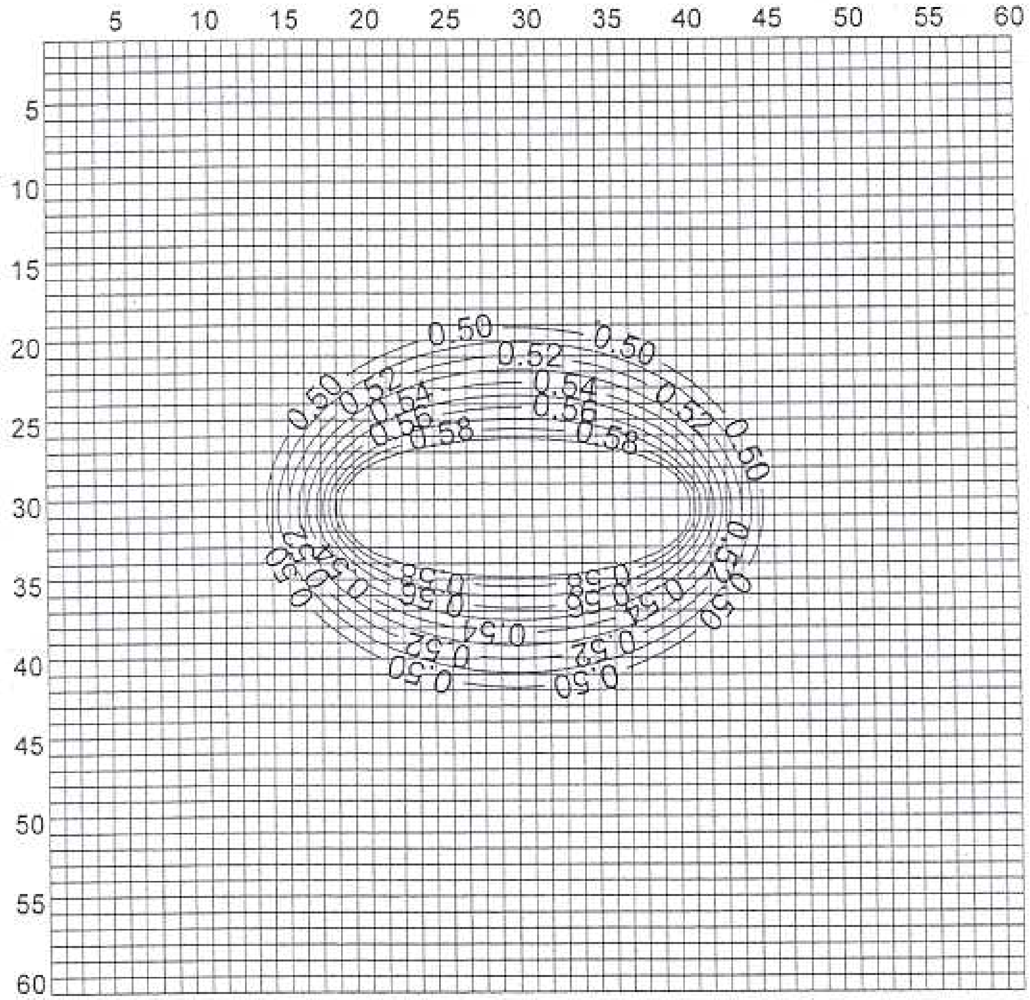

Figure D.81 Water saturation contours in plan view for SCLA9

Simulation-SCLA10-Sandy Clay Loam soil with ET domain type A
Time -300 days after beginning of simulation
Date-11/9/2000

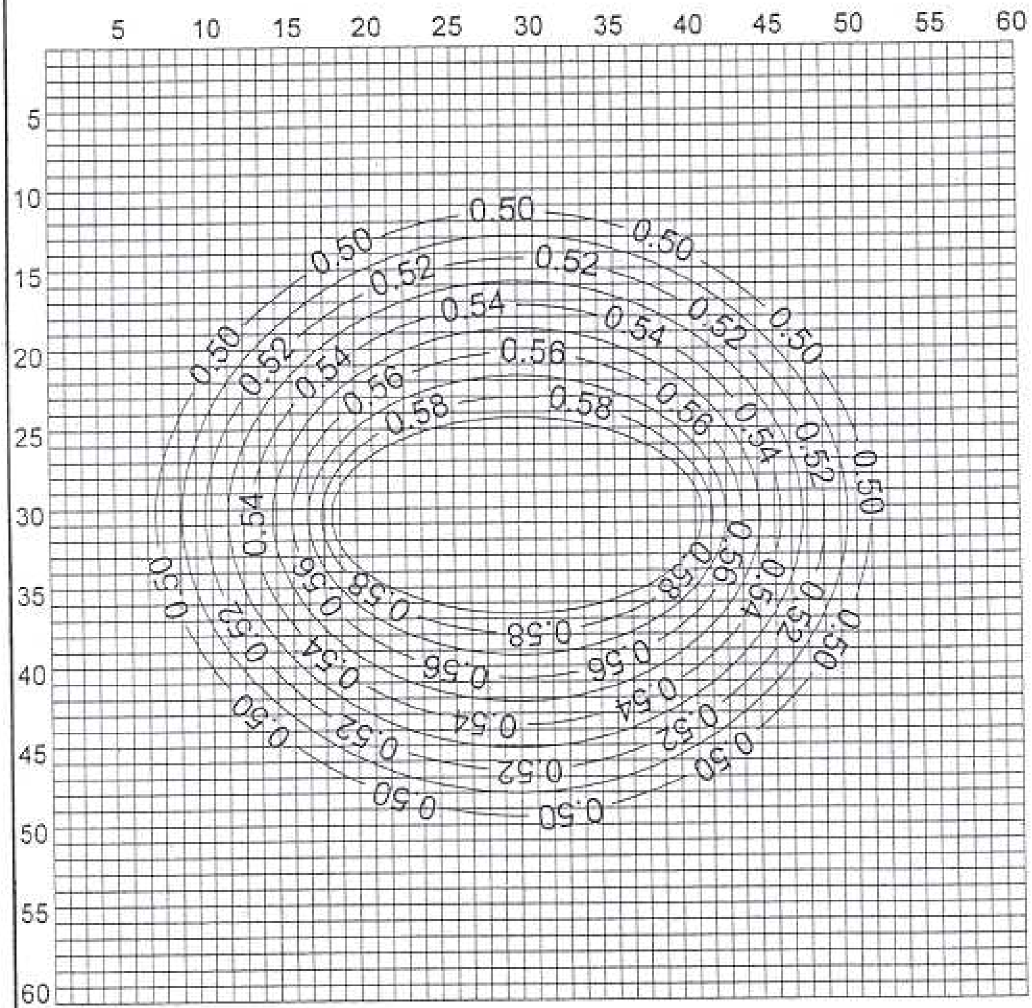

Figure D.82 Water saturation contours in plan view for SCLA10

Simulation-SCLA11-Sandy Clay Loam soil with ET domain type A
Time -330 days after beginning of simulation
Date-12/9/2000

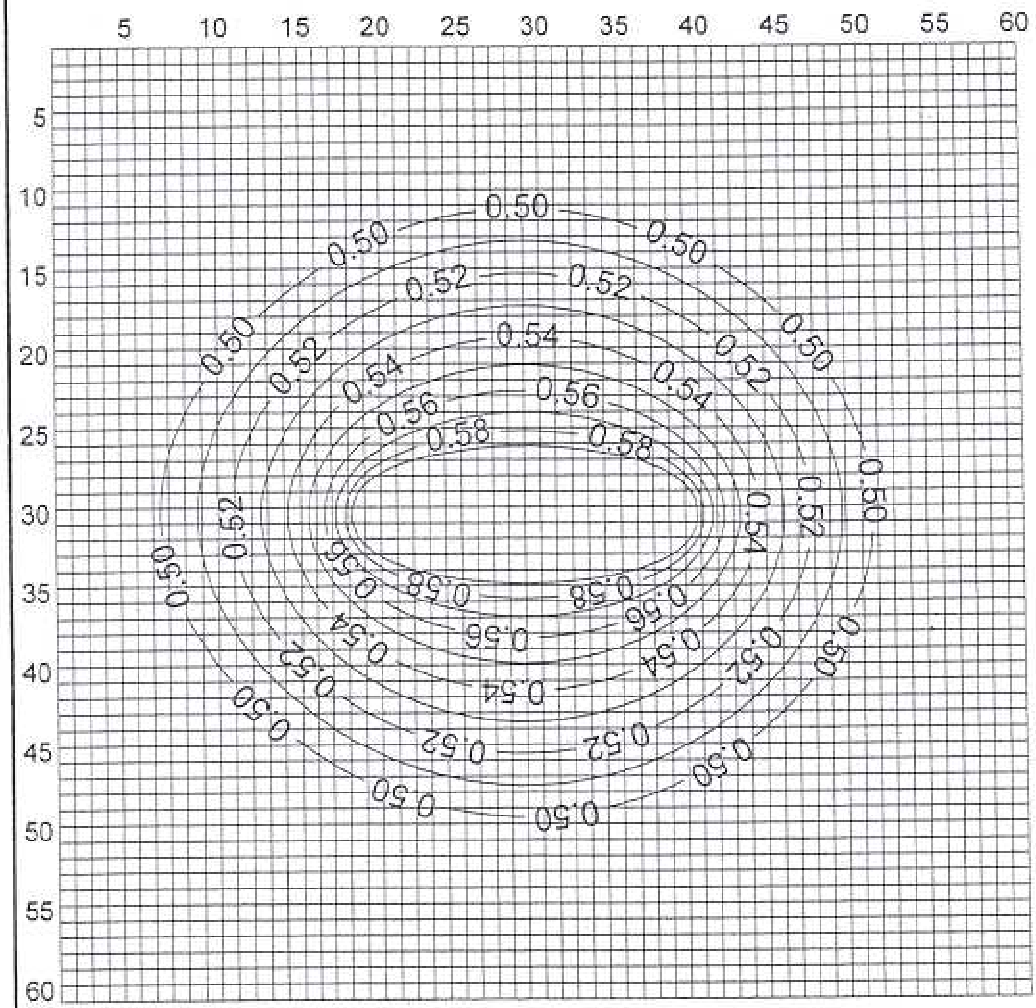

Figure D.83 Water saturation contours in plan view for SCLA11

Simulation-SCLA12-Sandy Clay Loam soil with ET domain type A
Time -352 days after beginning of simulation
Date-12/31/2000

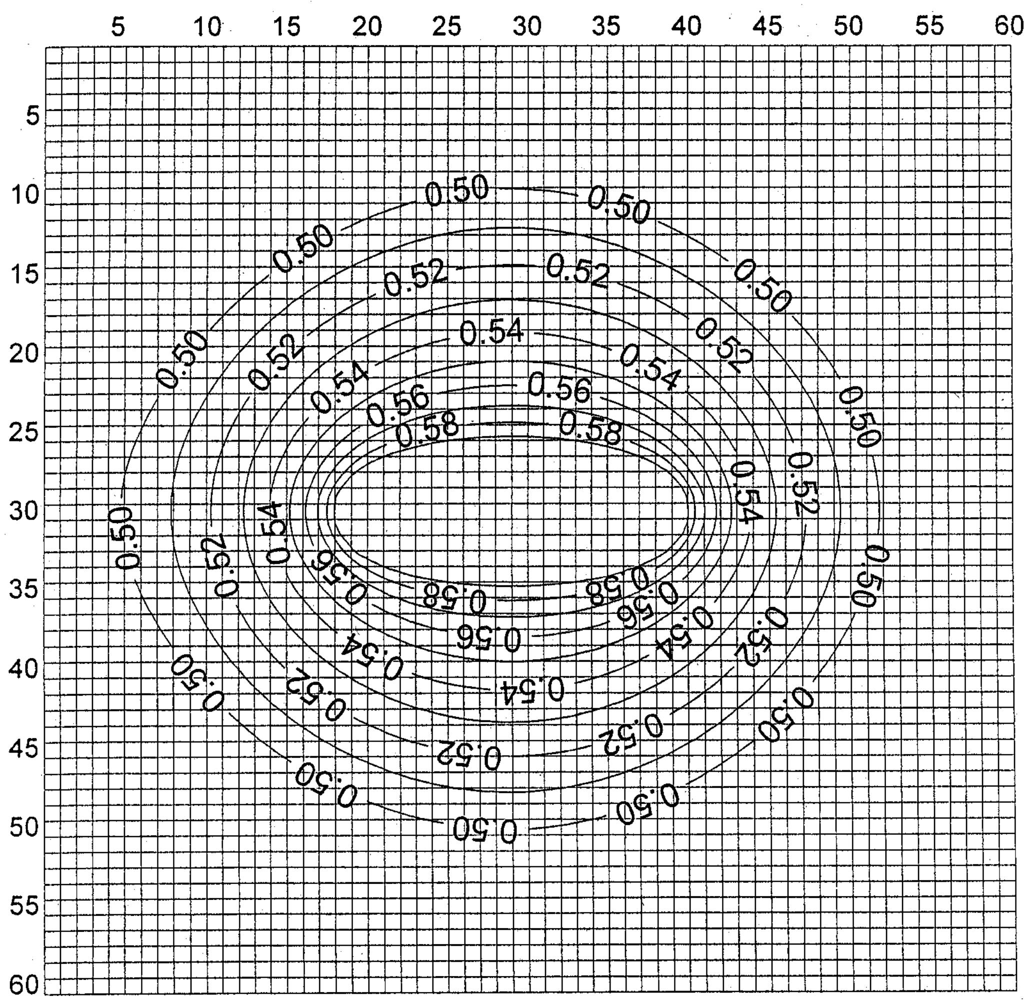

Figure D.84 Water saturation contours in plan view for SCLA12

Simulation-SLCA1-Sandy Clay Loam soil with ET domain type A
Time -30 days after beginning of simulation
Date-2/13/2000

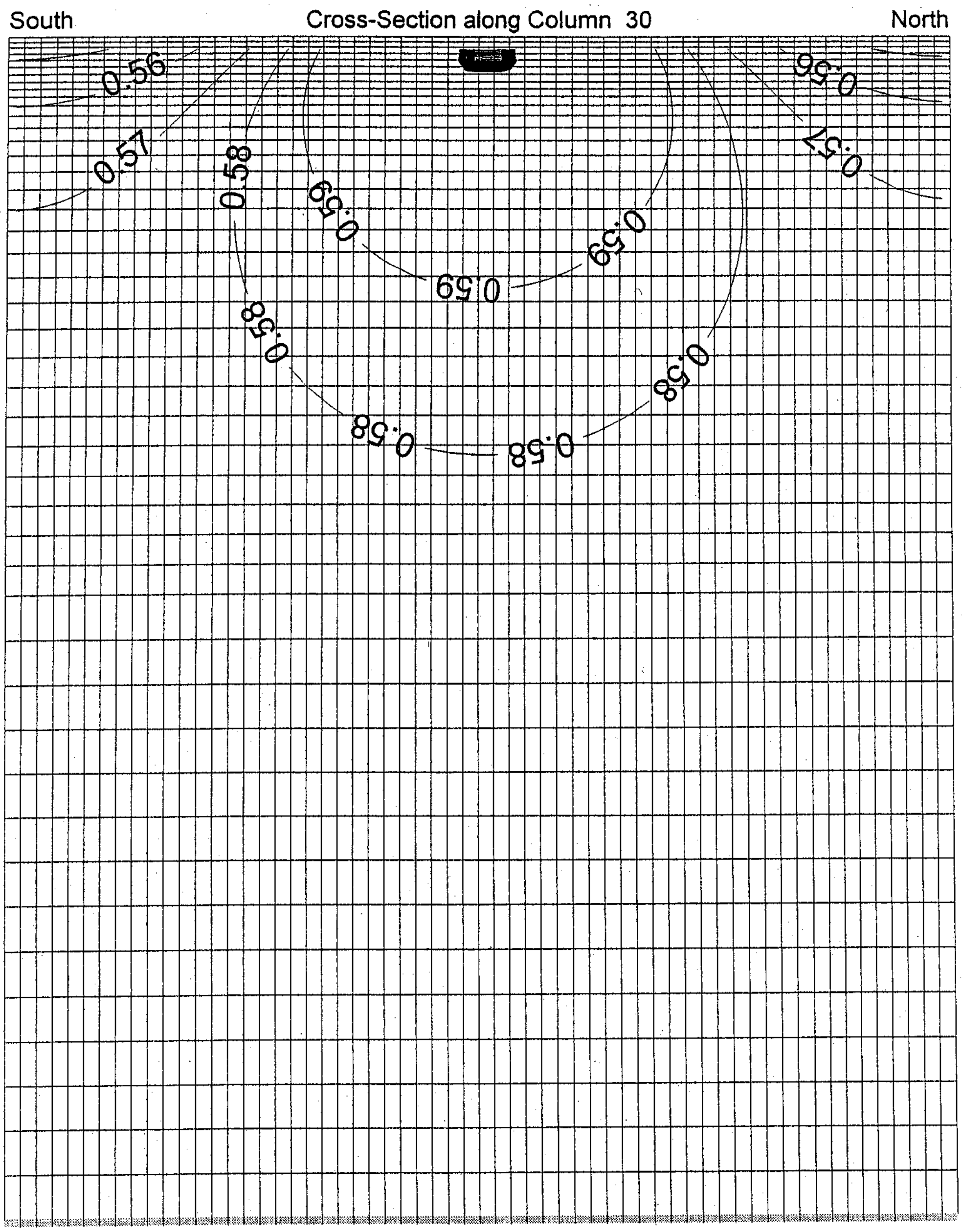

Figure D.85 Water saturation contours in cross-section for SCLA1

Simulation-SCLA2-Sandy Clay Loam soil with ET domain type A
Time -60 days after beginning of simulation
Date-3/14/2000

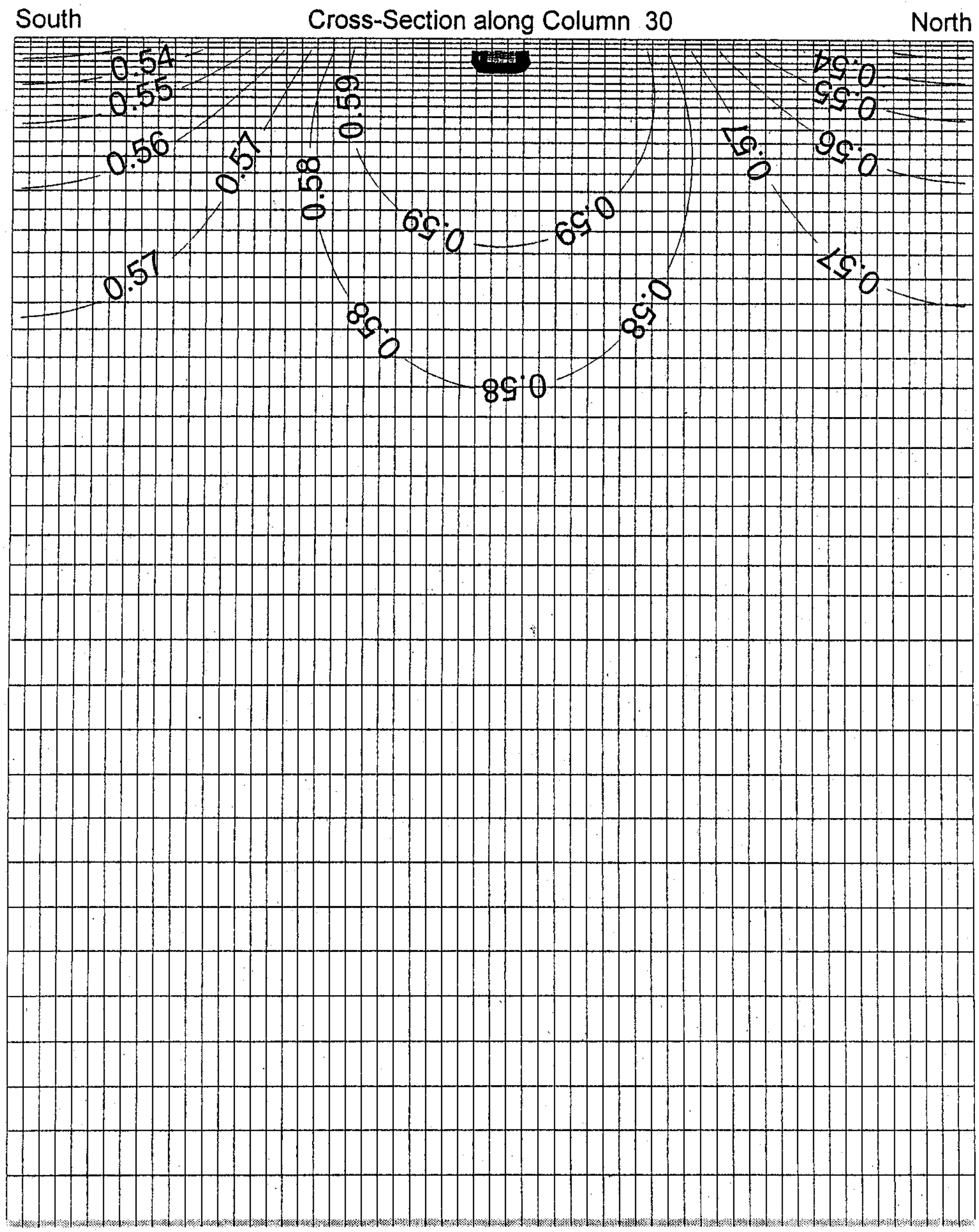

Figure D.86 Water saturation contours in cross-section for SCLA2

Simulation-SCLA3-Sandy Clay Loam soil with ET domain type A
Time -90 days after beginning of simulation
Date-4/13/2000

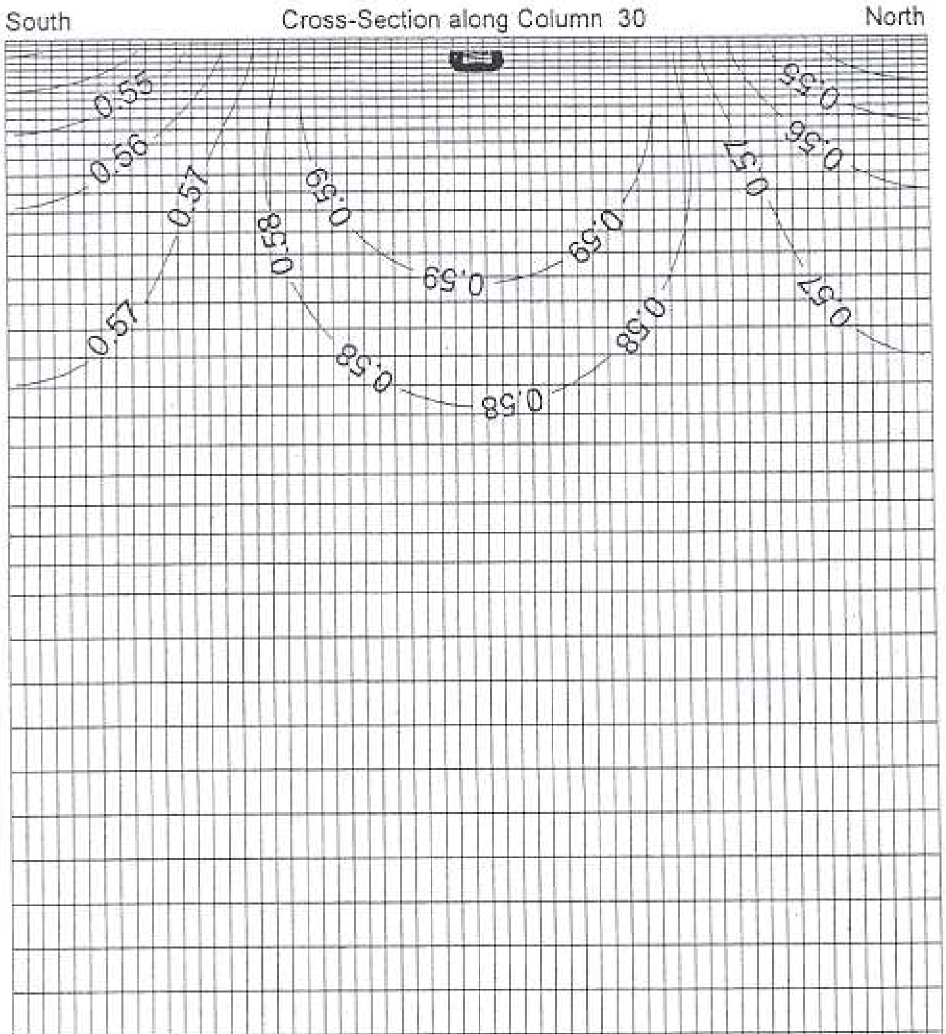

Figure D.87 Water saturation contours in cross-section for SCLA3

Simulation-SCLA4-Sandy Clay Loam soil with ET domain type A
Time -120 days after beginning of simulation
Date-5/13/2000

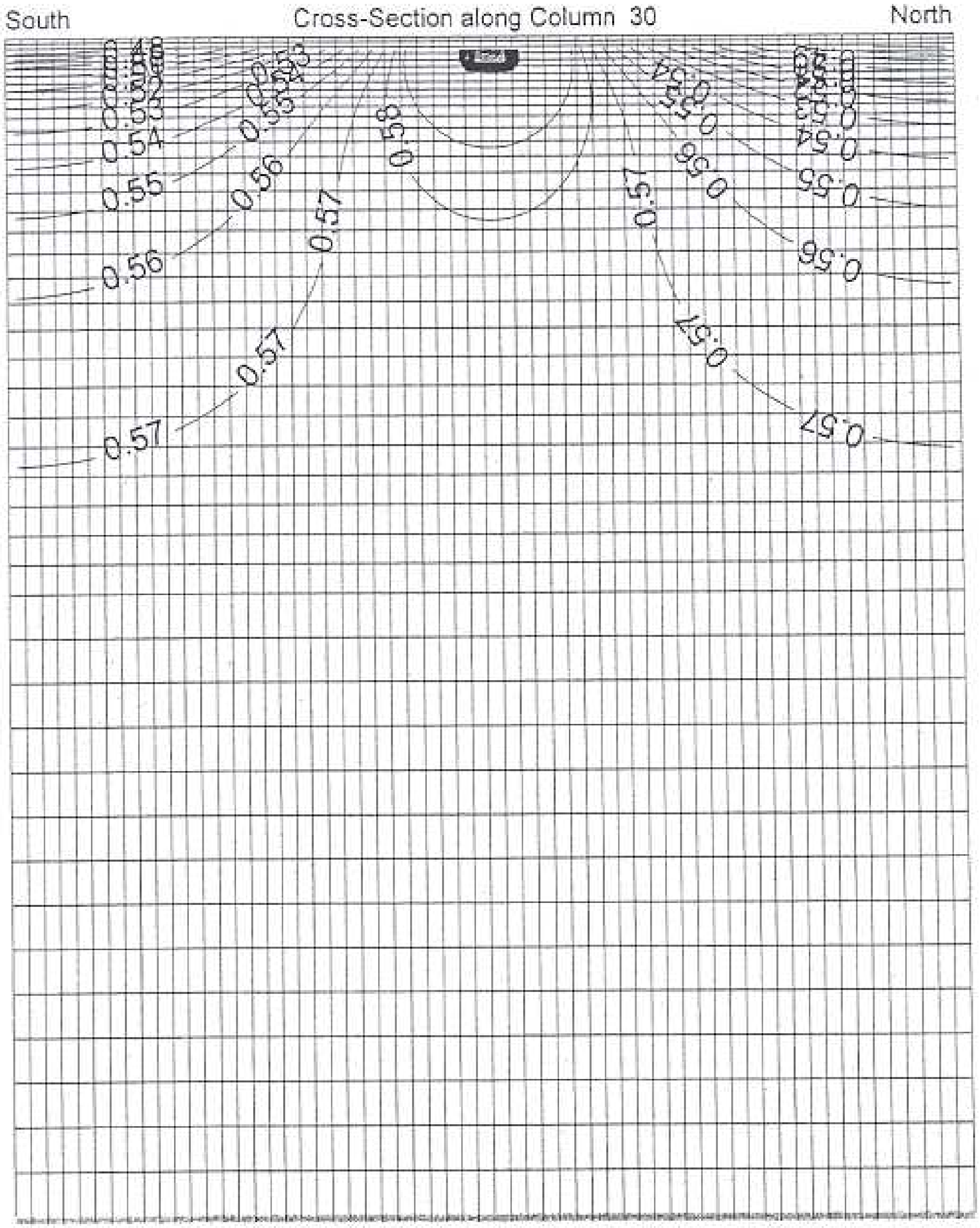

Figure D.88 Water saturation contours in cross-section for SCLA4

Simulation-SCLA5-Sandy Clay Loam soil with ET domain type A
Time -150 days after beginning of simulation
Date-6/12//2000

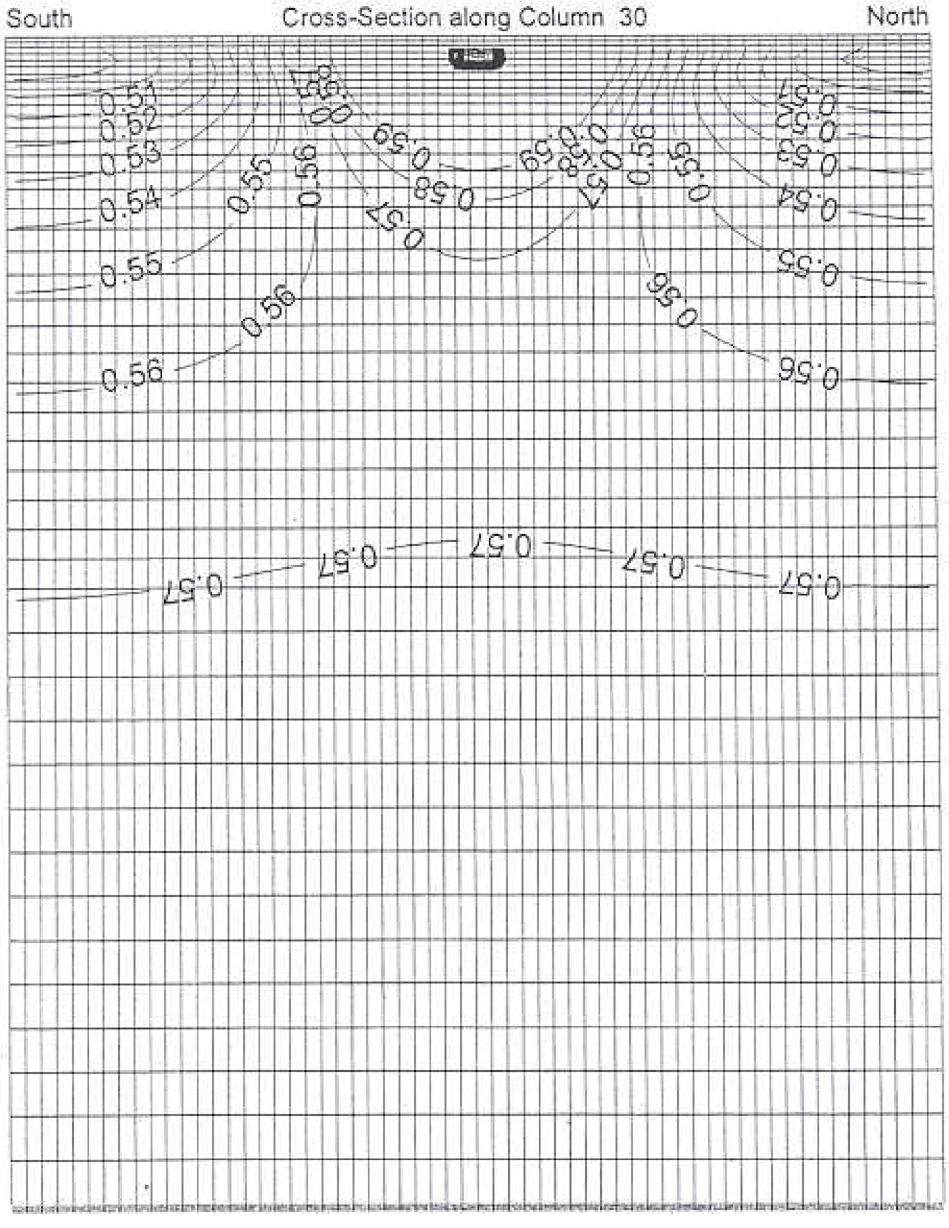

Figure D.89 Water saturation contours in cross-section for SCLA5

Simulation-SCLA6-Sandy Clay Loam soil with ET domain type A
Time -180 days after beginning of simulation
Date-7/12/2000

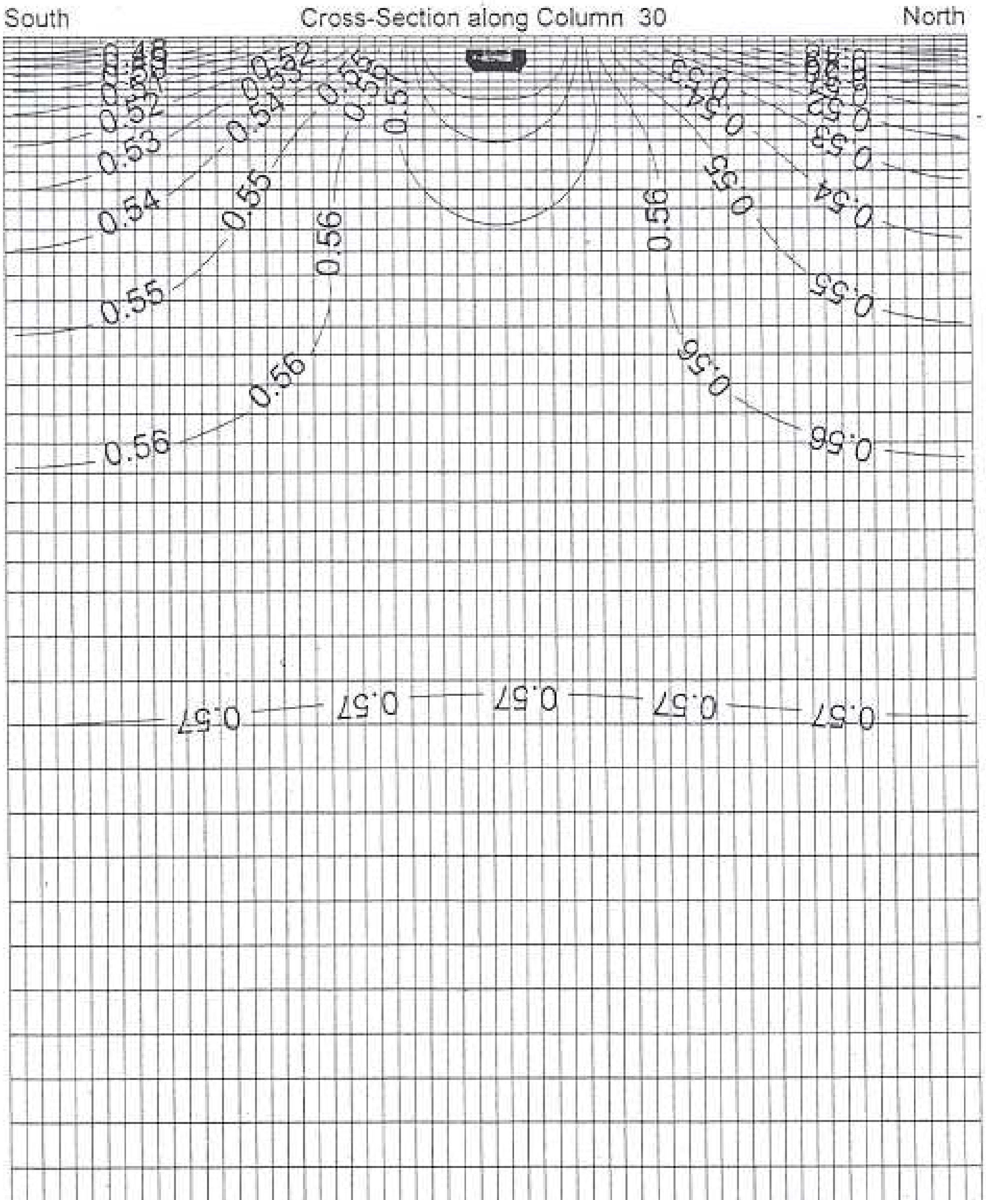

Figure D.90 Water saturation contours in cross-section for SCLA6

Simulation-SCLA7-Sandy Clay Loam soil with ET domain type A
Time -210 days after beginning of simulation
Date-8/11/2000

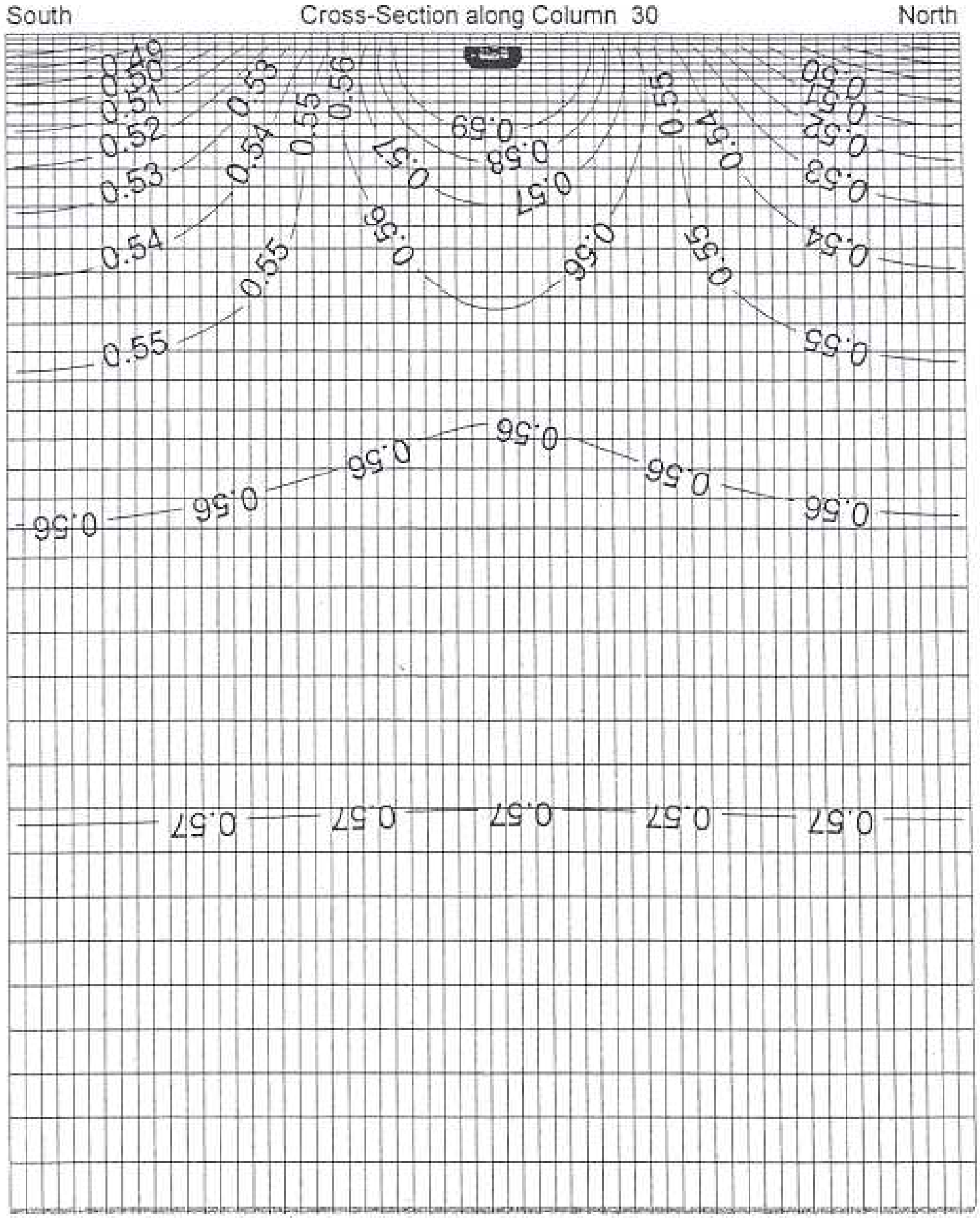

Figure D.91 Water saturation contours in cross-section for SCLA7

Simulation-SCLA8-Sandy Clay Loam soil with ET domain type A
Time -240 days after beginning of simulation
Date-9/10/2000

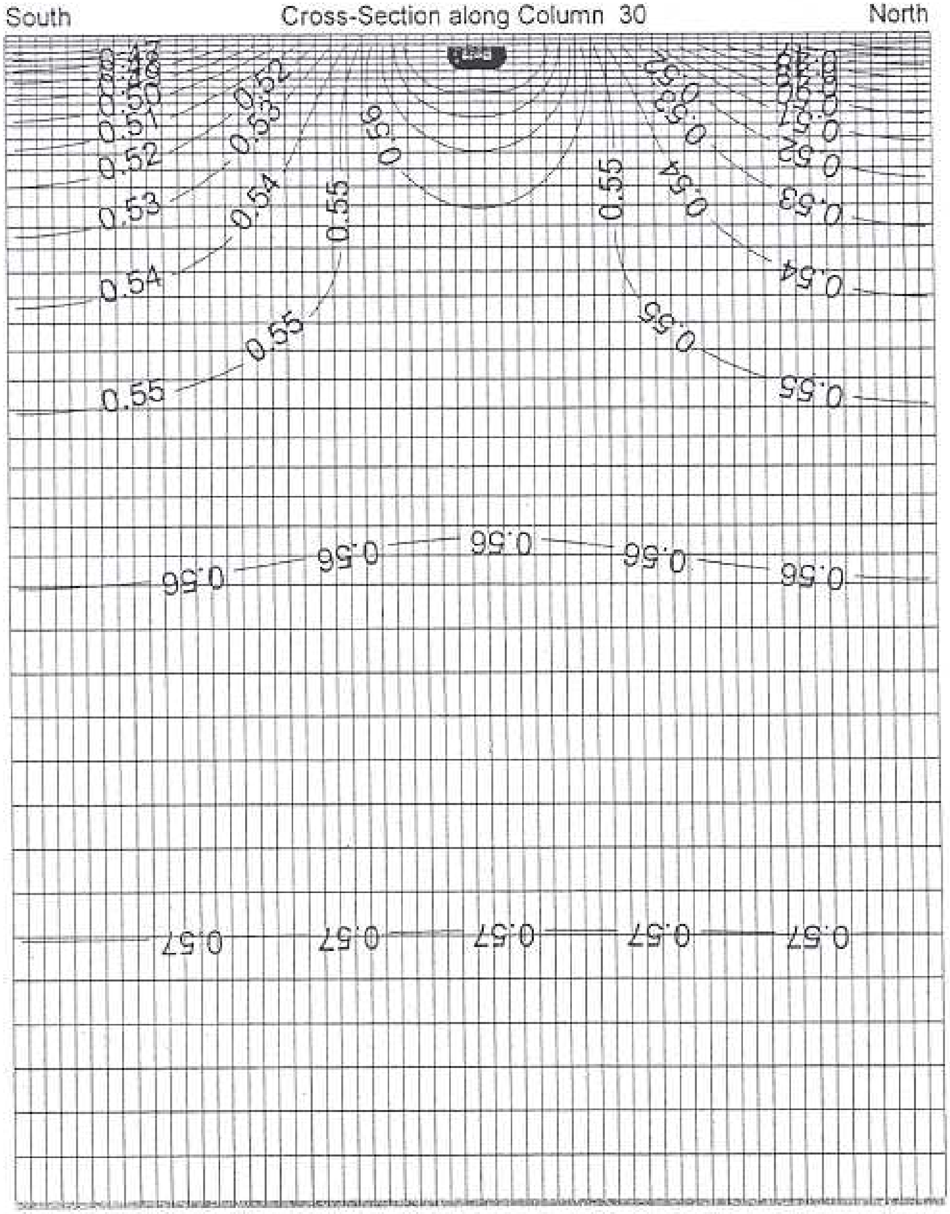

Figure D.92 Water saturation contours in cross-section for SCLA8

Simulation-SCLA9-Sandy Clay Loam soil with ET domain type A
Time -270 days after beginning of simulation
Date-10/10/2000

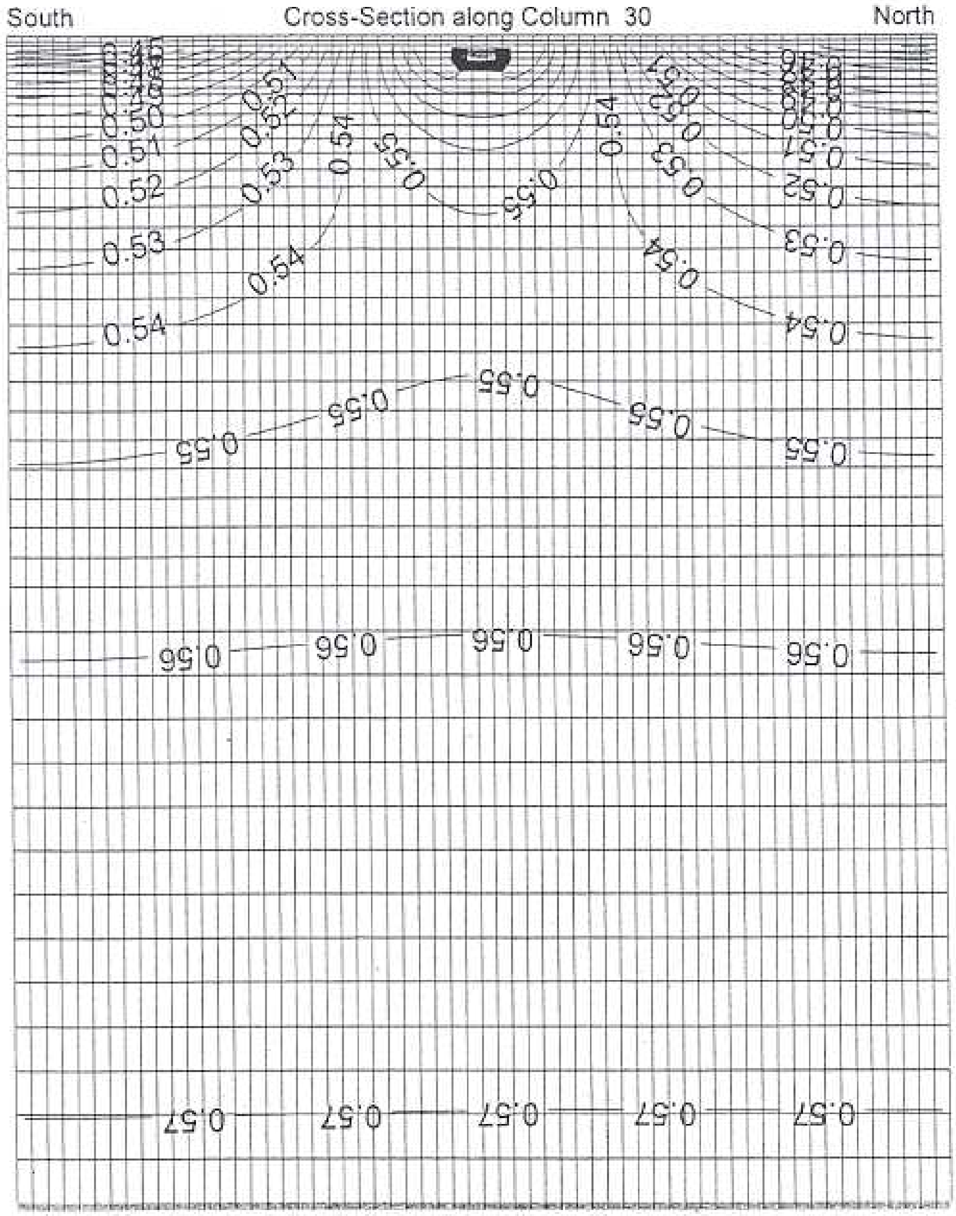

Figure D.93 Water saturation contours in cross-section for SCLA9

Simulation-SCLA10-Sandy Clay Loam soil with ET domain type A
Time -300 days after beginning of simulation
Date-11/9/2000

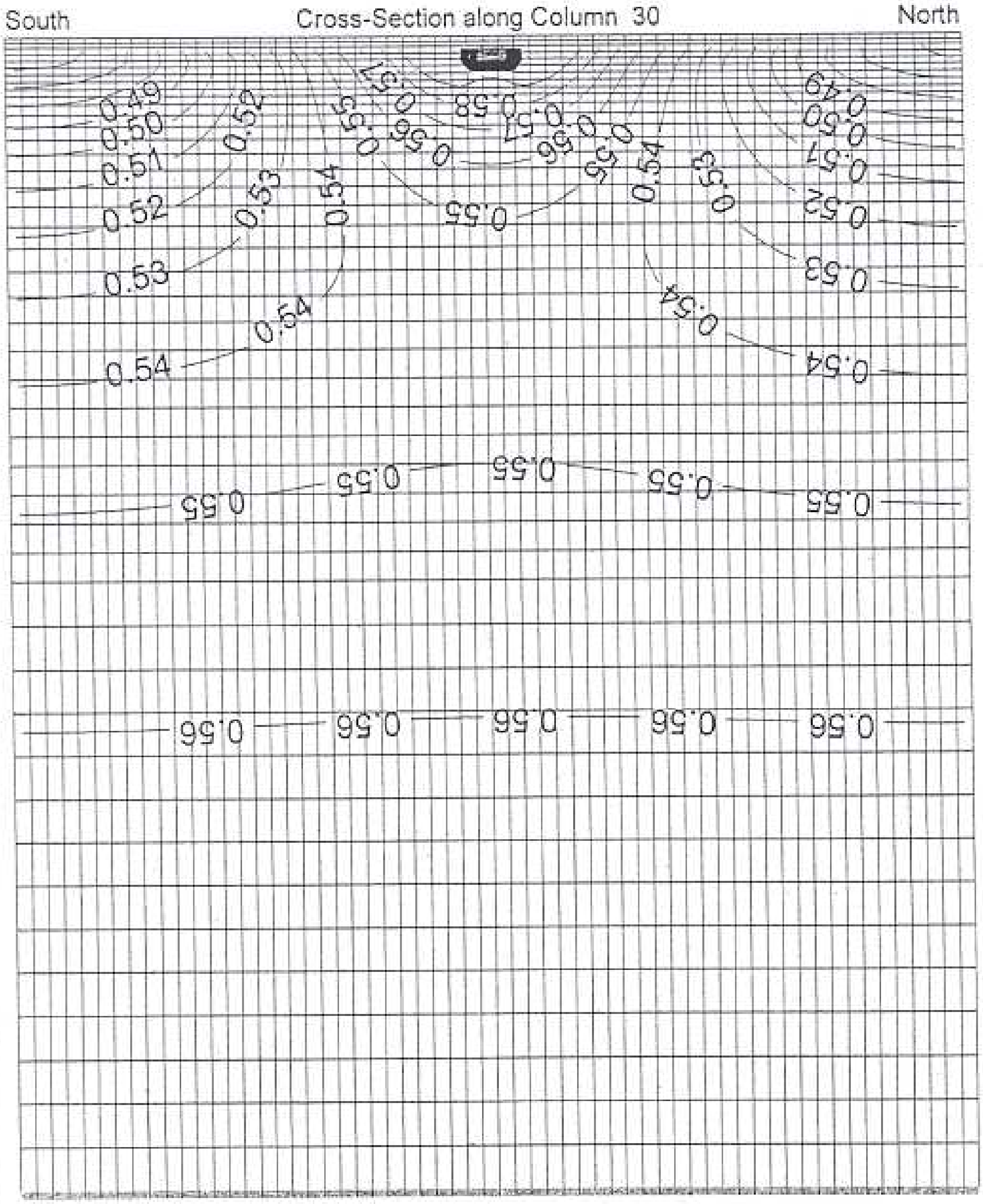

Figure D.94 Water saturation contours in cross-section for SCLA10

Simulation-SCLA11-Sandy Clay Loam soil with ET domain type A
Time -330 days after beginning of simulation
Date-12/9/2000

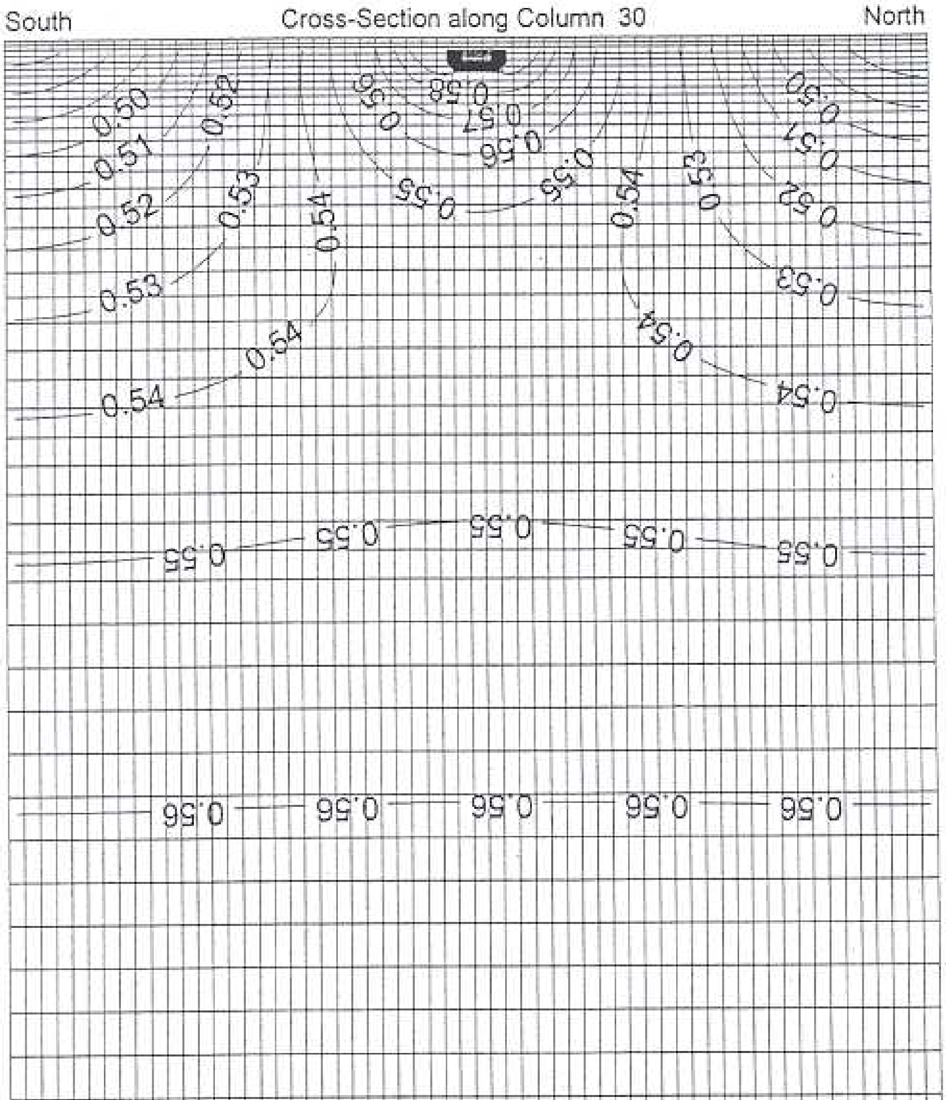

Figure D.95 Water saturation contours in cross-section for SCLA11

Simulation-SCLA12-Sandy Clay Loam soil with ET domain type A
Time -352 days after beginning of simulation
Date-12/31/2000

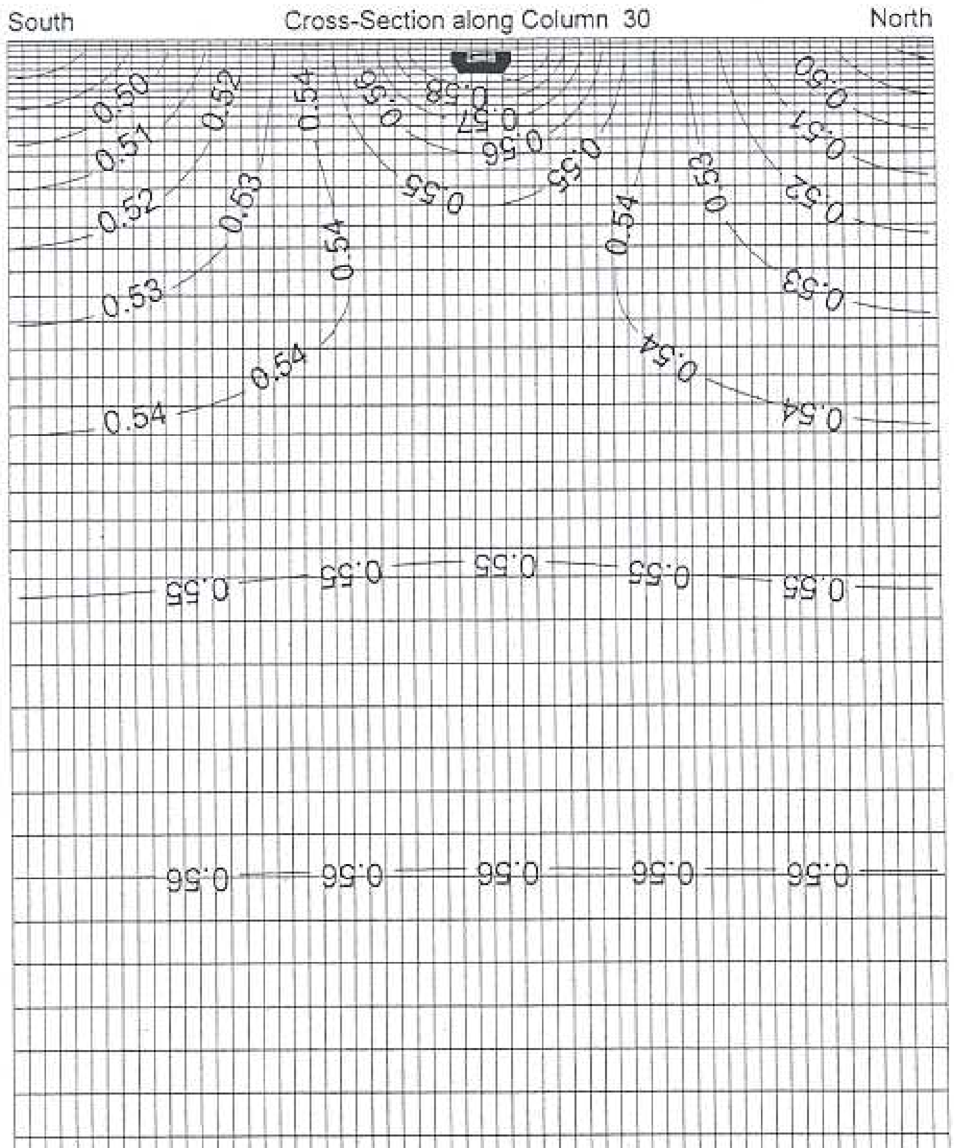

Figure D.96 Water saturation contours in cross-section for SCLA12

Simulation-SCLA1-Sandy Clay Loam soil with ET domain type A
Time -30 days after beginning of simulation
Date-2/13/2000

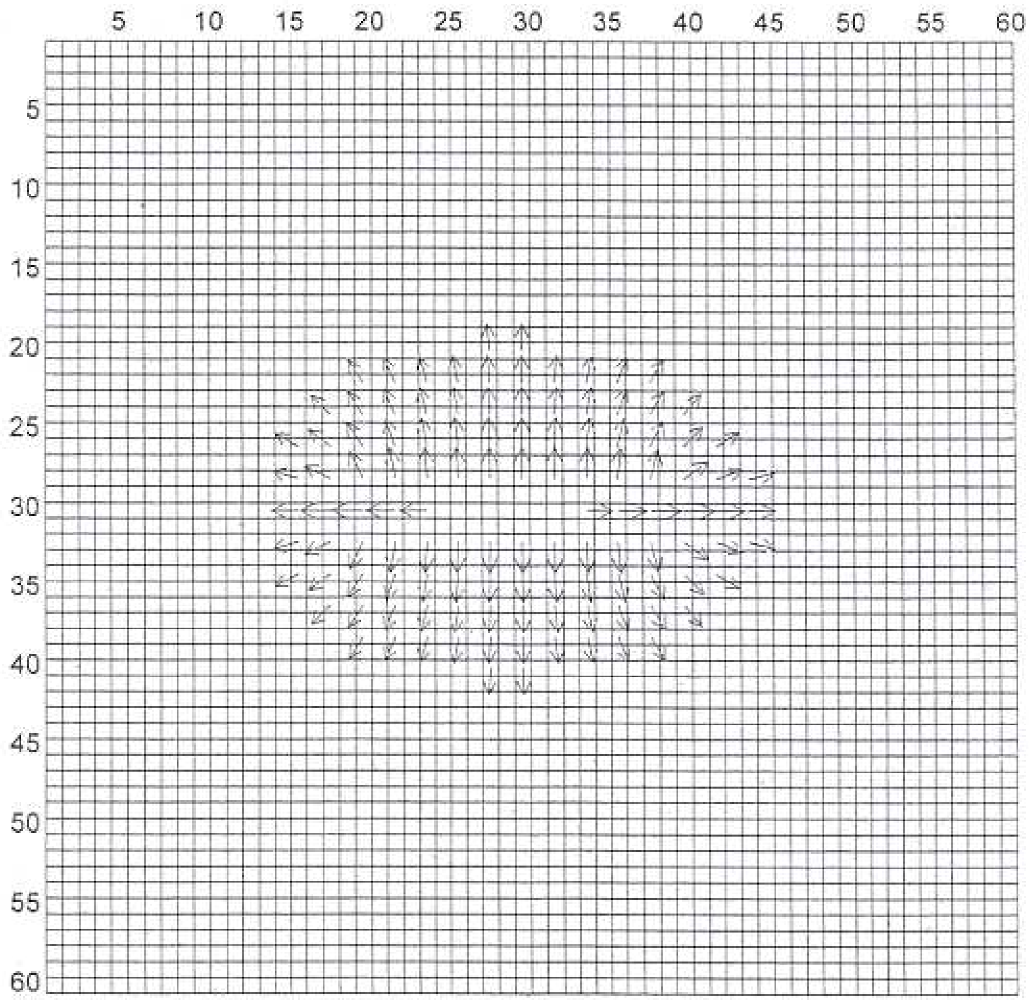

Figure D.97 Moisture movement vectors in plan view for SCLA1

Simulation-SCLA4-Sandy Clay Loam soil with ET domain type A
Time -120 days after beginning of simulation
Date-5/13/2000

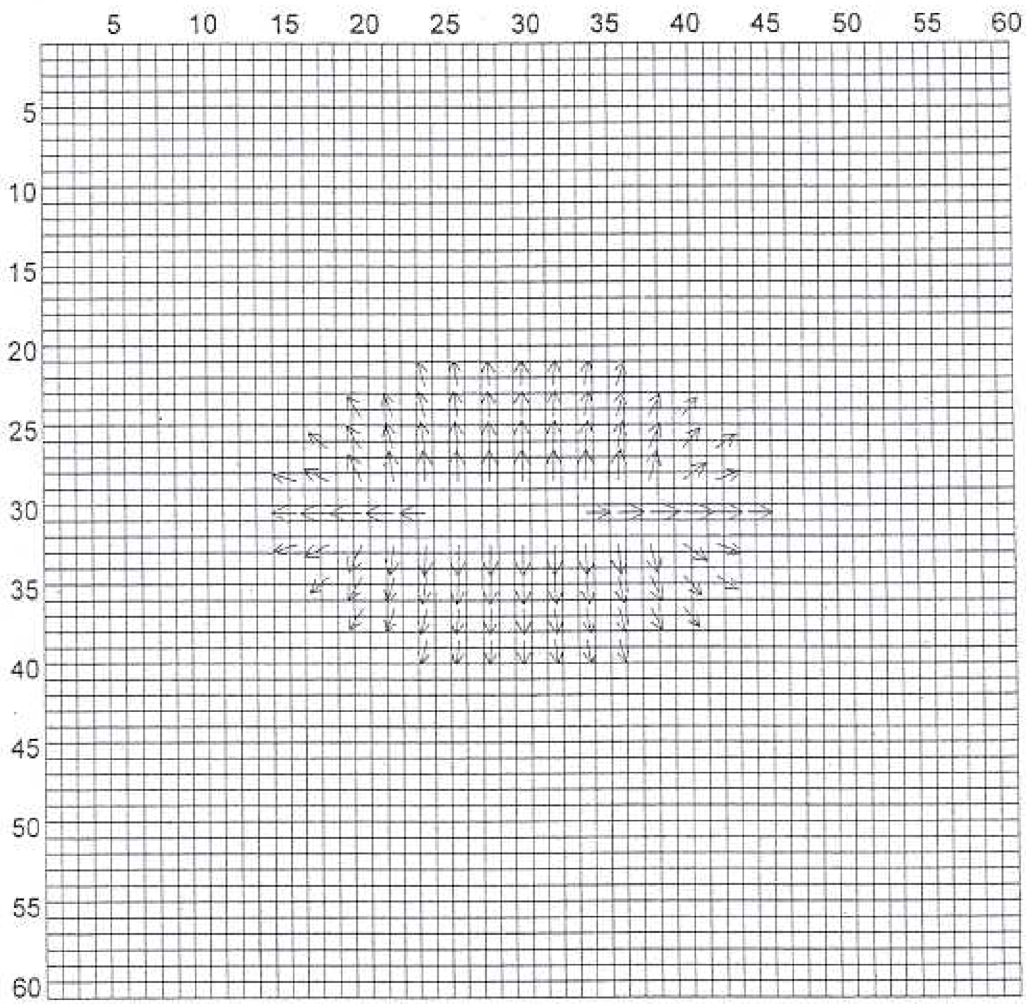

Figure D.98 Moisture movement vectors in plan view for SCLA4

Simulation-SCLA8-Sandy Clay Loam soil with ET domain type A
Time -240 days after beginning of simulation
Date-9/10/2000

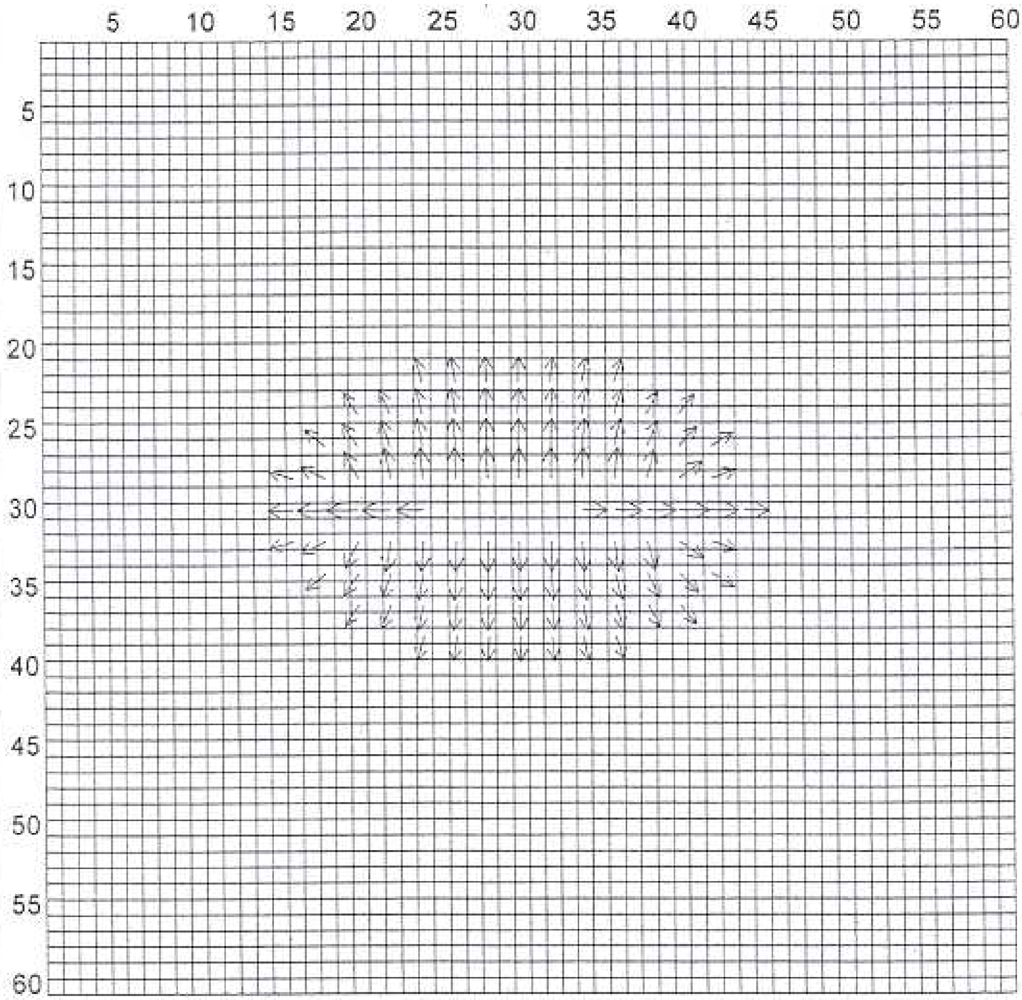

Figure D.99 Moisture movement vectors in plan view for SCLA8

Simulation-SCLA12-Sandy Clay Loam soil with ET domain type A
Time -352 days after beginning of simulation
Date-12/31/2000

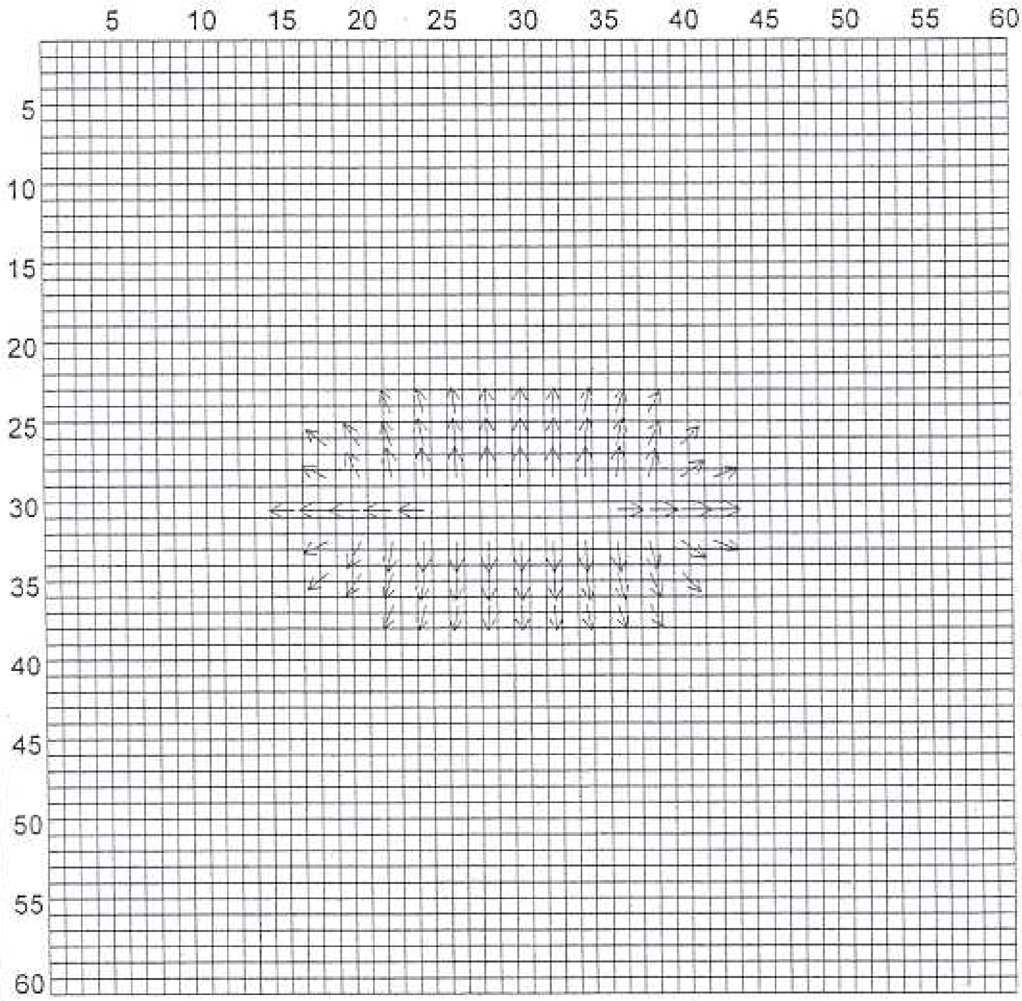

Figure D.100 Moisture movement vectors in plan view for SCLA12

Simulation-SCLA1-Sandy Clay Loam soil with ET domain type A
Time -30 days after beginning of simulation
Date-2/13/2000

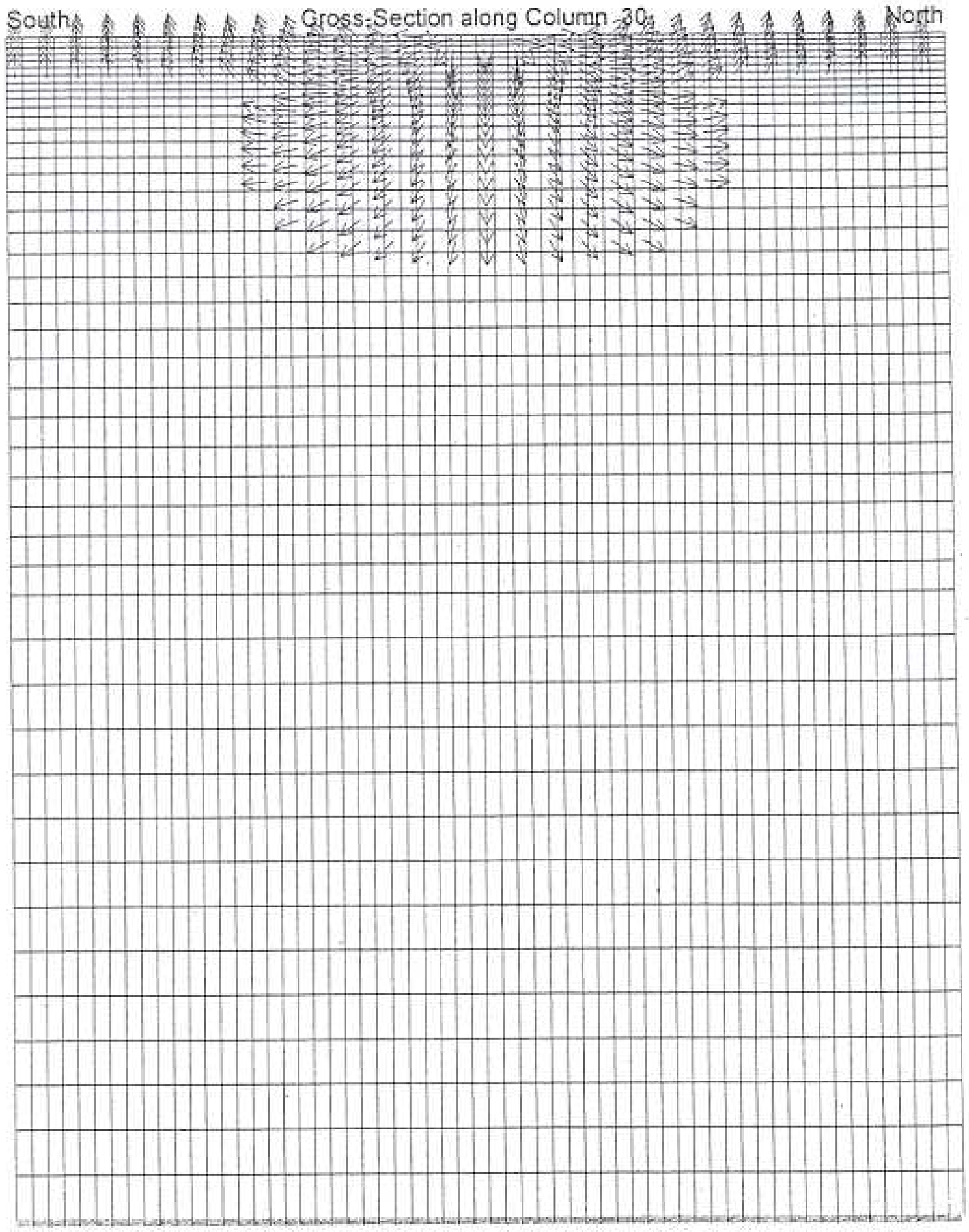

Figure D.101 Moisture movement vectors along C-30 for SCLA1

Simulation-SCLA4-Sandy Clay Loam soil with ET domain type A
Time -120 days after beginning of simulation
Date-5/13/2000

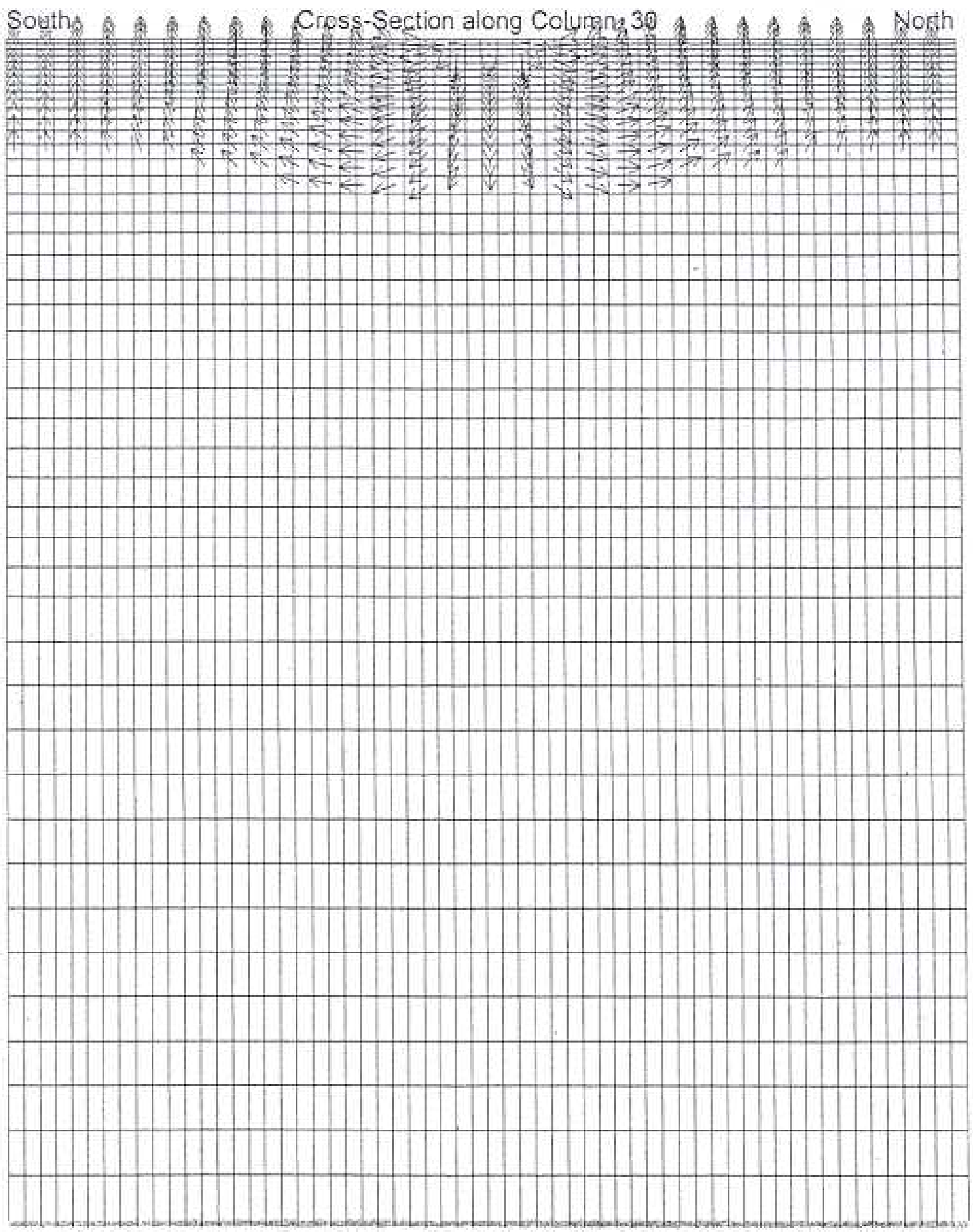

Figure D.102 Moisture movement vectors along C-30 for SCLA4

Simulation-SCLA8-Sandy Clay Loam soil with ET domain type A
Time -240 days after beginning of simulation
Date-9/10/2000

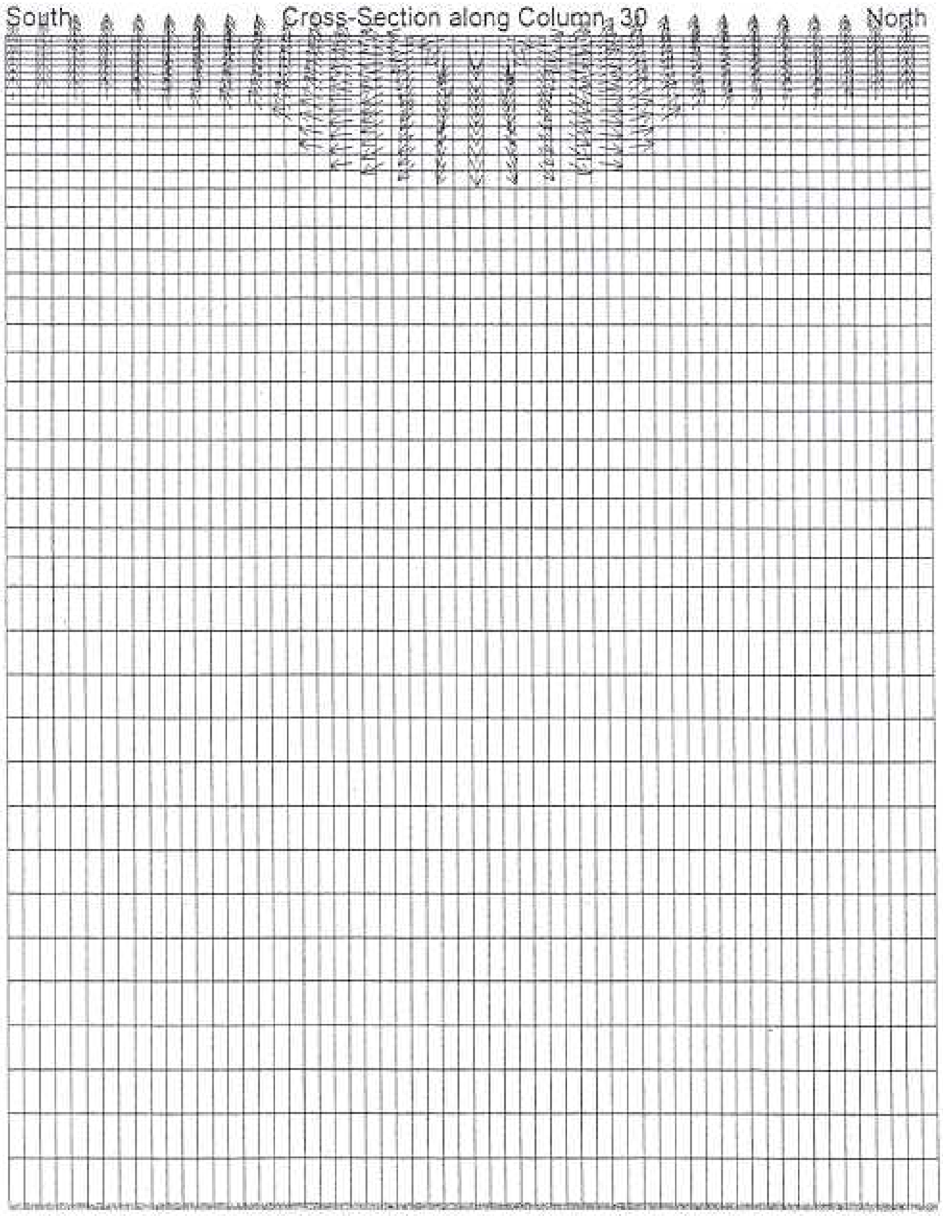

Figure D.103 Moisture movement vectors along C-30 for SCLA8

Simulation-SCLA12-Sandy Clay Loam soil with ET domain type A
Time -352 days after beginning of simulation
Date-12/31/2000

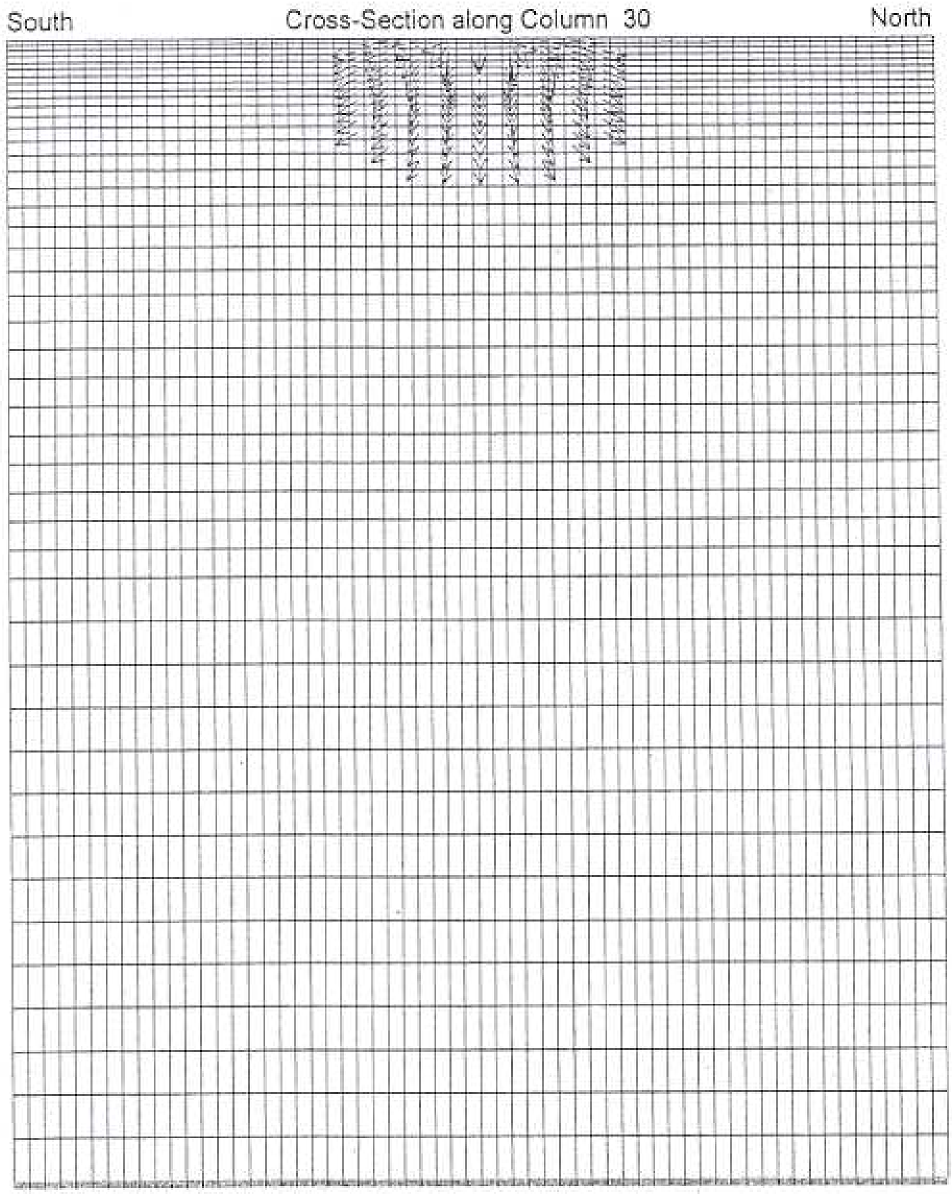

Figure D.104 Moisture movement vectors along C-30 for SCLA12

Simulation-SCLA1-Sandy Clay Loam soil with ET domain type A
Time -30 days after beginning of simulation
Date-2/13/2000

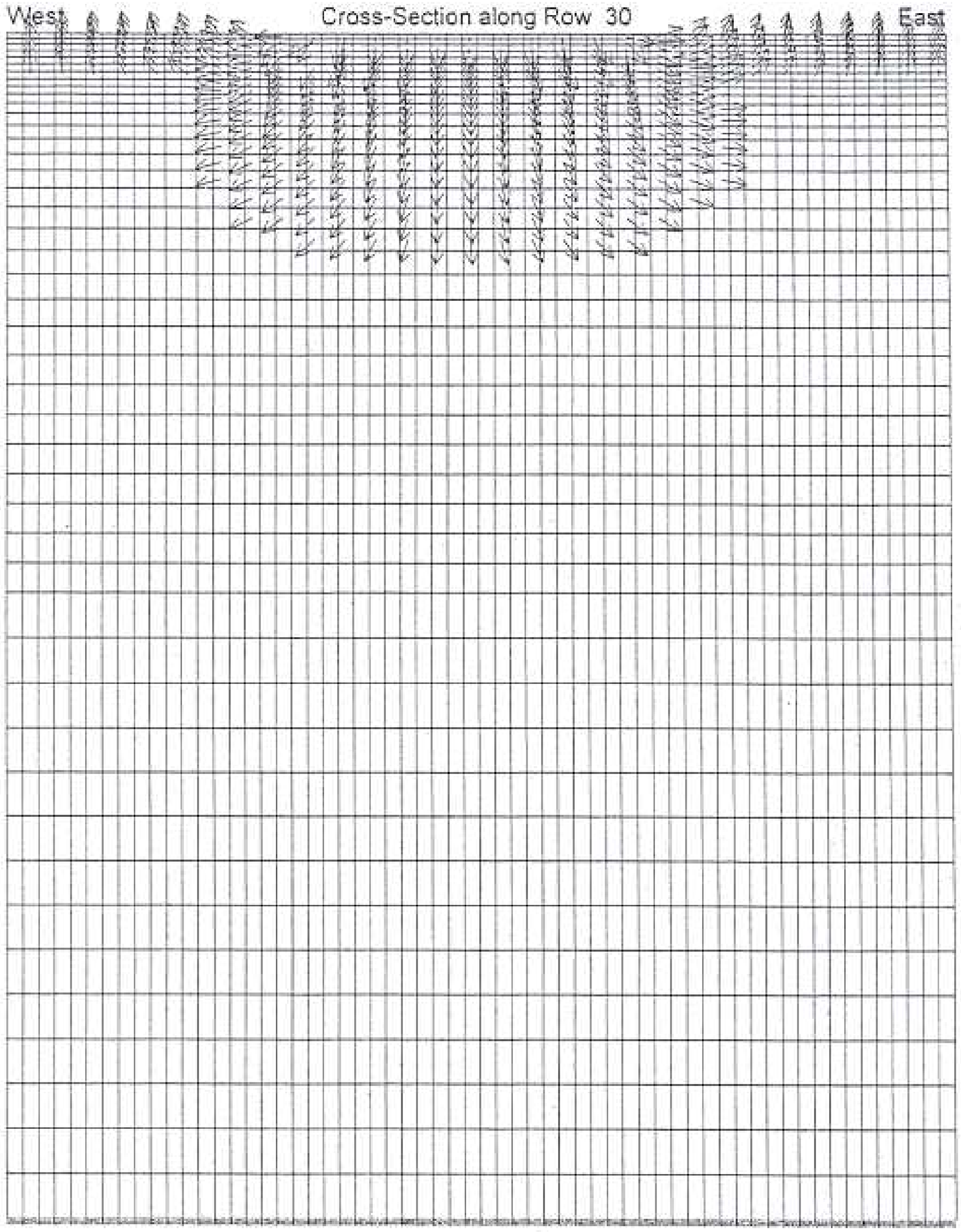

Figure D.105 Moisture movement vectors along R-30 for SCLA1

Simulation-SCLA4-Sandy Clay Loam soil with ET domain type A
Time -120 days after beginning of simulation
Date-5/13/2000

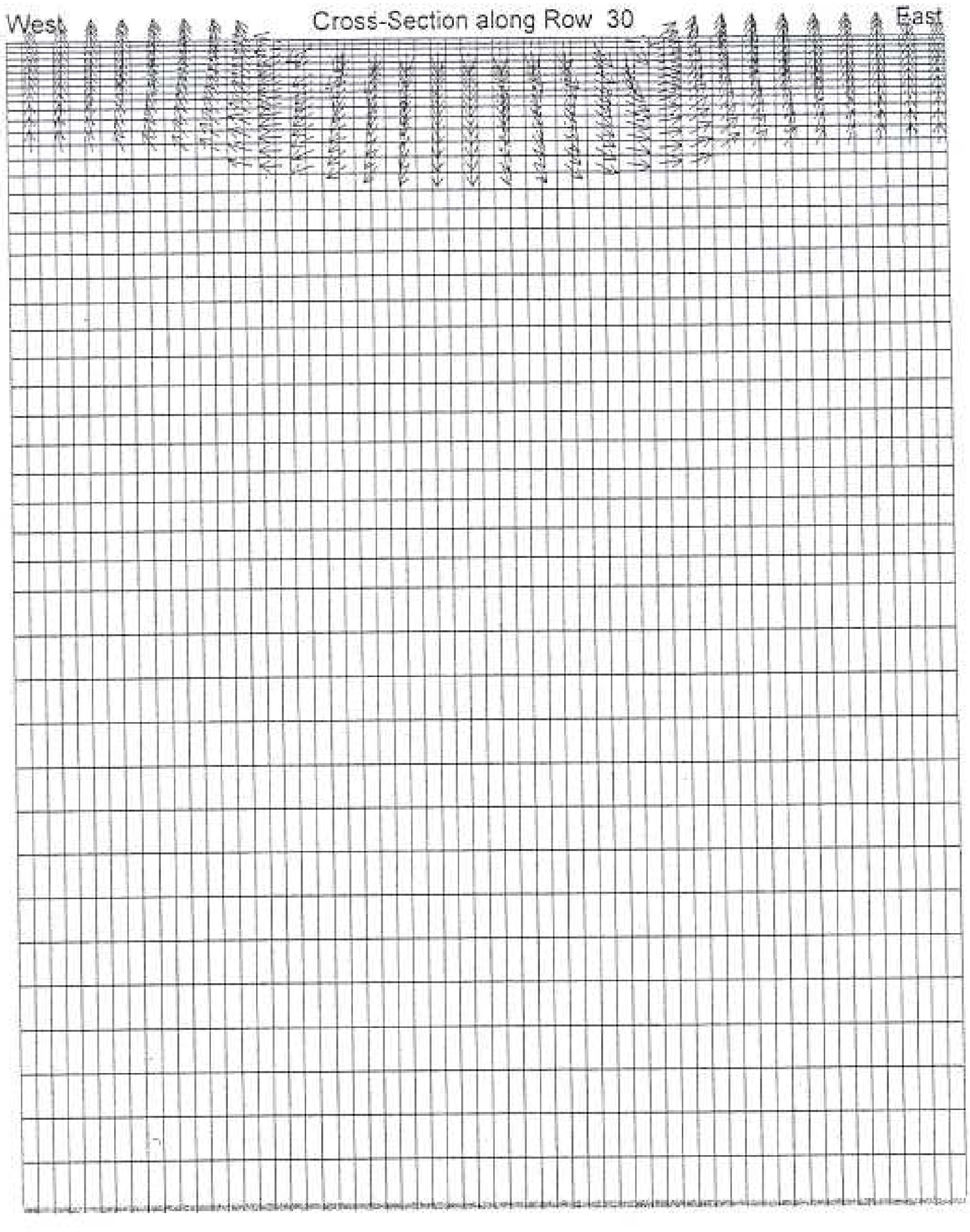

Figure D.106 Moisture movement vectors along R-30 for SCLA4

Simulation-SCLA8-Sandy Clay Loam soil with ET domain type A
Time -240 days after beginning of simulation
Date-9/10/2000

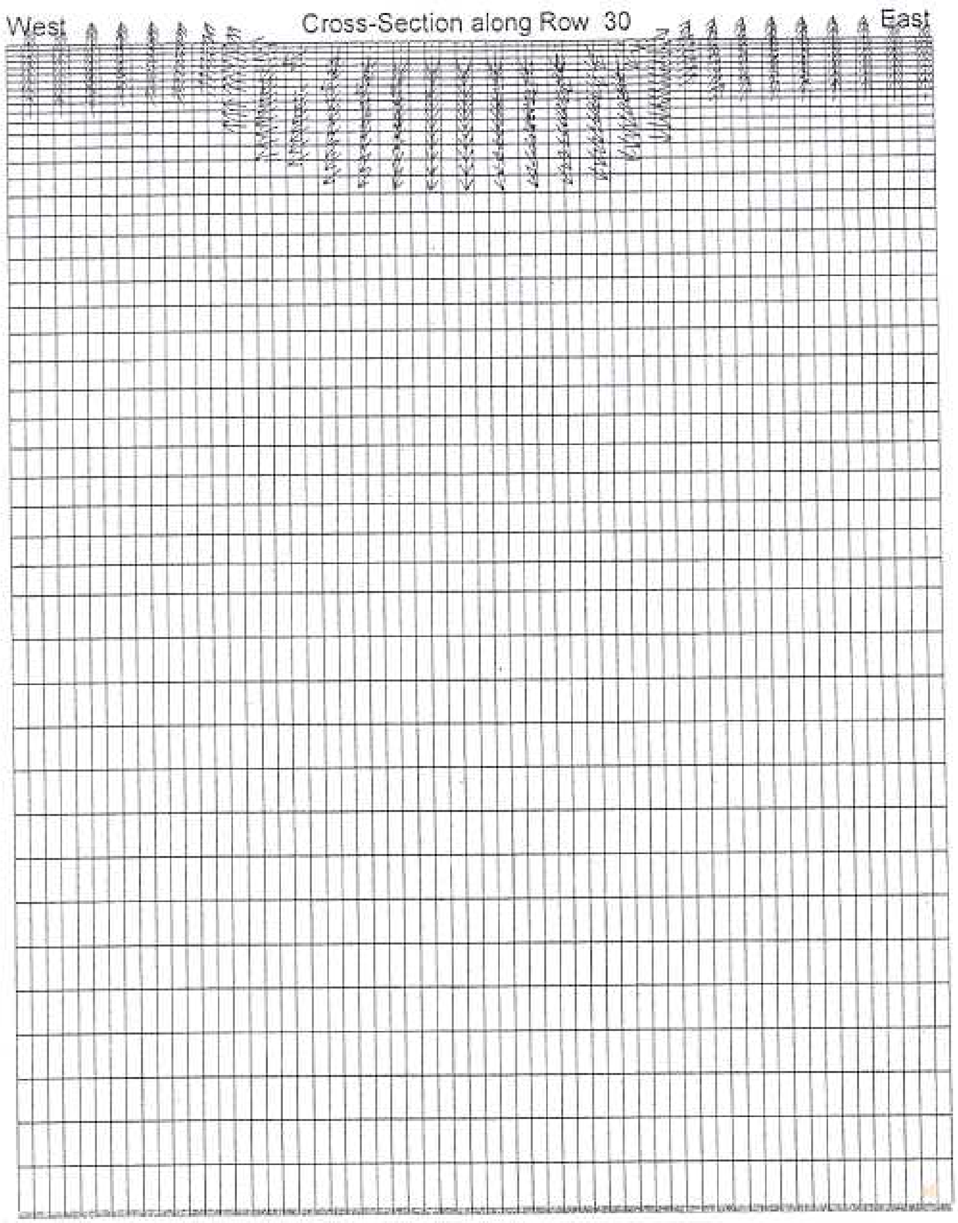

Figure D.107 Moisture movement vectors along R-30 for SCLA8

Simulation-SCLA12-Sandy Clay Loam soil with ET domain type A
Time -352 days after beginning of simulation
Date-12/31/2000

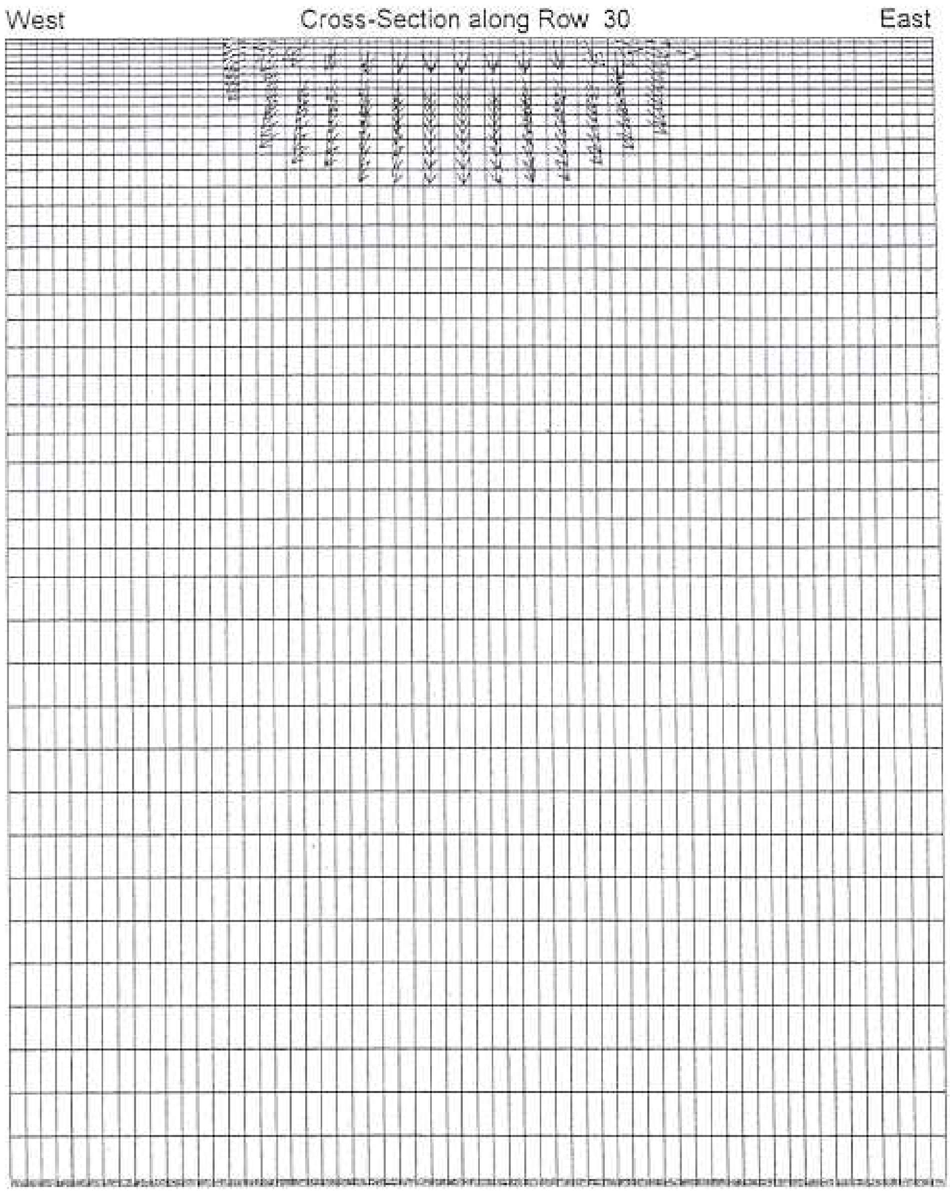

Figure D.108 Moisture movement vectors along R-30 for SCLA12

Simulation-SCLB1-Sandy Clay Loam soil with ET domain type B
Time -30 days after beginning of simulation
Date-2/13/2000

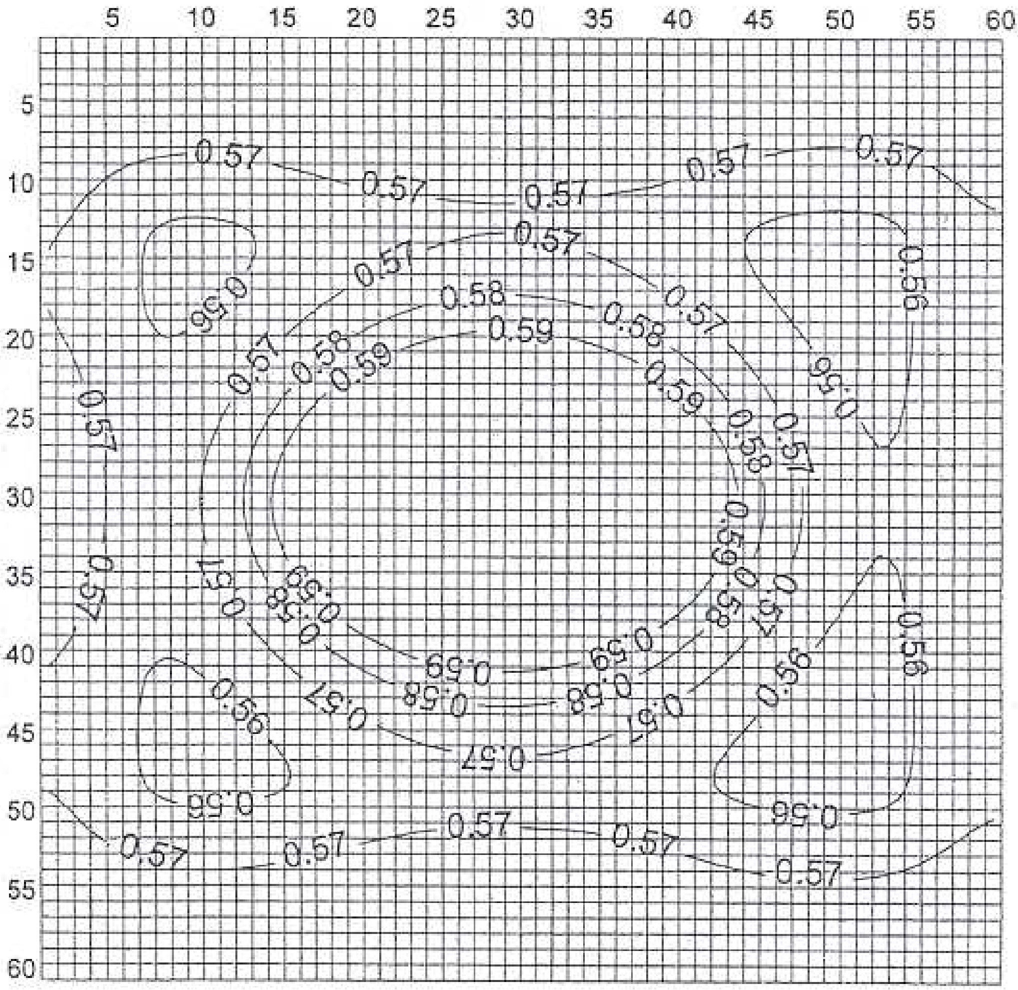

Figure D.109 Water saturation contours in plan view for SCLB1

Simulation-SCLB2-Sandy Clay Loam soil with ET domain type B
Time -60 days after beginning of simulation
Date-3/14/2000

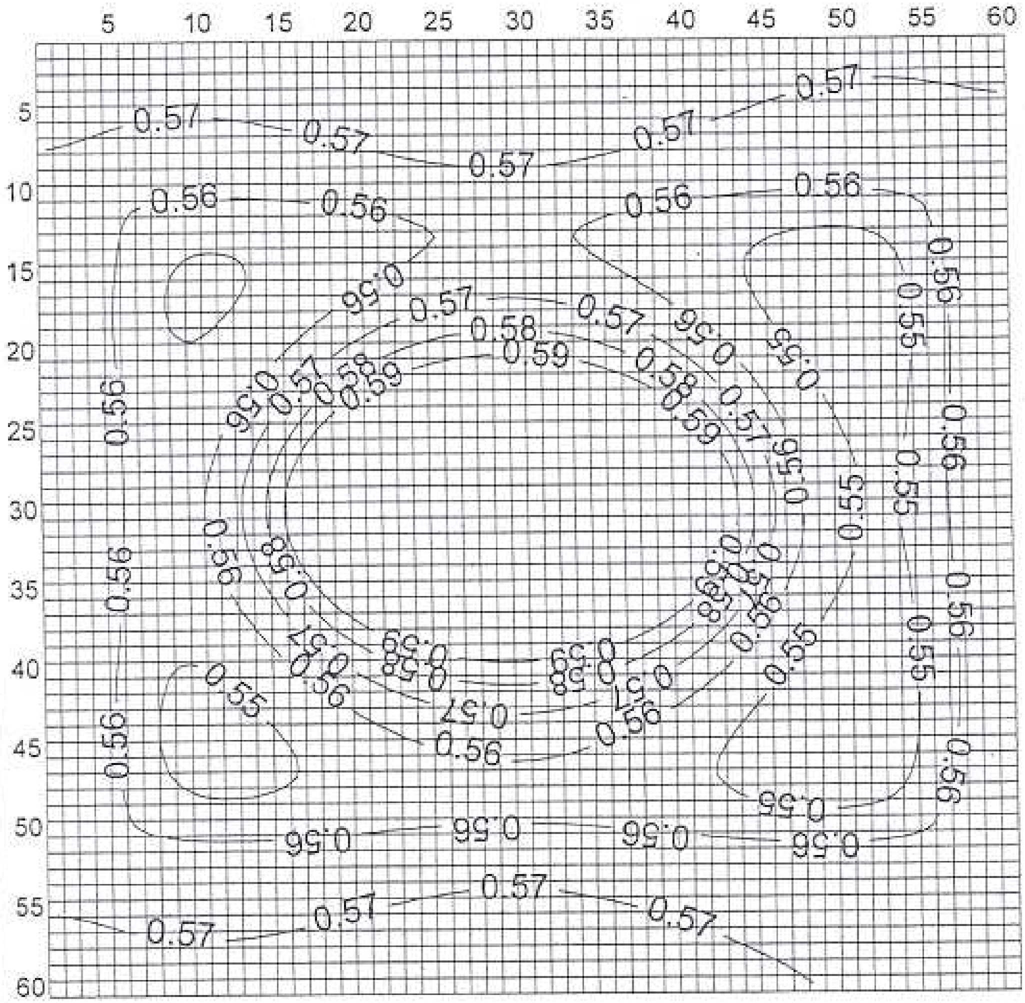

Figure D.110 Water saturation contours in plan view for SCLB2

Simulation-SCLB3-Sandy Clay Loam soil with ET domain type B
Time -90 days after beginning of simulation
Date-4/13/2000

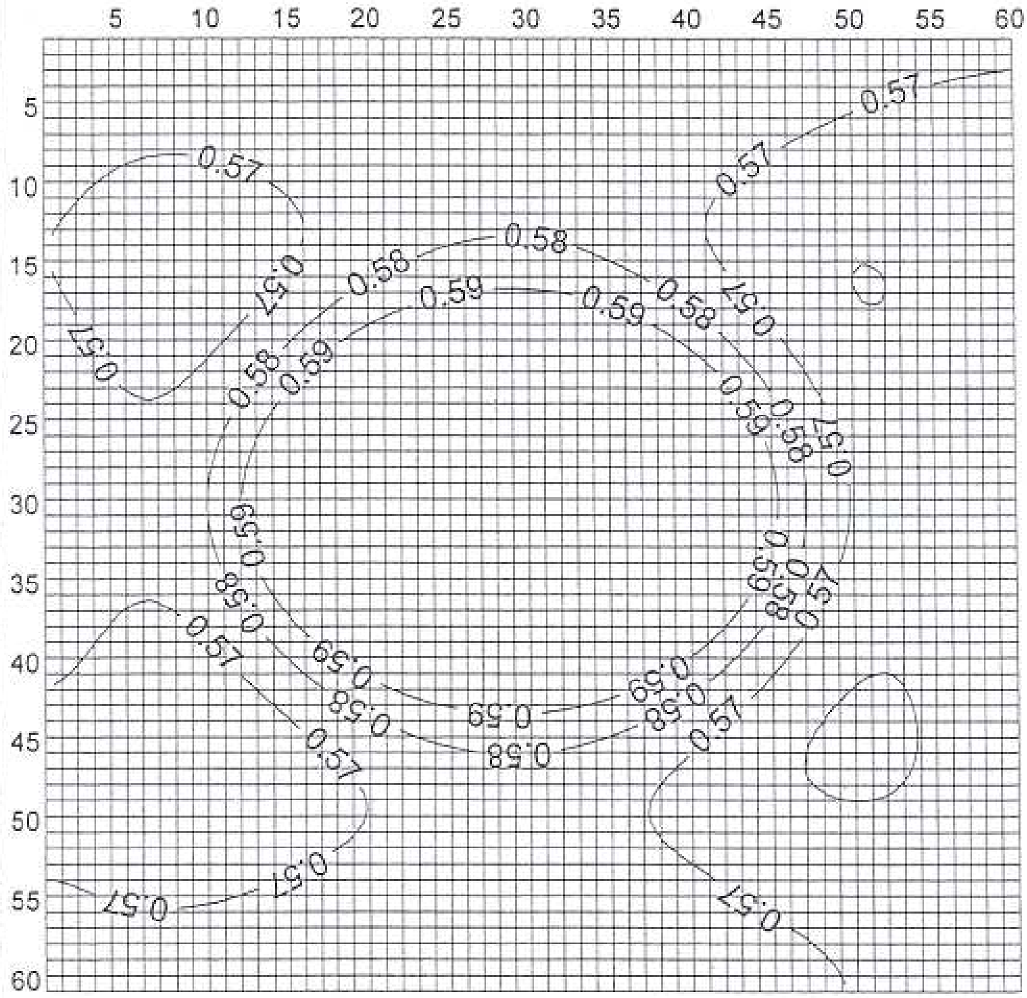

Figure D.111 Water saturation contours in plan view for SCLB3

Simulation-SCLB4-Sandy Clay Loam soil with ET domain type B
Time -120 days after beginning of simulation
Date-5/13/2000

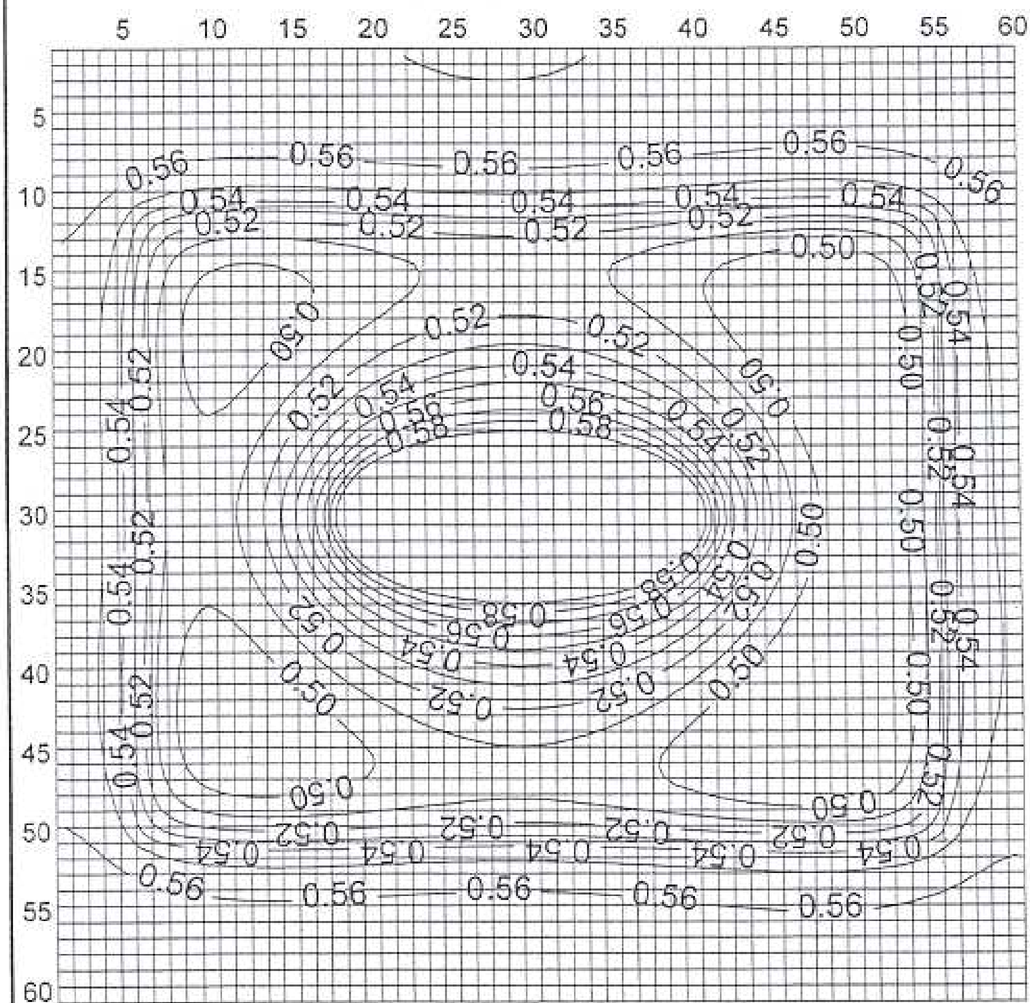

Figure D.112 Water saturation contours in plan view for SCLB4

Simulation-SCLB5-Sandy Clay Loam soil with ET domain type B
Time -150 days after beginning of simulation
Date-6/12//2000

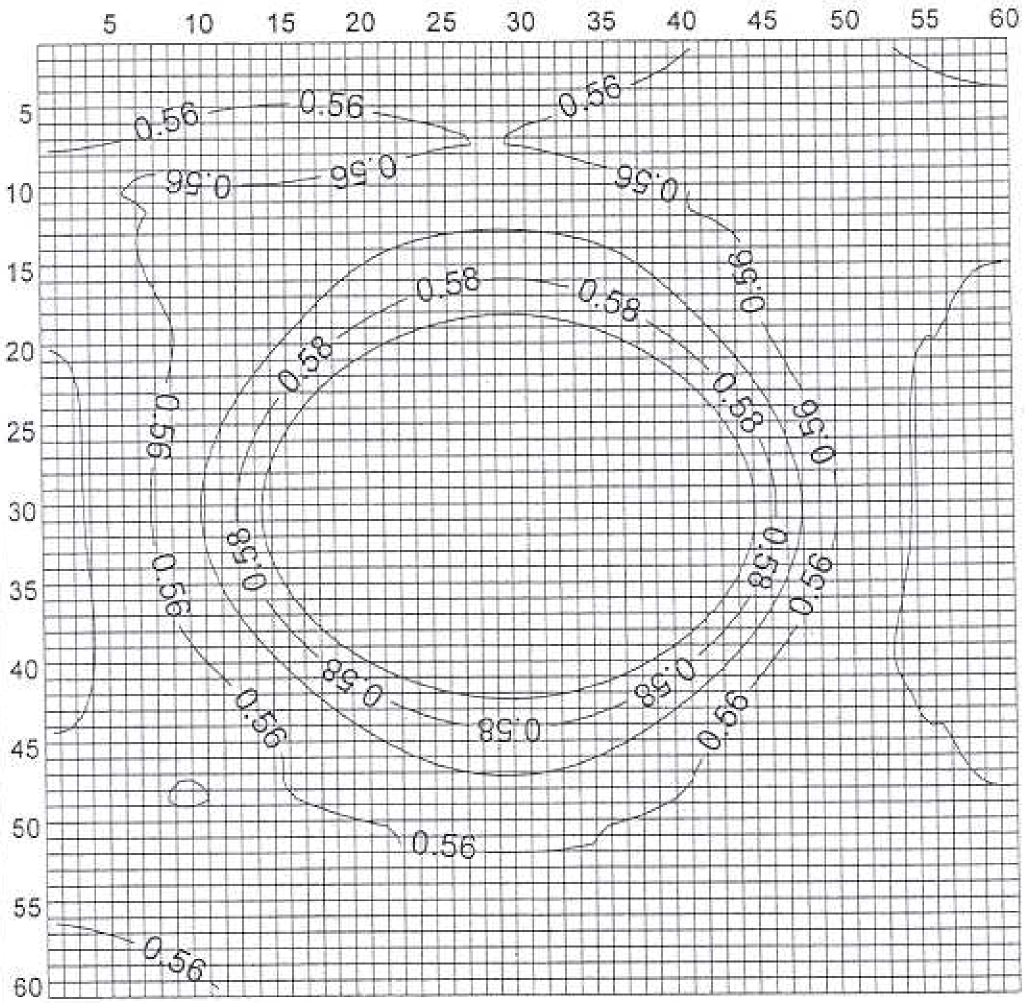

Figure D.113 Water saturation contours in plan view for SCLB5

Simulation-SCLB6-Sandy Clay Loam soil with ET domain type B
Time -180 days after beginning of simulation
Date-7/12/2000

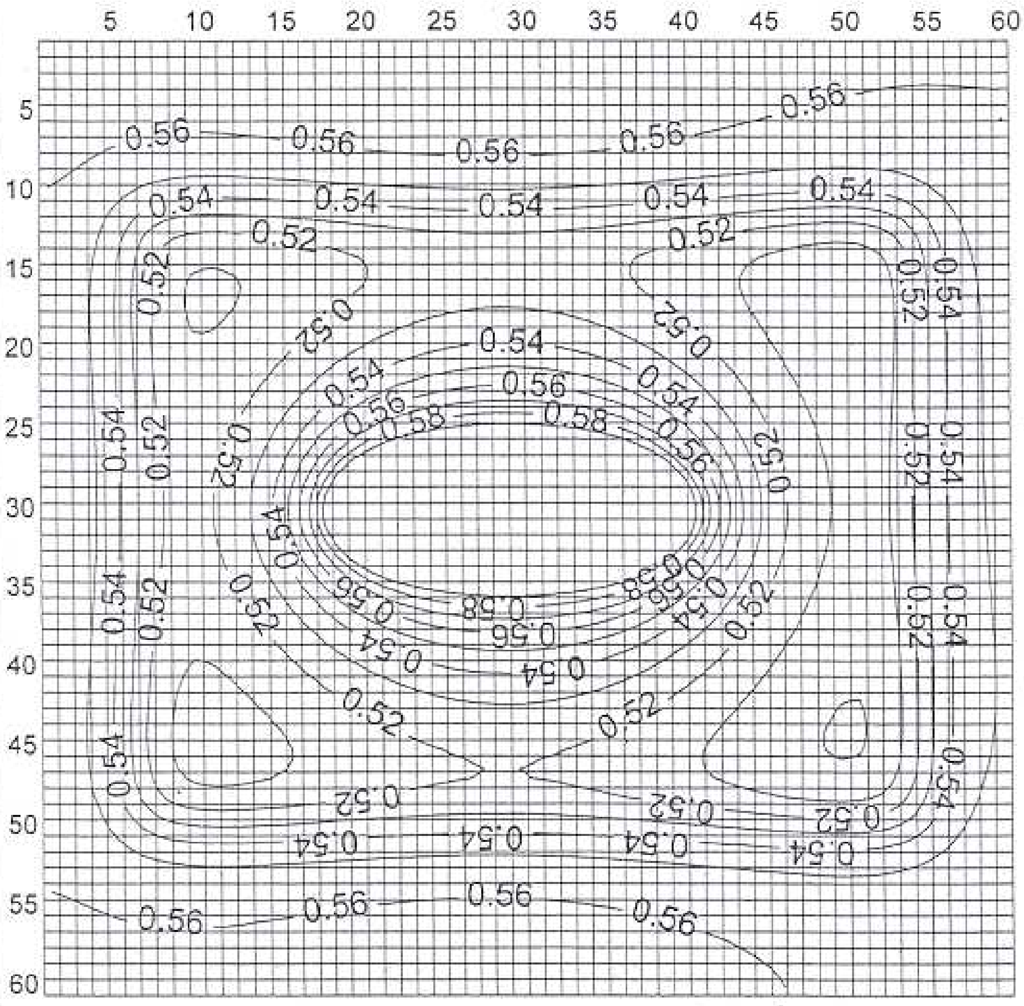

Figure D.114 Water saturation contours in plan view for SCLB6

Simulation-SCLB7-Sandy Clay Loam soil with ET domain type B
Time -210 days after beginning of simulation
Date-8/11/2000

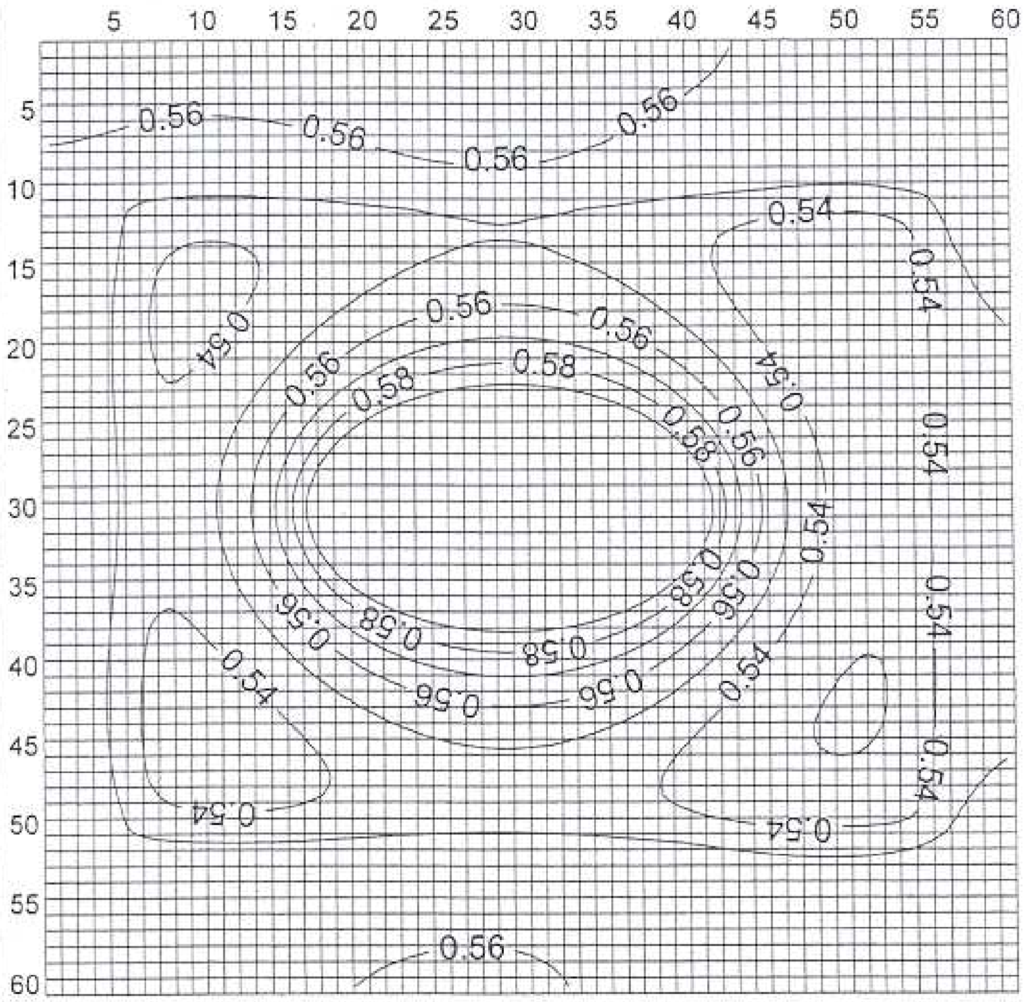

Figure D.115 Water saturation contours in plan view for SCLB7

Simulation-SCLB8-Sandy Clay Loam soil with ET domain type B
Time -240 days after beginning of simulation
Date-9/10/2000

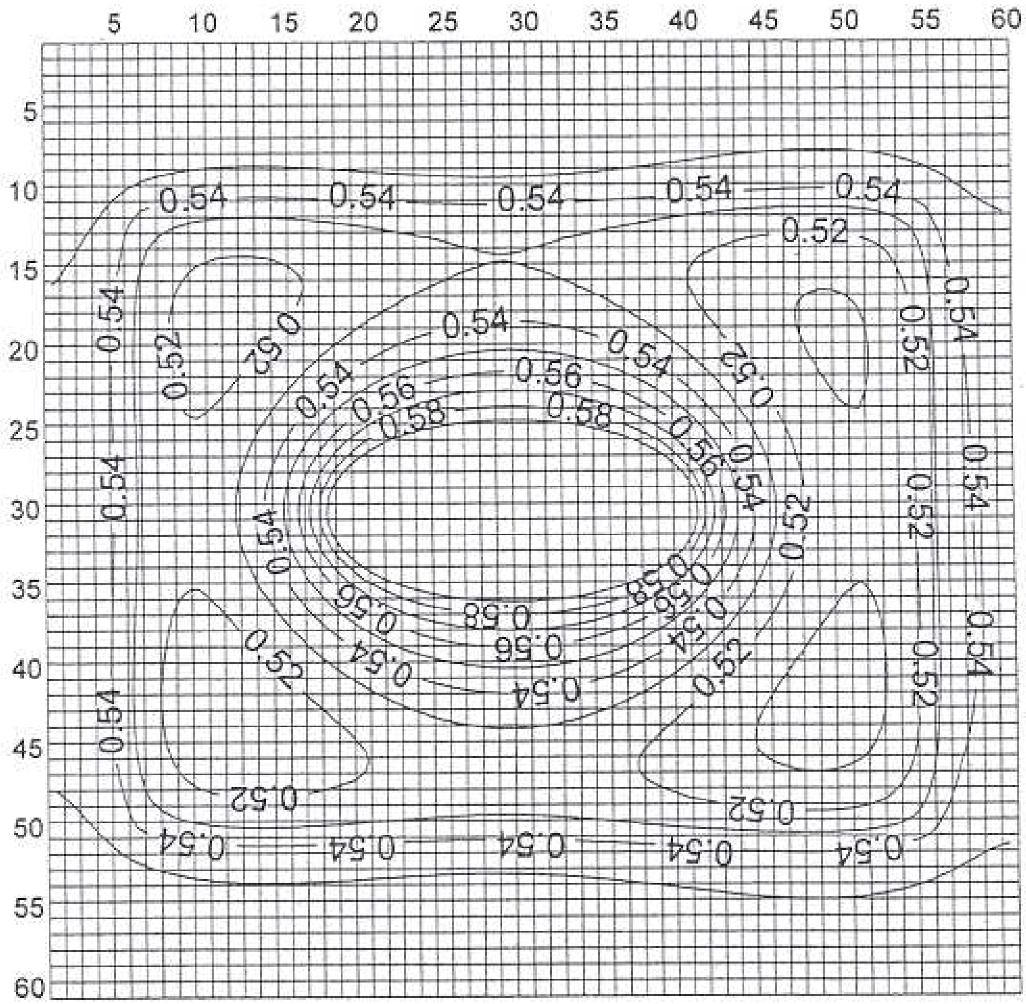

Figure D.116 Water saturation contours in plan view for SCLB8

Simulation-SCLB9-Sandy Clay Loam soil with ET domain type B
Time -270 days after beginning of simulation
Date-10/10/2000

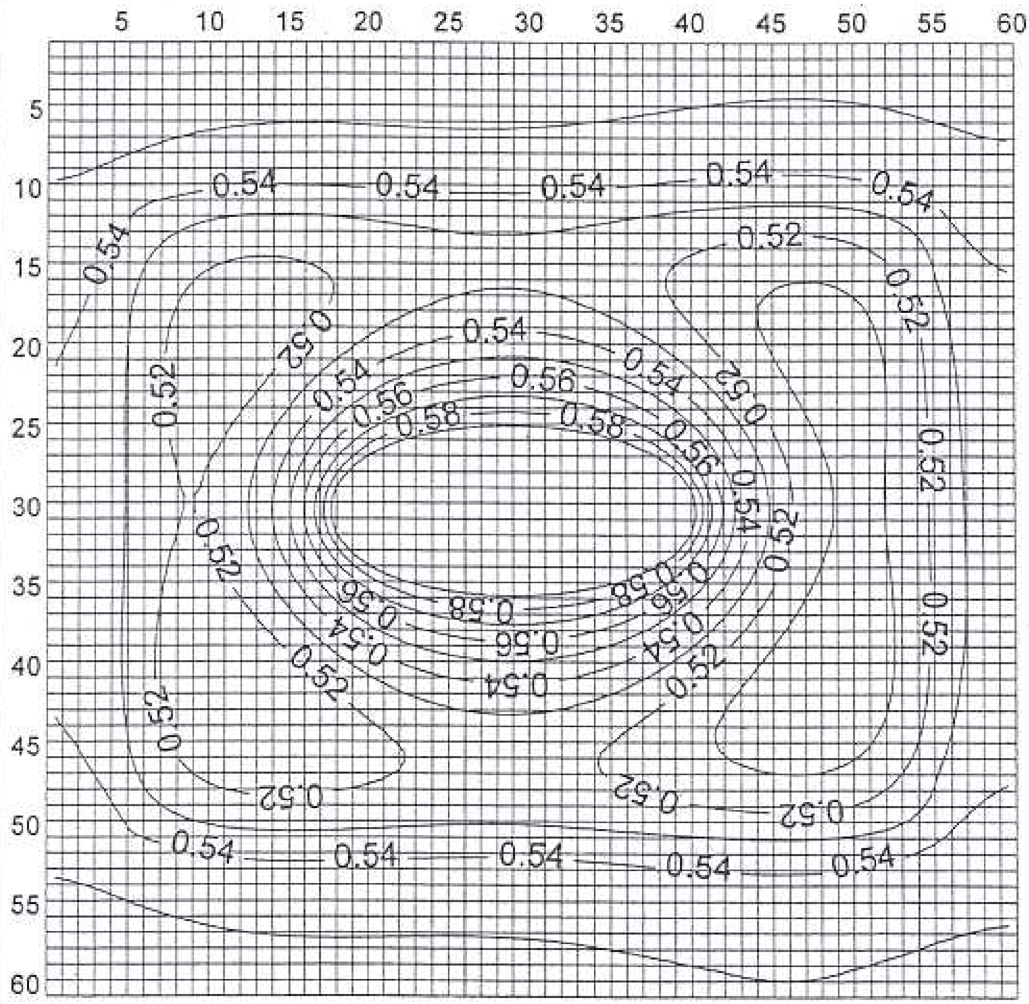

Figure D.117 Water saturation contours in plan view for SCLB9

Simulation-SCLB10-Sandy Clay Loam soil with ET domain type B
Time -300 days after beginning of simulation
Date-11/9/2000

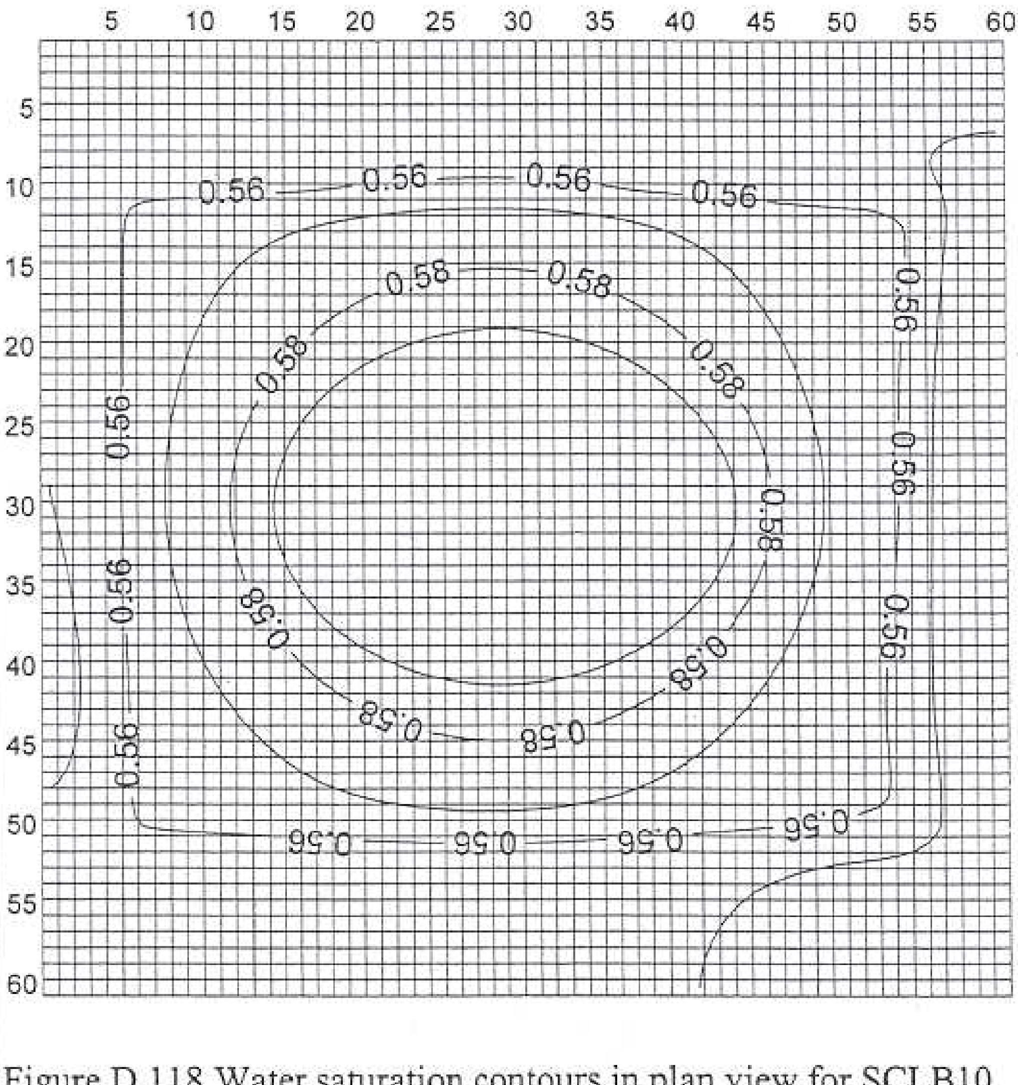

Figure D.118 Water saturation contours in plan view for SCLB10

Simulation-SCLB11-Sandy Clay Loam soil with ET domain type B
Time -330 days after beginning of simulation
Date-12/9/2000

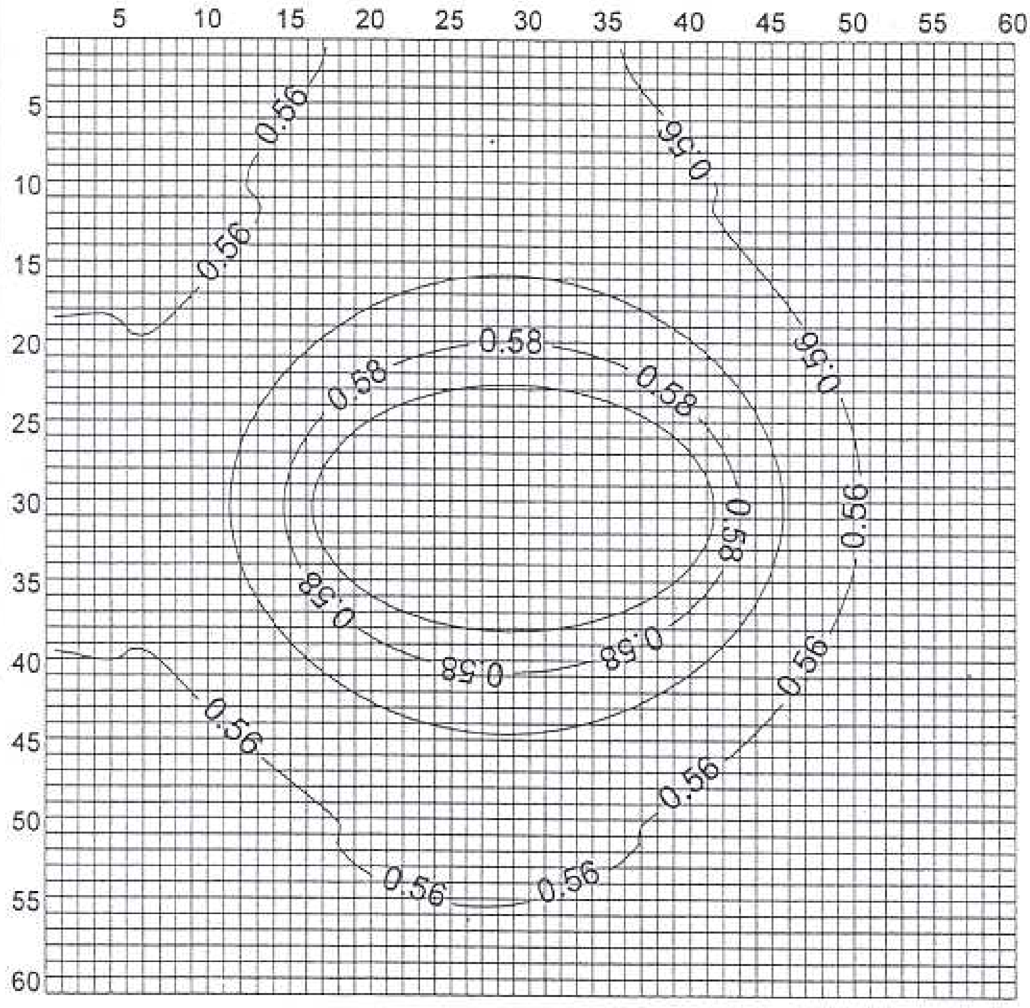

Figure D.119 Water saturation contours in plan view for SCLB11

Simulation-SCLB12-Sandy Clay Loam soil with ET domain type B
Time -352 days after beginning of simulation
Date-12/31/2000

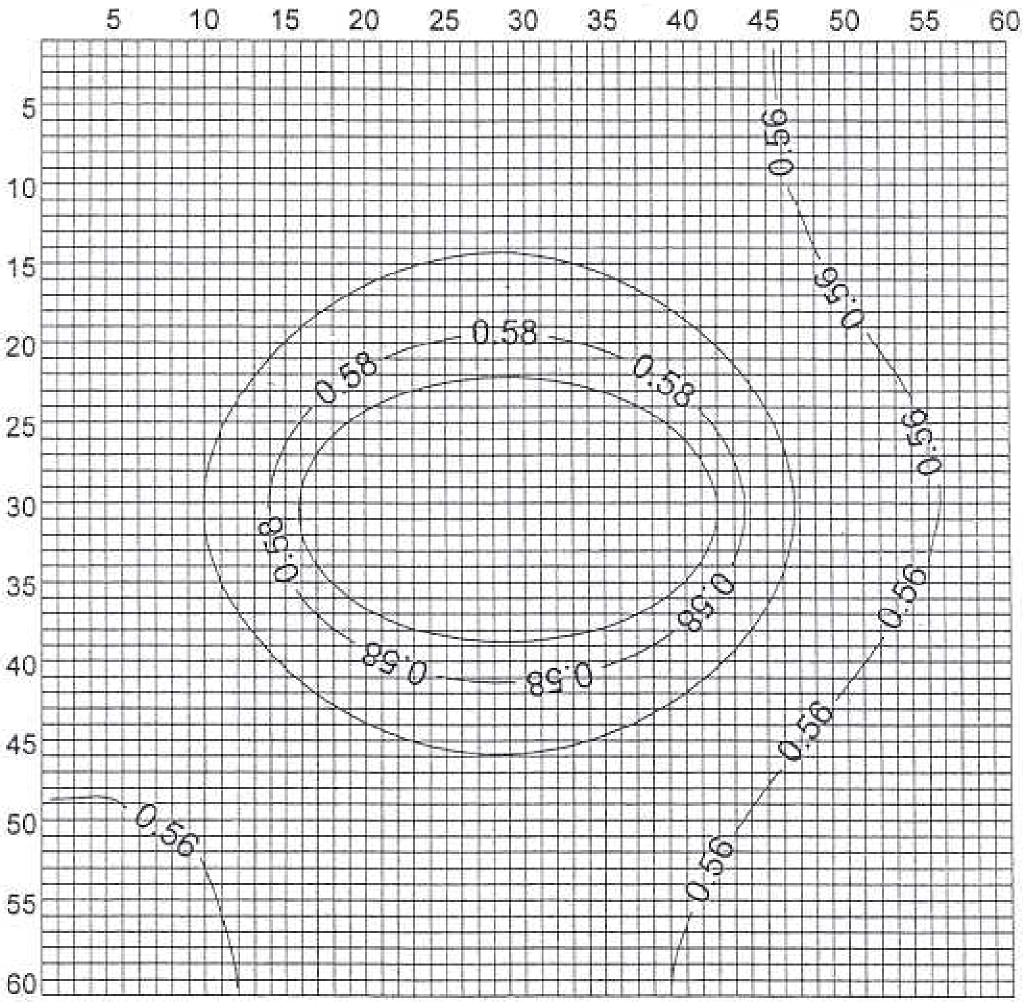

Figure D.120 Water saturation contours in plan view for SCLB12

Simulation-SCLB1-Sandy Clay Loam soil with ET domain type B
Time -30 days after beginning of simulation
Date-2/13/2000

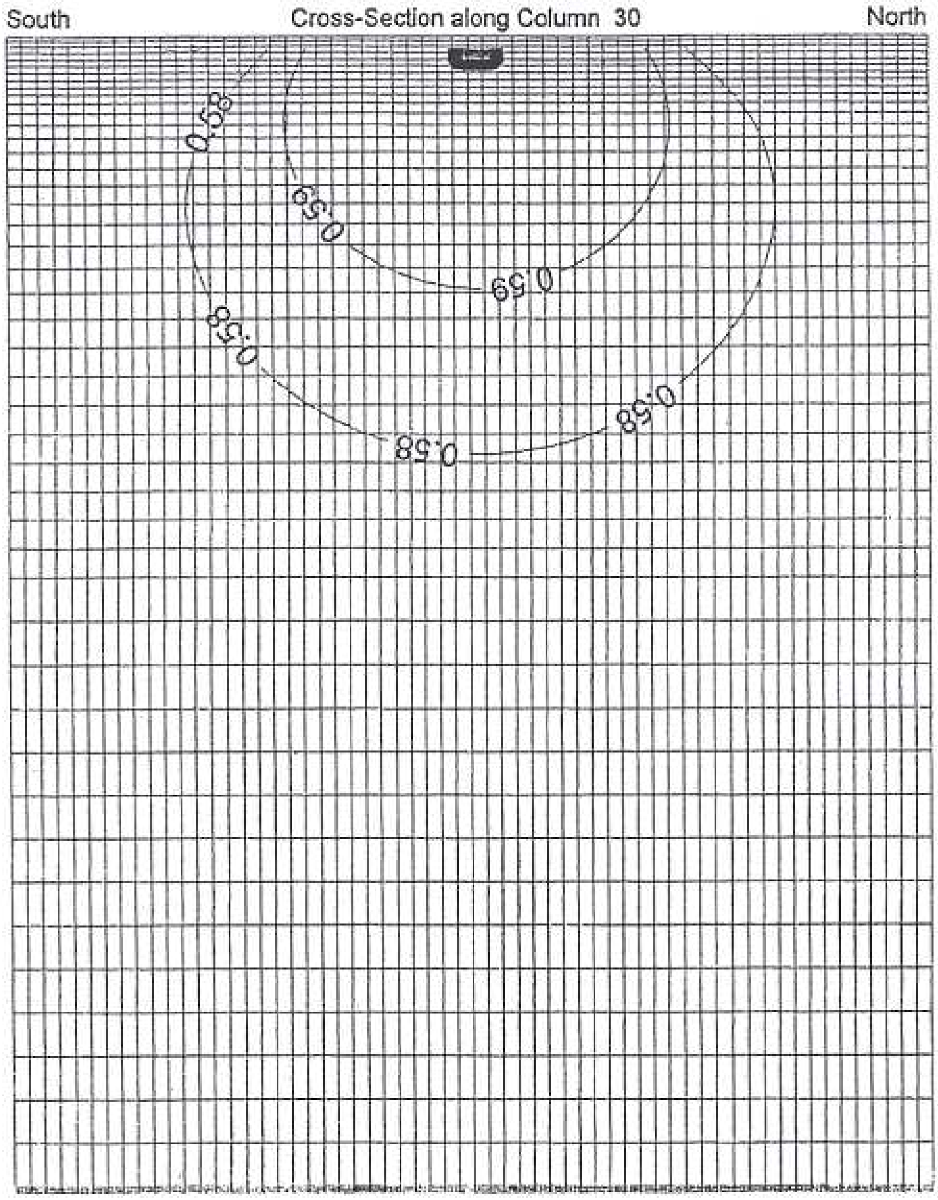

Figure D.121 Water saturation contours in cross-section for SCLB1

Simulation-SCLB2-Sandy Clay Loam soil with ET domain type B
Time -60 days after beginning of simulation
Date-3/14/2000

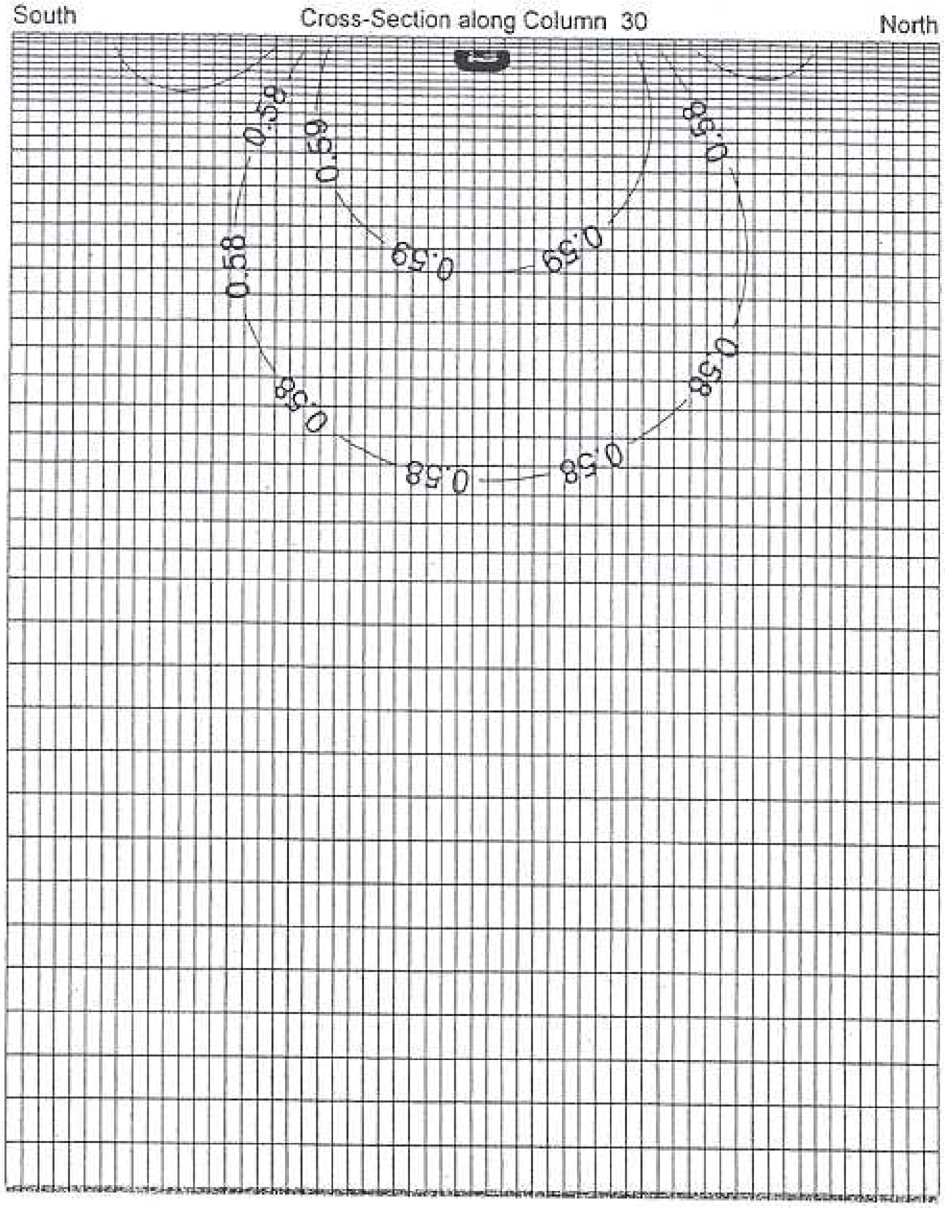

Figure D.122 Water saturation contours in cross-section for SCLB2

Simulation-SCLB3-Sandy Clay Loam soil with ET domain type B
Time -90 days after beginning of simulation
Date-4/13/2000

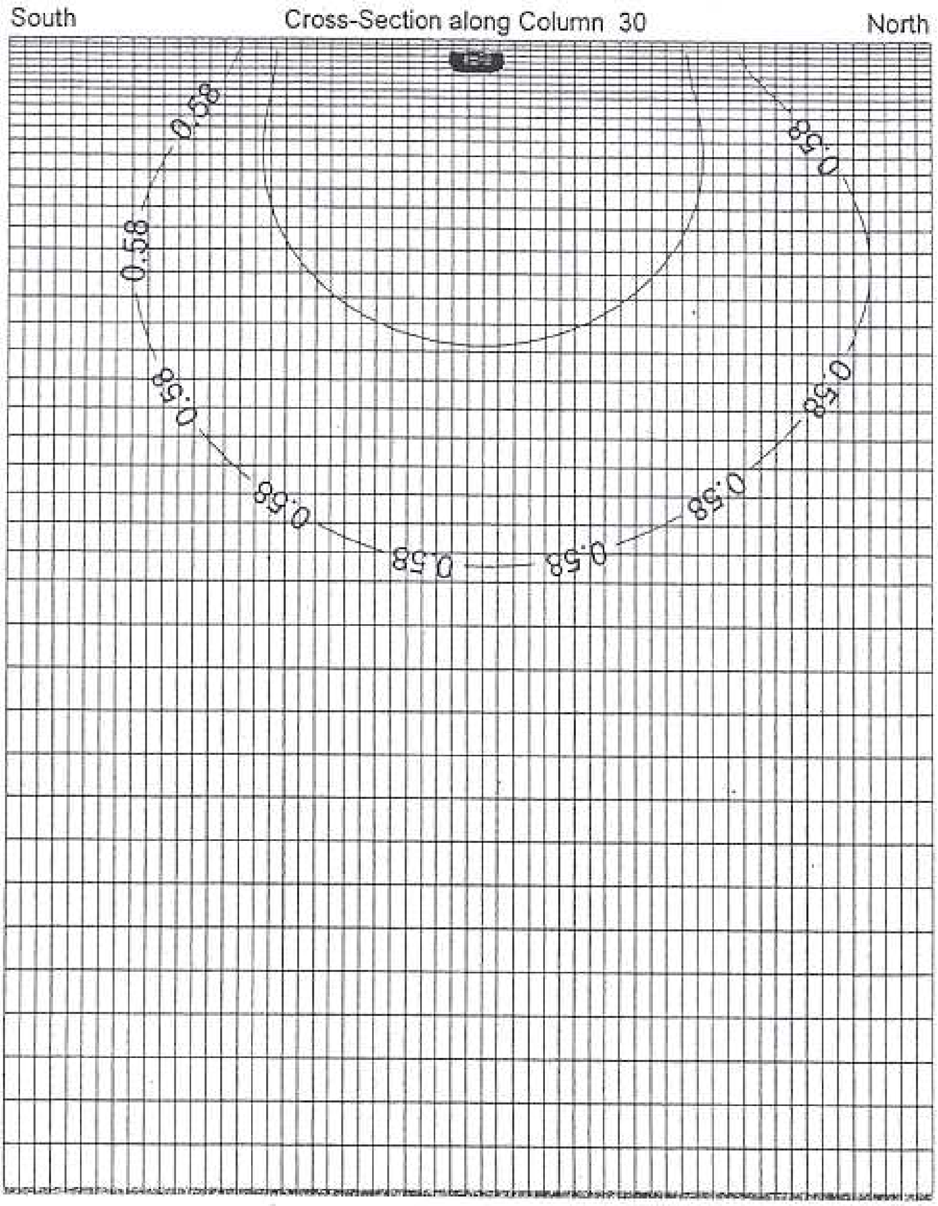

Figure D.123 Water saturation contours in cross-section for SCLB3

Simulation-SCLB4-Sandy Clay Loam soil with ET domain type B
Time -120 days after beginning of simulation
Date-5/13/2000

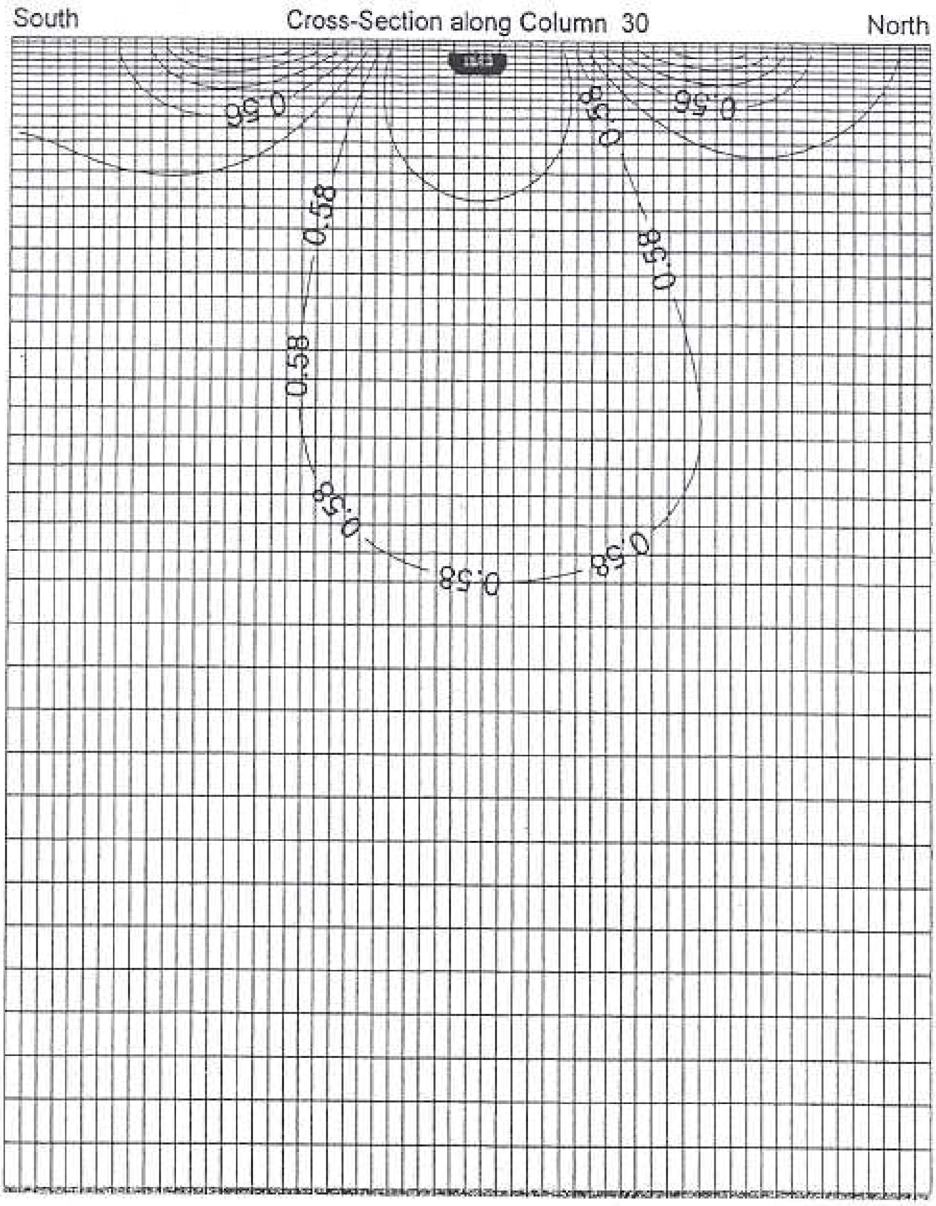

Figure D.124 Water saturation contours in cross-section for SCLB4

Simulation-SCLB5-Sandy Clay Loam soil with ET domain type B
Time -150 days after beginning of simulation
Date-6/12//2000

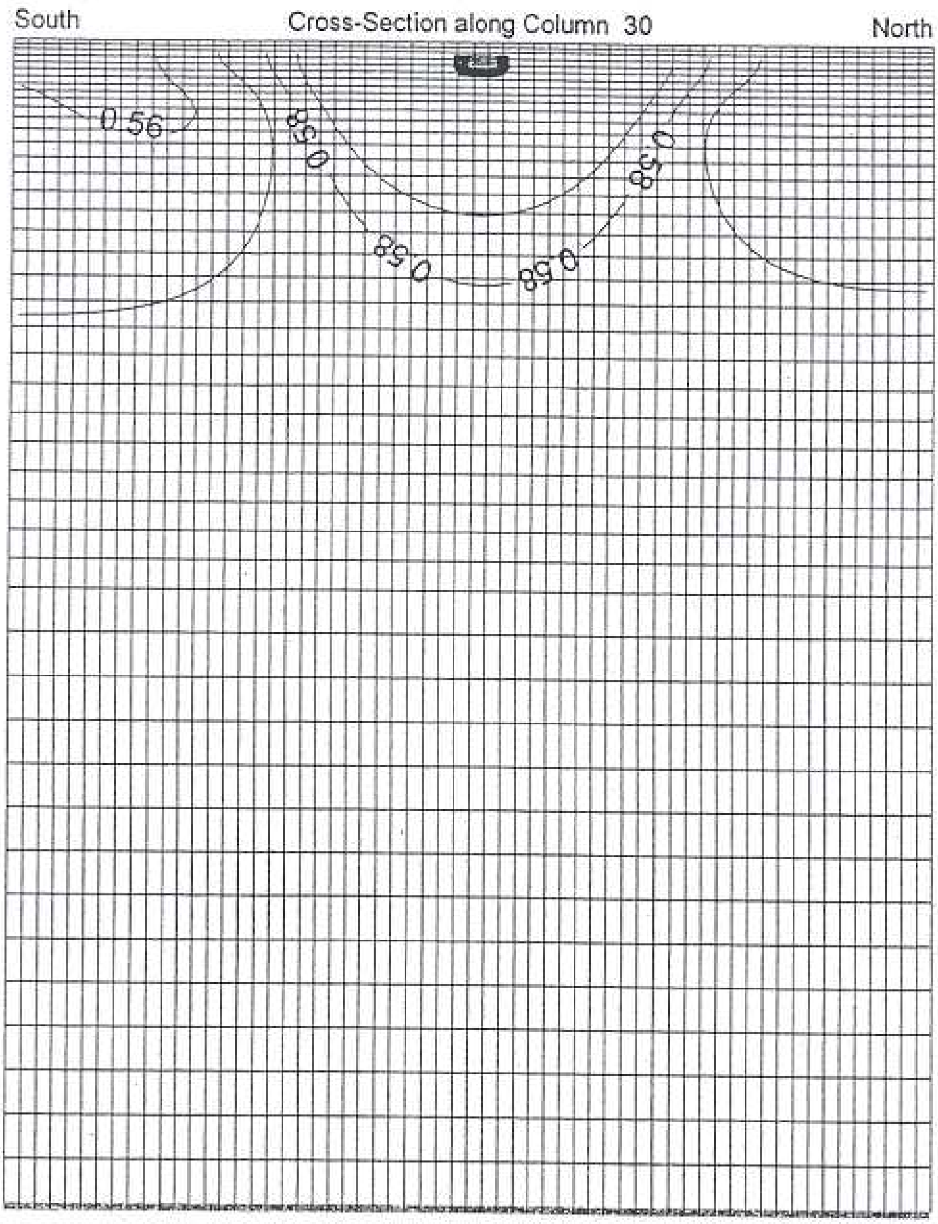

Figure D.125 Water saturation contours in cross-section for SCLB5

Simulation-SCLB6-Sandy Clay Loam soil with ET domain type B
Time -180 days after beginning of simulation
Date-7/12/2000

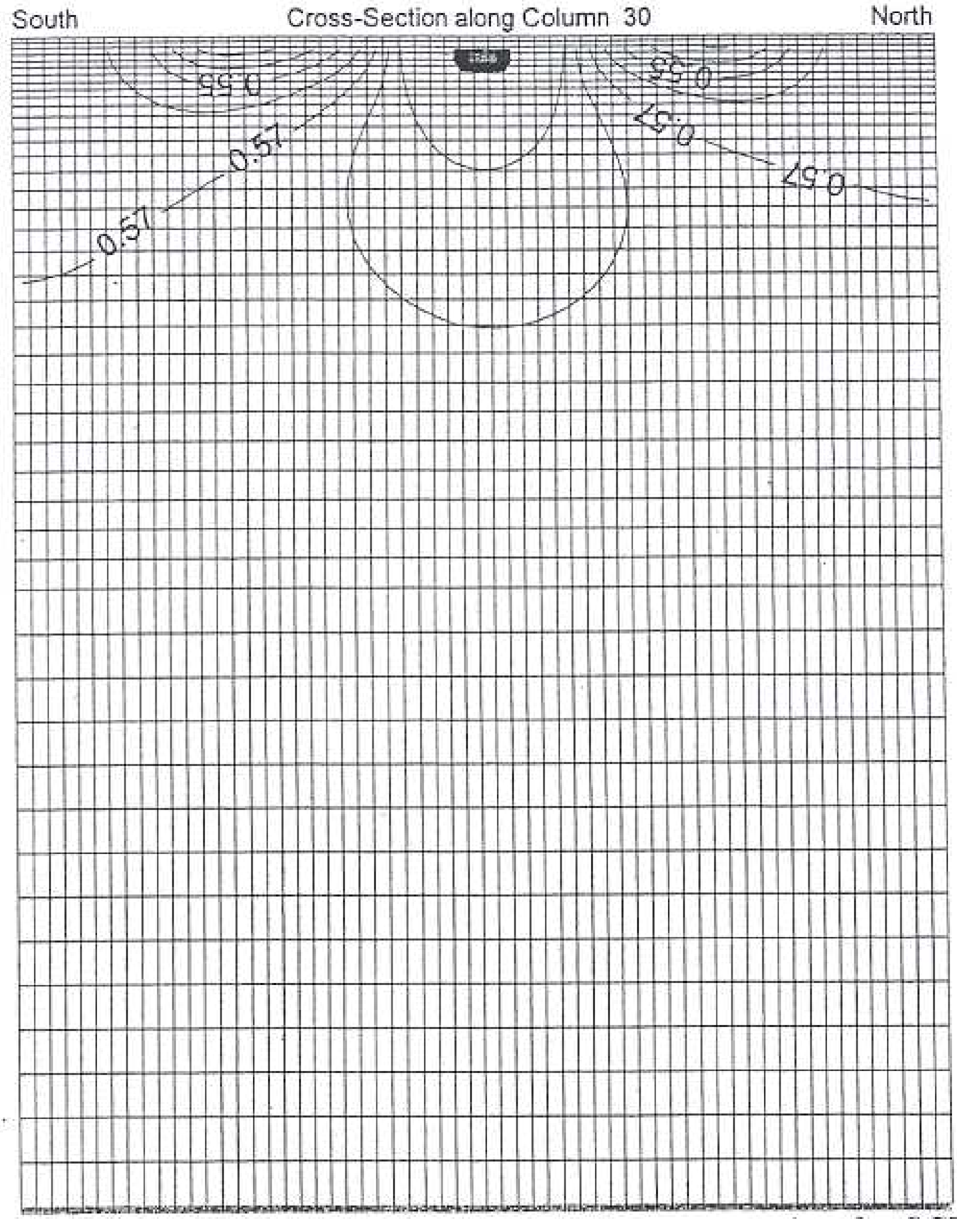

Figure D.126 Water saturation contours in cross-section for SCLB6

Simulation-SCLB7-Sandy Clay Loam soil with ET domain type B
Time -210 days after beginning of simulation
Date-8/11/2000

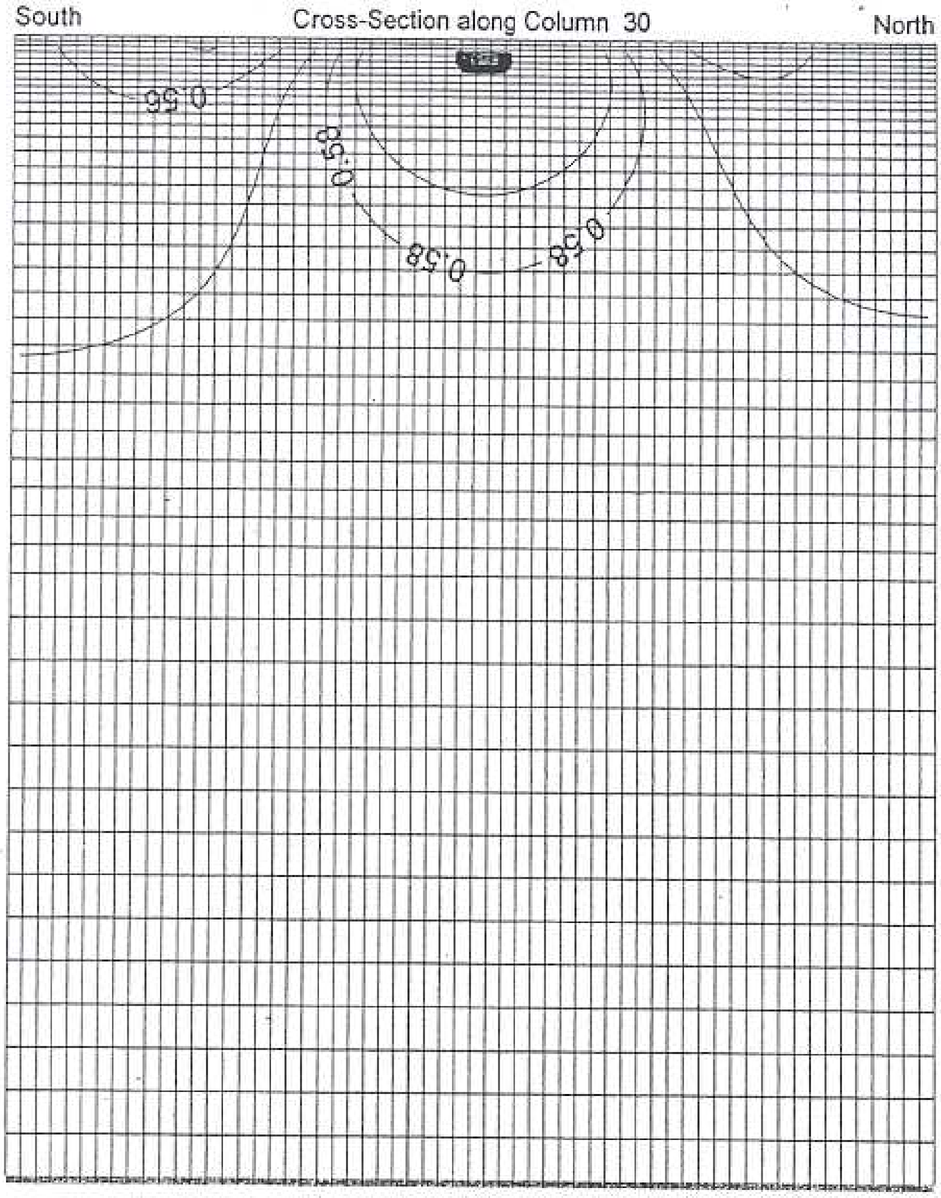

Figure D.127 Water saturation contours in cross-section for SCLB7

Simulation-SCLB8-Sandy Clay Loam soil with ET domain type B
Time -240 days after beginning of simulation
Date-9/10/2000

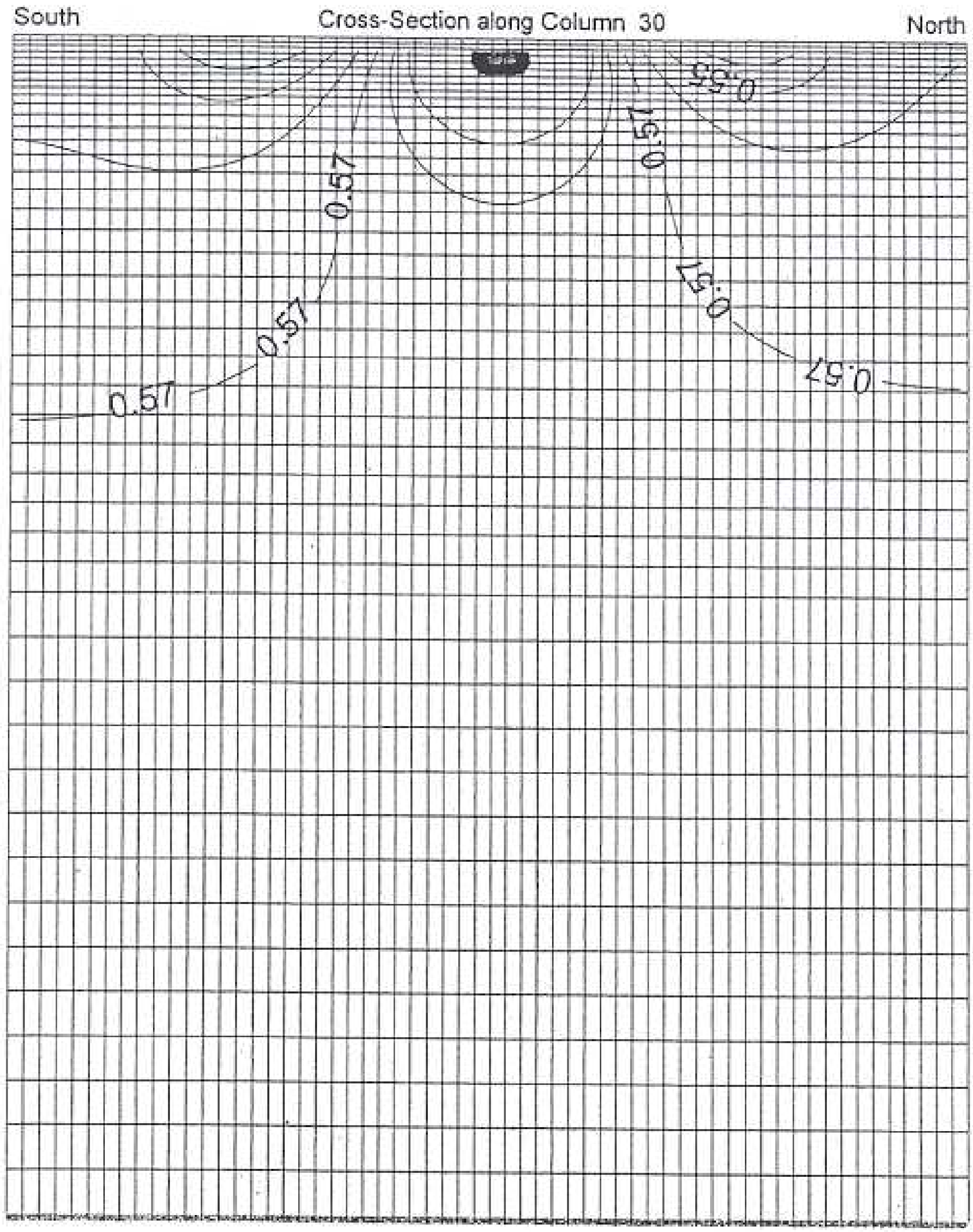

Figure D.128 Water saturation contours in cross-section for SCLB8

Simulation-SCLB9-Sandy Clay Loam soil with ET domain type B
Time -270 days after beginning of simulation
Date-10/10/2000

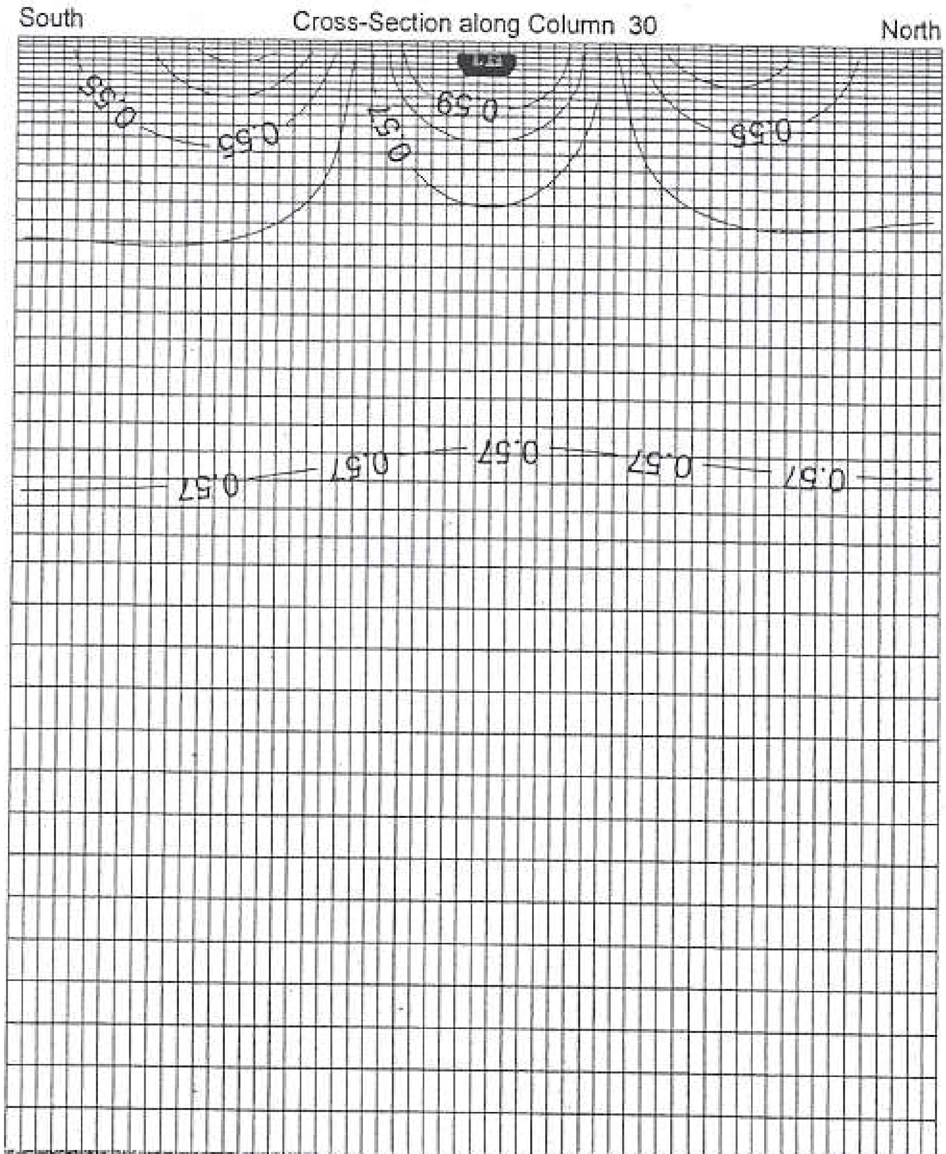

Figure D.129 Water saturation contours in cross-section for SCLB9

Simulation-SCLB10-Sandy Clay Loam soil with ET domain type B
Time -300 days after beginning of simulation
Date-11/9/2000

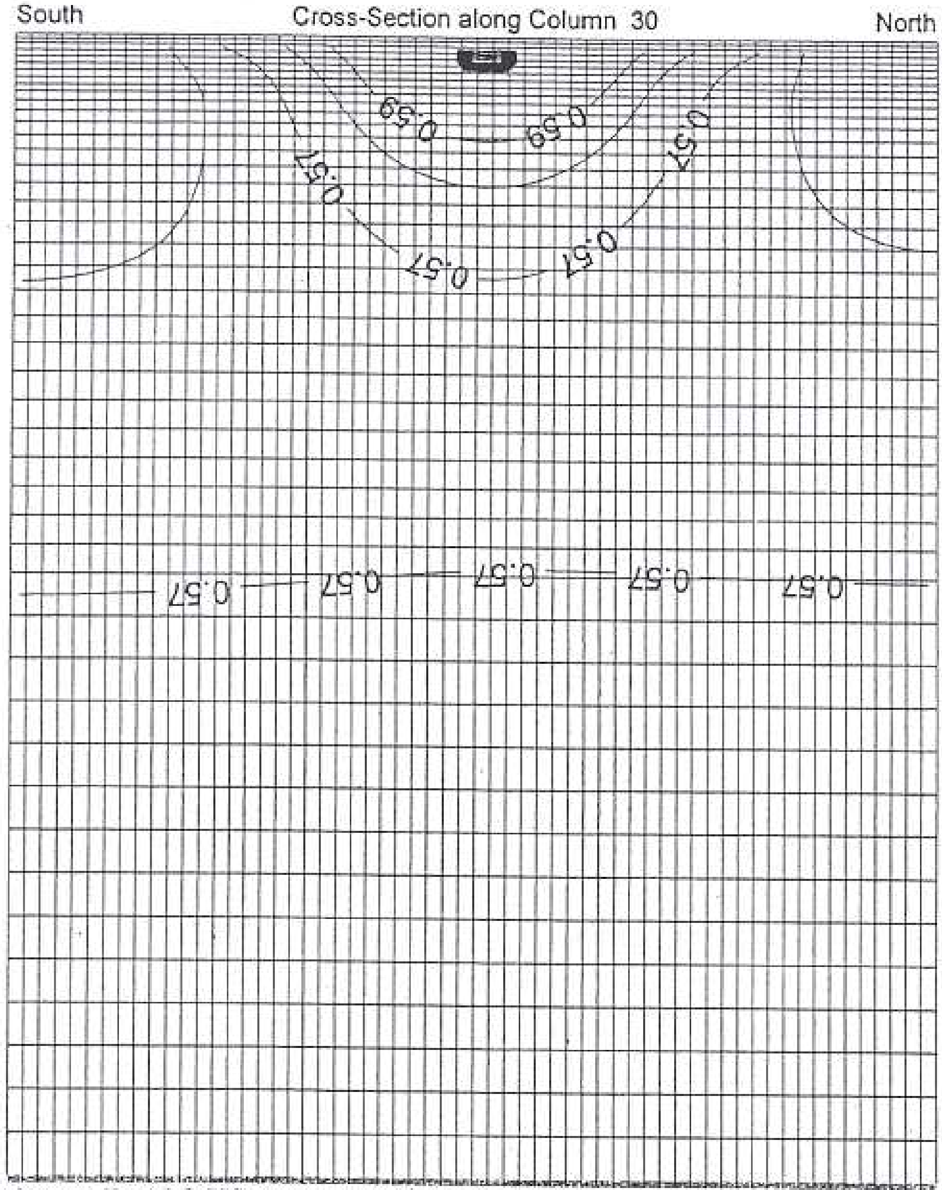

Figure D.130 Water saturation contours in cross-section for SCLB10

Simulation-SCLB11-Sandy Clay Loam soil with ET domain type B
Time -330 days after beginning of simulation
Date-12/9/2000

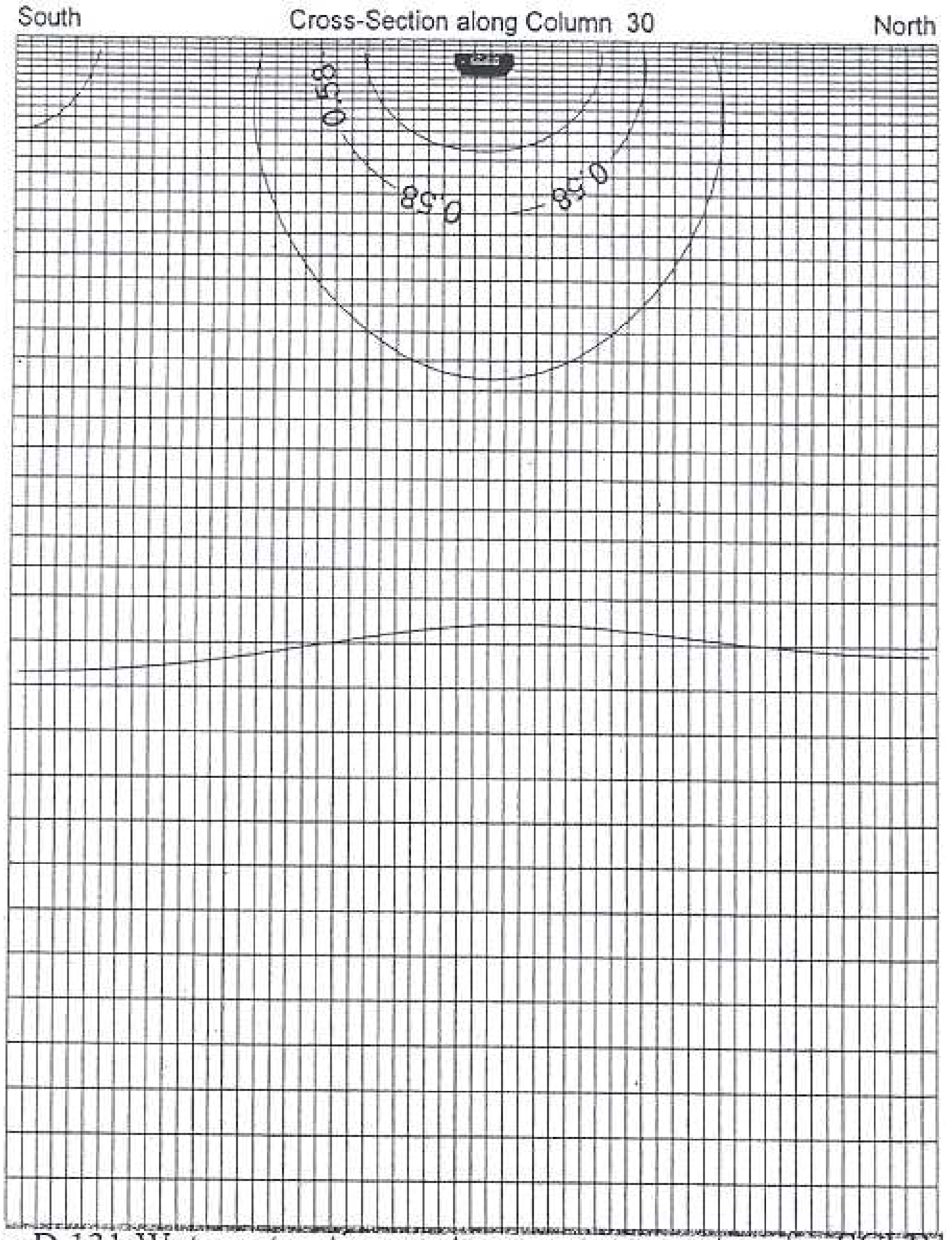

Figure D.131 Water saturation contours in cross-section for SCLB11

Simulation-SCLB12-Sandy Clay Loam soil with ET domain type B
Time -352 days after beginning of simulation
Date-12/31/2000

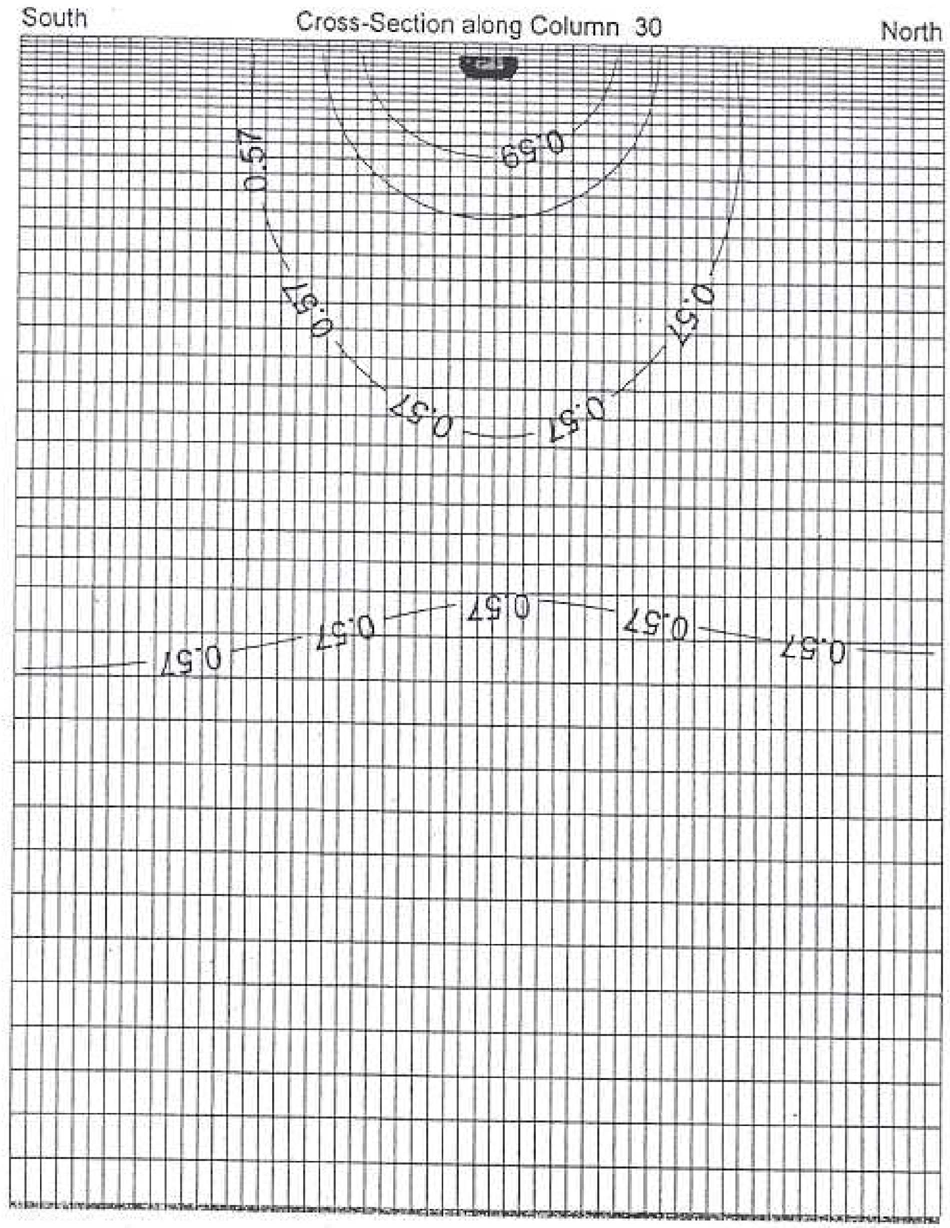

Figure D.132 Water saturation contours in cross-section for SCLB12

Simulation-SCLB1-Sandy Clay Loam soil with ET domain type B
Time -30 days after beginning of simulation
Date-2/13/2000

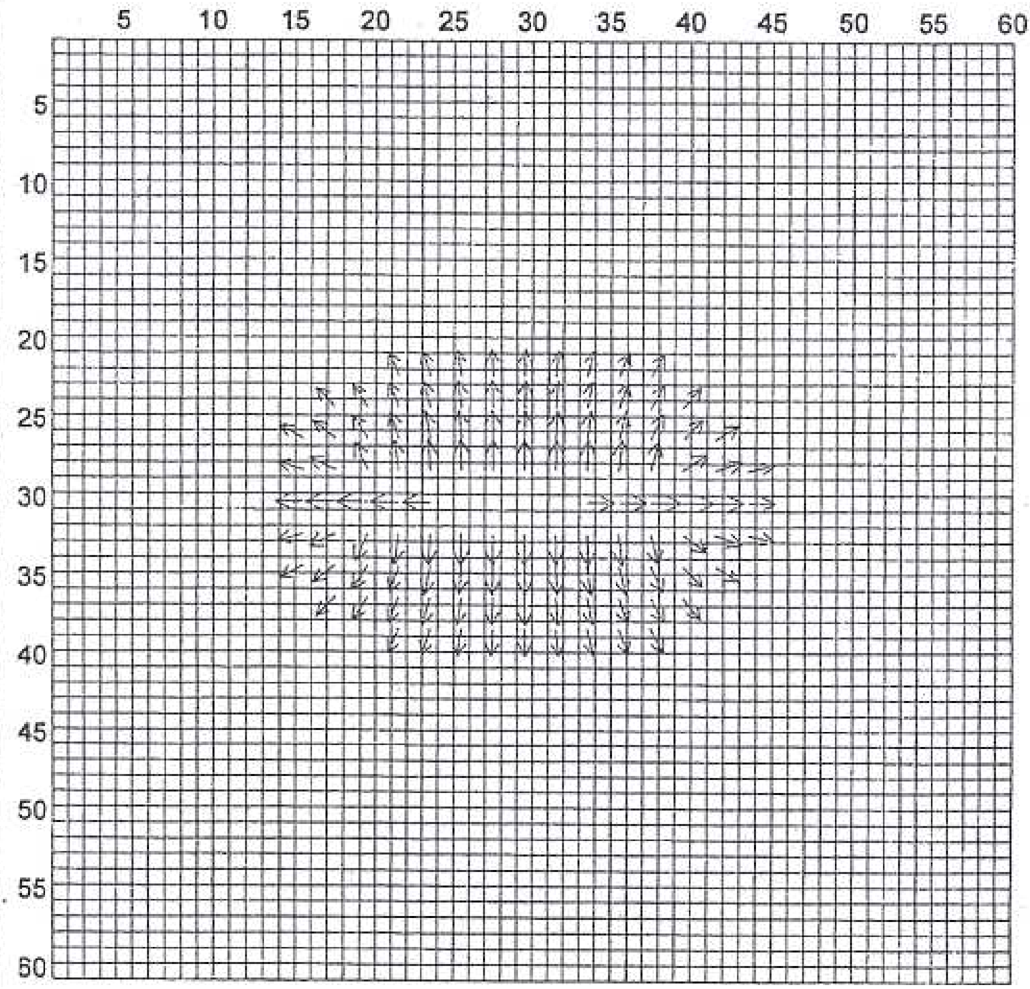

Figure D.133 Moisture movement vectors in plan view for SCLB1

Simulation-SCLB4-Sandy Clay Loam soil with ET domain type B
Time -120 days after beginning of simulation
Date-5/13/2000

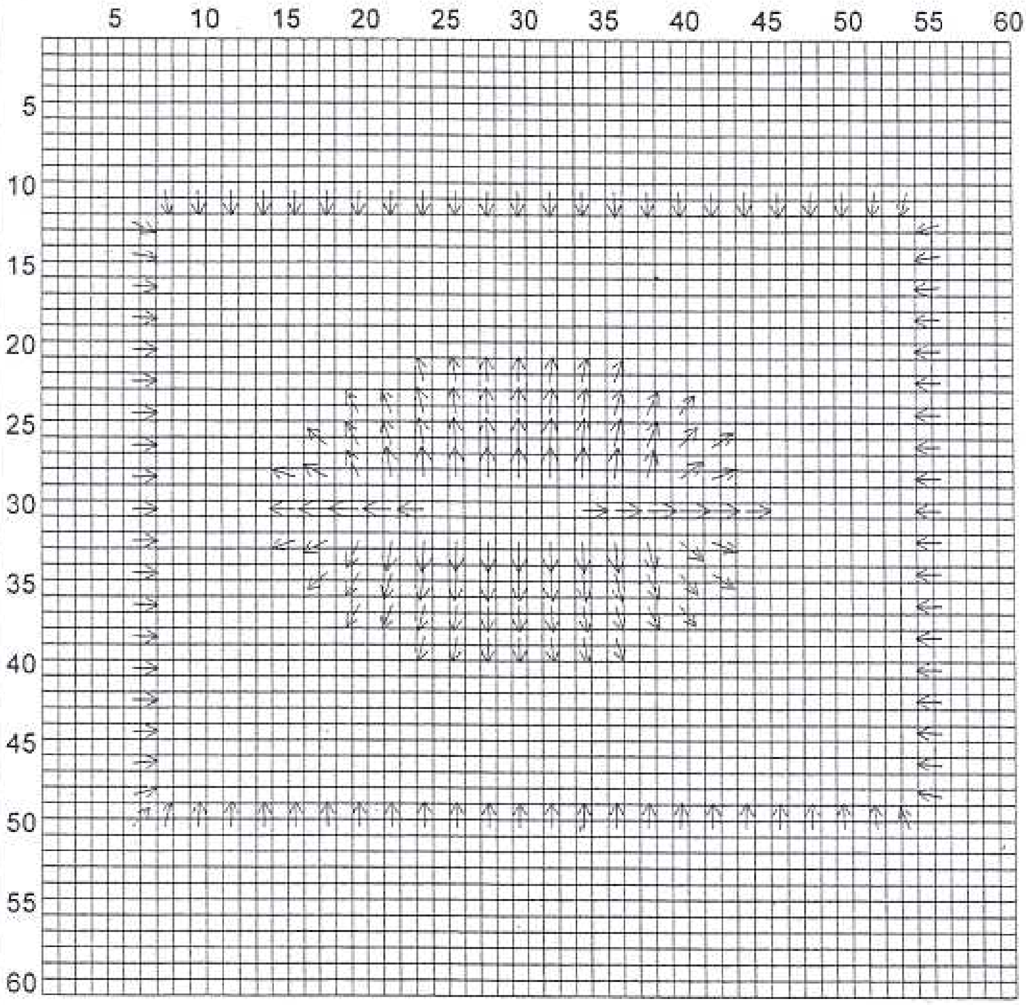

Figure D.134 Moisture movement vectors in plan view for SCLB4

Simulation-SCLB8-Sandy Clay Loam soil with ET domain type B
Time -240 days after beginning of simulation
Date-9/10/2000

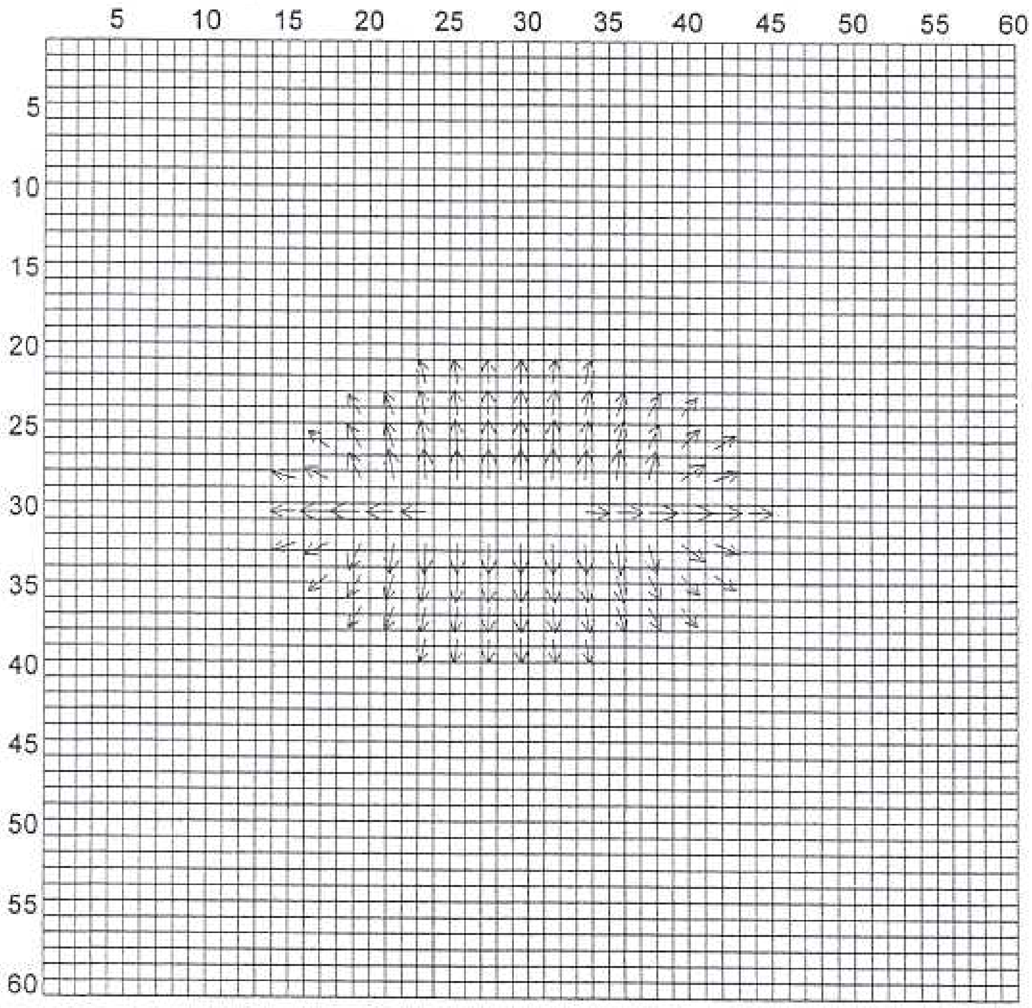

Figure D.135 Moisture movement vectors in plan view for SCLB8

Simulation-SCLB12-Sandy Clay Loam soil with ET domain type B
Time -352 days after beginning of simulation
Date-12/31/2000

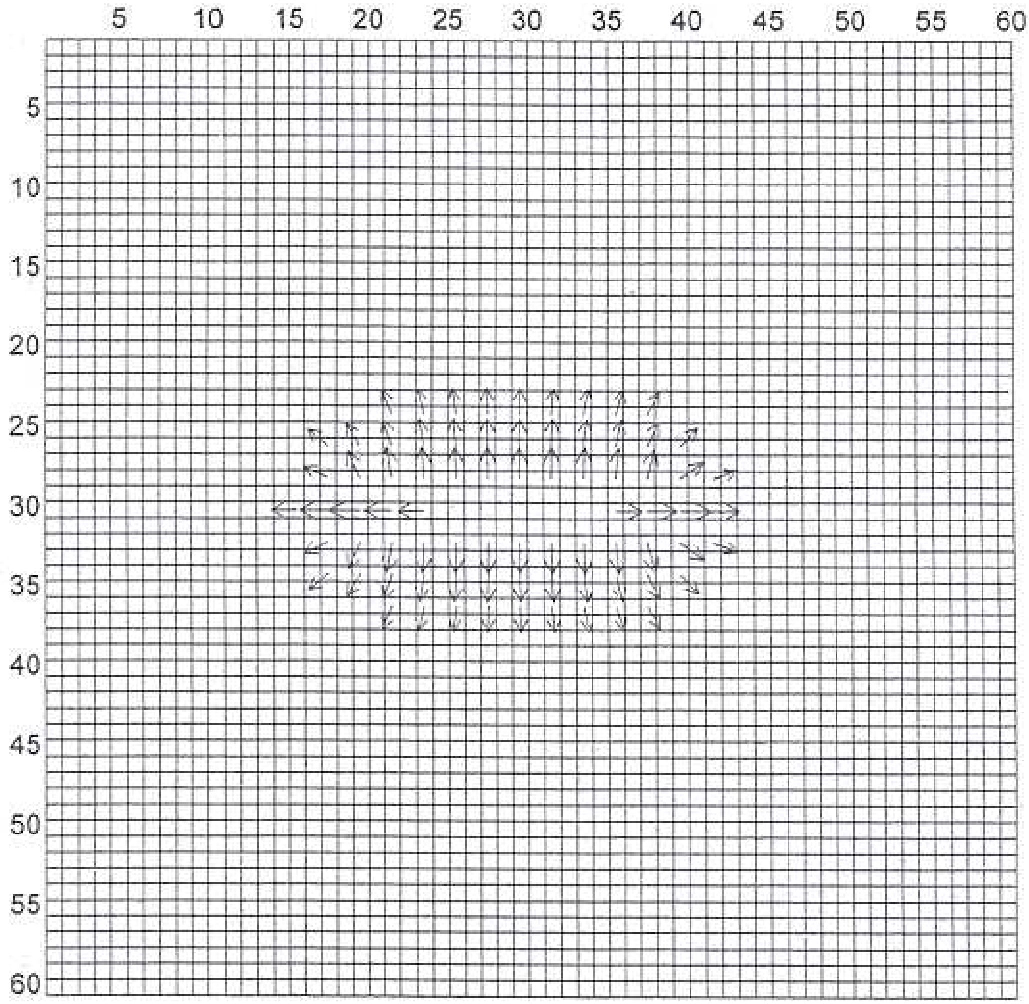

Figure D.136 Moisture movement vectors in plan view for SCLB12

Simulation-SCLB1-Sandy Clay Loam soil with ET domain type B
Time -30 days after beginning of simulation
Date-2/13/2000

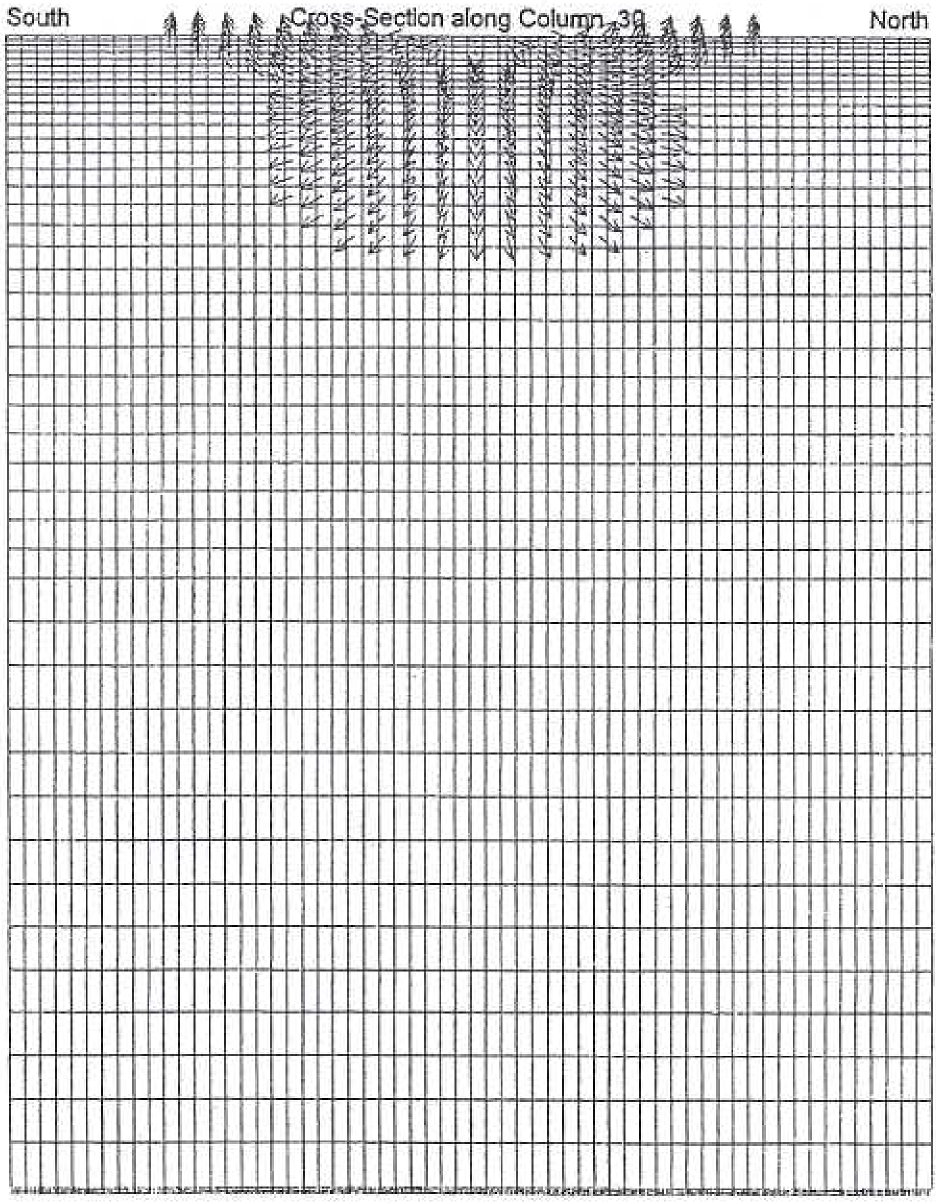

Figure D.137 Moisture movement vectors along C-30 for SCLB1

Simulation-SCLB4-Sandy Clay Loam soil with ET domain type B
Time -120 days after beginning of simulation
Date-5/13/2000

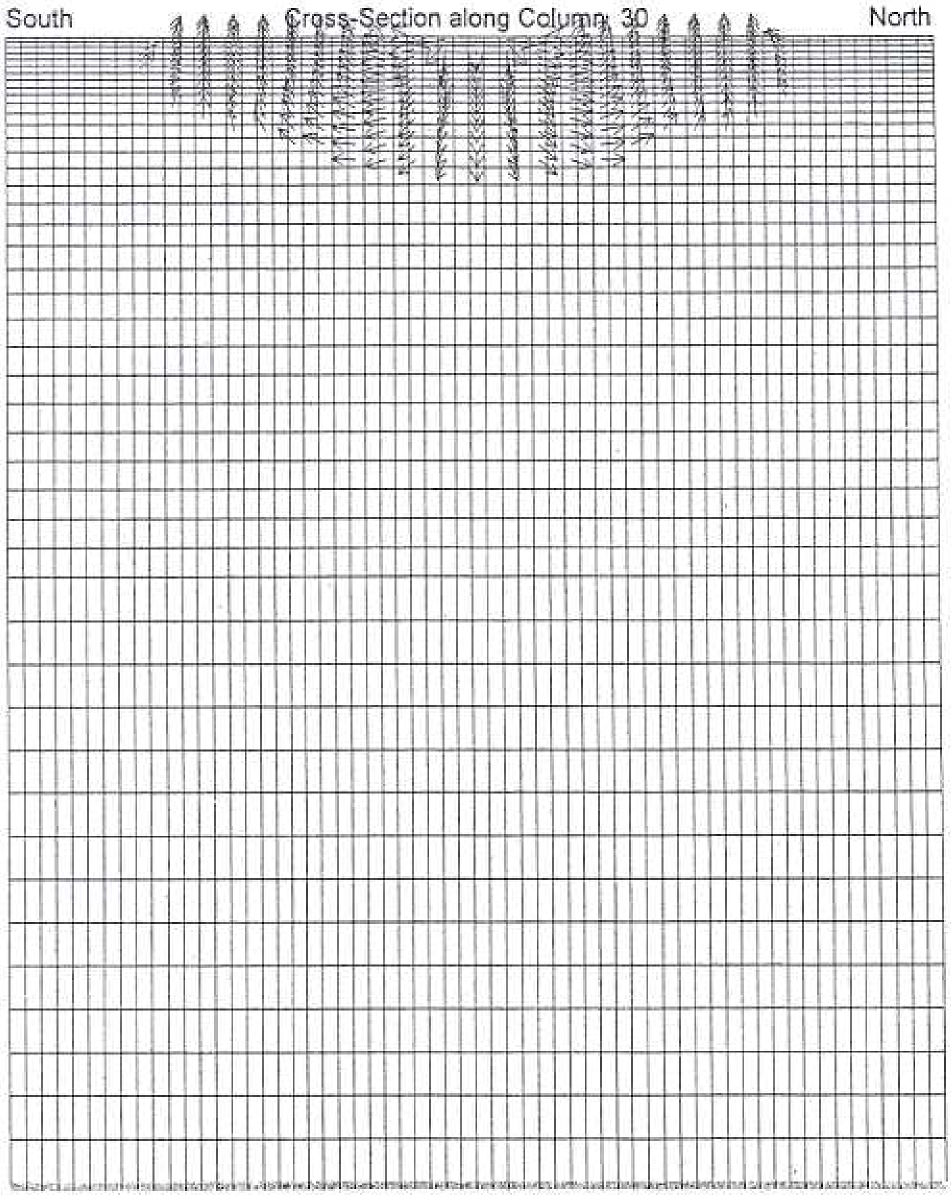

Figure D.138 Moisture movement vectors along C-30 for SCLB4

Simulation-SCLB8-Sandy Clay Loam soil with ET domain type B
Time -240 days after beginning of simulation
Date-9/10/2000

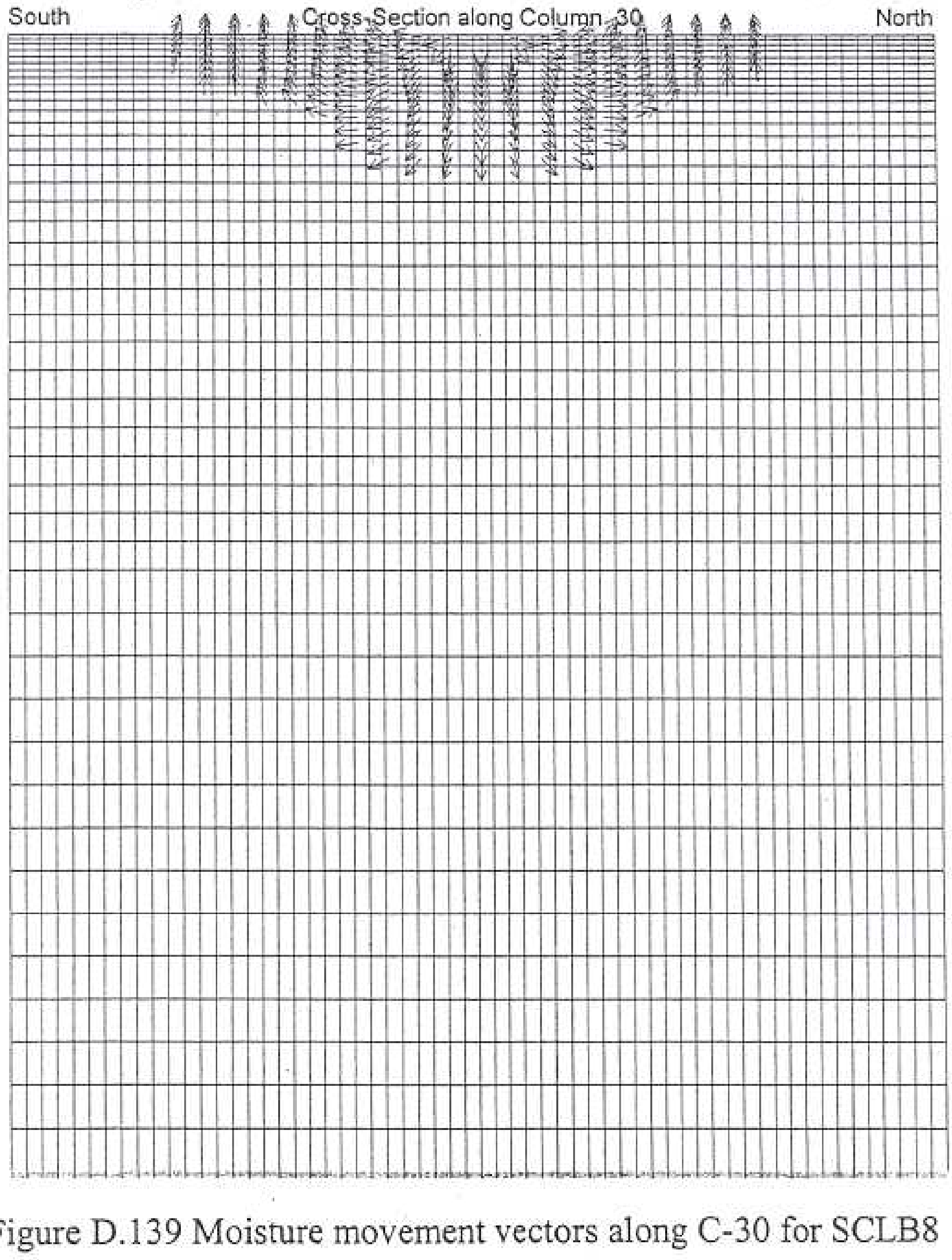

Figure D.139 Moisture movement vectors along C-30 for SCLB8

Simulation-SCLB12-Sandy Clay Loam soil with ET domain type B
Time -352 days after beginning of simulation
Date-12/31/2000

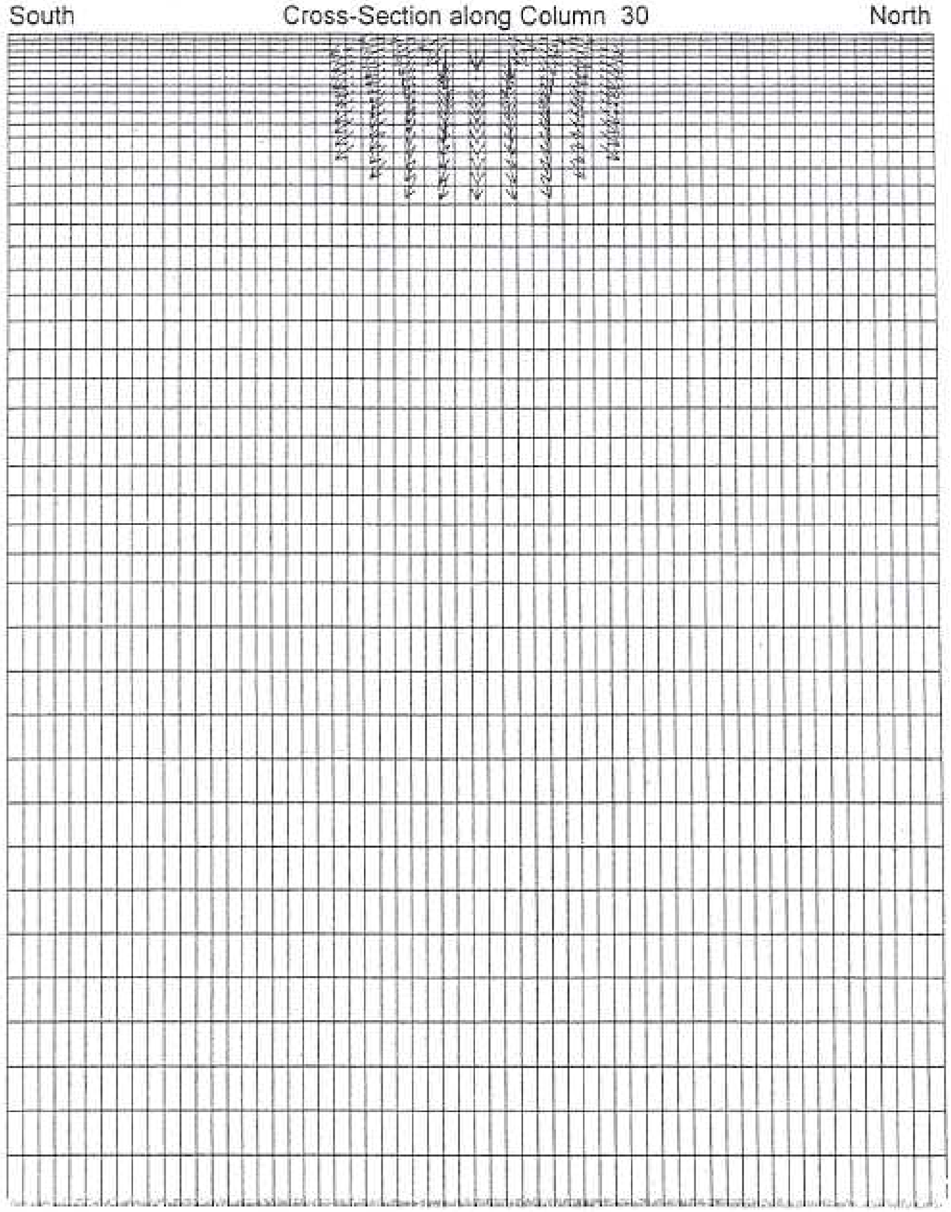

Figure D.140 Moisture movement vectors along C-30 for SCLB12

Simulation-SCLB1-Sandy Clay Loam soil with ET domain type B
Time -30 days after beginning of simulation
Date-2/13/2000

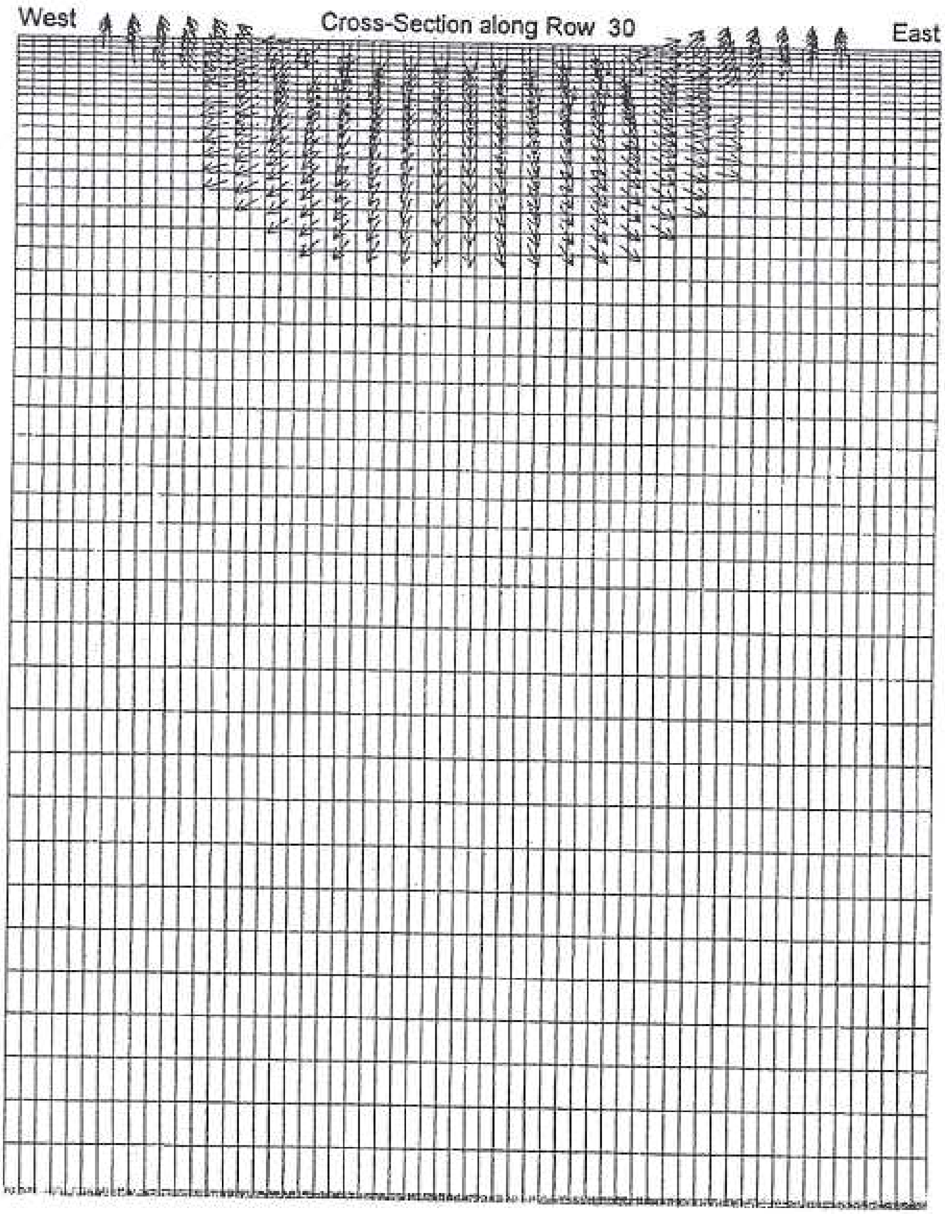

Figure D.141 Moisture movement vectors along R-30 for SCLB1

Simulation-SCLB4-Sandy Clay Loam soil with ET domain type B
Time -120 days after beginning of simulation
Date-5/13/2000

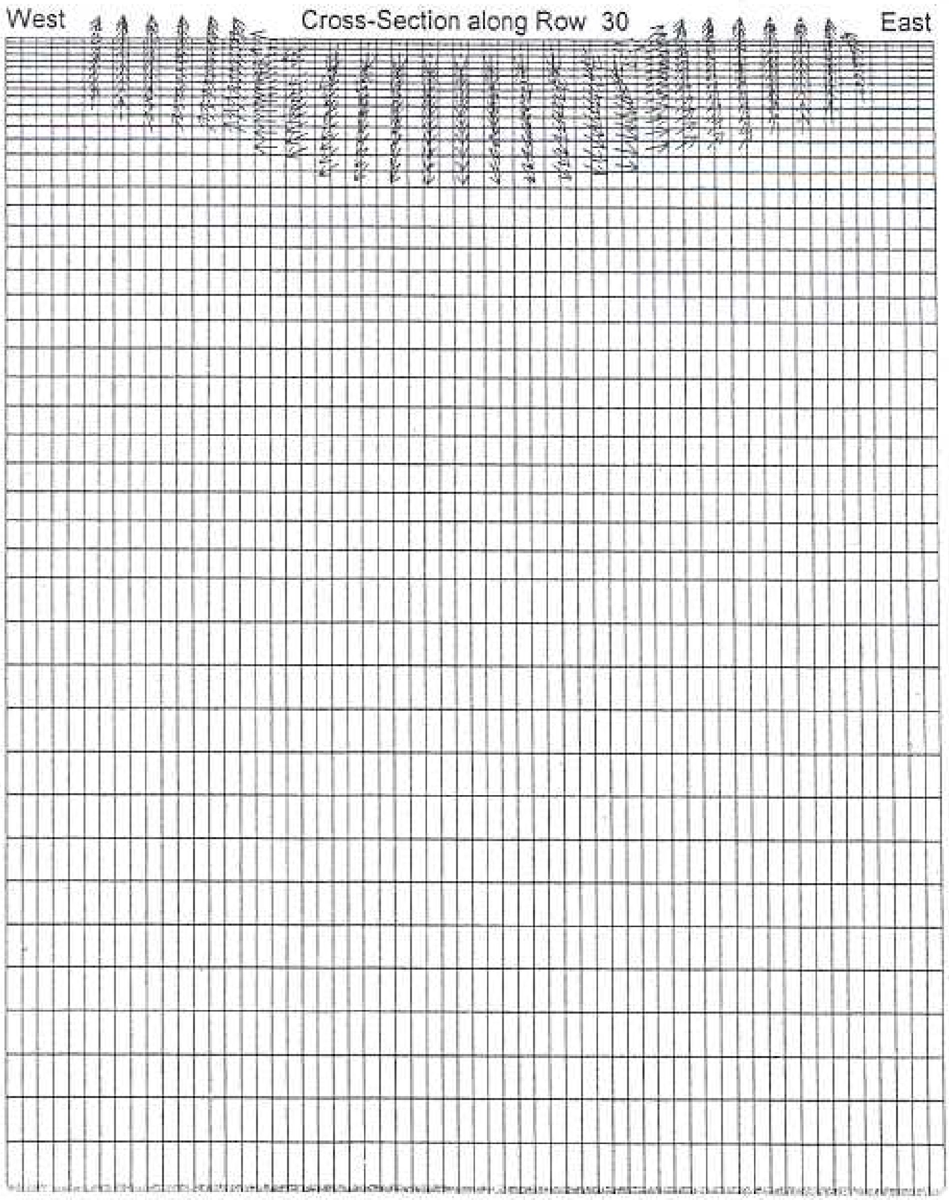

Figure D.142 Moisture movement vectors along R-30 for SCLB4

Simulation-SCLB8-Sandy Clay Loam soil with ET domain type B
Time -240 days after beginning of simulation
Date-9/10/2000

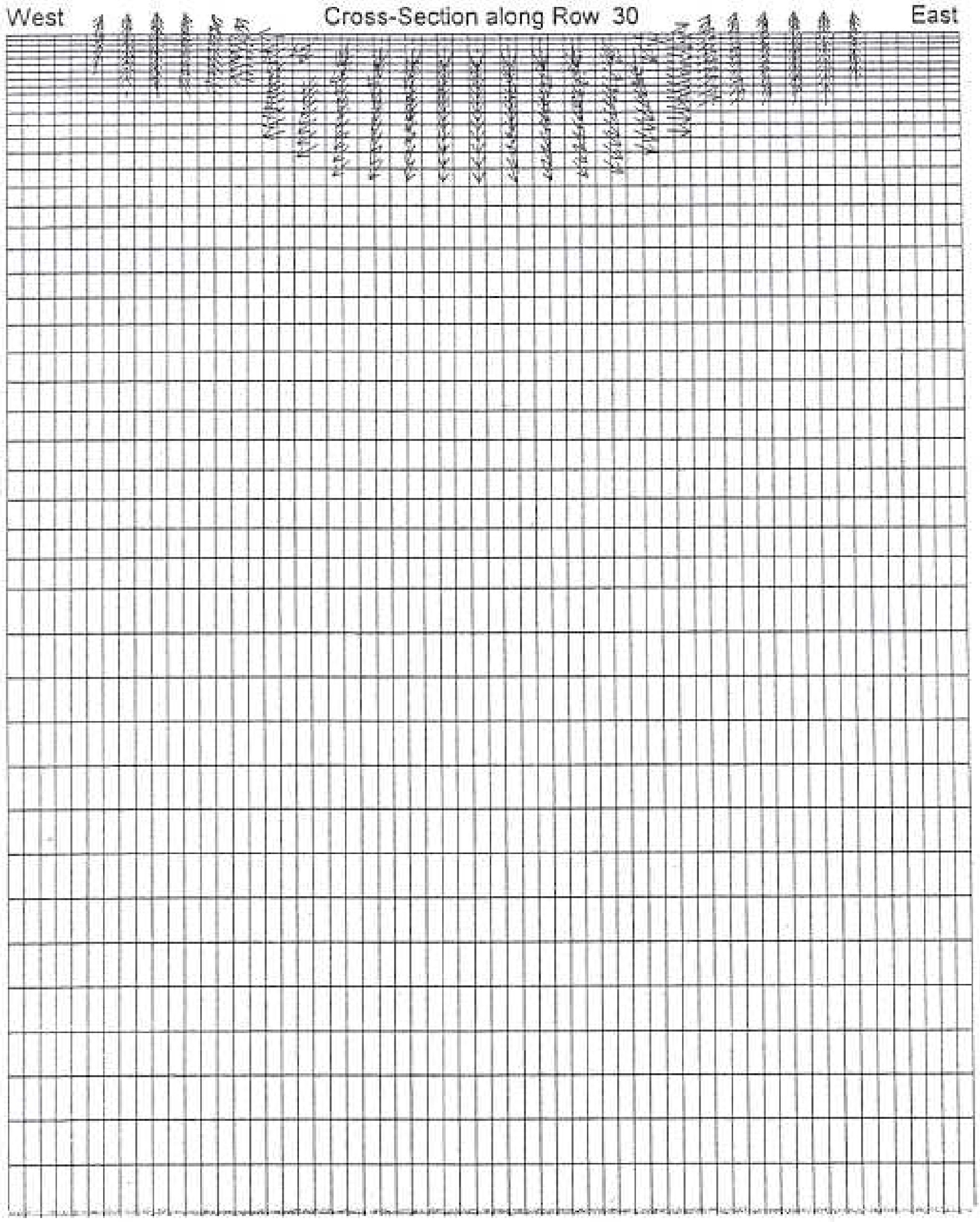

Figure D.143 Moisture movement vectors along R-30 for SCLB8

Simulation-SCLB12-Sandy Clay Loam soil with ET domain type B
Time -352 days after beginning of simulation
Date-12/31/2000

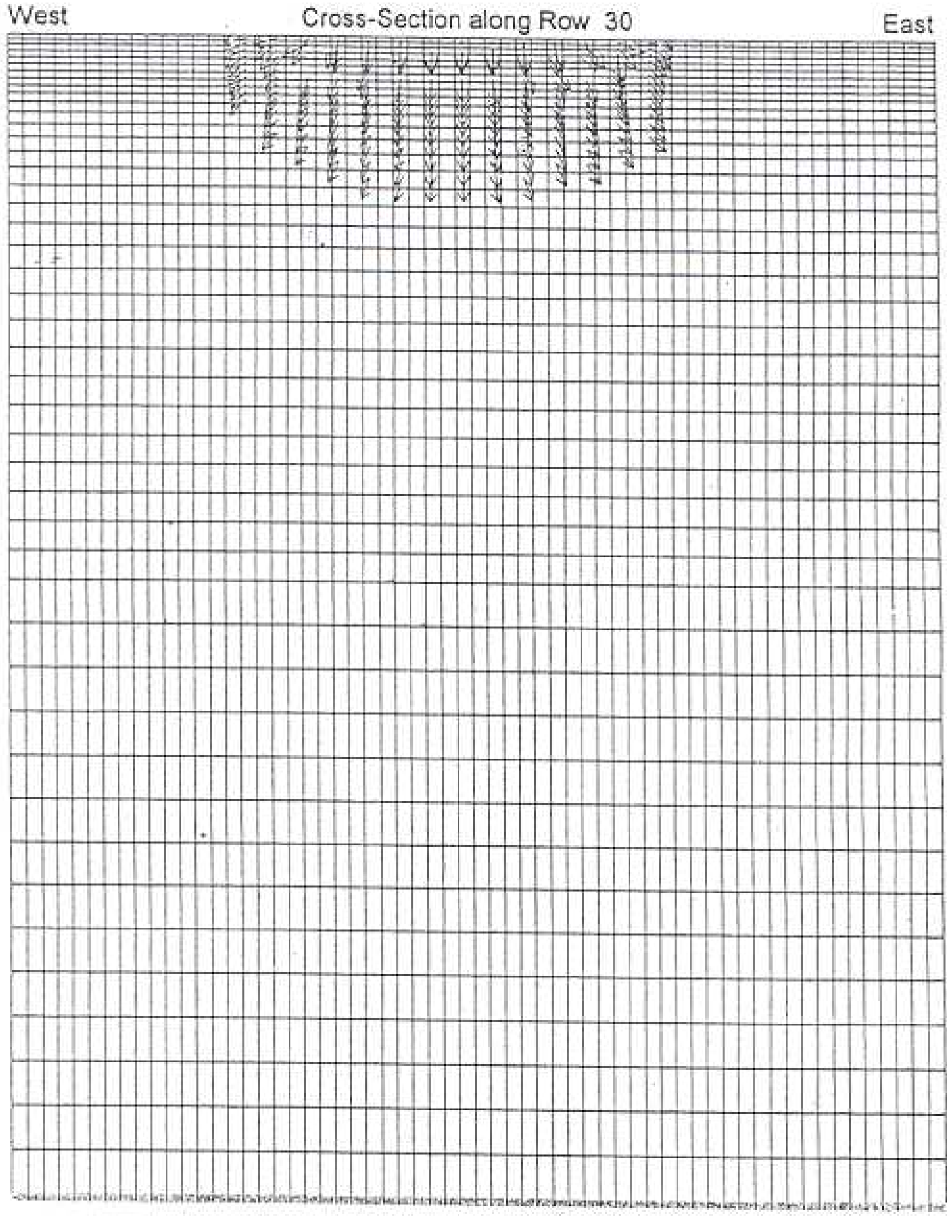

Figure D.144 Moisture movement vectors along R-30 for SCLB12